

FINAL REPORT

to

THE FLORIDA DEPARTMENT OF TRANSPORTATION
RESEARCH CENTER

on Project

“Managed Lane Operations –
Adjusted Time of Day Pricing vs. Near-Real Time Dynamic Pricing”

Volume II: Ramp Signaling and Variable Speed Limits (VSL)

FDOT Contract BDK77 977-04 (UF Project 00081551)



February 12, 2012

Transportation Research Center
The University of Florida

DISCLAIMER

The opinions, findings, and conclusions expressed in this publication are those of the authors and not necessarily those of the Florida Department of Transportation.

METRIC CONVERSION CHART

U.S. UNITS TO METRIC (SI) UNITS

LENGTH

SYMBOL	WHEN YOU KNOW	MULTIPLY BY	TO FIND	SYMBOL
in	Inches	25.4	millimeters	mm
ft	Feet	0.305	meters	m
yd	Yards	0.914	meters	m
mi	Miles	1.61	kilometers	km

METRIC (SI) UNITS TO U.S. UNITS

LENGTH

SYMBOL	WHEN YOU KNOW	MULTIPLY BY	TO FIND	SYMBOL
mm	millimeters	0.039	inches	in
m	Meters	3.28	feet	ft
m	Meters	1.09	yards	yd
km	kilometers	0.621	miles	mi

Technical Report Documentation Page

1. Report No.	2. Government Accession No.	3. Recipient's Catalog No.	
4. Title and Subtitle Managed Lane Operations – Adjusted Time of Day Pricing vs. Near-Real Time Dynamic Pricing Volume II: Ramp Signaling and Variable Speed Limits (VSL)		5. Report Date February 12, 2012	6. Performing Organization Code UF-TRC
7. Author(s) Lily Elefteriadou, Clark Letter, Evangelos Mintsis		8. Performing Organization Report No.	
9. Performing Organization Name and Address Transportation Research Center University of Florida 512 Weil Hall, PO Box 116580 Gainesville, FL 32611-6580		10. Work Unit No. (TRAIS)	11. Contract or Grant No. FDOT Contract BDK77 977-04
12. Sponsoring Agency Name and Address Florida Department of Transportation 605 Suwannee Street, MS 30 Tallahassee, FL 32399		13. Type of Report and Period Covered Final, 6/19/2009-2/12/2012	
15. Supplementary Notes		14. Sponsoring Agency Code	
16. Abstract <p>This report (Volume II) provides an overview of the research conducted for Task 5 and the Supplemental Task. Task 5 focused on interactions between congestion pricing and ramp signaling (also referred to as ramp metering), while the Supplemental Task focused on the potential impacts of a Variable Speed Limit (VSL) implementation along the I-95 HOT lanes. Each of these efforts is discussed separately in this report.</p> <p>The objectives of Task 5 were to explore interactions between congestion pricing and ramp signaling, and to provide recommendations for implementation of congestion pricing and ramp signaling when these operate concurrently at the same facility.</p> <p>A theoretical framework was first constructed, and then the I-95 HOT lanes corridor was simulated, and various pricing and signaling scenarios were tested. The analysis showed that an increase in the toll rate is rendering the HOT lanes less preferable with respect to travel cost, shifting traffic to the GP lanes. This causes the signaling rate to become more restrictive. Based on the analysis conducted, the optimal operation of the system would rely on maximizing the utilization of the HOT lanes. Therefore, it is suggested that one of the objectives of the pricing algorithm should be the maximization of the utilization of the HOT lanes.</p> <p>The objective of the Supplemental Task was to evaluate whether VSL could/should be considered for incorporation into managed lanes along the I-95 HOT lanes facility. The researchers used the CORSIM simulation model developed under Task 5 to replicate VSL operations along the I-95 HOT lanes facility. The throughput was found to increase for most of the VSL scenarios tested by a maximum of 30 to 90 vehicles over a given 15-minute time period. It was concluded that VSL has the potential to improve traffic operations along the I-95 corridor. Before implementing such a system, it is recommended that enforcement of speed limits is further considered.</p>			
17. Key Word Ramp Metering, Ramp Signaling, Variable Speed Limits, Freeway Management Strategies		18. Distribution Statement No restrictions	
19. Security Classif. (of this report) Unclassified.	20. Security Classif. (of this page) Unclassified.	21. No. of Pages 189	22. Price N/A

ACKNOWLEDGMENTS

The authors would like to express their sincere appreciation to Trey Tillander, Mark Plass, Rory Santana, Debora Rivera, David Chang and Gregg Letts of the Florida Department of Transportation for the guidance and support that they provided on this project.

EXECUTIVE SUMMARY

This report (Volume II) provides an overview of the research conducted for Task 5 and the Supplemental Task. Task 5 focused on interactions between congestion pricing and ramp signaling (also referred to as ramp metering), while the Supplemental Task focused on the potential impacts of a Variable Speed Limit (VSL) implementation along the I-95 HOT lanes. Each of these efforts is discussed separately in this report.

Congestion pricing and ramp metering are two different traffic management strategies which have been developed to manage and optimize freeway traffic operations. Existing research and practice have not evaluated the interaction of these strategies and their combined effect when they are implemented along the same facility. A thorough literature review did not identify any papers that discuss the interactions between pricing and ramp metering. Therefore, the objectives of this task (Task 5) were to:

- Explore interactions between congestion pricing and ramp signaling
- Propose recommendations for implementation of congestion pricing and ramp metering when these operate concurrently at the same facility.

To accomplish this task, the research team first developed a theoretical framework regarding the interaction of congestion pricing and ramp metering according to their respective locations on the network. This analysis suggested that an increase in the toll rates would cause a decrease in the metering rates at the ramp meters that are installed along the HOT lanes. This hypothesis was examined using simulation. The I-95 in Miami was simulated in CORSIM. A dynamic pricing algorithm (i.e., I-95 HOT Tolling Algorithm) and a dynamic ramp metering algorithm (i.e., Fuzzy Logic Ramp Metering Algorithm) were programmed and interfaced with CORSIM to conduct the experiments. The research team tested various scenarios related to the two types of management systems.

The simulation results were in agreement with the hypothesis made in the early stages of this task. The analysis showed that an increase in the toll rate renders the HOT

lanes less preferable with respect to travel cost, shifting traffic to the GP lanes. This causes the metering rate to become more restrictive. Based on the analysis conducted, the optimal operation of the system would rely on maximizing the utilization of the HOT lanes. Therefore, it is suggested that one of the objectives of the pricing algorithm should be the maximization of the utilization of the HOT lanes. The toll rate should always remain at a level that prevents the occurrence of breakdowns on the HOT lanes. The more traffic HOT lanes manage to service without the risk of congestion, the easier it becomes for ramp metering to regulate the mainline and on-ramp traffic.

Concurrently with the investigation of the interactions between ramp metering and pricing, the operation of different tolling algorithms and different combinations of ramp metering and pricing algorithms was evaluated. The evaluation revealed that the integrated control (i.e., ramp metering plus tolling) regulates traffic much more efficiently compared to the tolling only case. However, when both algorithms are implemented it is recommended that they operate in a dynamic way in order to mitigate congestion successfully both on the ramps and the mainline freeway.

Variable Speed Limit (VSL) systems have been used upstream of bottlenecks with recurring congestion as a way to dampen the shockwave produced once congestion starts. However, the exact effects of VSL on traffic flow are not well understood. An extensive literature review was performed to review previous studies that have assessed VSL or have replicated them in simulation. The literature provides conflicting conclusions with respect to the effectiveness of VSL installations in increasing overall speeds and throughput.

The objective of this task (Supplemental Task) was to evaluate whether VSL could/should be considered for incorporation into managed lanes along the I-95 HOT lanes facility. The researchers used the CORSIM simulation model developed under Task 5 to replicate VSL operations along the I-95 HOT lanes facility. Simulation is a very effective tool in evaluating alternatives under completely controlled conditions which cannot be achieved in the field. Current micro-simulators do not provide an interface to easily simulate VSLs and evaluate their impact on traffic, thus simulation must be carried out through additional coding. A run time extension (RTE) was developed and used to simulate VSL operations and to test their effectiveness under a

variety of conditions and algorithm settings.

Three different algorithms for VSL control were implemented into the CORSIM network and evaluated based on selected performance measures. These represent the major types of algorithms that have been tested and implemented to-date. An occupancy-based algorithm was selected because it is currently implemented on I-4 in Orlando, Florida. A volume-based algorithm was selected because it is implemented on the M25 in England (Robinson, 2000) with very good overall results. The third algorithm selected is based on a combination of flow, occupancy, and average travel speed, and it is based on a study of a freeway in Toronto, Canada (Allaby et al., 2007). This algorithm was selected because it seemed a promising alternative to the other two; however, has not been implemented in the field. Different threshold values as well as several different VSL sign locations were tested with each algorithm to evaluate their effectiveness under different settings. The following were concluded:

- All of the algorithms tested improved average travel speed and total travel time, though different thresholds needed to be tested to obtain a “best case” scenario.
- The throughput was found to increase for most of the VSL scenarios tested by a maximum of 30 to 90 vehicles over a given 15 minute time period.
- The effect of the VSL may not be immediately seen if one examines conditions only at the bottleneck. The area upstream of the bottleneck shows much greater traffic improvements than the bottleneck itself.
- Improper selection of thresholds or sign positioning can cause traffic conditions to deteriorate when compared to the no-VSL control case.
- The best performing algorithm and scenario was different between the two bottleneck locations, suggesting that there is no best implementation that applies to every bottleneck.
- There was no consistent trend in traffic conditions as a function of the number and location of speed limit signs. The best sign positioning was found to be highly dependent on the type of algorithm and specific thresholds selected.
- Implementing VSL at both bottlenecks simultaneously did not improve operations. However, additional testing of combinations of algorithms at the

two bottlenecks might reveal that another combination can further improve conditions.

- The results and conclusions of this study assume speed limit compliance from motorists. In order for the I-95 corridor to operate at similar levels, the same level of compliance must be achieved. Thus there is a need for enforcement of the speed limits when they are implemented in the field.

It can be concluded that VSL has the potential to improve traffic operations along the I-95 corridor. Before implementing such a system, it is recommended that enforcement of speed limits is further considered. Also, this study did not attempt to thoroughly evaluate and compare the three selected VSL algorithms, nor to obtain optimal thresholds for each type of algorithm. An optimization-type study could be performed to obtain optimal thresholds, sign locations, and detector locations. Research considering ramp metering in conjunction with VSL would be useful in determining the mechanism through which these two tools would interact, and developing recommendations for optimizing their joint operation.

TABLE OF CONTENTS

DISCLAIMER	II
ACKNOWLEDGMENTS	V
EXECUTIVE SUMMARY	VI
LIST OF FIGURES	XII
LIST OF TABLES	XV
1 INTRODUCTION	1
1.1 COORDINATION BETWEEN PRICING AND RAMP SIGNALING.....	1
1.2 VARIABLE SPEED LIMITS ON I-95 EXPRESS	2
2 COORDINATION BETWEEN PRICING AND RAMP SIGNALIZATION	4
2.1 THEORETICAL FRAMEWORK OF CONGESTION PRICING AND RAMP METERING INTERACTIONS.....	4
2.1.1 Case 1: Ramp metering installed upstream of the HOT lanes	4
2.1.2 Case 2: Ramp metering installed along the HOT lanes	5
2.1.3 Case 3: Ramp metering installed downstream of the HOT lanes	7
2.2 LANE-BY-LANE FLOW DISTRIBUTIONS	7
2.3 THE SIMULATION NETWORK FOR I-95 IN MIAMI	18
2.3.1 Configuration of the network.....	18
2.3.1.1 Network Geometry and Study Area	18
2.3.1.2 Incoming Volumes	20
2.3.1.3 Implementation of the Ramp Metering Algorithm.....	21
2.3.1.4 Detector Placement Throughout the Network	22
2.3.2 Calibration process	23
2.4 SIMULATION-BASED EXPERIMENTS.....	38
2.4.1 Architecture of the simulation model	38
2.4.2 The Fuzzy Logic ramp signaling algorithm.....	40
2.4.2.1 Fuzzy Logic Control in Ramp Signaling.....	40
2.4.2.2 Structure and Operation of the Fuzzy Logic Ramp Signaling Algorithm	41
2.4.3 Structure of the simulated experiments.....	45
2.4.4 Results.....	46
3 VARIABLE SPEED LIMITS ON I-95 EXPRESS	71
3.1 FORMULATION OF THE EXPERIMENTS.....	71
3.1.1 Study site	71
3.1.2 VSL algorithms.....	73
3.1.2.1 Algorithm Based on Occupancy.....	74
3.1.2.2 Algorithm Based on Flow	75
3.1.2.3 Algorithm Based on a Logic Tree including Flow, Occupancy, and Average Speed	76
3.1.3 Sign location variations	77
3.1.4 The CORSIM RTE Interface	82
3.2 IMPLEMENTATION AND ANALYSIS OF ALGORITHMS IN CORSIM.....	87
3.2.1 Implementation of RTE scenarios in CORSIM.....	87
3.2.2 Analysis of the No VSL Control Scenario.....	88
3.2.3 Implementation of VSL along Bottleneck 1	98
3.2.4 Implementation of VSL along Bottleneck 2	106
3.2.5 Simultaneous VSL control at the two bottlenecks.....	114

4 CONCLUSIONS AND RECCOMENDATIONS	128
4.1 COORDINATION BETWEEN PRICING AND RAMP SIGNALING.....	128
4.2 VARIABLE SPEED LIMITS ON I-95 EXPRESS	129
REFERENCES	132
APPENDIX A – CALIBRATION DATA.....	133
APPENDIX B - LITERATURE REVIEW ON VARIABLE SPEED LIMITS (VSL)..	136

LIST OF FIGURES

FIGURE 2.1 Ramp metering installed upstream of the HOT lanes	5
FIGURE 2.2 Ramp metering installed along the length of the HOT lanes	6
FIGURE 2.3 Potential interactions between pricing and ramp metering	6
FIGURE 2.4 Ramp metering installed downstream of the HOT lanes.....	7
FIGURE 2.5 Lane configuration at each of the twelve detector locations	9
FIGURE 2.6 Lane-by-lane flow distributions south of NW 119 St. - Pre-tolling	12
FIGURE 2.7 Lane-by-lane flow distributions south of NW 131 St. - Post-tolling/pre- signaling.....	13
FIGURE 2.8 Lane-by-lane flow distributions south of NW 131 St. - Post-tolling plus signaling.....	14
FIGURE 2.9 Lane-by-lane flow distributions north of NW 151 St. - Pre-tolling	15
FIGURE 2.10 Lane-by-lane flow distributions north of NW 151 St. - Post-tolling.....	16
FIGURE 2.11 Lane-by-lane flow distributions north of NW 151 St. - Post-tolling plus signaling.....	17
FIGURE 2.12 The I-95 Expressway at NW 62 nd Street before the modifications	19
FIGURE 2.13 The I-95 Expressway at NW 62 nd Street after the modifications	20
FIGURE 2.14 Location of detectors used for calibration on I-95 in Miami.....	22
FIGURE 2.15 Field and simulated speeds – 1 st time period.....	26
FIGURE 2.16 Field and simulated volumes – 1 st time period.....	26
FIGURE 2.17 Field and simulated speeds – 2 nd time period	27
FIGURE 2.18 Field and simulated volumes – 2 nd time period	27
FIGURE 2.19 Field and simulated speeds – 3 rd time period.....	28
FIGURE 2.20 Field and simulated volumes – 3 rd time period.....	28
FIGURE 2.21 Field and simulated speeds – 4 th time period.....	29
FIGURE 2.22 Field and simulated volumes – 4 th time period.....	29
FIGURE 2.23 Field and simulated speeds – 5 th time period.....	30
FIGURE 2.24 Field and simulated volumes – 5 th time period.....	30
FIGURE 2.25 Field and simulated speeds – 6 th time period.....	31
FIGURE 2.26 Field and simulated volumes – 6 th time period.....	31
FIGURE 2.27 Field and simulated speeds – 7 th time period.....	32
FIGURE 2.28 Field and simulated volumes – 7 th time period.....	32
FIGURE 2.29 Field and simulated speeds – 8 th time period.....	33
FIGURE 2.30 Field and simulated volumes – 8 th time period.....	33
FIGURE 2.31 Field and simulated speeds – 9 th time period.....	34
FIGURE 2.32 Field and simulated volumes – 9 th time period.....	34
FIGURE 2.33 Field and simulated speeds – 10 th time period.....	35
FIGURE 2.34 Field and simulated volumes – 10 th time period.....	35
FIGURE 2.35 Field and simulated speeds – 11 th time period.....	36
FIGURE 2.36 Field and simulated volumes – 11 th time period.....	36
FIGURE 2.37 Field and simulated speeds – 12 th time period.....	37
FIGURE 2.38 Field and simulated volumes – 12 th time period.....	37
FIGURE 2.39 Architecture of the simulation	39
FIGURE 2.40 Fuzzy classes for local and downstream occupancy	42
FIGURE 2.41 Fuzzy classes for local and downstream speed	43
FIGURE 2.42 Fuzzy classes for local and downstream speed	43
FIGURE 2.43 Fuzzy classes for metering rates.....	44
FIGURE 2.44 Scenario #6: Metering rate of ramp at 62 nd Street.....	47

FIGURE 2.45 Scenario #6: Toll rate imposed on vehicles entering the HOT Lanes every time interval (i.e., 15 min).....	48
FIGURE 2.46 Scenario #6: Percent of traffic entering GP and HOT Lanes every time interval (i.e., 15 min).....	49
FIGURE 2.47 Scenario #5: Metering rate of ramp at 62 nd Street.....	50
FIGURE 2.48 Scenario #5: Toll rate imposed on vehicles entering the HOT lanes every time interval (i.e., 15 min).....	51
FIGURE 2.49 Scenario #5: Percent of traffic entering GP and HOT lanes every time interval (i.e., 15 min).....	52
FIGURE 2.50 Scenario #1: Average speeds along I-95 Northbound GP lanes during 17:30 – 17:45 pm.....	54
FIGURE 2.51 Scenario #2: Average speeds along I-95 Northbound GP lanes during 17:30 – 17:45 pm.....	55
FIGURE 2.52 Scenario #3: Average speeds along I-95 Northbound GP lanes during 17:30 – 17:45 pm.....	56
FIGURE 2.53 Scenario #4: Average speeds along I-95 Northbound GP lanes during 17:30 – 17:45 pm.....	57
FIGURE 2.54 Scenario #5: Average speeds along I-95 Northbound GP lanes during 17:30 – 17:45 pm.....	58
FIGURE 2.55 Scenario #6: Average speeds along I-95 Northbound GP lanes during 17:30 – 17:45 pm.....	59
FIGURE 2.56 Scenario #1: Average travel time per vehicle from NW 81 st St. to North Golden Glades.....	61
FIGURE 2.57 Scenario #2: Average travel time per vehicle from NW 81 st St. to North Golden Glades.....	62
FIGURE 2.58 Scenario #3: Average travel time per vehicle from NW 81 st St. to North Golden Glades.....	63
FIGURE 2.59 Scenario #4: Average travel time per vehicle from NW 81 st St. to North Golden Glades.....	64
FIGURE 2.60 Scenario #5: Average travel time per vehicle from NW 81 st St. to North Golden Glades.....	65
FIGURE 2.61 Scenario #6: Average travel time per vehicle from NW 81 st St. to North Golden Glades.....	66
FIGURE 2.62 Scenario #2: Total delay at the first on-ramp downstream of NW 95 th Street.....	68
FIGURE 2.63 Scenario #4: Total delay at the first on-ramp downstream of NW 95 th Street.....	69
FIGURE 2.64 Scenario #6: Total delay at the first on-ramp downstream of NW 95 th Street.....	70
FIGURE 3.1 Speed profile of the I-95 section at the onset of congestion (4:15 p.m. to 4:30 p.m.).....	72
FIGURE 3.2 Decision tree logic for combined flow/occupancy/speed algorithm.....	77
FIGURE 3.3 Use of one sign located approximately one-half mile upstream of Bottleneck 1.....	78
FIGURE 3.4 Use of one sign located approximately one mile upstream of Bottleneck 1.....	78
FIGURE 3.5 Use of two signs spaced approximately one-half mile apart upstream of Bottleneck 1.....	79
FIGURE 3.6 Use of two signs spaced approximately one mile apart upstream of Bottleneck 1.....	79

FIGURE 3.7 Use of one sign located approximately one half mile upstream of Bottleneck 2	80
FIGURE 3.8 Use of one sign located approximately one mile upstream from Bottleneck 2	80
FIGURE 3.9 Use of two signs spaced approximately one half mile apart upstream of Bottleneck 2	81
FIGURE 3.10 Use of two signs spaced approximately one mile apart upstream of Bottleneck 2	81
FIGURE 3.11 Flowchart of RTE logic	83
FIGURE 3.12 Screen shot of computer run indicating a change in the speed limit	84
FIGURE 3.13 Speed limit propagation downstream from VSL sign location. Simulation time from change of speed limit:	85
FIGURE 3.14 Speed profile for no-control scenario over time the 12 periods at Bottleneck 1.	89
FIGURE 3.15. Speed profile for no-control scenario over time the 12 periods at Bottleneck 2.	94
FIGURE 3.16. Speed profile for the volume-based algorithm using one sign spaced 1 mile from the bottleneck (threshold scenario 1) compared to the no-control scenario.	100
FIGURE 3.17. Throughput for the volume-based algorithm using one sign spaced 1 mile from the bottleneck (threshold scenario 1) compared to the no-control scenario.	105
FIGURE 3.18. Speed profile for the occupancy-based algorithm using two signs spaced 1/2 mile apart (threshold scenario 1) compared to the no-control scenario.	108
FIGURE 3.19 Throughput for the occupancy-based algorithm using two signs spaced 1/2 mile apart (threshold scenario 1) compared to the no-control scenario.....	113
FIGURE 3.20 Speed profile for the combination VSL control compared to the no-control scenario.	116

LIST OF TABLES

TABLE 2.1 Data collection locations for pre-tolling and post tolling plus signaling	9
TABLE 2.2 Locations and detector identification – Tolling/pre-signaling only	10
TABLE 2.3 Location and metering rate of each ramp signal along I-95	21
TABLE 2.4 Location of field and simulated detectors	23
TABLE 2.5 Average network speed for each simulation run.....	24
TABLE 2.6 Field and simulated speeds and volumes – 1 st time period	26
TABLE 2.7 Field and simulated speeds and volumes – 2 nd time period	27
TABLE 2.8 Field and simulated speeds and volumes – 3 rd time period	28
TABLE 2.9 Field and simulated speeds and volumes – 4 th time period	29
TABLE 2.10 Field and simulated speeds and volumes – 5 th time period.....	30
TABLE 2.11 Field and simulated speeds and volumes – 6 th time period	31
TABLE 2.12 Field and simulated speeds and volumes – 7 th time period	32
TABLE 2.13 Field and simulated speeds and volumes – 8 th time period	33
TABLE 2.14 Field and simulated speeds and volumes – 9 th time period	34
TABLE 2.15 Field and simulated speeds and volumes – 10 th time period	35
TABLE 2.16 Field and simulated speeds and volumes – 11 th time period	36
TABLE 2.17 Field and simulated speeds and volumes – 12 th time period	37
TABLE 2.18 Description of fuzzy logic ramp metering algorithm inputs	42
TABLE 2.19 Rule base for fuzzy ramp metering algorithm	44
TABLE 2.20 Scenarios tested regarding ramp metering and tolling interactions	45
TABLE 3.1 Occupancy thresholds for displayed speed limits (scenario 1)	74
TABLE 3.2 Occupancy thresholds for displayed speed limits (scenario 2)	75
TABLE 3.3 Occupancy thresholds for displayed speed limits (scenario 3)	75
TABLE 3.4 Volume thresholds for displayed speed limits (scenario 1)	76
TABLE 3.5 Volume thresholds for displayed speed limits (scenario 2)	76
TABLE 3.6. Description of scenarios tested	88
TABLE 3.7. Network performance measures for Bottleneck 1.....	99
TABLE 3.8. Network performance measures for Bottleneck 2.....	107
TABLE 3.9 Network performance measures for corridor analysis	115

1 INTRODUCTION

This report (Volume II) provides an overview of the research conducted for Tasks 5 and the Supplemental Task. Task 5 focused on interactions between congestion pricing and ramp metering, while the Supplemental Task focused on the potential impacts of a Variable Speed Limit (VSL) implementation along the I-95 HOT lanes. Each of these efforts is discussed separately in this report.

1.1 Coordination Between Pricing and Ramp Signaling

Congestion pricing and ramp metering are two different traffic management strategies which have been developed to manage and optimize freeway traffic operations. Existing research and practice has not evaluated the interaction of these strategies and their combined effect when they are implemented along the same facility. A thorough literature review did not identify any papers that discuss the interactions between pricing and ramp metering. The majority of the papers identified to be relevant to the topic of this task simply mention the possibility of interactions between those types of systems (Swenson and Poole, 2009; Shen and Zhang, 2009; FHWA, 2008.) Specific adjustments may be required to one or both of these strategies to achieve optimal operations when these systems are implemented concurrently.

Therefore, the objectives of this task are to:

- Explore interactions between congestion pricing and ramp metering.
- Propose recommendations for implementation of congestion pricing and ramp metering when these operate concurrently at the same facility.

To accomplish this task, the research team observed lane distributions before and after the installation of the two systems at the I-95 HOT lanes section in Miami, FL. It then simulated this freeway section, implemented both congestion pricing and ramp metering, and tested various scenarios related to the two types of management systems.

1.2 Variable Speed Limits on I-95 Express

Static speed limits are designed to provide motorists with a safe speed at which to drive. While these safe speeds are effective during ideal conditions, they fail to provide recommended safe speeds during adverse weather or congested driving conditions (Sisiopiku 2001). Variable speed limits (VSLs) are a way of recommending safe driving speeds during less than ideal conditions. VSL systems have produced safety benefits such as a reduced number of rear end collisions and traffic homogenization.

In addition to their safety benefits, VSL have been used upstream of bottlenecks with recurring congestion as a way to dampen the shockwave produced once congestion starts. However, the exact effects of VSL on traffic flow are not well understood. An extensive literature review was performed to review previous studies that have assessed VSL or have replicated them in simulation. The literature provides conflicting conclusions with respect to the effectiveness of VSL installations in increasing overall speeds and throughput. The complete literature review can be found in Appendix B.

The objective of this task was to evaluate whether VSL could/should be considered for incorporation into managed lanes along the I-95 HOT lanes facility. The researchers used the CORSIM simulation model developed under Task 5 to replicate VSL operations along the I-95 HOT lanes facility. Various types of VSL algorithms were implemented at specific locations along the simulated I-95 freeway section to evaluate the effectiveness of these algorithms.

Simulation is a very effective tool in evaluating alternatives under completely controlled conditions which cannot be achieved in the field. It is also very effective in providing a comprehensive picture of traffic operations in time and space. To-date, few micro-simulators possess the ability to simulate VSL systems. Simulators such as AIMSUN and PARAMICS have the ability to simulate variable message signs, but require additional coding to simulate VSLs. No micro-simulator has a built-in interface that allows the simulation of different VSL algorithms. There are few tools or guidelines available for simulating VSLs, which makes simulating them a difficult and time-consuming process. CORSIM does not have an interface to directly

simulate VSLs, however, it has a run time extension (RTE) interface that allows users to define or modify operations of the simulation program. This interface can be used to simulate VSL operations and to test their effectiveness under a variety of conditions and algorithm settings.

Three different algorithms for VSL control are implemented into the CORSIM network and evaluated based on selected performance measures. Different threshold values as well as several different VSL sign locations are tested with each algorithm to evaluate their effectiveness under different settings.

The remainder of this report is organized as follows. Chapter 2 presents the research related to pricing and ramp metering, while Chapter 3 presents the research related to Variable Speed Limits (VSL). Chapter 4 summarizes the conclusions and recommendations based on the findings of Chapters 2 and 3.

2 COORDINATION BETWEEN PRICING AND RAMP SIGNALIZATION

This chapter is organized as follows. Section 2.1 presents a theoretical framework regarding the interaction of congestion pricing and ramp metering considering various possible types of concurrent installations. Section 2.2 examines the lane-by-lane flow distributions along the I-95 HOT lanes section before and after the installation of each system. Section 2.3 describes the I-95 HOT lanes network, demands and other inputs, as well as the calibration of the simulated network. Section 2.4 discusses the scenarios tested, their implementation and the results of the simulation experiments.

2.1 Theoretical Framework of Congestion Pricing and Ramp Metering Interactions

The researchers first considered possible cases of interactions between pricing and ramp metering, based on the relative location of each system. Three potential cases were identified and are discussed in this section.

2.1.1 Case 1: Ramp metering installed upstream of the HOT lanes

The case where ramp metering is installed in the section upstream of the HOT lanes is illustrated in Figure 2.1. Ramp metering algorithms generally set the ramp flow as a function of the flow or occupancy along the freeway facility. The presence of HOT lanes downstream of a metered ramp would affect the lane-by-lane flows as vehicles would distribute themselves across the facility based on whether they intend to use the HOT lanes. Thus, lane changes around the detectors which are used in setting ramp metering rates might affect the flow at the detector, which in turn would affect the flow levels from the ramp. Conversely, the presence of a ramp metering system might affect the operations of the freeway section upstream of the HOT lanes. Congestion in that section could affect the ability of vehicles to change lanes and position themselves to use the HOT lanes or the General Purpose (GP) lanes.

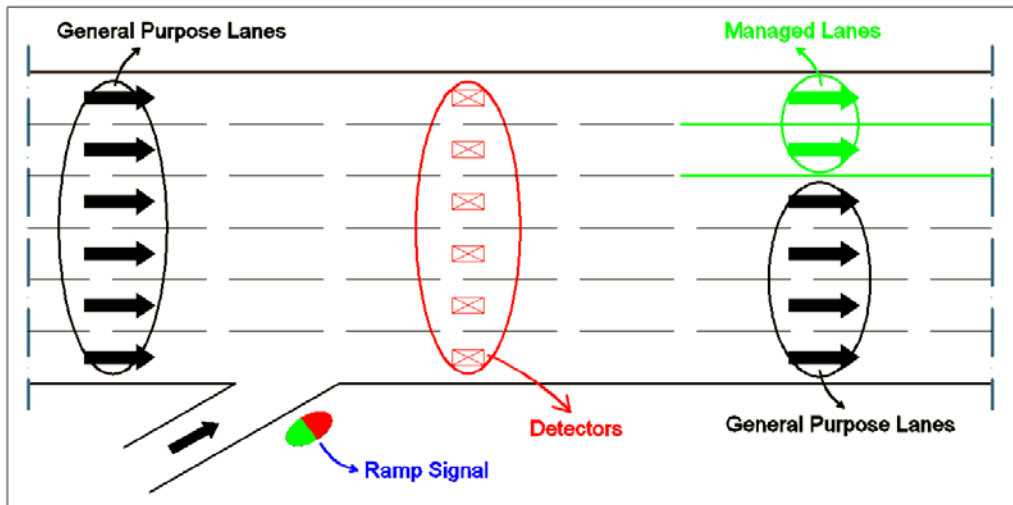


FIGURE 2.1 Ramp metering installed upstream of the HOT lanes

2.1.2 Case 2: Ramp metering installed along the HOT lanes

In this case ramp metering is installed along the HOT lanes, as shown in Figure 2.2. The I-95 HOT lanes section belongs in this category. Ramp meters installed along such a facility would use as input the flows or occupancies along the GP lanes only. However, the flows and occupancies along the GP lanes are a function of the tolling strategy. As flows in the GP lanes increase, the metering would reduce the ramp flows and would potentially result in longer queues at the ramps. Conversely, a change in the ramp metering algorithm that increases the ramp metering rates would affect the flow in the GP lanes. Increasing congestion in the GP lanes could result in higher demand for the HOT lanes.

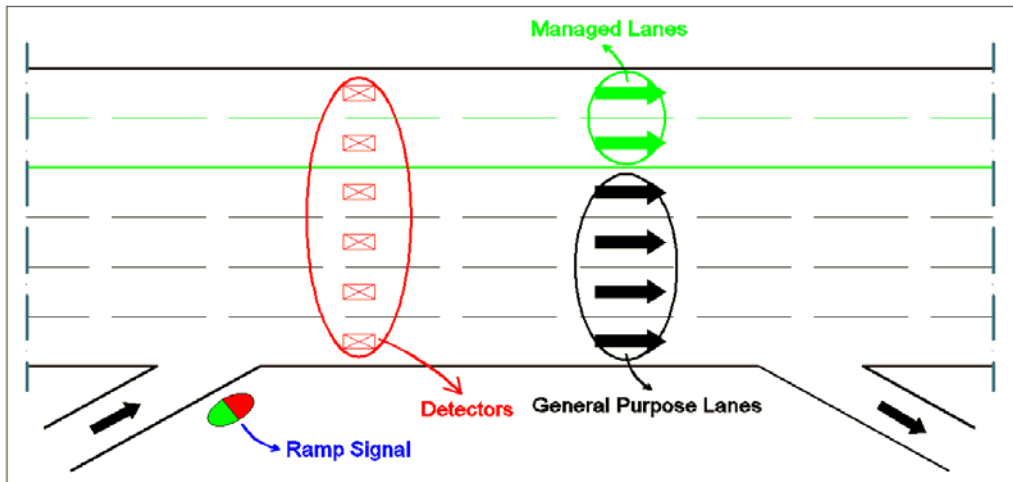


FIGURE 2.2 Ramp metering installed along the length of the HOT lanes

Figure 2.3 provides an overview of the potential interactions between system components for Case 2. The components shown in yellow indicate the ramp metering components. The metering rates are set so that capacity along the mainline is not exceeded (i.e., to avoid congestion) without causing spillback from the ramp queues to the surface network. An increase in the ramp queues (leftmost component of Figure 2.3) beyond a certain level would result in an increase of the metering rate. Such an increase would cause an increase of the GP lane flows and potential deterioration of traffic operations. If the HOT lanes toll is set considering GP lane operations, the increase in GP flows might result in higher tolls (rightmost component of Figure 2.3).

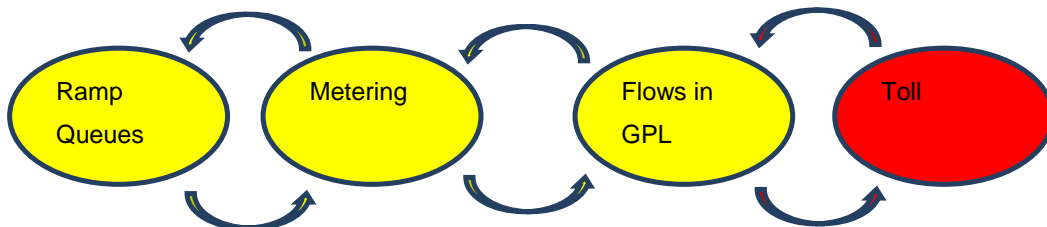


FIGURE 2.3 Potential interactions between pricing and ramp metering

Continuing in the other direction (Figure 2.3), a toll increase would likely increase GP lanes demand, which would cause a reduction in the metering rate.

2.1.3 Case 3: Ramp metering installed downstream of the HOT lanes

In Case 3, ramp metering is installed downstream of the HOT lanes as illustrated in Figure 2.4. In this case the lane changes potentially occurring downstream of the end of the HOT lanes might affect flow and eventually the ramp metering rates. Furthermore, any congestion in the vicinity of the ramp meter might spill back into the HOT lanes area.

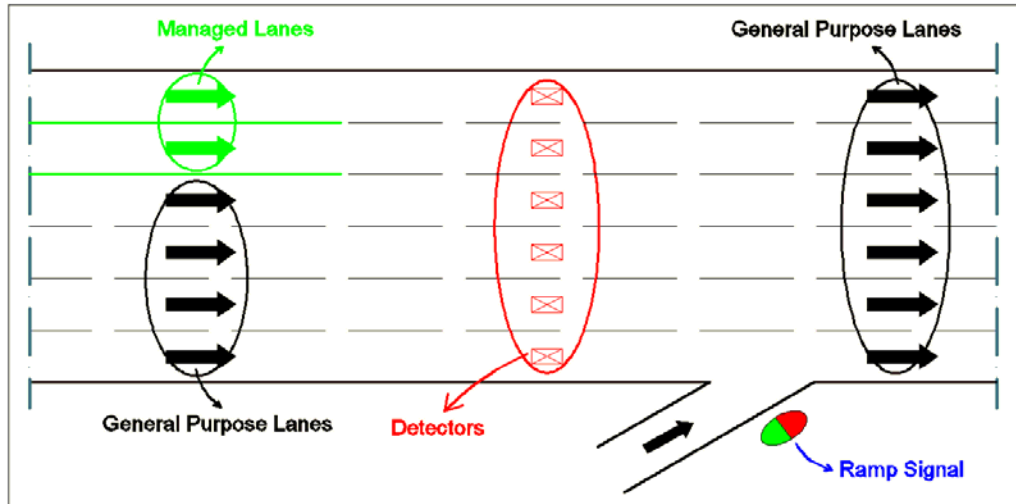


FIGURE 2.4 Ramp metering installed downstream of the HOT lanes

This section described conceptually some of the potential interactions between the two systems. For all three cases discussed here, the occurrence and magnitude of the effects would depend on various factors including the exact and relative locations of each of the implementations, as well as the specific algorithms used.

2.2 Lane-By-Lane Flow Distributions

This chapter develops and discusses the lane-by-lane flow distributions at the I-95 HOT lanes installation in Miami, FL, before and after the installation of each system (tolling and ramp metering). The primary purpose of conducting a lane-by-lane flow distribution analysis is to investigate the general impacts of the implementation of tolling and ramp metering on freeway traffic operations. Examining these distributions can help in understanding vehicle positioning under various scenarios and at various locations along the study site. The analysis evaluates the following conditions: pre-tolling, post-tolling and post-tolling plus ramp signaling. Data were

obtained from the STEWARD database at the following locations: upstream and downstream of on-ramps, and entry and exit points of the HOT lanes.

The tolling system was launched on December 5, 2008, and the ramp signaling system became active on February 4, 2009. Thus there was only a two-month period when only the tolling system was operational. This created some challenges in identifying detectors that could provide complete datasets for the post tolling/pre-metering condition. Also, during this time, the ramp metering algorithm implemented was “time-of-day” with a constant metering rate.

The distributions for the pre-tolling and for the post-tolling plus signaling were created using data from two days during the month of October in 2008 and 2009 respectively. The data were from the first Thursday and the first Tuesday of October 2008 (i.e., Thursday 1st and Tuesday 6th) and October 2009 (i.e., Thursday 2nd and Tuesday 7th). Diagrams were created for each day using data from twelve locations, where RTMS detectors are placed. The analysis time period is between 6:00 am and 22:00 pm. The locations data were collected, along with the detectors’ identification numbers are presented in Table 2.1. The lane configuration at each location is shown in Figure 2.5.

For the post-tolling/pre-signaling condition, data were obtained for the following three days: Tuesday, December 9, 2008; Tuesday, December 13, 2008; and Wednesday, January 21, 2009. Diagrams were created for each day using data from four locations. Those four locations were the only ones among those listed in Table 2.1 which had data available for that two-month time period. The data analysis period was 6:00 am to 10:00 pm. The locations along with the detectors’ identification numbers are presented in Table 2.2. The lane configurations at each location are identical to those shown in Figure 2.5.

TABLE 2.1 Data collection locations for pre-tolling and post tolling plus ramp signaling

	Detector Identification Number	Description
1	600641/690641	I-95 SOUTH OF NW 103 ST
2	600701/690701	I-95 NORTH OF NW 103 ST
3	600711/690711	I-95 SOUTH OF NW 111 ST
4	600731/690731	I-95 SOUTH OF NW 119 ST
5	600781/690781	I-95 NORTH OF NW 119 ST
6	600791/690791	I-95 SOUTH OF NW 131 ST (Before Merging)
7	600801/690801	I-95 SOUTH OF NW 131 ST (After Merging)
8	600831/690831	I-95 SOUTH OF NW 135 ST
9	600841/690841	I-95 NORTH OF OPA-LOCKA BLVD (Before
10	600851/690851	I-95 NORTH OF OPA-LOCKA BLVD (After
11	600891/690891	I-95 SOUTH OF NW 151 ST
12	600921/690921	I-95 NORTH OF NW 151 ST

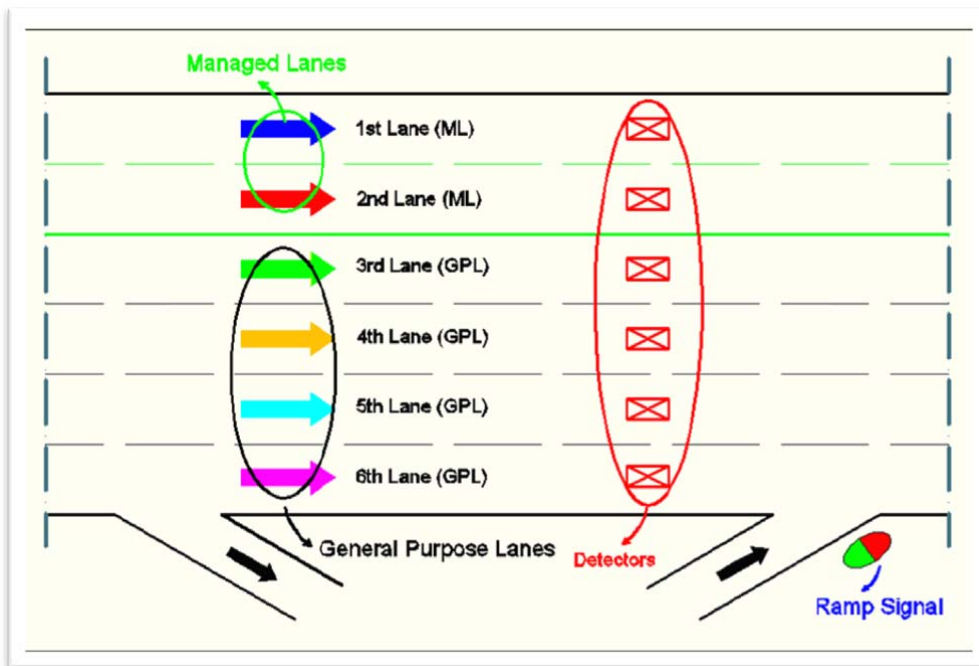


FIGURE 2.5 Lane configuration at each of the twelve detector locations

TABLE 2.2 Locations and detector identification – Tolling/pre-signaling only

	Identification Number	Description
1	670701/660701	I-95 NORTH OF NW 103 ST
2	670791/660791	I-95 SOUTH OF NW 131 ST (Before Merging)
3	670841/660841	I-95 NORTH OF OPA-LOCKA BLVD (Before Merging)
4	600921/690921	I-95 NORTH OF NW 151 ST

The lane-by-lane flow distributions for locations 2 and 4 of Table 2.2 are presented here for each of the three conditions (pre-tolling, post-tolling/pre-signaling, post-tolling plus signaling). For the pre-tolling period there are no available data for location I-95 south of NW 131. Thus, location I-95 south of NW 119 is used instead, as this is fairly close and it is a geometrically similar location. Also, at I-95 north of NW 151 St. there is only one HOT lane. Figures 2.6, 2.7, and 2.8 present the lane-by-lane distributions for location 2, while Figures 2.9, 2.10, and 2.11 present the same information for location 4.

As shown, in the pre-tolling period volumes on the left-most lanes are more equally balanced. The highest flows are observed in the 4th and 5th lane for both time periods. The high volumes on the right-most general purpose lane (Lane 6) at south of NW 151 St. are due to the existence of an exit ramp just downstream of the detector.

The data also show that there is no major shift of traffic to or from the GP lanes to the managed ones after the establishment of the tolls. There is only a slight increase in the GP lanes volumes. Also, there does not appear to be a significant change in the lane-by-lane distributions due to the ramp metering.

Generally, the analysis demonstrated that both the pricing and tolling algorithms did not cause any major changes in the lane distributions along the I-95 HOT lanes freeway section. It should be noted that the data were obtained during the early days of the systems installation and thus there may be additional changes that will be observed as the systems mature. The tolling algorithm does not consider operations

on the GP lanes, and thus the relationship between the two volumes may not be as strong. Also, the ramp metering algorithm currently operating is based on fuzzy logic. Thus the metering operation has become dynamic and more robust, allowing for a more efficient and effective management of traffic in the merging areas. Under this metering scheme shockwaves on the outer lane are less likely to occur. This change may result in further changes in traffic distributions across the lanes.

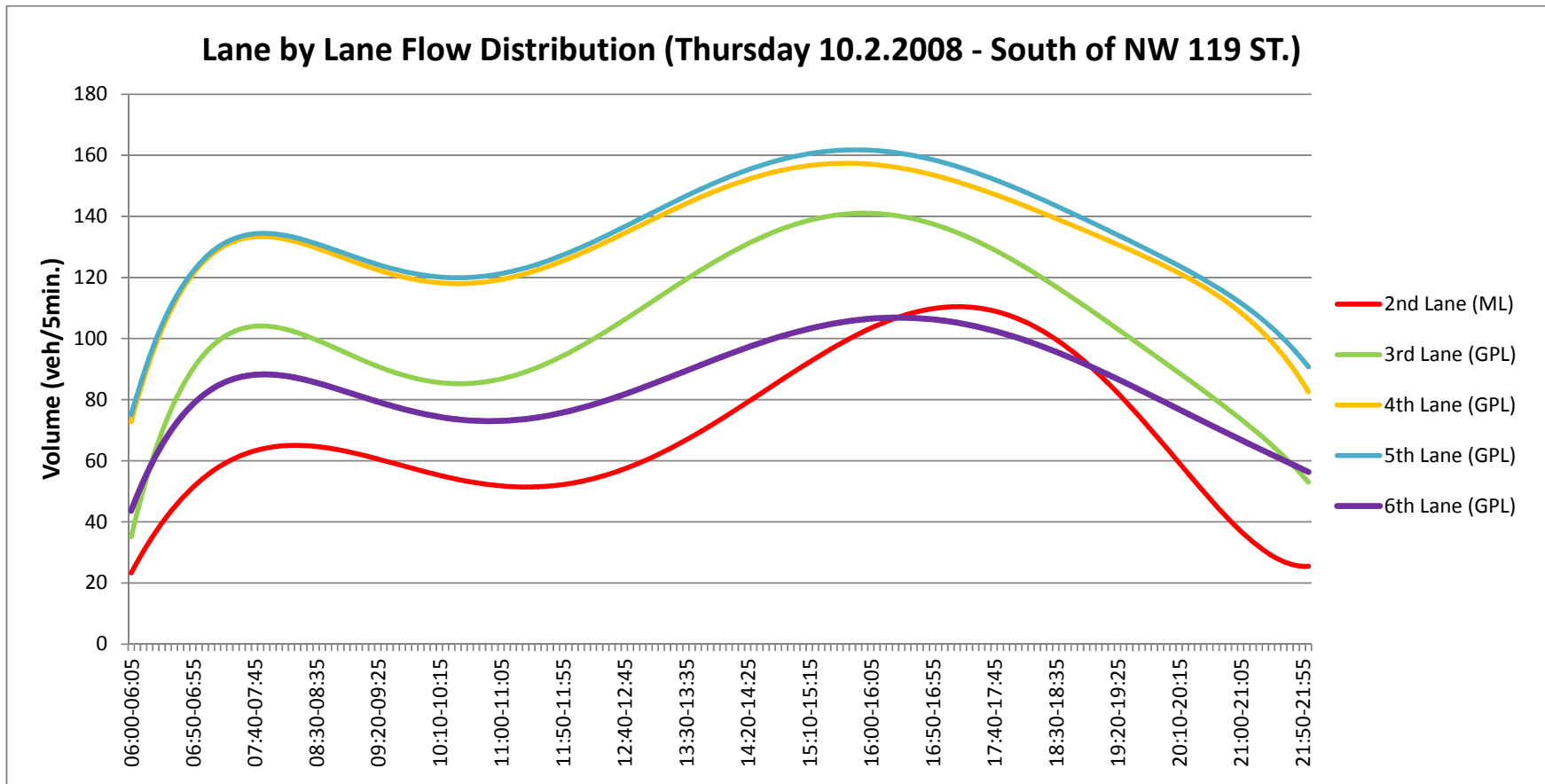


FIGURE 2.6 Lane-by-lane flow distributions south of NW 119 St. - Pre-tolling

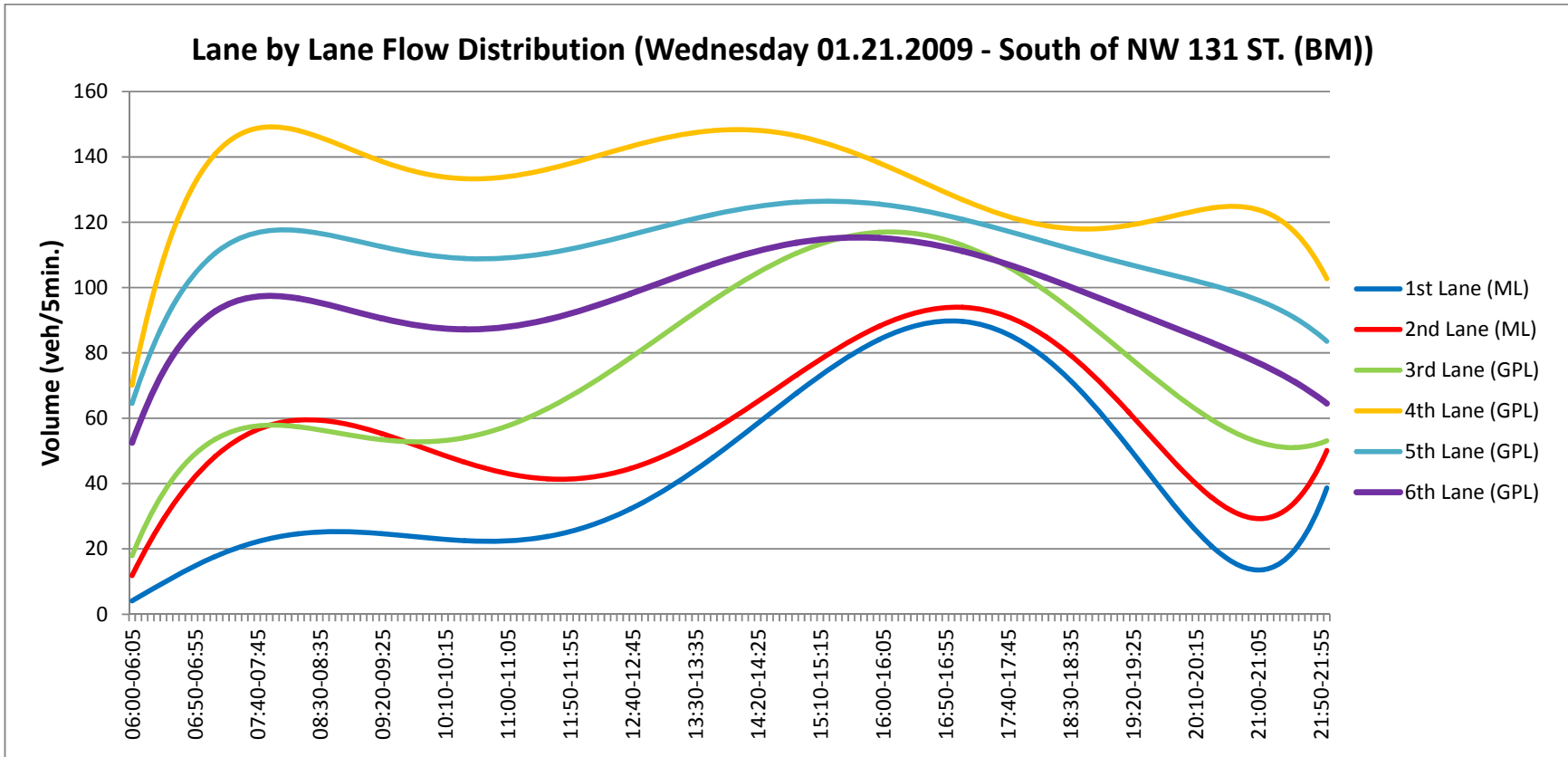


FIGURE 2.7 Lane-by-lane flow distributions south of NW 131 St. - Post-tolling/pre-signaling

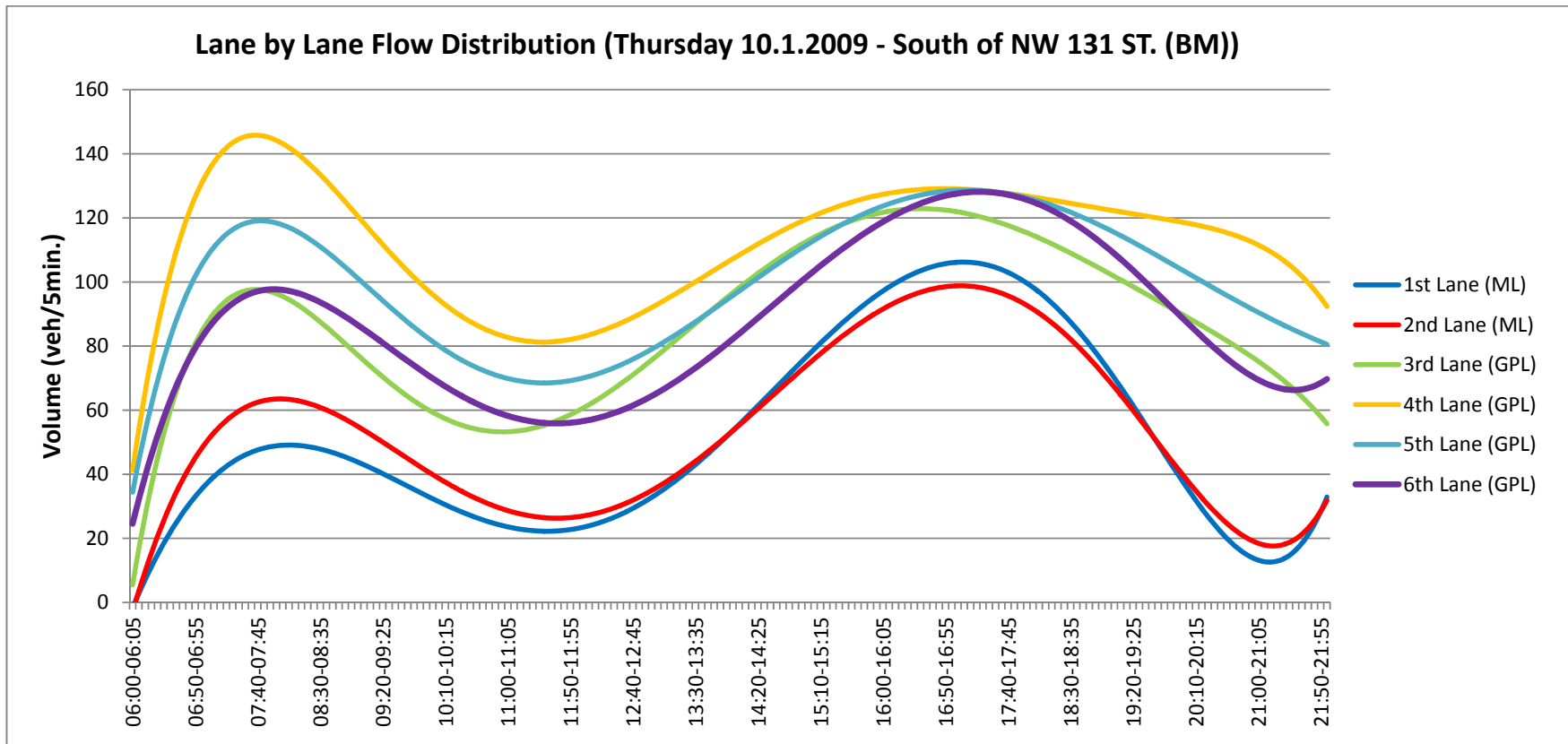


FIGURE 2.8 Lane-by-lane flow distributions south of NW 131 St. - Post-tolling plus signaling

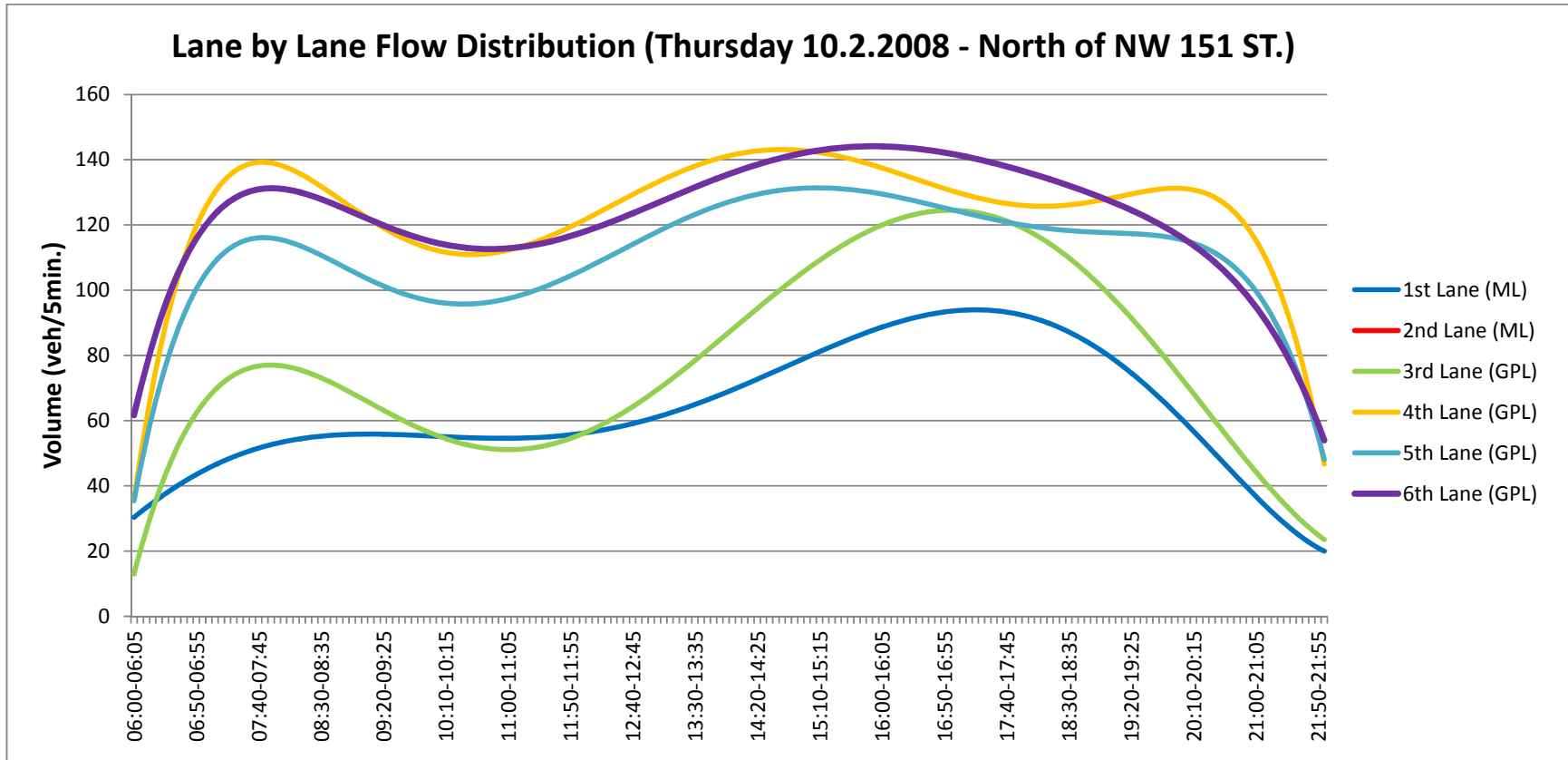


FIGURE 2.9 Lane-by-lane flow distributions north of NW 151 St. - Pre-tolling

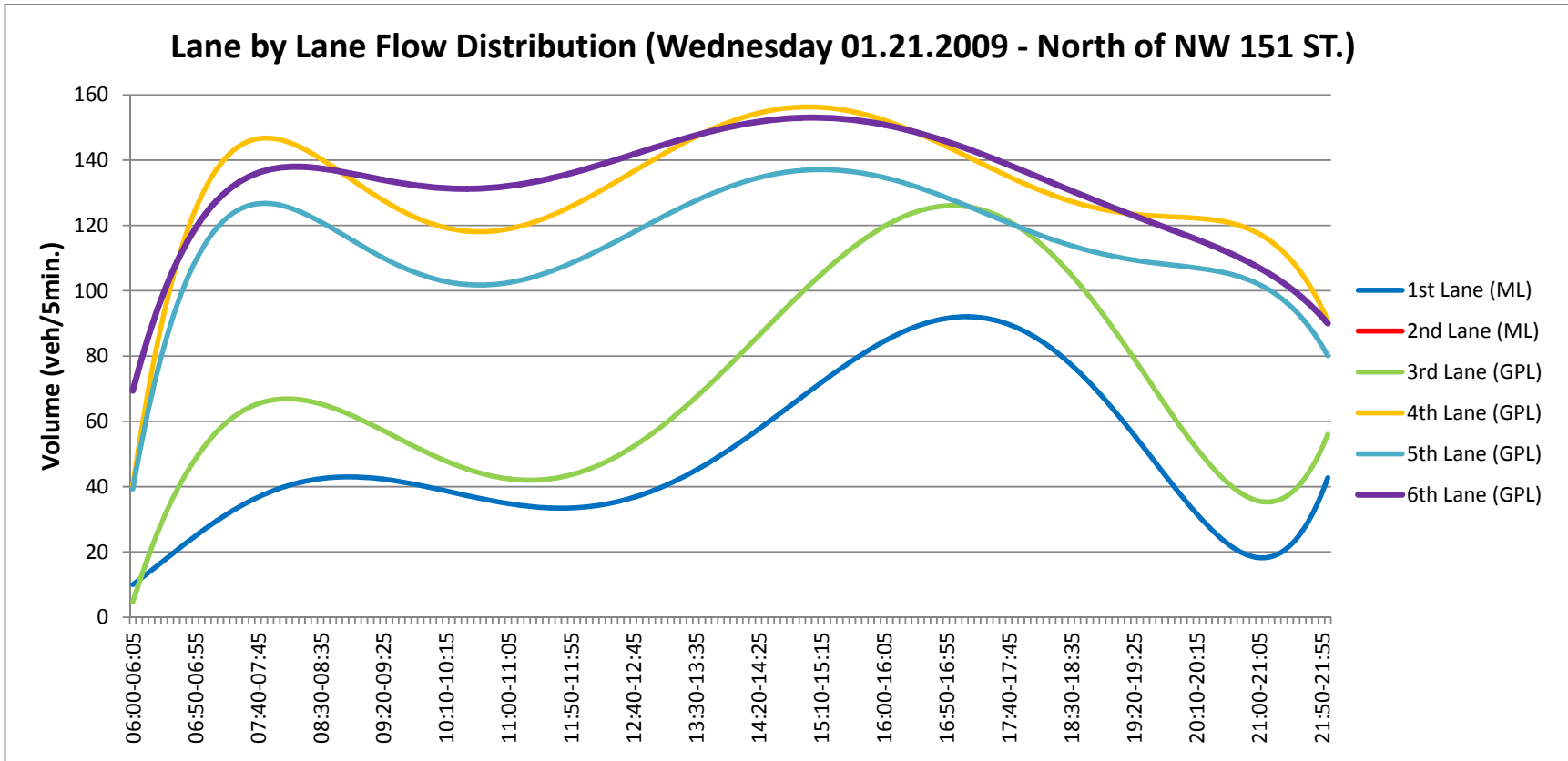


FIGURE 2.10 Lane-by-lane flow distributions north of NW 151 St. - Post-tolling

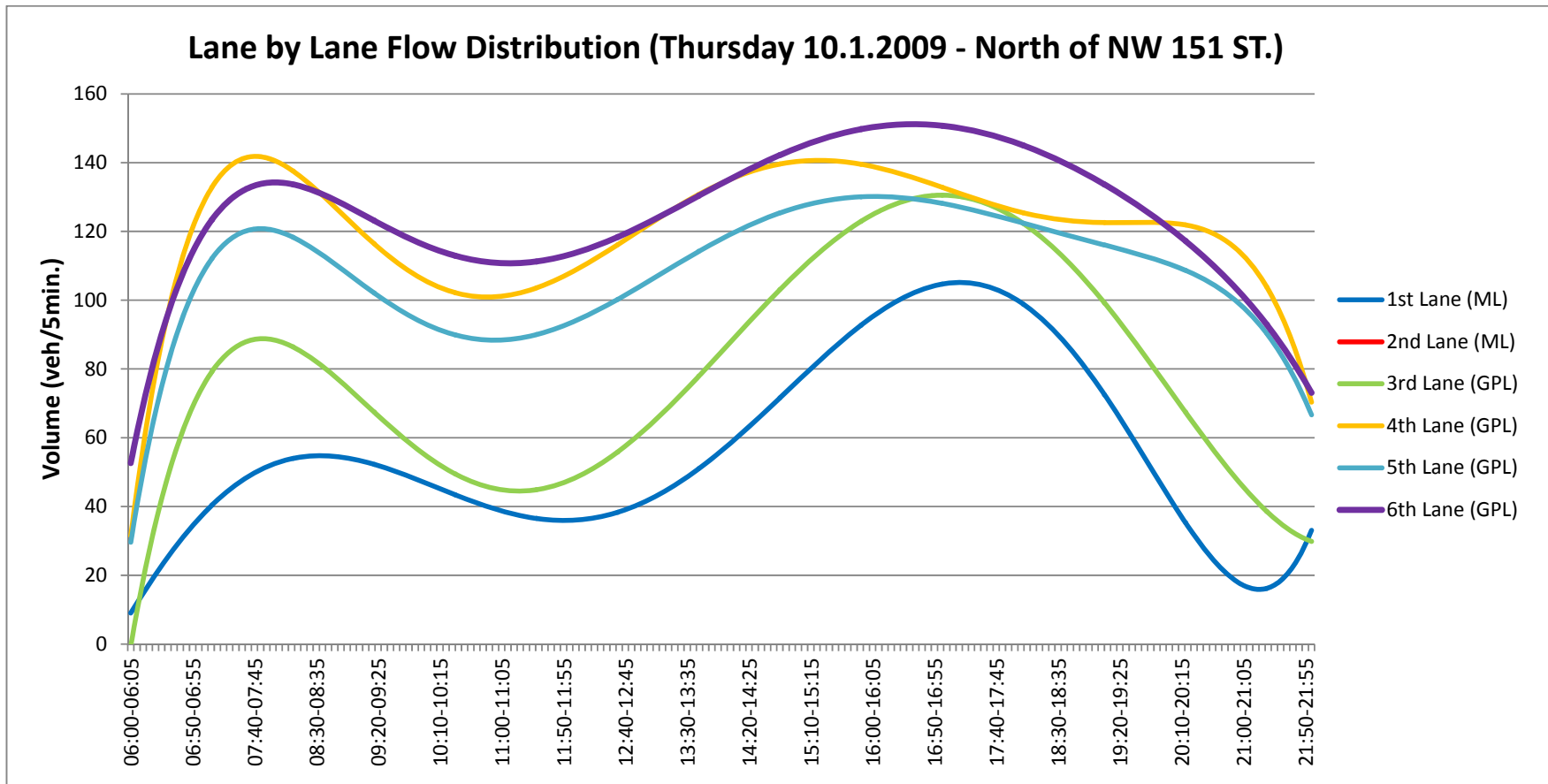


FIGURE 2.11 Lane-by-lane flow distributions north of NW 151 St. - Post-tolling plus signaling

2.3 The Simulation Network for I-95 in Miami

This section describes the simulation effort conducted to evaluate the relationships between tolling and metering operations under various scenarios. Simulation was used to accomplish this since it allows us to experiment with various algorithms and conditions and easily measure their impacts on the freeway network.

The I-95 HOT lanes network in Miami, FL, was used for this analysis. This network had already been simulated in CORSIM by the FDOT during the process of the HOT lanes design. However, the objectives of this project required the reconfiguration and calibration of the initial CORSIM files provided by FDOT to consider the actual post-implementation conditions. The following sections describe the configuration of the network and the calibration process to ensure that the simulator accurately reflects field conditions before experiments are conducted.

2.3.1 Configuration of the Network

Several changes were made to the initial CORSIM files to ensure that the network accurately replicated the existing post-tolling conditions, and to focus on the interactions between ramp metering and tolling operations. The changes implemented are related to the geometry and the extent of the study area, the volumes entering the network, the implementation of the ramp metering algorithm, and the simulated detector locations used in calibrating the model. The remainder of this section describes these four types of changes.

2.3.1.1 Network Geometry and Study Area

The initial CORSIM file provided by FDOT was replicating the traffic conditions on both directions of I-95 in Miami. The file included the interchanges of the Expressway with I-395, I-195 and all the local arterials connecting the urban streets with the freeway network through ramps. Part of the Turnpike was also included in the network. Thus this original file was very extensive and required extensive computational resources (each run needed approximately 45 minutes to be completed). Since the objective of this research did not require the simulation of all these roadway sections the network was modified to replicate the operation of northbound I-95 in Miami together with all the ramps merging and diverging from the

freeway. These segments were sufficient for evaluating the interactions between the ramp signaling and the tolling system. In the southbound direction the two strategies (i.e., ramp signaling and tolling) had not been implemented until recently and thus only a limited amount of data is available for that section. Therefore the analysis in this task focuses on the northbound direction. Operations on I-395, I-195, the Turnpike and local arterials were not important for the purposes of this project, and only their connections with I-95 were kept and modified appropriately. This modification of the network allowed focusing the team's resources on the freeway operations. As an example, Figure 2.12 illustrates the geometry of the NW 62nd Street interchange before the changes, and Figure 2.13 illustrates the same interchange after the changes were implemented.

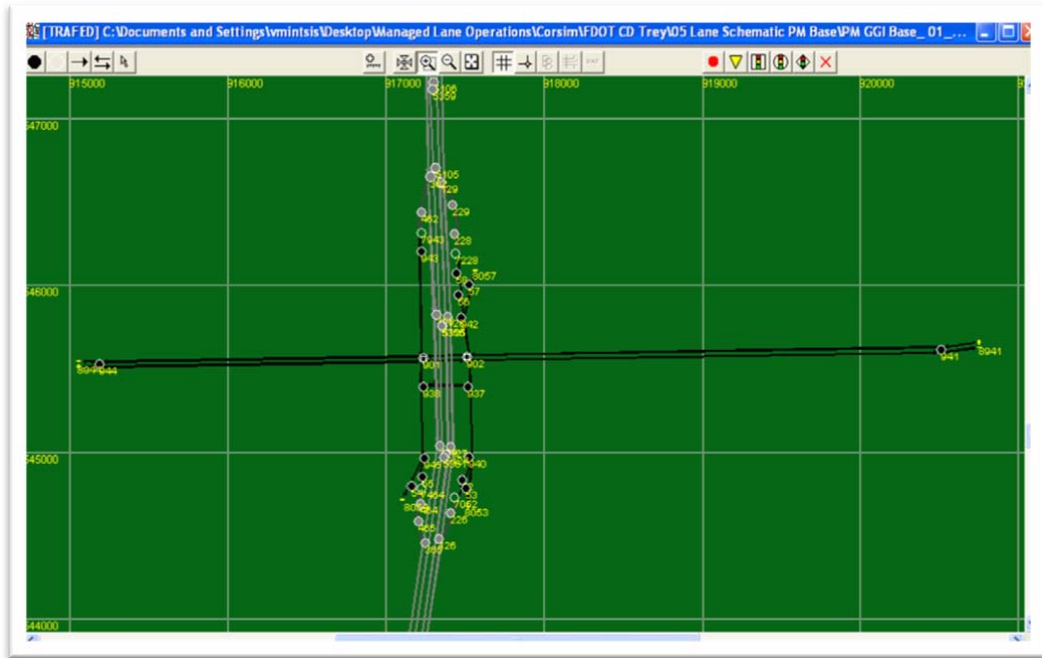


FIGURE 2.12 The I-95 Expressway at NW 62nd Street before the modifications

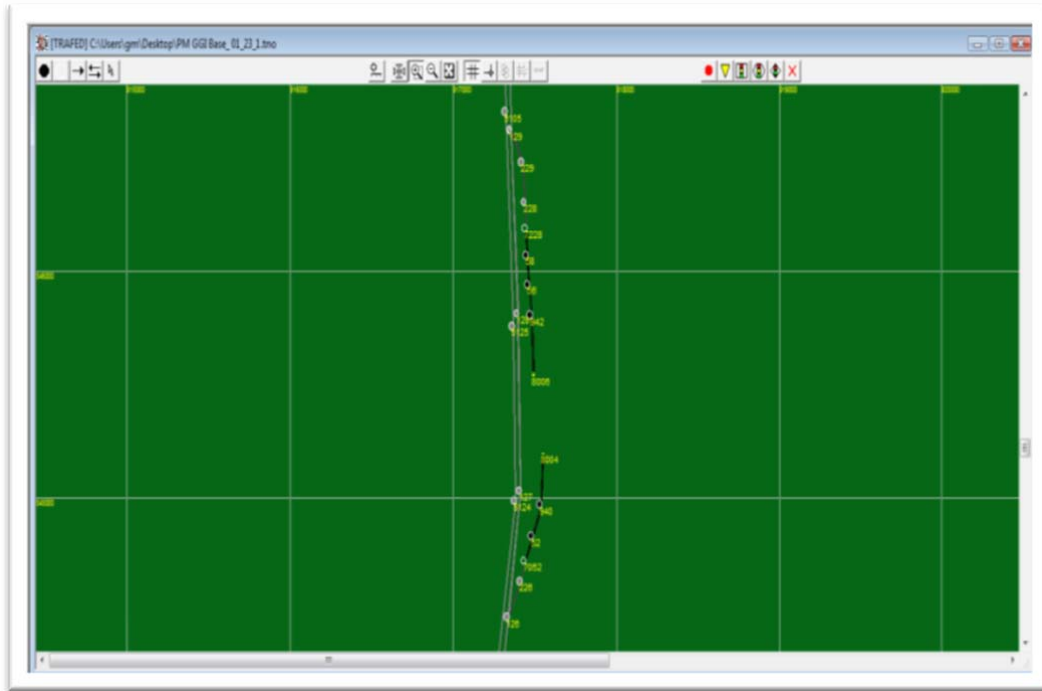


FIGURE 2.13 The I-95 Expressway at NW 62nd Street after the modifications

2.3.1.2 Incoming Volumes

Field data from the STEWARD database were used to obtain incoming volumes for “loading” of the network. Volume data from the 7th of October 2009 were extracted from the database and were input into CORSIM. Data from that particular day had been previously selected for the lane-by-lane flow distribution analysis and were considered appropriate for loading the network for two reasons. First, during that time period the ramp signaling and the tolling system had been operating under the strategies that will constitute our base case scenario: the ramp metering system was operating on a pre-timed schedule, and the tolls were set as a function of the density on the HOT lanes. Second, the quality and amount of data from that day are sufficient compared to those of nearby dates.

Data from the time period between 15:30-18:30 pm of the selected day were used. That time represents the peak period on the northbound direction. Volumes were obtained in 15-minute intervals, and the simulation contains a total of 12 analysis periods. The volumes input at the entry nodes were mainly derived from data provided from the inductive loop-detectors at the on-ramps. For on-ramps where loop

detector data were not available, data from two detectors (one upstream of the merge point and one downstream) were utilized and the entry volume was estimated as the difference between the two counts. At diverge points, the amount of traffic exiting from the mainline was calculated either by using the upstream and downstream detectors as mentioned above, or by keeping the same percentage of exiting traffic as specified in the CORSIM files provided by FDOT. The split of traffic between HOT and general purpose lanes was derived from station ID #: 600471/690471, which is located north of NW 62nd St. just upstream of the diverge point.

Appendix A provides the relevant data regarding the loading of the network (mainline traffic volumes, entering traffic and exiting traffic at entry and diverge nodes respectively).

2.3.1.3 Implementation of the Ramp Metering Algorithm

In the original CORSIM file, traffic entering from the on-ramps onto the I-95 in Miami was not regulated by any control strategy. Thus, it was necessary to replicate the ramp metering algorithm in effect at the time the data were collected (October, 2009). That algorithm, which is a pre-timed, fixed rate algorithm, can easily be replicated in CORSIM. Therefore, the metering rates, as were provided by the SunGuide Transportation Management Center and the control strategy were coded within CORSIM as shown in Table 2.3.

TABLE 2.3 Location and metering rate of each ramp signal along I-95

	Location	Metering Rate (veh/min)
1	I-95 NORTH OF NW 62 ST	20
2	I-95 AT NW 69 ST	20
3	I-95 NORTH OF NW 81 ST	20
4	I-95 AT NW 96 ST	20
5	I-95 NORTH OF NW 103 ST	20
6	I-95 SOUTH OF NW 131 ST	20
7	I-95 NORTH OF OPA-LOCKA BLVD	24
8	I-95 SOUTH OF US 441	24

2.3.1.4 Detector Placement Throughout the Network

Calibration involves the comparison of traffic operations in the field to the simulated network and adjustment of the simulation as necessary. To complete the process of calibration it is necessary to install simulated detectors in the field, and collect various performance measures related to traffic operations. The detectors that are supplying the STEWARD database with data are providing measurements of volume, speed and occupancy at particular locations along the network. Thus, for calibration and validation purposes eleven detectors were installed throughout the CORSIM network at locations that correspond to those of the actual detectors in the field. The first eight detectors were set up along the General Purpose Lanes, while the last three along the HOT Lanes. The actual and simulated locations of those detectors are provided in Figure 2.14 and Table 2.4.

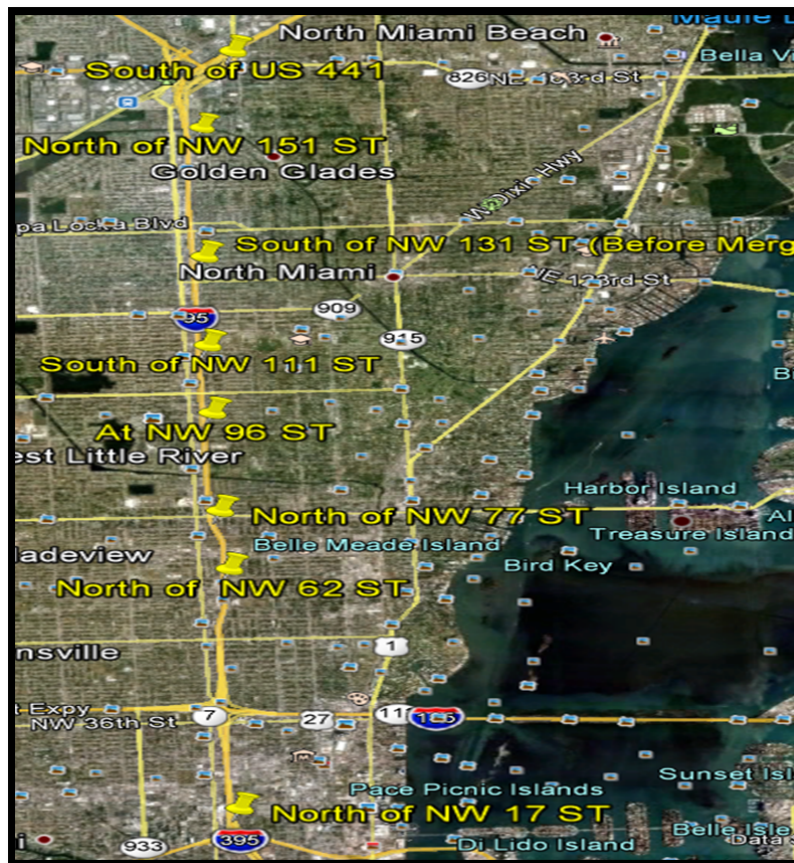


FIGURE 2.14 Location of detectors used for calibration on I-95 in Miami.

TABLE 2.4 Location of field and simulated detectors

	Location	Actual Station ID#	CORSIM Station ID#
1	I-95 NORTH OF NW 17 ST	600291	1
2	I-95 NORTH OF NW 62 ST	600471	2
3	I-95 NORTH OF NW 77 ST	600521	3
4	I-95 AT NW 96 ST	600621	4
5	I-95 SOUTH OF NW 111	600711	5
6	I-95 SOUTH OF NW 131	600791	6
7	I-95 SOUTH OF NW 151	600921	7
8	I-95 SOUTH OF US 441	600981	8
9	I-95 NORTH OF NW 62 ST	690471	9
10	I-95 AT NW 96 ST	690621	10
11	I-95 SOUTH OF NW 131	690791	11

2.3.2 Calibration process

Calibration is the process of model adjustment to ensure that the network performs accurately and that the assumptions made in developing the model are reasonable. Calibration involves a comparison of selected performance measures between the simulated corridor and the field data. For the purposes of this project, network volumes and speeds were monitored throughout the simulated network to identify potential significant differences at specific locations.

Since CORSIM is a stochastic simulator, it uses random number generators to replicate traffic conditions, and each run should be viewed as one sample of the experiment. Several runs of the simulator are needed to obtain an estimate of the “average” conditions in the network. Thus, after the completion of the modifications outlined in the previous section, the required number of runs was determined. Initially, the model was executed 10 times, and the average network speed was obtained (Table 2.5). Based on these, and assuming an allowable error of $e=0.05$ mph and 95% confidence level, the required number of runs was estimated to be 7. Thus, in subsequent analysis 10 runs will be conducted, which are more than adequate for the project purposes.

TABLE 2.5 Average network speed for each simulation run.

Run #	1	2	3	4	5	6	7	8	9	10
Average Network Speed (mph)	49.13	49.20	49.09	49.12	49.25	49.26	49.13	49.11	49.13	49.04

The reconciliation of field and simulated traffic counts was achieved after an extensive experimentation process with the available calibration parameters in CORSIM. The adjustments to the values of these parameters were finalized through trial-and-error after several iterations. The calibration parameter with the most profound effect on the simulated traffic operations was found to be the car-following sensitivity factor. This factor determines the desired time headway during car-following. Therefore, this factor was the one that was mostly modified in order to calibrate the network. Appendix A includes the value of that factor per network link, together with the free-flow speed at each link. Parameters affecting the lane changing activity, the start-up delay of vehicles in front of meters, and the arrival rate of traffic into the network were also adjusted.

Tables 2.6 to 2.17 and Figures 2.15 to 2.38 compare the field counts to those obtained in the simulation after the completion of the calibration. The first eight locations in the graphs correspond to detectors in the general purpose lanes, while the last three to detectors in the high occupancy toll lanes. As can be seen in the figures, generally there is a good match in the trends of the volumes and speeds from one location to the next, and from one time period to the next. One exception is the volumes and speeds of locations 6 and 7, between 16:45 and 17:45 (Figures 2.15 to 2.38). At that location both the simulated volumes and speeds are higher than those in the field. This discrepancy should be ascribed to the simulator's intrinsic limitations to replicate reality. For example, in CORSIM drivers do not adjust their speed to reduce speed differential between lanes. Drivers in the field are more prone to consider their broader environment and be affected by it.

Simulated speeds deviate from field measurements more than volumes, but they are still very close to field conditions at most instances. Location 4 breaks down earlier in the simulation than in the field, causing the queue to dissipate earlier as well.

Generally, in the simulation the beginning and build-up of congestion follows a similar pattern to that observed in the field. The calibration was based on both traffic speeds and volumes over multiple time periods and for 11 different locations. Simulated mean speeds deviate about 7.00 mph from the field observations, while traffic volumes deviate around 100 vehicles from the corresponding field data. Therefore, it was concluded that the simulated network is replicating actual traffic conditions sufficiently.

TABLE 2.6 Field and simulated speeds and volumes – 1st time period

1 st Time period (15:30 - 15:45)						
Freeway Link	Detector ID#	Location	Field Speeds	Sim. Speeds	Field Vol.	Sim. Vol.
[112, 113]	600291	I-95 NORTH OF NW 17 ST	42.27	53.16	796	783
[129, 130]	600471	I-95 NORTH OF NW 62 ST	30.55	22.67	1607	1622
[132, 133]	600521	I-95 NORTH OF NW 77 ST	31.35	39.30	1539	1660
[139, 140]	600621	I-95 AT NW 96 ST	40.32	37.32	1570	1588
[145, 146]	600711	I-95 SOUTH OF NW 111 ST	35.07	41.76	1675	1711
[153, 154]	600791	I-95 SOUTH OF NW 131 ST	51.96	46.66	1529	1607
[159, 161]	600921	I-95 SOUTH OF NW 151 ST	54.70	43.72	2218	2114
[170, 171]	600981	I-95 SOUTH OF US 441	54.70	57.92	861	839
[5125, 5105]	690471	I-95 NORTH OF NW 62 ST	63.42	66.88	514	609
[5138, 5139]	690621	I-95 AT NW 96 ST	66.94	65.98	491	611
[5153, 5154]	690791	I-95 SOUTH OF NW 131 ST	62.55	65.32	586	606

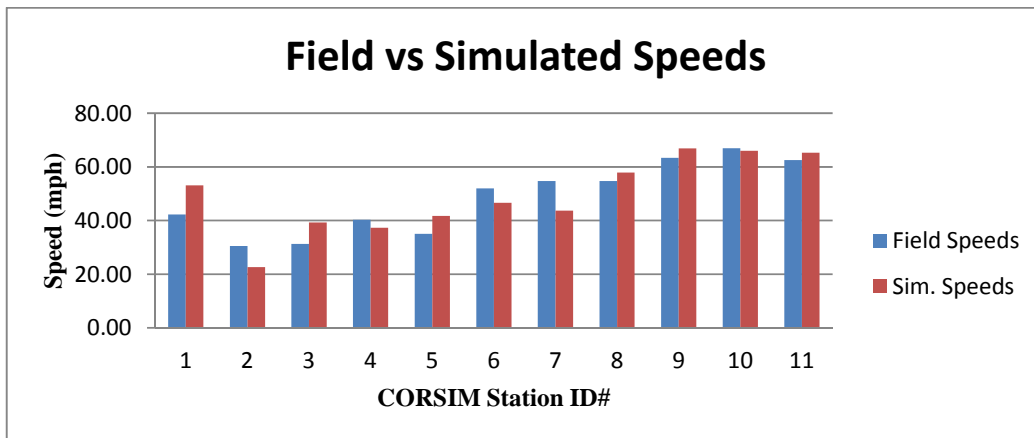


FIGURE 2.15 Field and simulated speeds – 1st time period

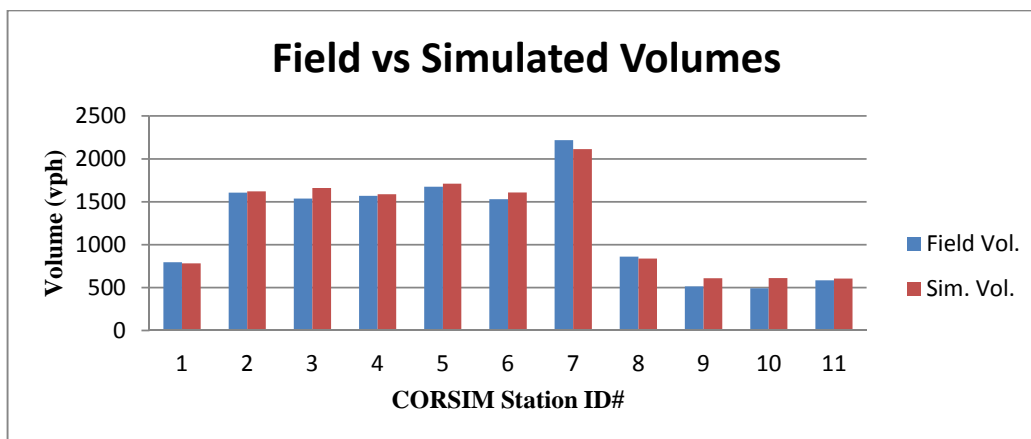


FIGURE 2.16 Field and simulated volumes – 1st time period

TABLE 2.7 Field and simulated speeds and volumes – 2nd time period

2 nd Time period (15:45 - 16:00)						
Freeway Link	Detector ID#	Location	Field Speeds	Sim. Speeds	Field Vol.	Sim. Vol.
[112, 113]	600291	I-95 NORTH OF NW 17 ST	48.04	52.82	851	862
[129, 130]	600471	I-95 NORTH OF NW 62 ST	32.10	31.50	1642	1749
[132, 133]	600521	I-95 NORTH OF NW 77 ST	33.81	40.69	1465	1630
[139, 140]	600621	I-95 AT NW 96 ST	42.54	24.47	1602	1552
[145, 146]	600711	I-95 SOUTH OF NW 111 ST	37.83	41.73	1741	1712
[153, 154]	600791	I-95 SOUTH OF NW 131 ST	46.37	46.78	1474	1576
[159, 161]	600921	I-95 SOUTH OF NW 151 ST	54.98	43.74	2107	2042
[170, 171]	600981	I-95 SOUTH OF US 441	55.41	58.09	832	804
[5125, 5105]	690471	I-95 NORTH OF NW 62 ST	61.28	67.27	531	544
[5138, 5139]	690621	I-95 AT NW 96 ST	65.36	66.31	440	554
[5153, 5154]	690791	I-95 SOUTH OF NW 131 ST	59.53	65.90	549	564

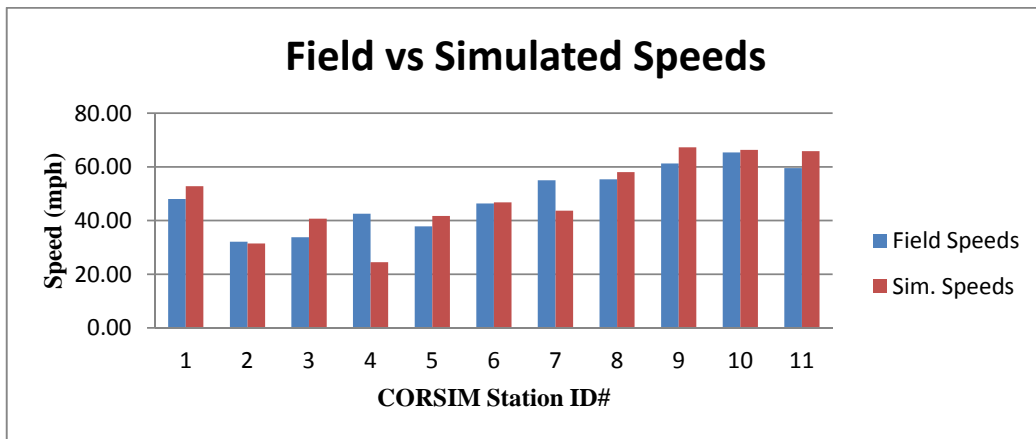


FIGURE 2.17 Field and simulated speeds – 2nd time period

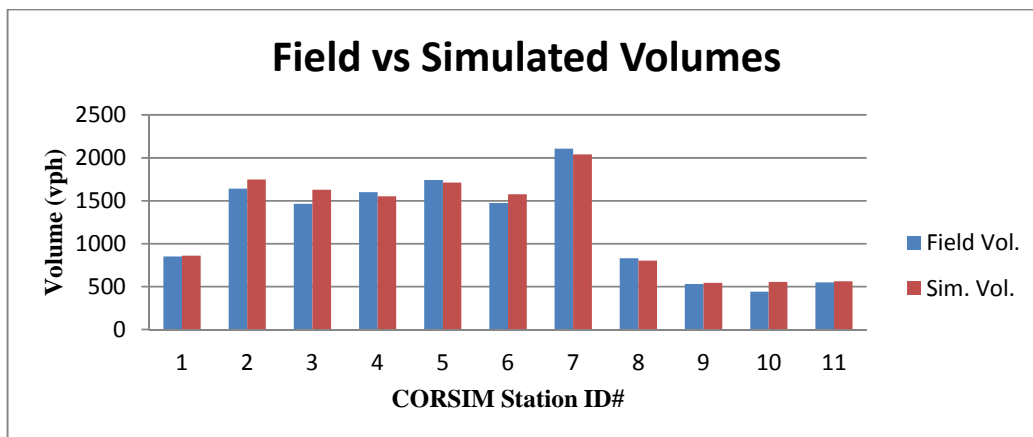


FIGURE 2.18 Field and simulated volumes – 2nd time period

TABLE 2.8 Field and simulated speeds and volumes – 3rd time period

3 rd Time period (16:00 - 16:15)						
Freeway Link	Detector ID#	Location	Field Speeds	Sim. Speeds	Field Vol.	Sim. Vol.
[112, 113]	600291	I-95 NORTH OF NW 17 ST	36.12	52.40	862	932
[129, 130]	600471	I-95 NORTH OF NW 62 ST	43.75	50.02	1634	1656
[132, 133]	600521	I-95 NORTH OF NW 77 ST	35.15	45.89	1521	1567
[139, 140]	600621	I-95 AT NW 96 ST	44.13	23.36	1651	1545
[145, 146]	600711	I-95 SOUTH OF NW 111 ST	38.38	41.76	1790	1721
[153, 154]	600791	I-95 SOUTH OF NW 131 ST	49.94	46.93	1588	1565
[159, 161]	600921	I-95 SOUTH OF NW 151 ST	44.75	40.76	2292	1993
[170, 171]	600981	I-95 SOUTH OF US 441	55.64	58.30	890	740
[5125, 5105]	690471	I-95 NORTH OF NW 62 ST	63.05	66.41	616	681
[5138, 5139]	690621	I-95 AT NW 96 ST	68.47	65.58	516	661
[5153, 5154]	690791	I-95 SOUTH OF NW 131 ST	62.52	65.21	610	638

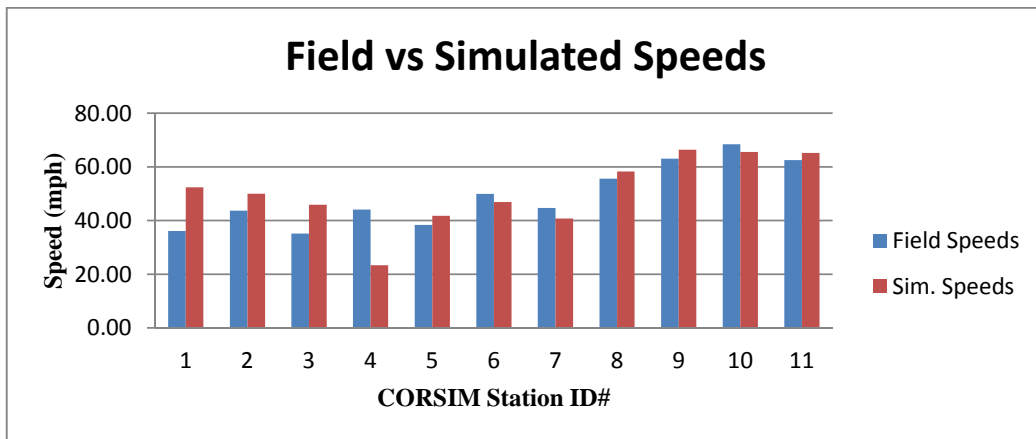


FIGURE 2.19 Field and simulated speeds – 3rd time period

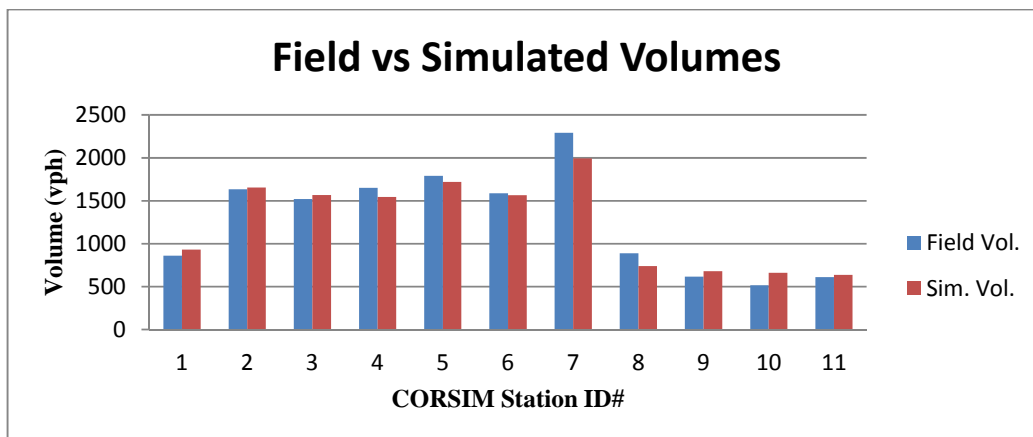


FIGURE 2.20 Field and simulated volumes – 3rd time period

TABLE 2.9 Field and simulated speeds and volumes – 4th time period

4 th Time period (16:15 - 16:30)						
Freeway Link	Detector ID#	Location	Field Speeds	Sim. Speeds	Field Vol.	Sim. Vol.
[112, 113]	600291	I-95 NORTH OF NW 17 ST	57.84	53.16	813	799
[129, 130]	600471	I-95 NORTH OF NW 62 ST	53.83	50.95	1616	1570
[132, 133]	600521	I-95 NORTH OF NW 77 ST	36.35	45.59	1568	1585
[139, 140]	600621	I-95 AT NW 96 ST	42.70	21.87	1601	1569
[145, 146]	600711	I-95 SOUTH OF NW 111 ST	36.45	41.58	1742	1709
[153, 154]	600791	I-95 SOUTH OF NW 131 ST	49.92	46.96	1446	1553
[159, 161]	600921	I-95 SOUTH OF NW 151 ST	31.01	27.03	1912	1972
[170, 171]	600981	I-95 SOUTH OF US 441	55.93	58.44	766	725
[5125, 5105]	690471	I-95 NORTH OF NW 62 ST	63.07	66.75	619	636
[5138, 5139]	690621	I-95 AT NW 96 ST	68.45	65.91	481	637
[5153, 5154]	690791	I-95 SOUTH OF NW 131 ST	63.07	65.51	573	650

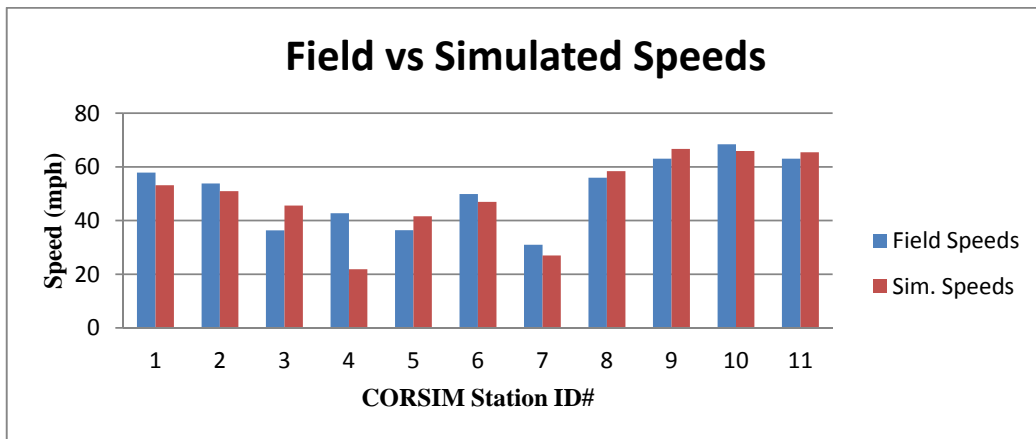


FIGURE 2.21 Field and simulated speeds – 4th time period

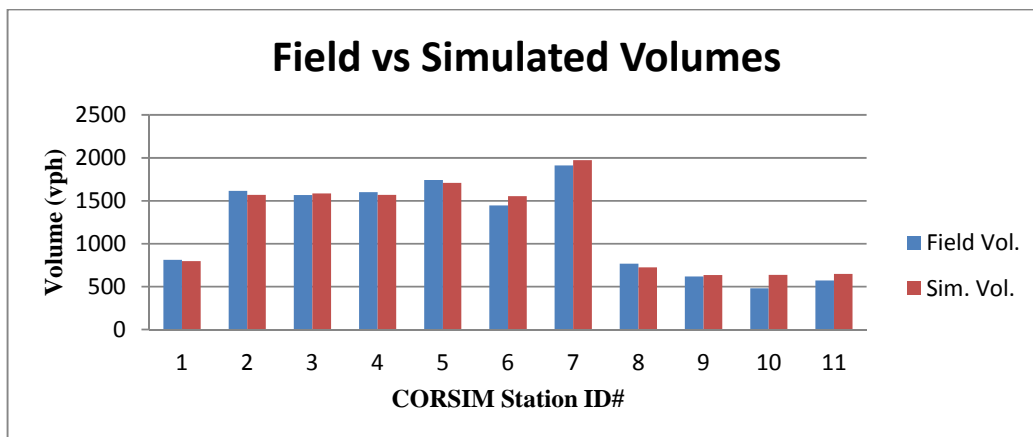


FIGURE 2.22 Field and simulated volumes – 4th time period

TABLE 2.10 Field and simulated speeds and volumes – 5th time period

5 th Time period (16:30 - 16:45)						
Freeway Link	Detector ID#	Location	Field Speeds	Sim. Speeds	Field Vol.	Sim. Vol.
[112, 113]	600291	I-95 NORTH OF NW 17 ST	58.83	53.11	807	799
[129, 130]	600471	I-95 NORTH OF NW 62 ST	56.61	51.57	1560	1509
[132, 133]	600521	I-95 NORTH OF NW 77 ST	56.80	52.58	1505	1456
[139, 140]	600621	I-95 AT NW 96 ST	41.86	24.72	1616	1586
[145, 146]	600711	I-95 SOUTH OF NW 111 ST	36.60	41.56	1725	1720
[153, 154]	600791	I-95 SOUTH OF NW 131 ST	36.33	46.82	1346	1582
[159, 161]	600921	I-95 SOUTH OF NW 151 ST	28.75	30.70	1928	1935
[170, 171]	600981	I-95 SOUTH OF US 441	55.31	58.43	776	733
[5125, 5105]	690471	I-95 NORTH OF NW 62 ST	62.57	67.24	620	585
[5138, 5139]	690621	I-95 AT NW 96 ST	68.08	66.27	518	602
[5153, 5154]	690791	I-95 SOUTH OF NW 131 ST	62.64	65.81	549	608

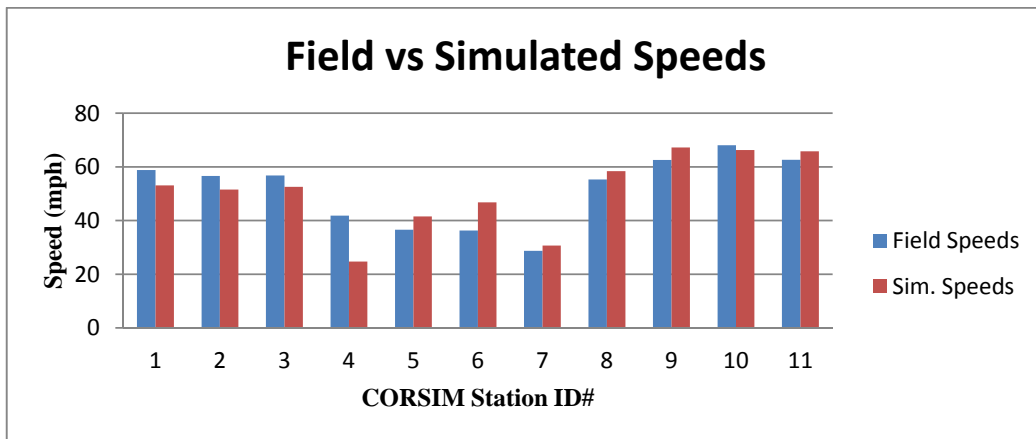


FIGURE 2.23 Field and simulated speeds – 5th time period

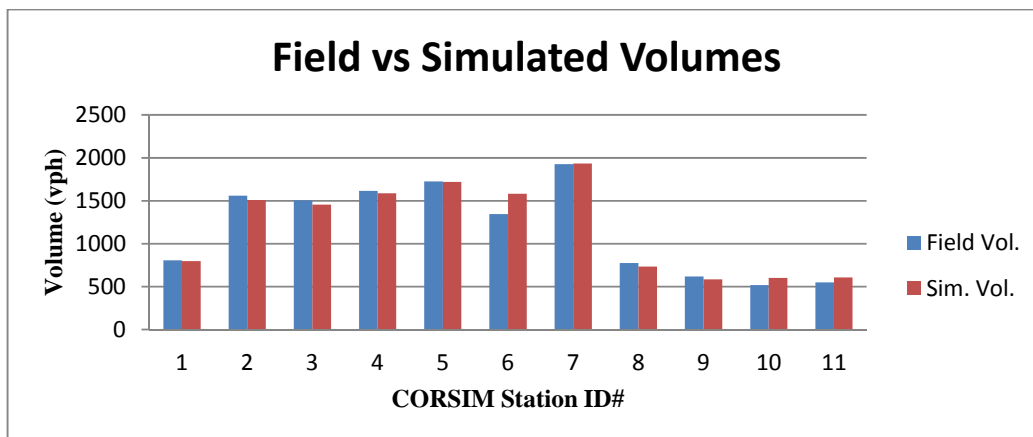


FIGURE 2.24 Field and simulated volumes – 5th time period

TABLE 2.11 Field and simulated speeds and volumes – 6th time period

6 th Time period (16:45 - 17:00)						
Freeway Link	Detector ID#	Location	Field Speeds	Sim. Speeds	Field Vol.	Sim. Vol.
[112, 113]	600291	I-95 NORTH OF NW 17 ST	57.31	52.68	949	917
[129, 130]	600471	I-95 NORTH OF NW 62 ST	56.86	51.32	1622	1554
[132, 133]	600521	I-95 NORTH OF NW 77 ST	56.20	53.88	1555	1486
[139, 140]	600621	I-95 AT NW 96 ST	43.97	46.42	1583	1495
[145, 146]	600711	I-95 SOUTH OF NW 111 ST	37.90	41.85	1747	1722
[153, 154]	600791	I-95 SOUTH OF NW 131 ST	28.18	40.08	1340	1731
[159, 161]	600921	I-95 SOUTH OF NW 151 ST	24.57	28.74	1799	2059
[170, 171]	600981	I-95 SOUTH OF US 441	55.31	58.02	790	875
[5125, 5105]	690471	I-95 NORTH OF NW 62 ST	63.51	66.95	636	623
[5138, 5139]	690621	I-95 AT NW 96 ST	67.58	65.91	504	616
[5153, 5154]	690791	I-95 SOUTH OF NW 131 ST	61.16	65.67	571	605

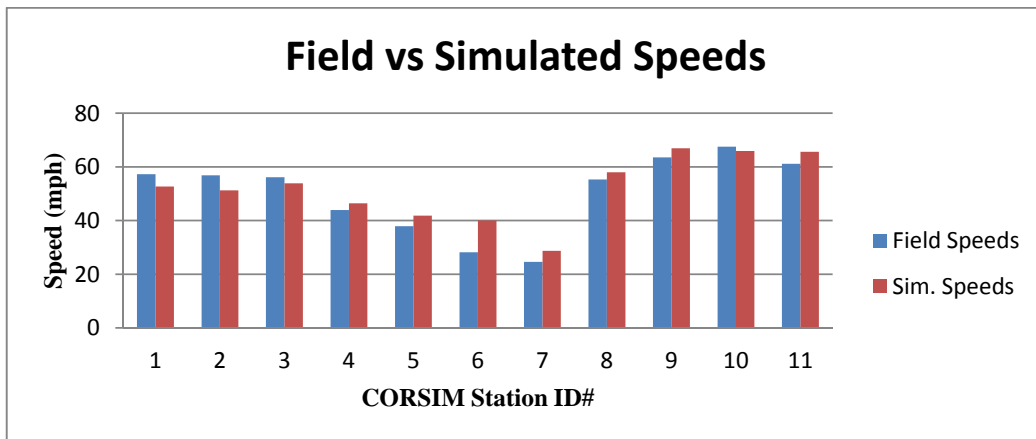


FIGURE 2.25 Field and simulated speeds – 6th time period

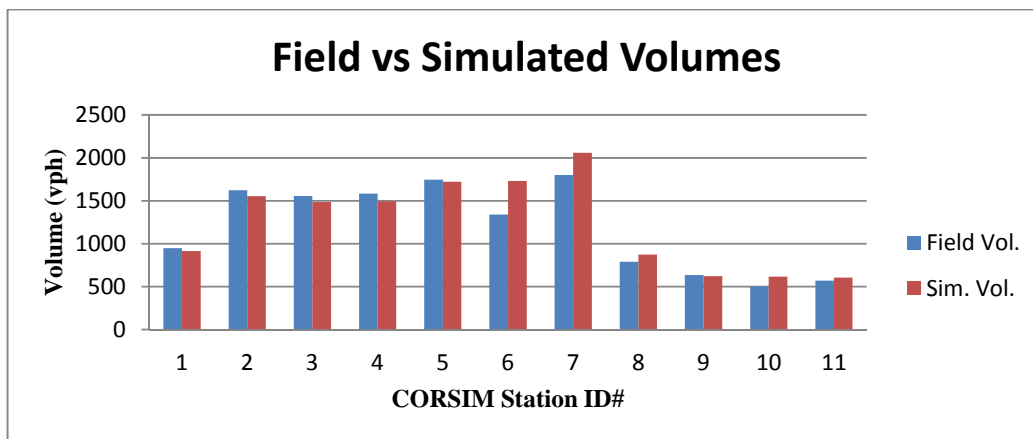


FIGURE 2.26 Field and simulated volumes – 6th time period

TABLE 2.12 Field and simulated speeds and volumes – 7th time period

7 th Time period (17:00 - 17:15)						
Freeway Link	Detector ID#	Location	Field Speeds	Sim. Speeds	Field Vol.	Sim. Vol.
[112, 113]	600291	I-95 NORTH OF NW 17 ST	46.69	52.05	926	986
[129, 130]	600471	I-95 NORTH OF NW 62 ST	56.39	50.99	1649	1604
[132, 133]	600521	I-95 NORTH OF NW 77 ST	55.07	47.97	1603	1580
[139, 140]	600621	I-95 AT NW 96 ST	50.01	52.49	1563	1552
[145, 146]	600711	I-95 SOUTH OF NW 111 ST	33.36	42.02	1565	1709
[153, 154]	600791	I-95 SOUTH OF NW 131 ST	23.43	33.98	1221	1739
[159, 161]	600921	I-95 SOUTH OF NW 151 ST	26.62	33.26	1680	2097
[170, 171]	600981	I-95 SOUTH OF US 441	56.25	57.77	681	939
[5125, 5105]	690471	I-95 NORTH OF NW 62 ST	64.76	66.93	637	589
[5138, 5139]	690621	I-95 AT NW 96 ST	69.99	66.34	533	588
[5153, 5154]	690791	I-95 SOUTH OF NW 131 ST	64.79	65.71	564	594

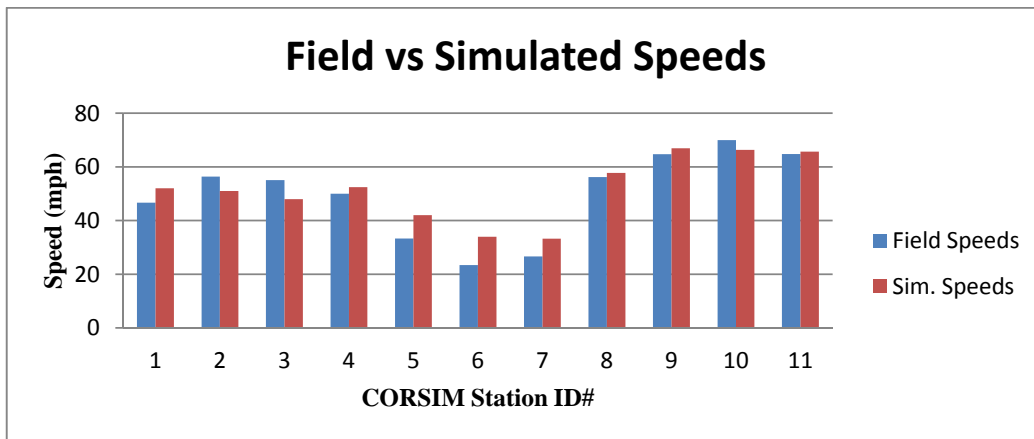


FIGURE 2.27 Field and simulated speeds – 7th time period

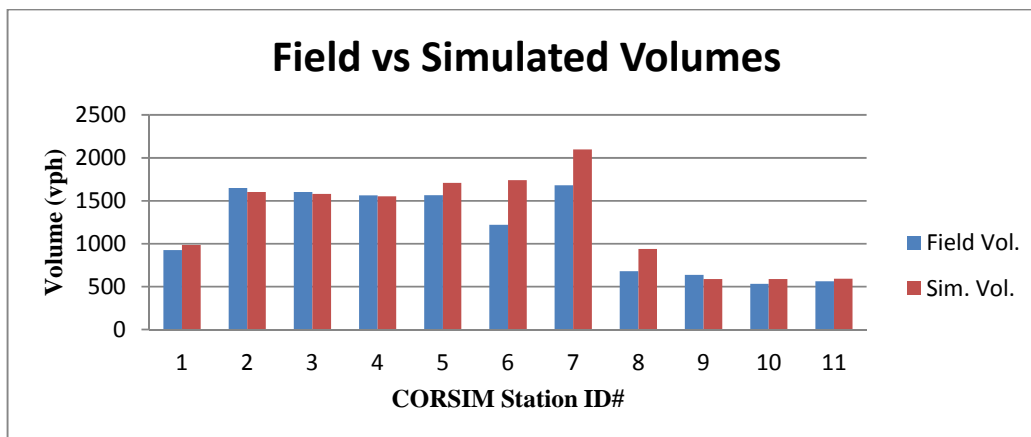


FIGURE 2.28 Field and simulated volumes – 7th time period

TABLE 2.13 Field and simulated speeds and volumes – 8th time period

8 th Time period (17:15 - 17:30)						
Freeway Link	Detector ID#	Location	Field Speeds	Sim. Speeds	Field Vol.	Sim. Vol.
[112, 113]	600291	I-95 NORTH OF NW 17 ST	44.58	52.45	927	923
[129, 130]	600471	I-95 NORTH OF NW 62 ST	56.40	50.49	1719	1679
[132, 133]	600521	I-95 NORTH OF NW 77 ST	49.17	40.49	1620	1614
[139, 140]	600621	I-95 AT NW 96 ST	31.85	52.57	1512	1638
[145, 146]	600711	I-95 SOUTH OF NW 111 ST	28.68	42.28	1476	1700
[153, 154]	600791	I-95 SOUTH OF NW 131 ST	21.68	30.12	1201	1688
[159, 161]	600921	I-95 SOUTH OF NW 151 ST	25.04	29.61	1679	2041
[170, 171]	600981	I-95 SOUTH OF US 441	56.63	58.08	698	825
[5125, 5105]	690471	I-95 NORTH OF NW 62 ST	64.81	67.21	582	527
[5138, 5139]	690621	I-95 AT NW 96 ST	70.98	66.37	436	536
[5153, 5154]	690791	I-95 SOUTH OF NW 131 ST	67.20	65.96	545	550

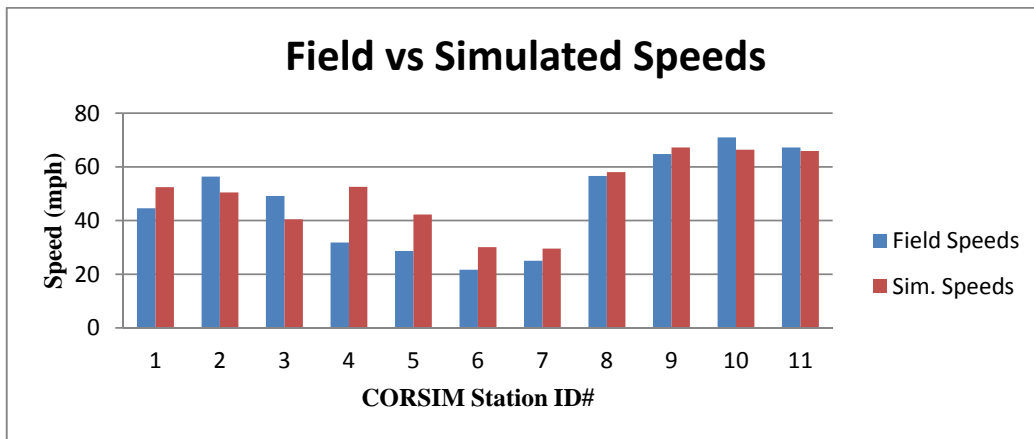


FIGURE 2.29 Field and simulated speeds – 8th time period

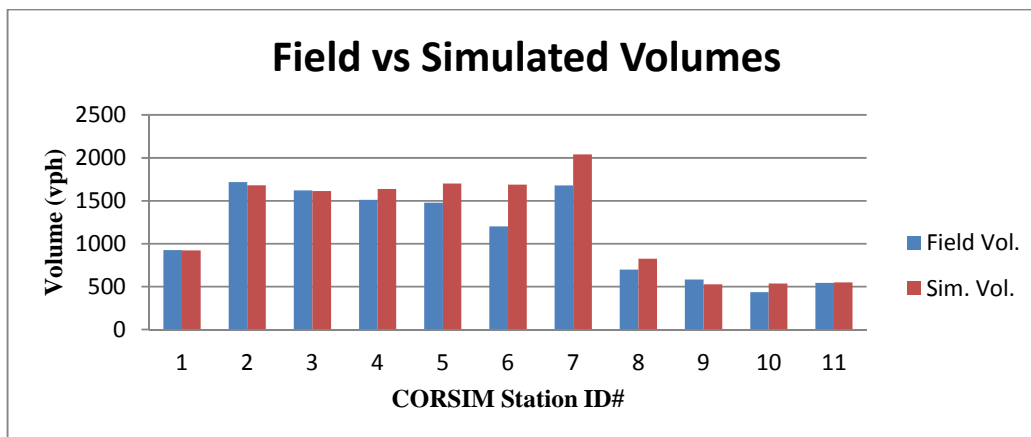


FIGURE 2.30 Field and simulated volumes – 8th time period

TABLE 2.14 Field and simulated speeds and volumes – 9th time period

9 th Time period (17:30 - 17:45)						
Freeway Link	Detector ID#	Location	Field Speeds	Sim. Speeds	Field Vol.	Sim. Vol.
[112, 113]	600291	I-95 NORTH OF NW 17 ST	54.27	52.38	924	952
[129, 130]	600471	I-95 NORTH OF NW 62 ST	53.97	49.91	1598	1596
[132, 133]	600521	I-95 NORTH OF NW 77 ST	35.80	44.35	1407	1593
[139, 140]	600621	I-95 AT NW 96 ST	30.04	46.00	1396	1641
[145, 146]	600711	I-95 SOUTH OF NW 111 ST	31.10	41.52	1485	1702
[153, 154]	600791	I-95 SOUTH OF NW 131 ST	22.94	20.43	1114	1603
[159, 161]	600921	I-95 SOUTH OF NW 151 ST	28.83	27.77	1843	2023
[170, 171]	600981	I-95 SOUTH OF US 441	55.74	57.94	750	859
[5125, 5105]	690471	I-95 NORTH OF NW 62 ST	65.41	67.08	625	596
[5138, 5139]	690621	I-95 AT NW 96 ST	67.57	66.32	474	580
[5153, 5154]	690791	I-95 SOUTH OF NW 131 ST	64.88	65.69	530	567

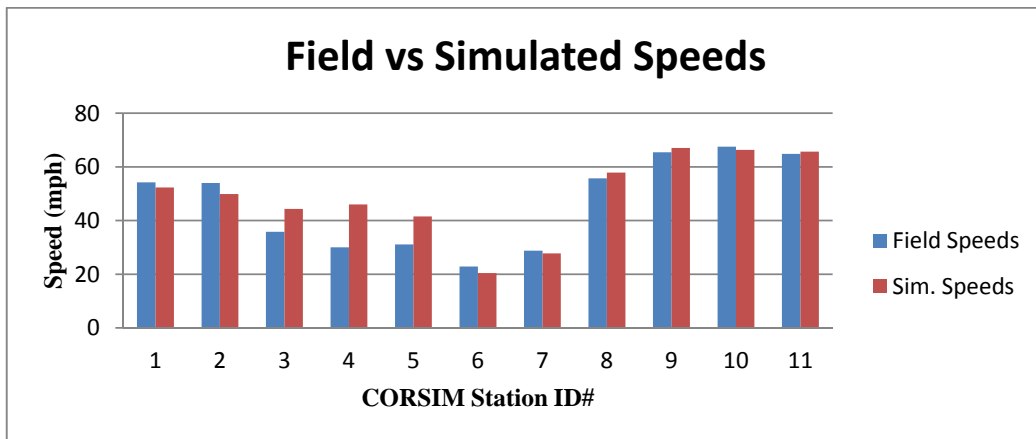


FIGURE 2.31 Field and simulated speeds – 9th time period

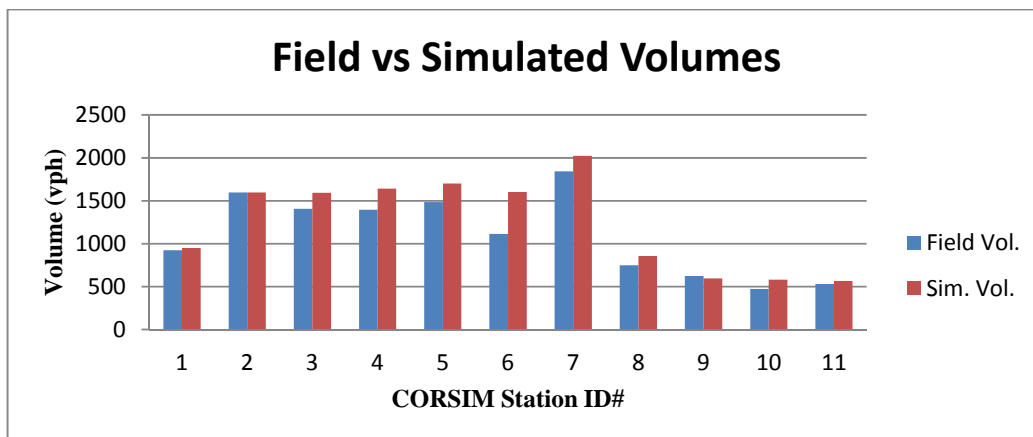


FIGURE 2.32 Field and simulated volumes – 9th time period

TABLE 2.15 Field and simulated speeds and volumes – 10th time period

10 th Time period (17:45 - 18:00)						
Freeway Link	Detector ID#	Location	Field Speeds	Sim. Speeds	Field Vol.	Sim. Vol.
[112, 113]	600291	I-95 NORTH OF NW 17 ST	64.87	52.46	885	926
[129, 130]	600471	I-95 NORTH OF NW 62 ST	56.20	51.10	1540	1511
[132, 133]	600521	I-95 NORTH OF NW 77 ST	38.10	53.80	1339	1401
[139, 140]	600621	I-95 AT NW 96 ST	31.23	45.15	1371	1479
[145, 146]	600711	I-95 SOUTH OF NW 111 ST	27.97	40.32	1460	1700
[153, 154]	600791	I-95 SOUTH OF NW 131 ST	31.79	16.60	1458	1463
[159, 161]	600921	I-95 SOUTH OF NW 151 ST	34.02	27.85	2055	2013
[170, 171]	600981	I-95 SOUTH OF US 441	56.10	57.80	811	939
[5125, 5105]	690471	I-95 NORTH OF NW 62 ST	65.74	67.63	559	492
[5138, 5139]	690621	I-95 AT NW 96 ST	71.00	66.70	397	514
[5153, 5154]	690791	I-95 SOUTH OF NW 131 ST	63.72	65.88	503	531

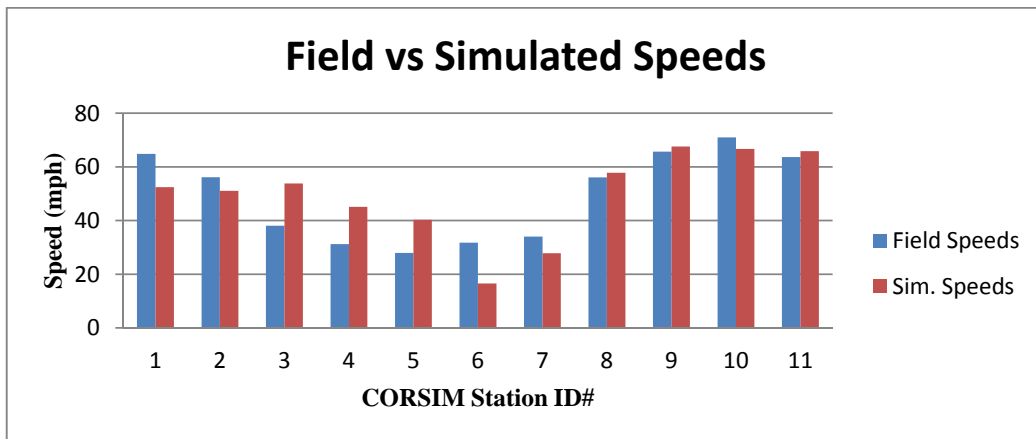


FIGURE 2.33 Field and simulated speeds – 10th time period

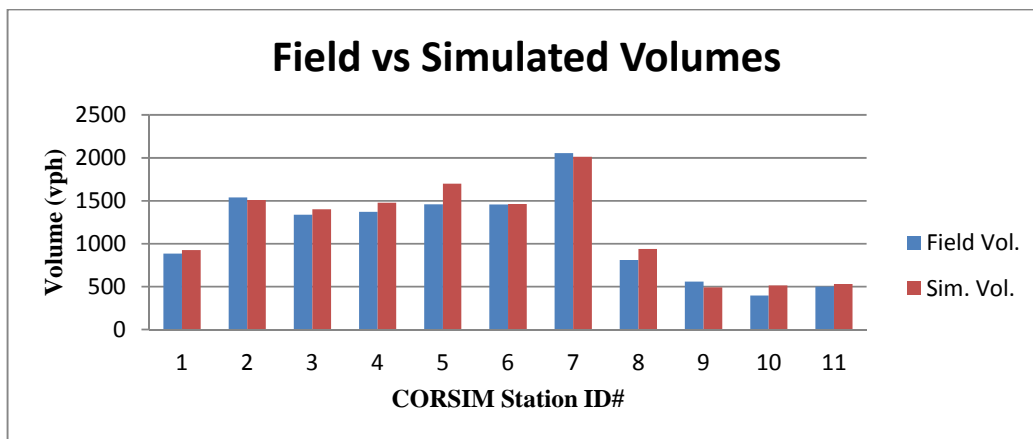


FIGURE 2.34 Field and simulated volumes – 10th time period

TABLE 2.16 Field and simulated speeds and volumes – 11th time period

11 th Time period (18:00 - 18:15)						
Freeway Link	Detector ID#	Location	Field Speeds	Sim. Speeds	Field Vol.	Sim. Vol.
[112, 113]	600291	I-95 NORTH OF NW 17 ST	65.16	52.29	909	927
[129, 130]	600471	I-95 NORTH OF NW 62 ST	55.01	51.28	1550	1506
[132, 133]	600521	I-95 NORTH OF NW 77 ST	34.39	53.56	1425	1454
[139, 140]	600621	I-95 AT NW 96 ST	42.19	51.34	1599	1530
[145, 146]	600711	I-95 SOUTH OF NW 111 ST	35.75	42.21	1694	1673
[153, 154]	600791	I-95 SOUTH OF NW 131 ST	42.22	27.42	1501	1474
[159, 161]	600921	I-95 SOUTH OF NW 151 ST	38.01	29.54	2143	2058
[170, 171]	600981	I-95 SOUTH OF US 441	55.90	57.82	880	868
[5125, 5105]	690471	I-95 NORTH OF NW 62 ST	66.20	67.08	563	569
[5138, 5139]	690621	I-95 AT NW 96 ST	70.55	66.60	427	560
[5153, 5154]	690791	I-95 SOUTH OF NW 131 ST	64.10	66.20	533	544

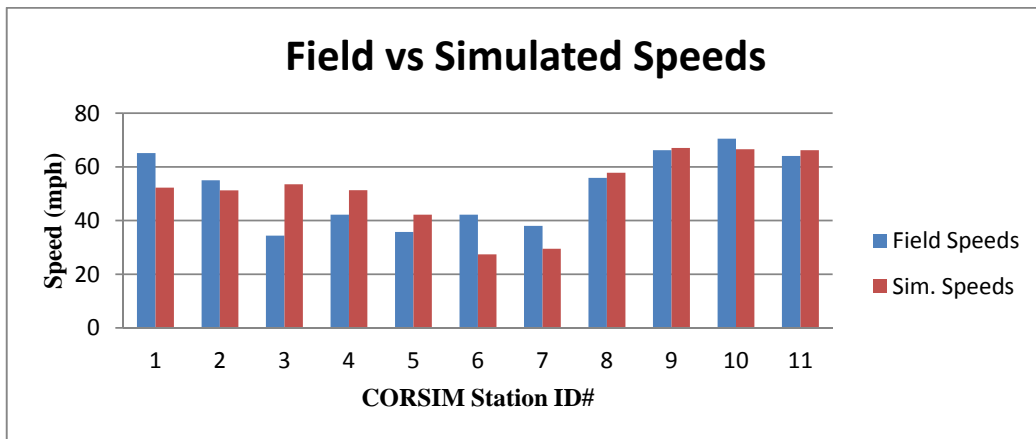


FIGURE 2.35 Field and simulated speeds – 11th time period

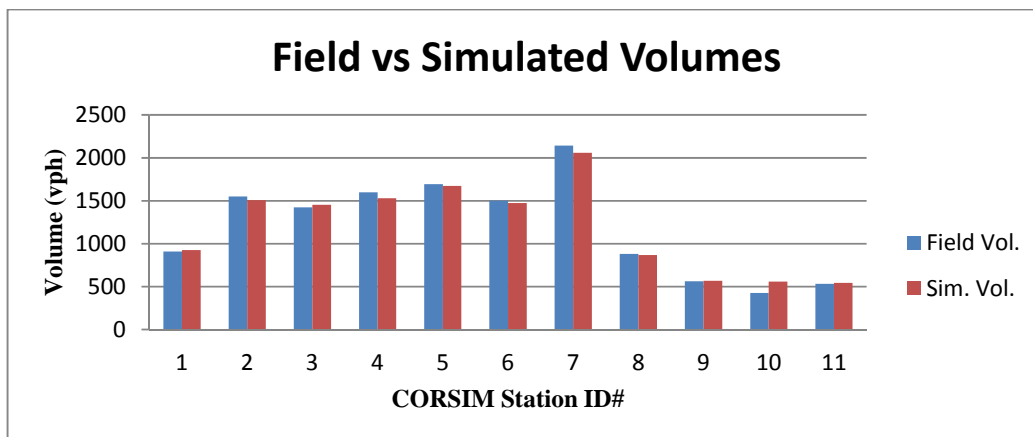


FIGURE 2.36 Field and simulated volumes – 11th time period

TABLE 2.17 Field and simulated speeds and volumes – 12th time period

12 th Time period (18:15 - 18:30)						
Freeway Link	Detector ID#	Location	Field Speeds	Sim. Speeds	Field Vol.	Sim. Vol.
[112, 113]	600291	I-95 NORTH OF NW 17 ST	66.26	52.54	873	908
[129, 130]	600471	I-95 NORTH OF NW 62 ST	57.06	51.29	1467	1487
[132, 133]	600521	I-95 NORTH OF NW 77 ST	62.20	54.29	1363	1421
[139, 140]	600621	I-95 AT NW 96 ST	55.30	52.34	1526	1544
[145, 146]	600711	I-95 SOUTH OF NW 111 ST	41.54	41.43	1698	1736
[153, 154]	600791	I-95 SOUTH OF NW 131 ST	51.56	46.52	1426	1259
[159, 161]	600921	I-95 SOUTH OF NW 151 ST	48.08	43.83	2074	1816
[170, 171]	600981	I-95 SOUTH OF US 441	56.42	58.27	889	774
[5125, 5105]	690471	I-95 NORTH OF NW 62 ST	64.09	67.10	483	539
[5138, 5139]	690621	I-95 AT NW 96 ST	71.51	66.75	400	537
[5153, 5154]	690791	I-95 SOUTH OF NW 131 ST	64.41	66.00	503	547

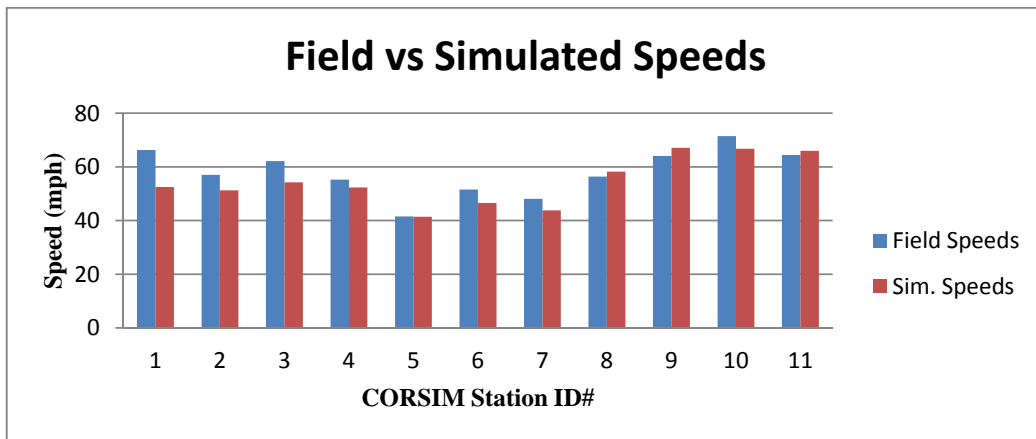


FIGURE 2.37 Field and simulated speeds – 12th time period

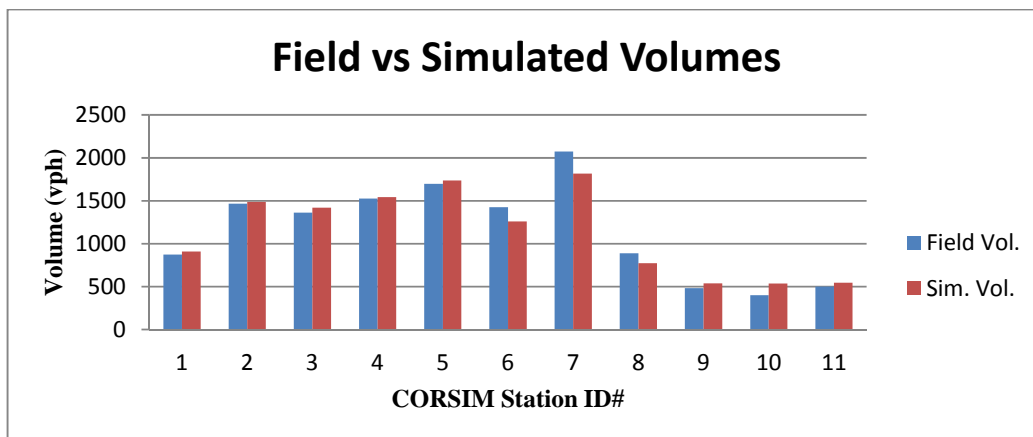


FIGURE 2.38 Field and simulated volumes – 12th time period

2.4 Simulation-Based Experiments

This section describes the simulation experiments conducted to evaluate the relationships between tolling and signaling algorithms when these operate along the same freeway section. The simulated network described in Section 4 was used for these experiments.

CORSIM's current version does not replicate tolling algorithms. Thus, an external module which simulates the operation of HOT lanes was developed in MATLAB. CORSIM can simulate a few ramp metering algorithms, but the Fuzzy Logic Ramp Metering Algorithm implemented along the I-95 in Miami since February 2009, is not among them. Thus, a Run-Time Extension (RTE) was built to replicate its operation in the simulation model.

The following subsections describe the process used to run the experiments, the fuzzy logic metering algorithm implementation, the experiments conducted, and their results.

2.4.1 Architecture of the simulation model

The architecture of the modified simulation model is presented in Figure 2.39. As shown, the initial demand for the general purpose and the managed lanes is specified and input into CORSIM. The model is then executed and results are obtained regarding the performance of both types of lanes (i.e., travel time, density and traffic volumes). Those are then used by the HOT Lane external module to predict the toll rate, the route choice behavior of drivers and consequently the utilization of the GP and managed lanes for the next time period. This procedure is repeated for each time period.

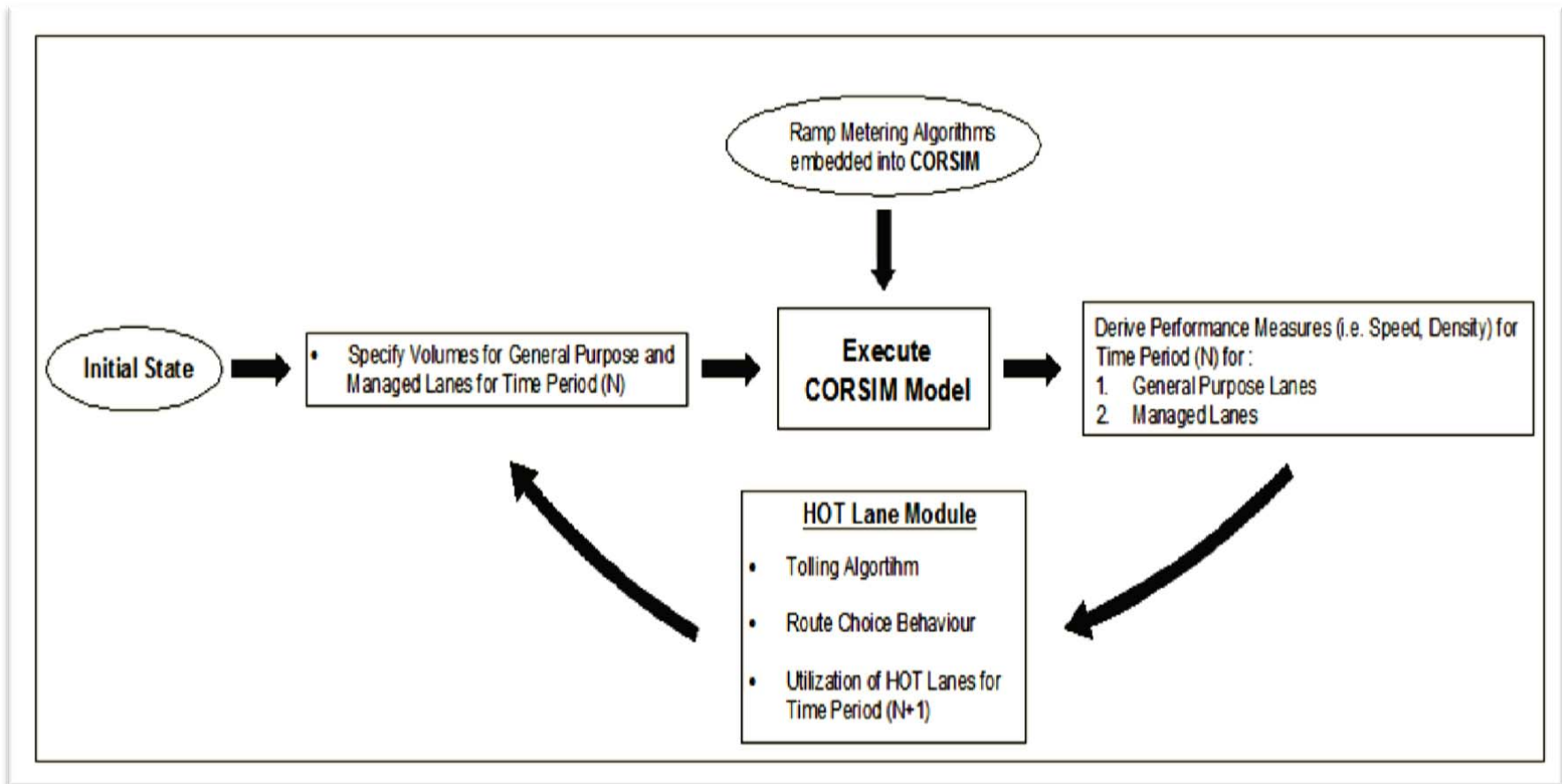


FIGURE 2.39 Architecture of the simulation

2.4.2 The Fuzzy Logic ramp signaling algorithm

This section describes the structure and the operation of the fuzzy logic ramp signaling algorithm. This algorithm was implemented by the Washington State Department of Transportation in the Northwest Region of Washington State to manage on-line the operation of over 100 on-ramps (Meldrum and Taylor, 2000). FDOT has rewritten the fuzzy logic ramp signaling algorithm based on the Washington DOT algorithm, and now owns this ramp metering firmware. In this report the algorithm appears with slight modifications compared to the initial one, to allow for its implementation in a simulated environment.

2.4.2.1 Fuzzy Logic Control in Ramp Signaling

In fuzzy logic the membership of an element into a set is not a matter of affirmation or denial. On the contrary, fuzzy logic deals with degrees of membership of elements into different fuzzy sets, sets that have no sharp boundaries. Consequently through the application of natural linguistic variables, heuristics of human reasoning and rule-based logic, fuzzy logic control (FLC) can handle imprecise or incomplete information. This attribute of FLC is one of the most important that makes it appropriate to ramp signaling. However, there are a few more reasons why FLC is well-suited for ramp metering:

- It can utilize incomplete or inaccurate data.

- It can balance conflicting objectives.

- It does not require extensive system modeling.

- It is easy to tune.

Fuzzy logic control does not require extensive system modeling. Freeway systems are quite difficult to model as they are nonlinear, chaotic and non-stationary. Many algorithms depend significantly on the accuracy of the system model, such as those that assume a constant freeway capacity for a given location. However, capacity may vary dynamically due to weather conditions, incidents, work zones or demand fluctuation. As FLC is using congestion indicators as inputs, it takes implicitly into account all these factors that affect the system's performance. Therefore, most ramps can operate properly using system-wide control parameters. Moreover, the fact that FLC uses linguistic variables and rule-based logic that mimics the way an operator

thinks about ramp metering, allows for the easy tuning of the algorithm, as the performance objective (e.g., longer or shorter queues) are different among various locations.

2.4.2.2 Structure and Operation of the Fuzzy Logic Ramp Signaling Algorithm

In general, fuzzy logic control involves three main steps: 1) fuzzification to convert the quantitative inputs into natural language variables; 2) rule evaluation to implement the control heuristics; and 3) defuzzification to map the qualitative rule outcomes to a numerical output.

The first step in the FLC is fuzzification, which preprocesses the inputs to the controller. The inputs to the controller are presented in Table 2.18. Fuzzification translates each numerical input into a set of fuzzy classes, also known as linguistic variables. For the local occupancy and local speed, the fuzzy classes used are very small (VS), small (S), medium (M), big (B), and very big (VB). The degree of activation indicates how true that class is on a scale of 0 to 1. Figures 2.40 through 2.42 represent the fuzzy classes for local and downstream occupancy, local and downstream speed, queue and advance queue occupancy.

TABLE 2.18 Description of fuzzy logic ramp metering algorithm inputs

Input	Typical Detector Locations
Local Occupancy	Mainline Station just upstream of merge
Local Speed	Same as for Local Occupancy
Downstream Occupancy	Multiple downstream stations
Downstream Speed	Same as for downstream occupancy
Queue Occupancy	Queue detector on the ramp
Advance Queue Occupancy	Tail end of the available queue storage

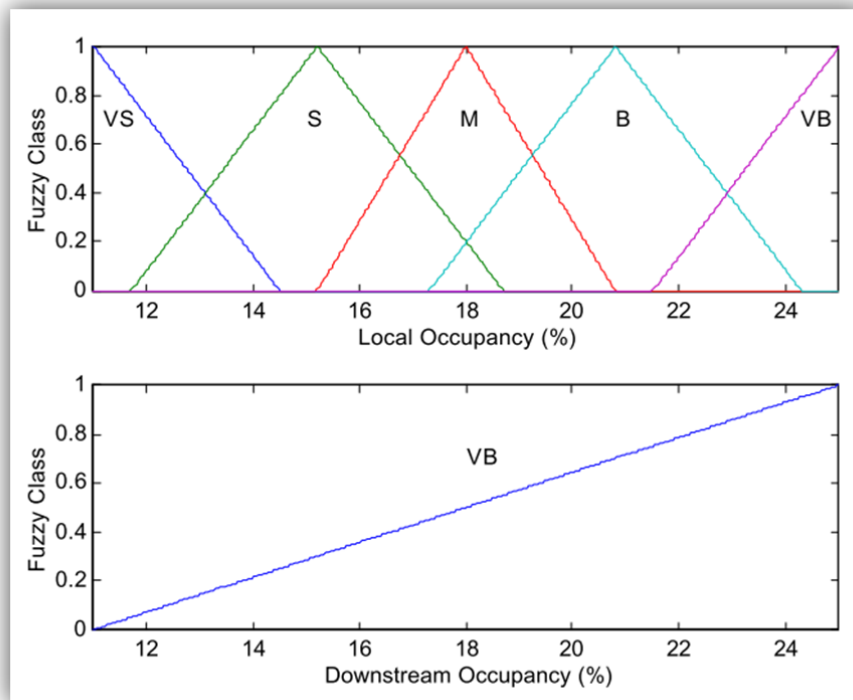


FIGURE 2.40 Fuzzy classes for local and downstream occupancy

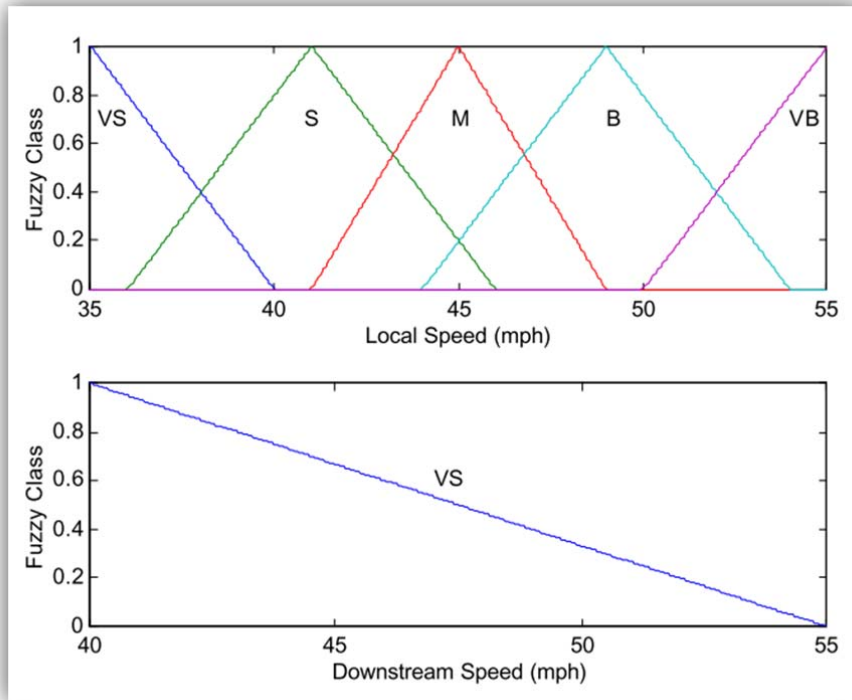


FIGURE 2.41 Fuzzy classes for local and downstream speed

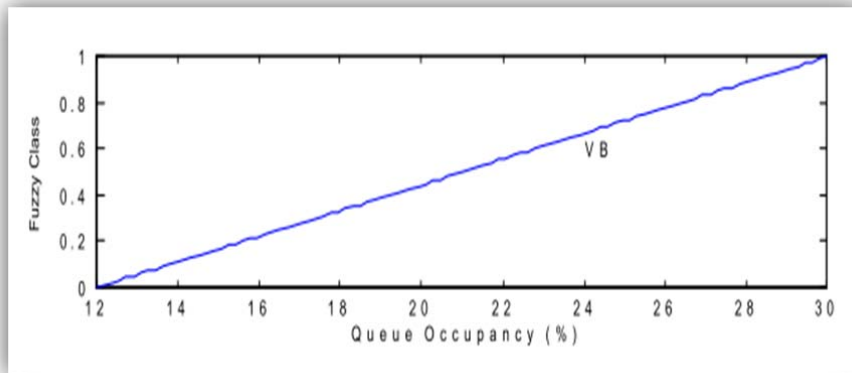


FIGURE 2.42 Fuzzy classes for local and downstream speed

After fuzzification, the rule base is evaluated. The rules are a set of if-then statements similar to the heuristics an operator would use to control the system (Table 2.19). For a given premise, a fuzzy class of metering rates is specified, either VS, S, M, B, or VB. The rule outcome is equal to the degree of activation of the rule premise. Each rule has a weighting that reflects its relative importance within the rule base. By adjusting these rule weights, the operator can balance the performance objectives.

TABLE 2.19 Rule base for fuzzy ramp metering algorithm

Rule	Rule Weight	Rule Premise	Rule Outcome
1	2.5	If local occupancy is VB	Metering rate is
2	1.0	If local occupancy is B	Metering rate is
3	1.0	If local occupancy is M	Metering rate is
4	1.0	If local occupancy is S	Metering rate is
5	1.0	If local occupancy is VS	Metering rate is
6	3.0	If local speed is VS AND local occupancy is VB	Metering rate is
7	1.0	If local speed is S	Metering rate is
8	1.0	If local speed is B	Metering rate is
9	1.0	If local speed is VB AND local occupancy is VS	Metering rate is
10	4.0	If downstream speed is VS AND downstream	Metering rate is
11	2.0	If queue occupancy is VB	Metering rate is
12	4.0	If advance queue occupancy is VB	Metering rate is

The last step in the FLC is to produce a numerical metering rate given all of the rule outcomes. Just as the inputs to the controller are represented by fuzzy classes to translate from a numerical input to a set of linguistic variables, so is the metering rate represented by a set of fuzzy classes to convert from a set of linguistic variables to a single metering rate. This reverse process from a fuzzy to a crisp, or quantitative state, is known as de-fuzzification. The fuzzy classes for a metered lane are shown in Figure 2.43.

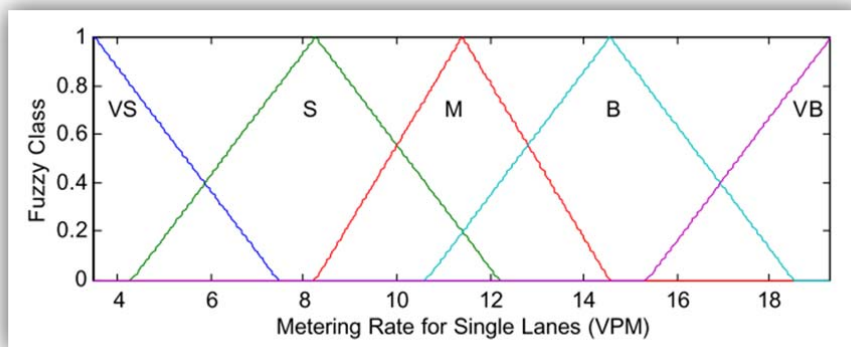


FIGURE 2.43 Fuzzy classes for metering rates

The implicated area of each rule outcome is found by scaling its fuzzy metering class by its activation degree. The centroid of the rule outcomes is found with the following equation, where each rule's implicated area is multiplied by the rule weighting:

$$Metering\ Rate = \frac{\sum_{i=1}^N w_i c_i I_i}{\sum_{i=1}^N w_i I_i} \quad (1)$$

where w_i is the weighting of the i_{th} rule, c_i is the centroid of the output class, and I_i is the implicated area of the output class. The discrete fuzzy centroid calculation produces a metering rate value.

2.4.3 Structure of the simulated experiments

A set of scenarios was developed for the implementation of the objectives of this task. The scenarios were structured so that the interactions between ramp metering and pricing could be identified and the impact of their combined operation on vehicular traffic flow could be assessed. The complete list of the simulated scenarios is presented in Table 2.20.

TABLE 2.20 Scenarios tested regarding ramp metering and tolling interactions

Scenario #	Ramp Signaling Algorithm	Tolling Algorithm
1	No Metering	Time of Day
2	No Metering	Existing (HOT performance based)
3	Constant Rate	Time of Day
4	Constant Rate	Existing (HOT performance based)
5	Fuzzy Logic	Time of Day
6	Fuzzy Logic	Existing (HOT performance based)

2.4.4 Results

The interactions between pricing and ramp metering are best captured by examining the last two scenarios of Table 2.20. In both cases, the metering and the toll rate are updated at specific time intervals (i.e., metering rate every minute, toll rate every 15 minutes) making it possible to examine how one algorithm responds when changes to the operation of the other occur according to the prevailing traffic conditions.

The metering rate profile (at the first on-ramp located upstream of the entry point to the HOT lanes), the toll rate profile and the route choice behavior of drivers throughout the simulation time-line are presented in Figures 2.44 to 2.49. According to Figures 2.45 and 2.48, during both scenarios the proportion of traffic traveling on the GP lanes in the beginning of the simulation is far higher than that traveling on the HOT lanes. Therefore, the metering rate imposed on the traffic entering from NW 62nd St. is restrictive (i.e., 4-8 veh/min). The toll rate (i.e., \$2.50) for this initial time period was selected arbitrarily, so that the tolling algorithm could predict the values for the following ones.

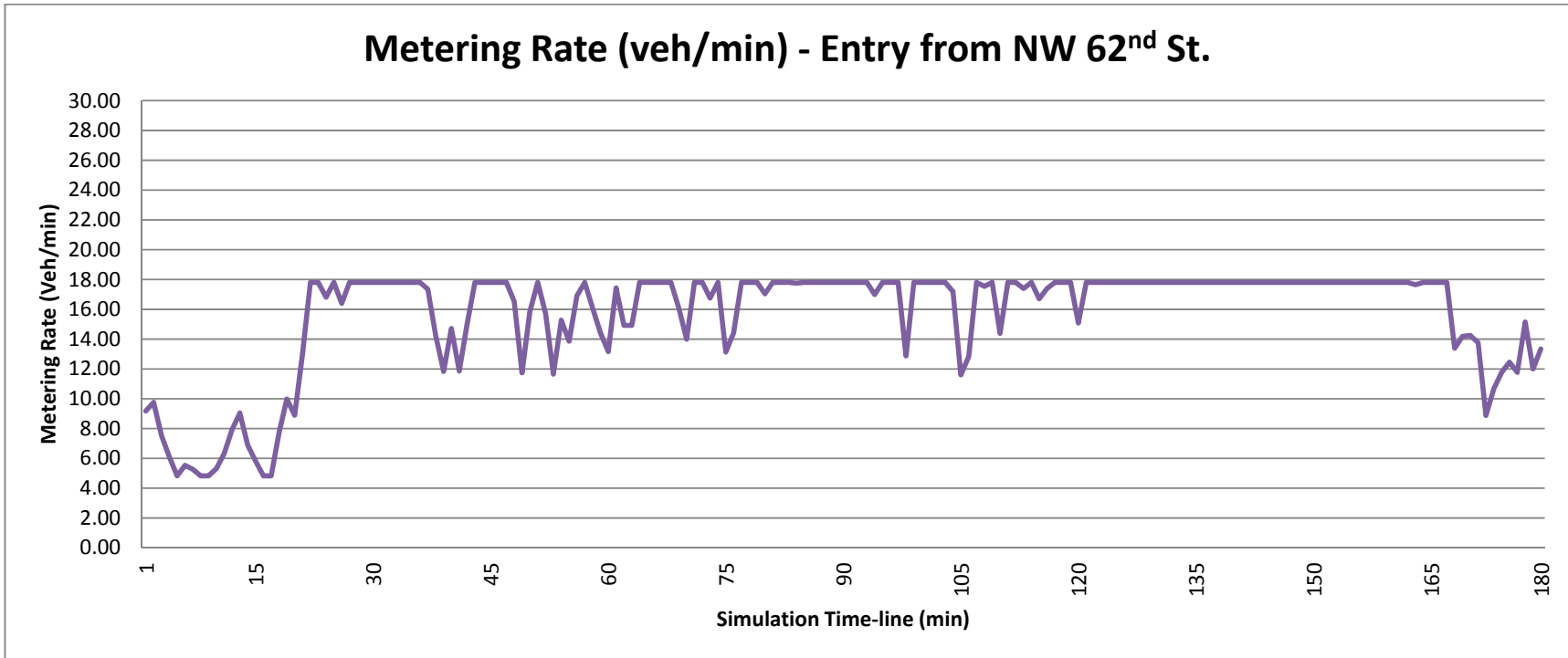


FIGURE 2.44 Scenario #6: Metering rate of ramp at 62nd Street

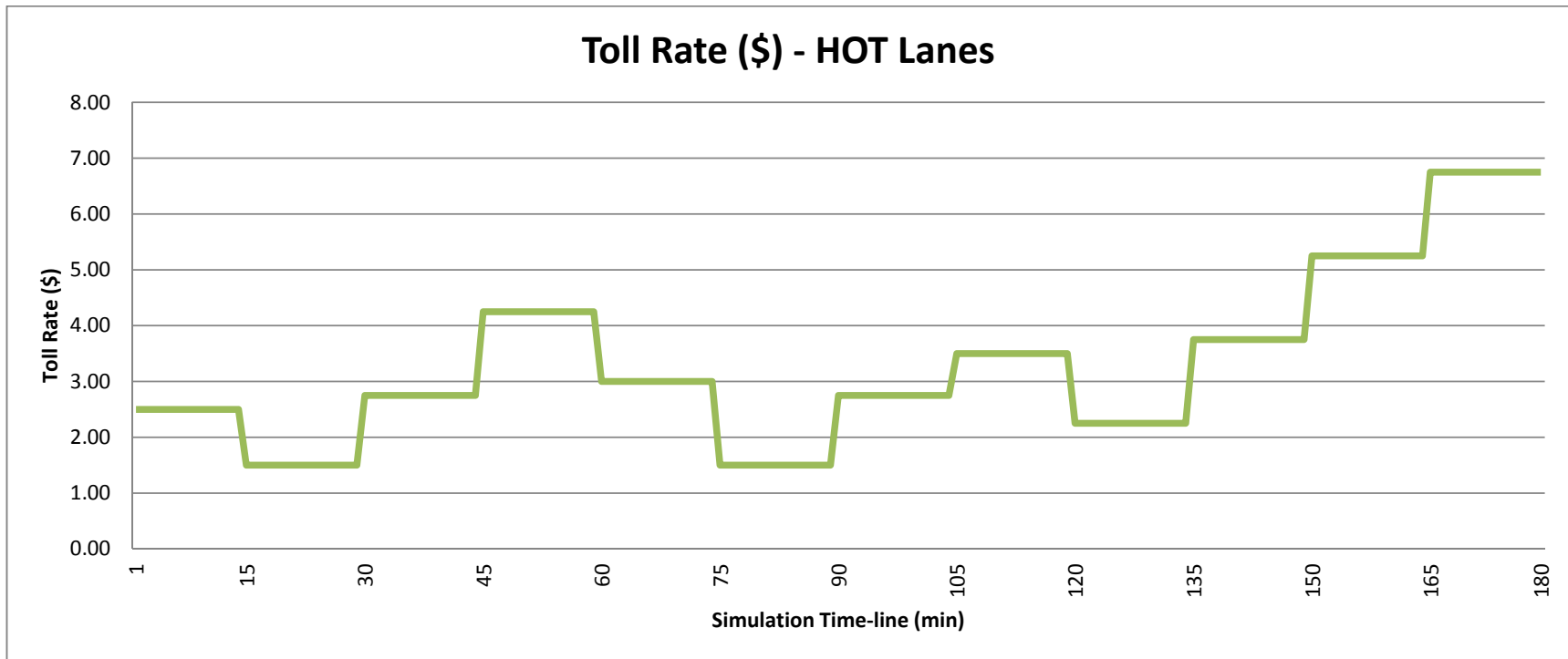


FIGURE 2.45 Scenario #6: Toll rate imposed on vehicles entering the HOT Lanes every time interval (i.e., 15 min).

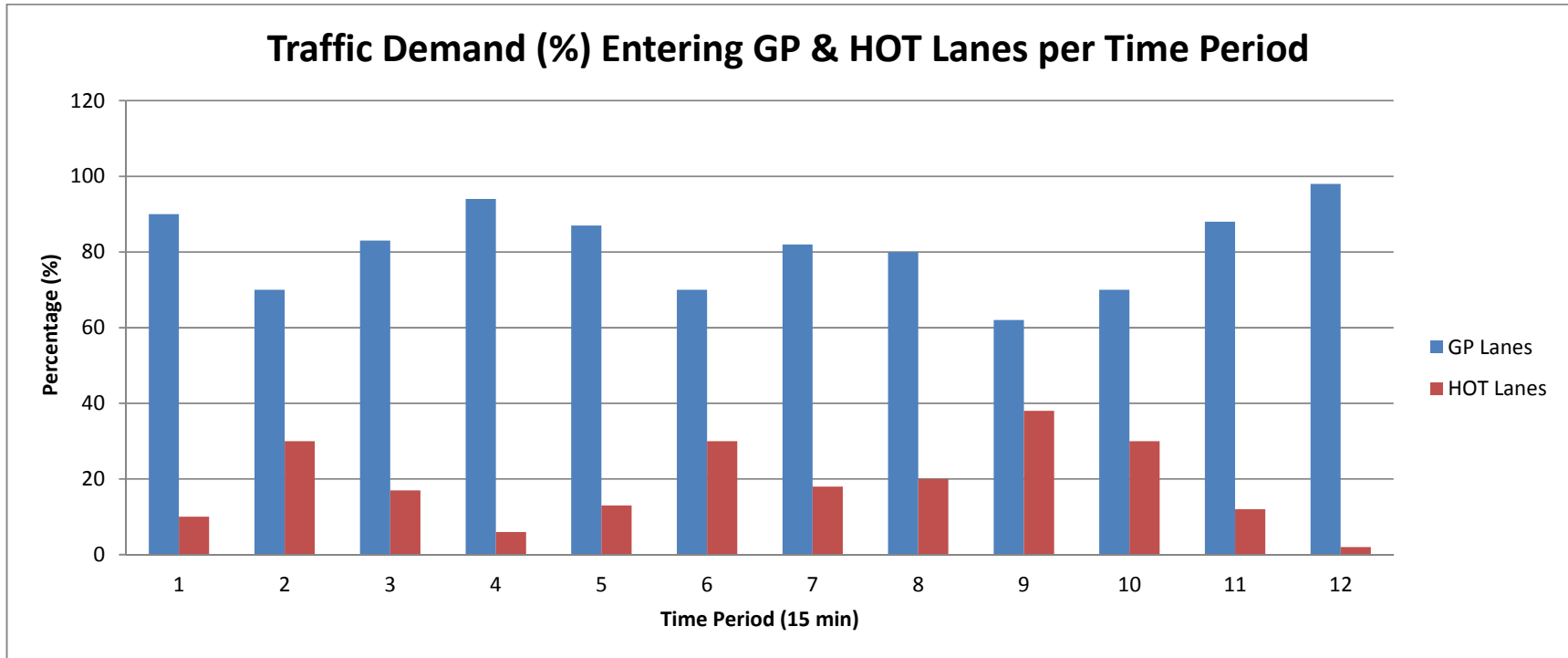


FIGURE 2.46 Scenario #6: Percent of traffic entering GP and HOT Lanes every time interval (i.e., 15 min).

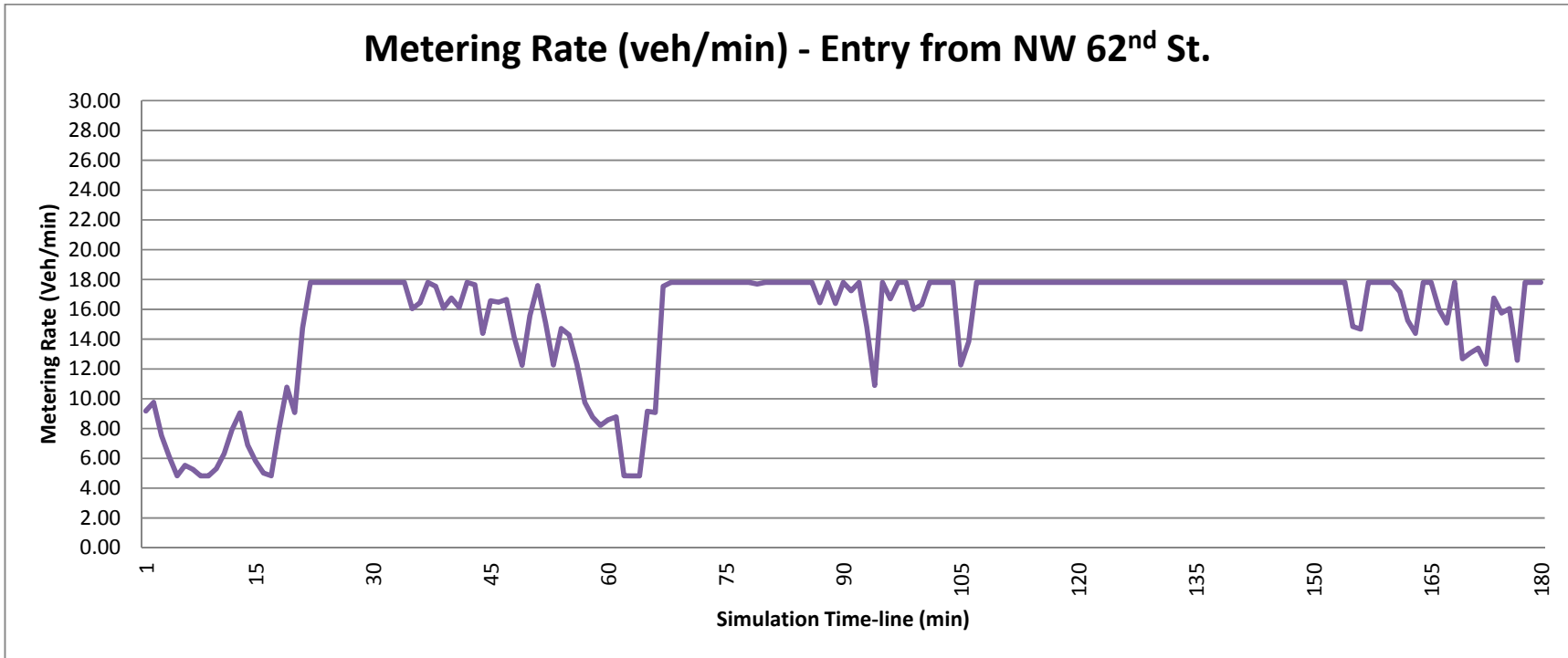


FIGURE 2.47 Scenario #5: Metering rate of ramp at 62nd Street

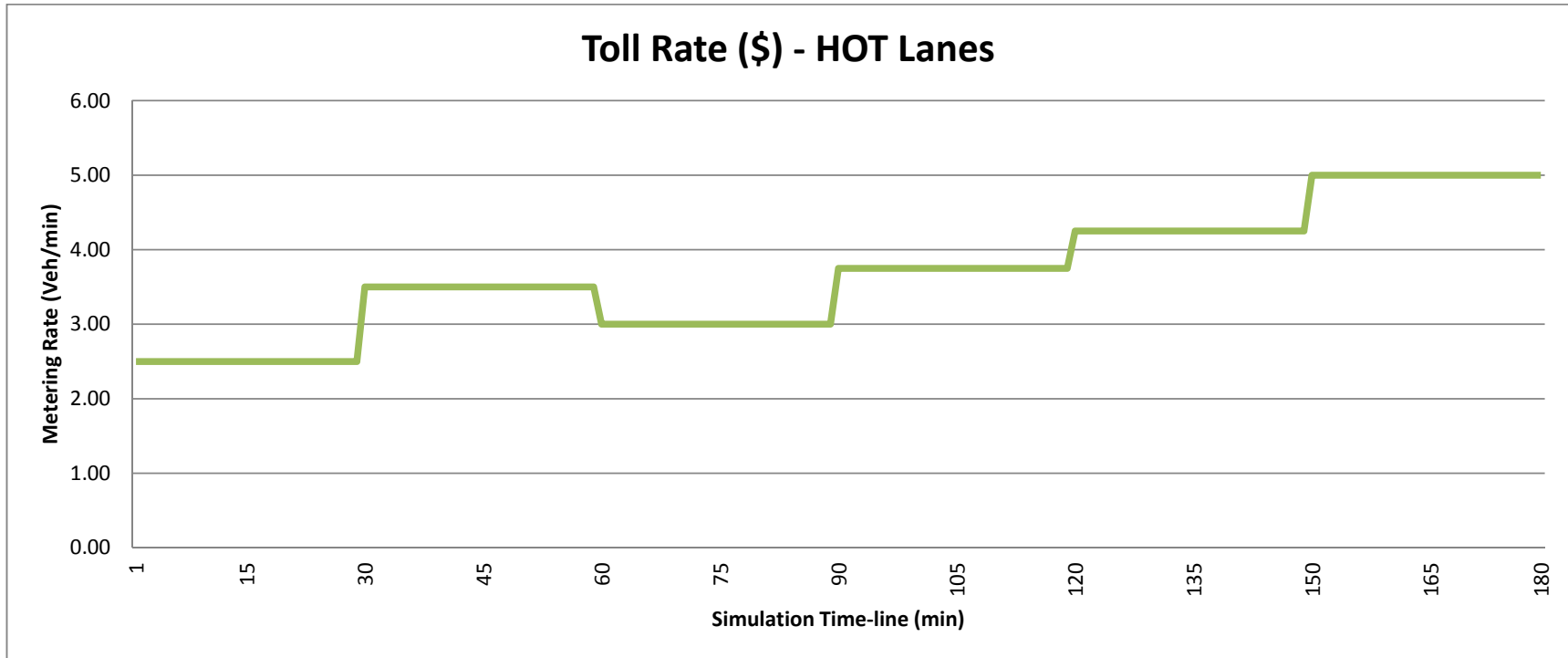


FIGURE 2.48 Scenario #5: Toll rate imposed on vehicles entering the HOT lanes every time interval (i.e., 15 min).

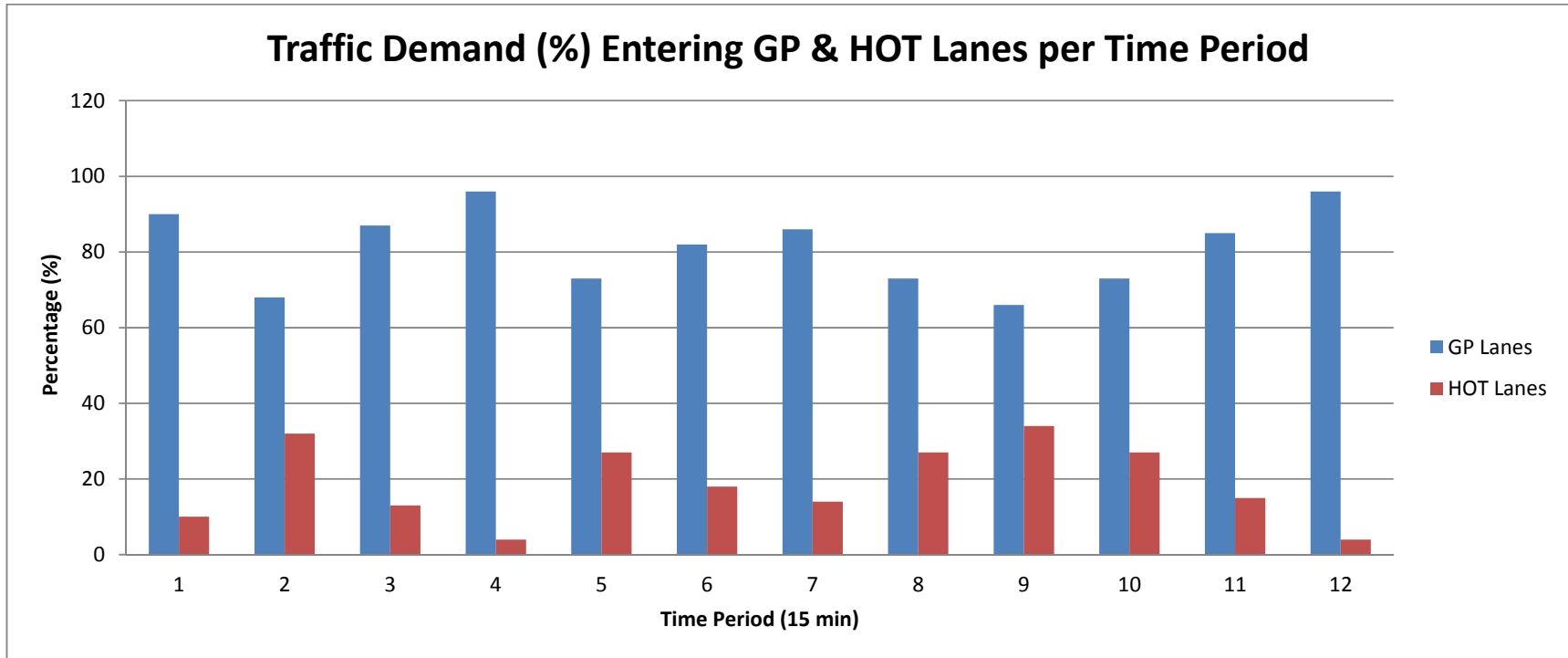


FIGURE 2.49 Scenario #5: Percent of traffic entering GP and HOT lanes every time interval (i.e., 15 min)

In the case of the traffic responsive pricing scheme (i.e., Scenario #6), the toll rate for the second time period is reduced to \$1.50. The estimation of the toll rate for each subsequent time period is based on the traffic conditions that prevailed on the HOT lanes (i.e., average density) during the previous one. Thus, more traffic is attracted into the HOT lanes during the second time period, as the travel cost (i.e., travel time plus toll rate) on the HOT lanes is lower. As the traffic demand on the GP lanes decreases, the ramp metering algorithm operates less restrictively allowing more traffic to enter the freeway.

The same phenomenon also occurs when a Time of Day (TOD) pricing scheme is active. In the predetermined tolling scheme that appears in Figure 2.47 the toll rate is updated every 30 minutes. It is obvious that after the transition to a higher toll value in the third time period the metering rate starts decreasing. The increase of the toll renders the HOT lanes less attractive with respect to travel cost, traffic demand increases on the GP lanes, and thus the operation of the meters becomes more restrictive. Thus, there is a clear relationship between ramp metering and pricing. An increase of the toll rate causes the metering rates to decrease at the meters that are placed along the HOT lanes.

Along with the interactions between ramp metering and pricing, the impacts of different tolling algorithms and combinations of tolling and ramp metering algorithms on freeway traffic operations were investigated. Figures 2.50 to 2.55 show the average speed (i.e., space mean speed per link) per location on the GP lanes of the I-95 Miami Expressway for the tested control schemes.

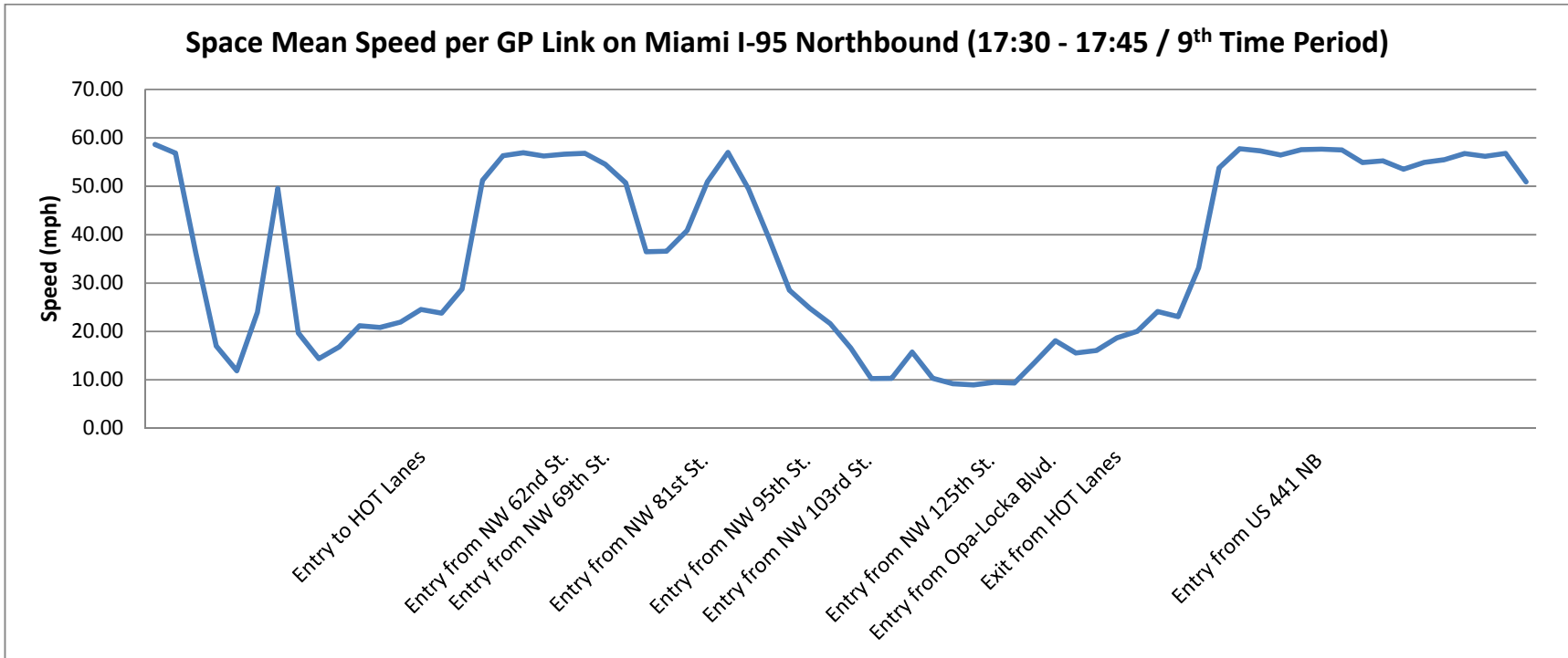


FIGURE 2.50 Scenario #1: Average speeds along I-95 Northbound GP lanes during 17:30 – 17:45 pm

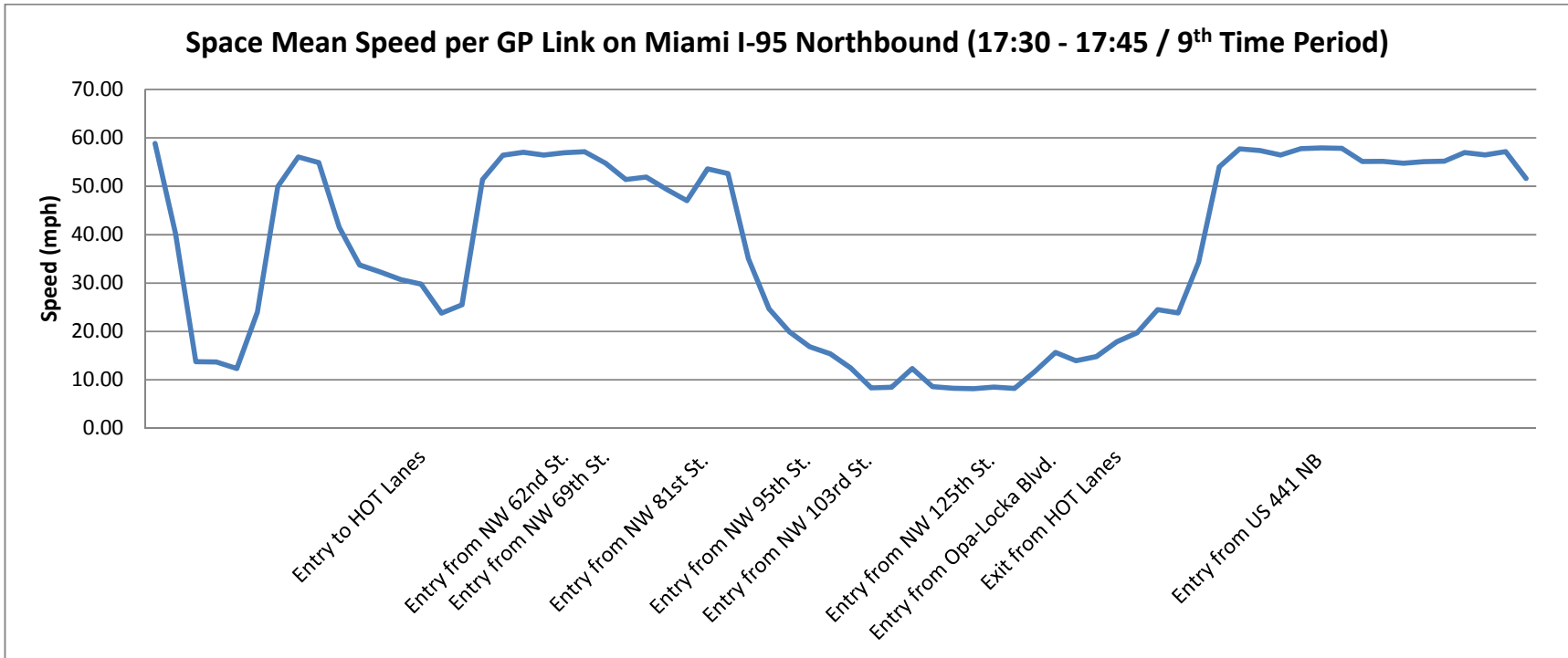


FIGURE 2.51 Scenario #2: Average speeds along I-95 Northbound GP lanes during 17:30 – 17:45 pm

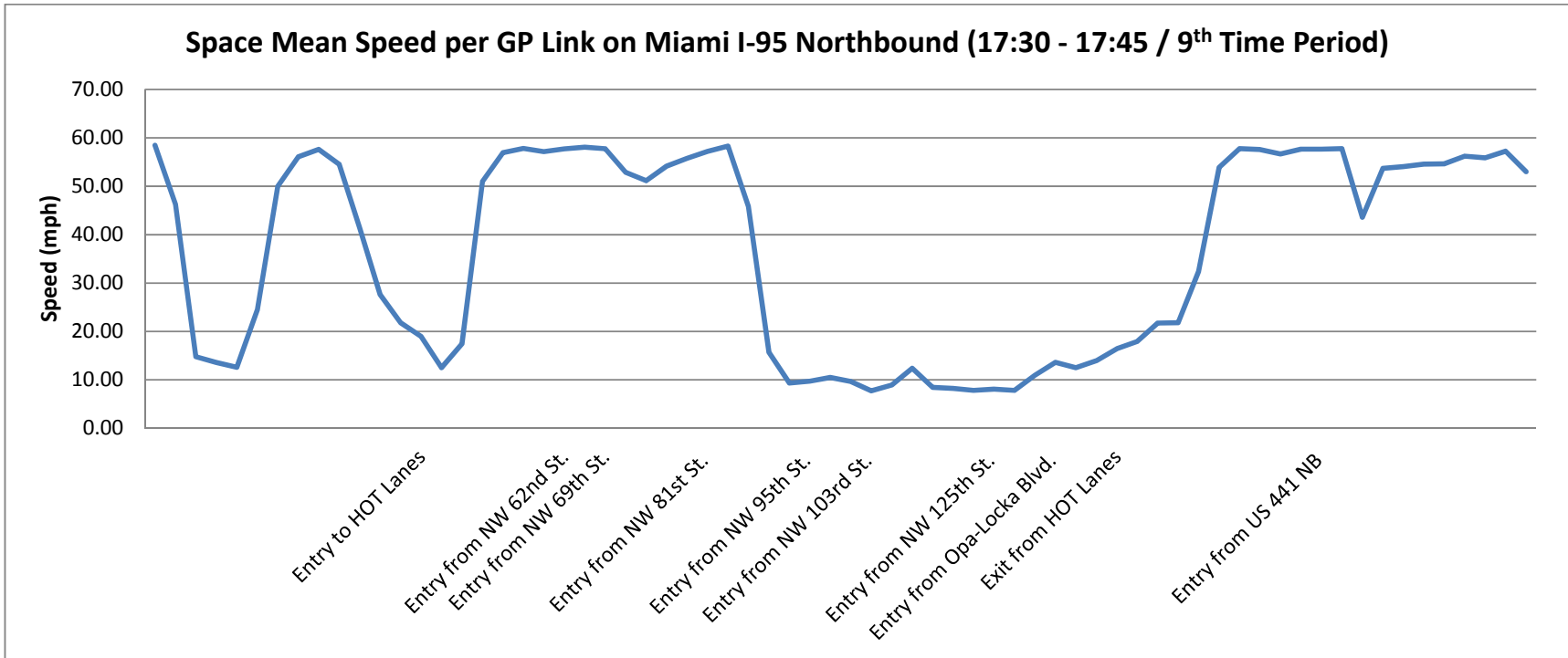


FIGURE 2.52 Scenario #3: Average speeds along I-95 Northbound GP lanes during 17:30 – 17:45 pm

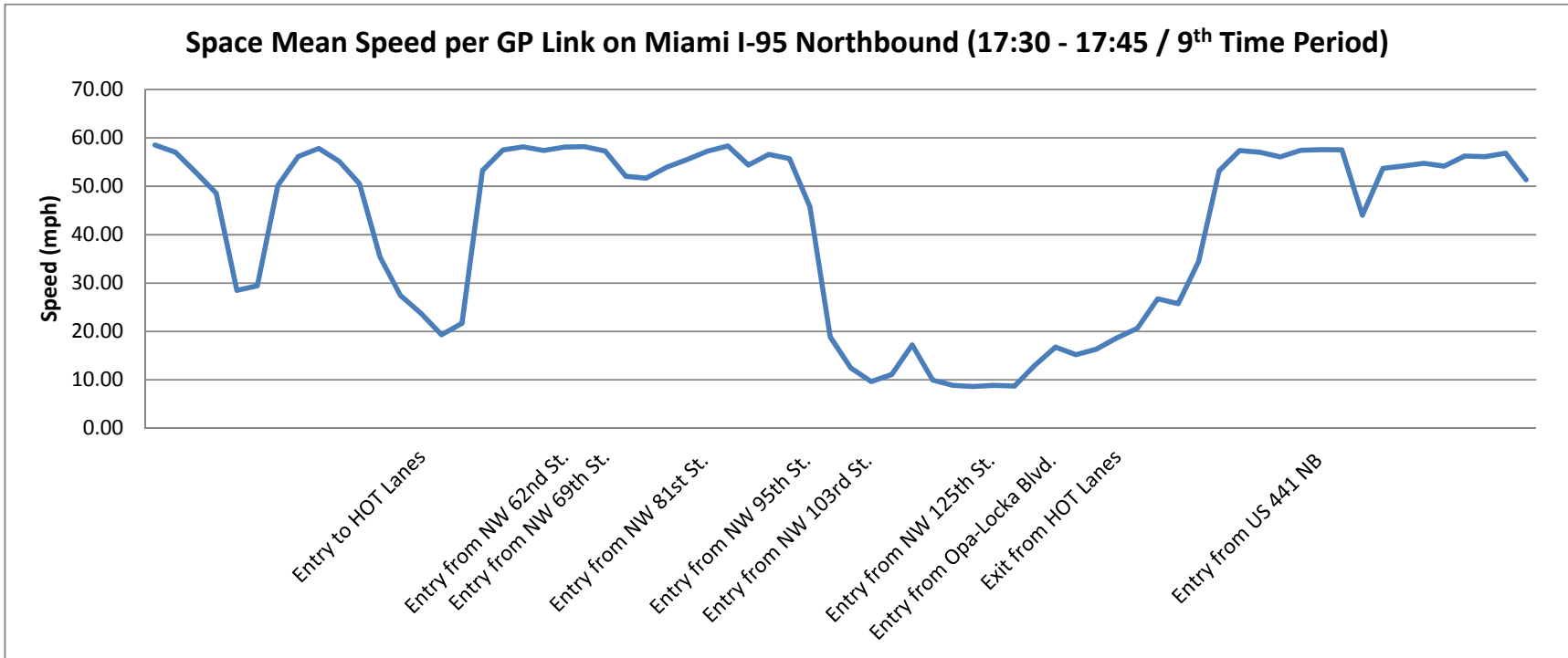


FIGURE 2.53 Scenario #4: Average speeds along I-95 Northbound GP lanes during 17:30 – 17:45 pm

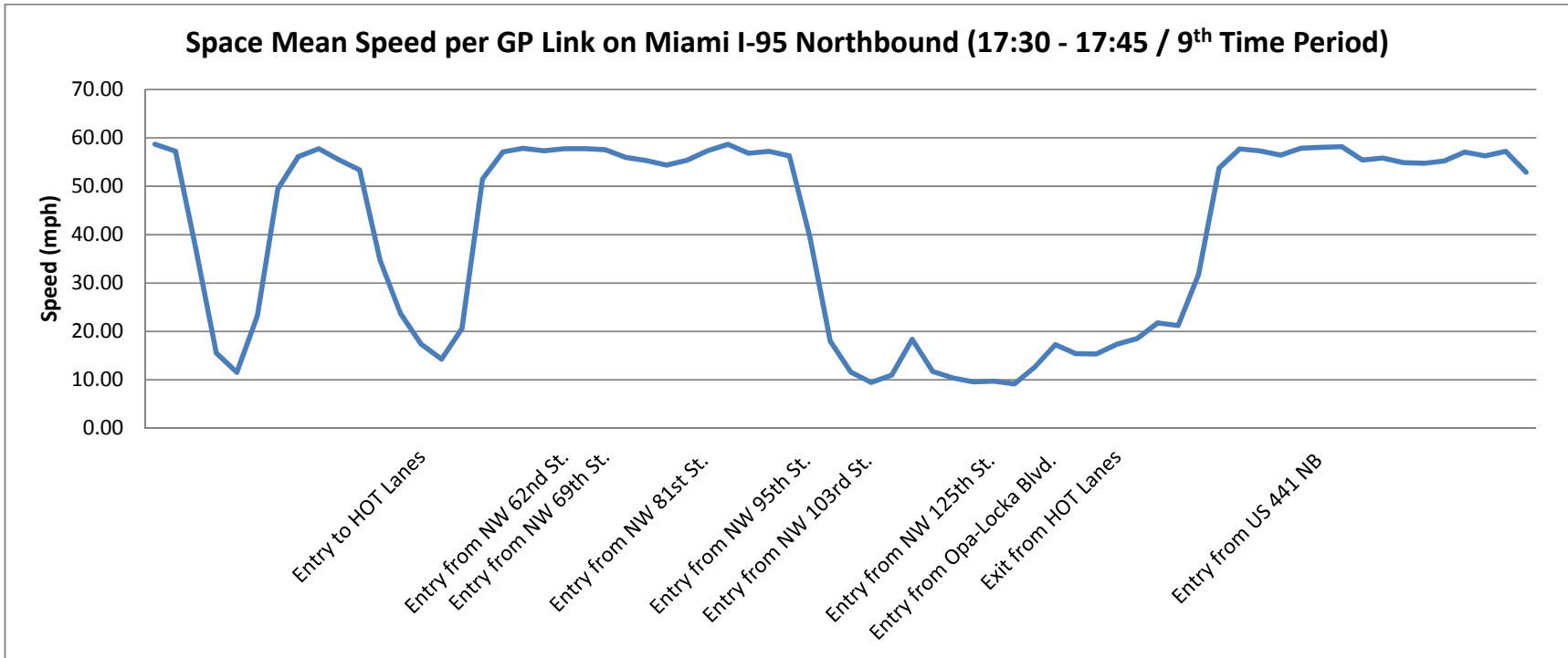


FIGURE 2.54 Scenario #5: Average speeds along I-95 Northbound GP lanes during 17:30 – 17:45 pm

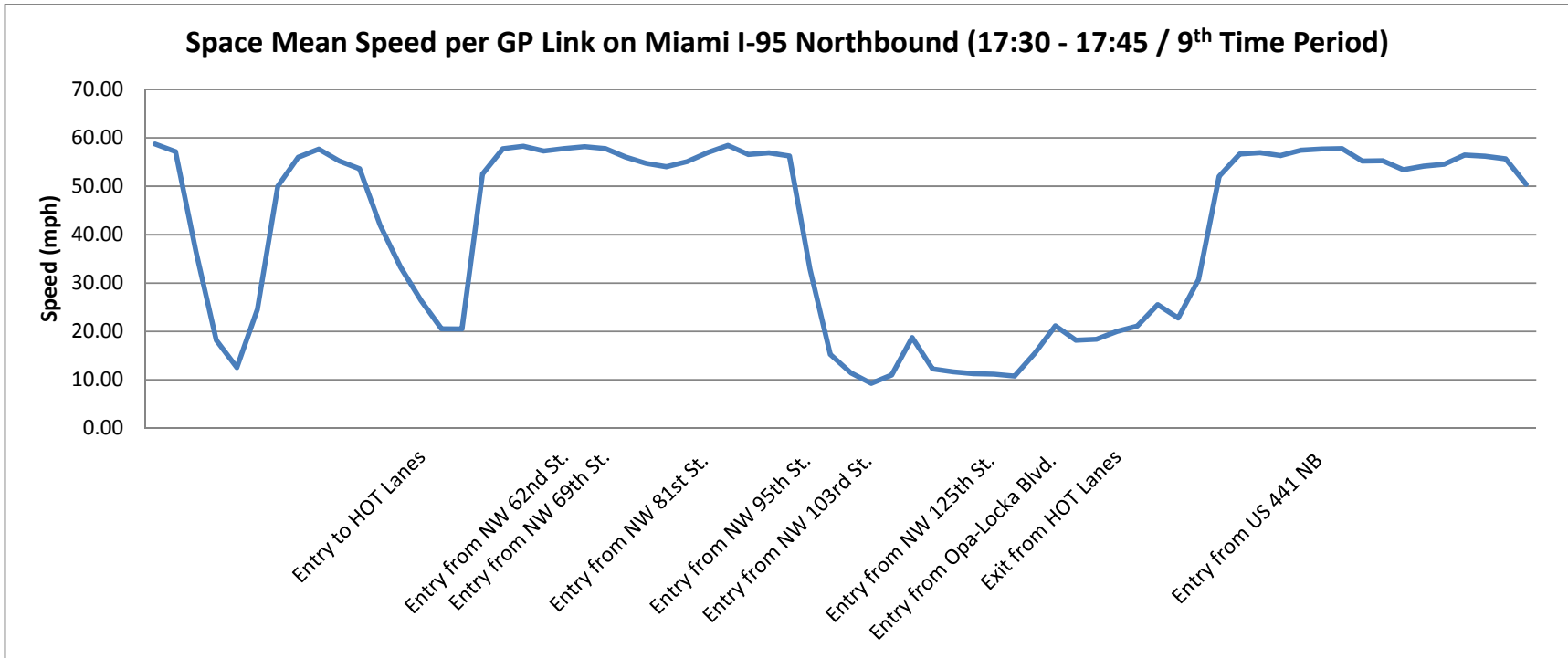


FIGURE 2.55 Scenario #6: Average speeds along I-95 Northbound GP lanes during 17:30 – 17:45 pm

According to these figures, when the entering traffic from the on-ramps is unregulated, and only a tolling algorithm is operating, almost the whole network breaks down during high demand periods (i.e., 17:30-17:45). However, when ramp metering (either pre-timed or traffic responsive control) is implemented along with pricing, congestion upstream of 95th St. is reduced. In the case that ramp metering is implemented and tolling becomes traffic responsive (Figures 2.53 and 2.55) the severity of the breakdown diminishes.

Next, to compare quantitatively traffic conditions under each traffic control scheme, the average travel time per vehicle to cross the congested part of the network (i.e., from 81st St. till the exit to the Golden Glades Dr.) every time interval (i.e., 15 min) is obtained (Figures 2.56 to 2.61). This route is 4.8 miles long and can be crossed in 5.8 min if a free flow speed of 50 mph is assumed. It is clear from the figures that the Fuzzy Logic Ramp Metering Algorithm manages to decrease that travel time per vehicle at least 2 min per time interval compared to the pre-timed control case. Under pre-timed metering and TOD tolling control the average travel time reaches 25 min during the 9th time period. Compared to the dynamic metering and pricing case this is a difference of 7 minutes.

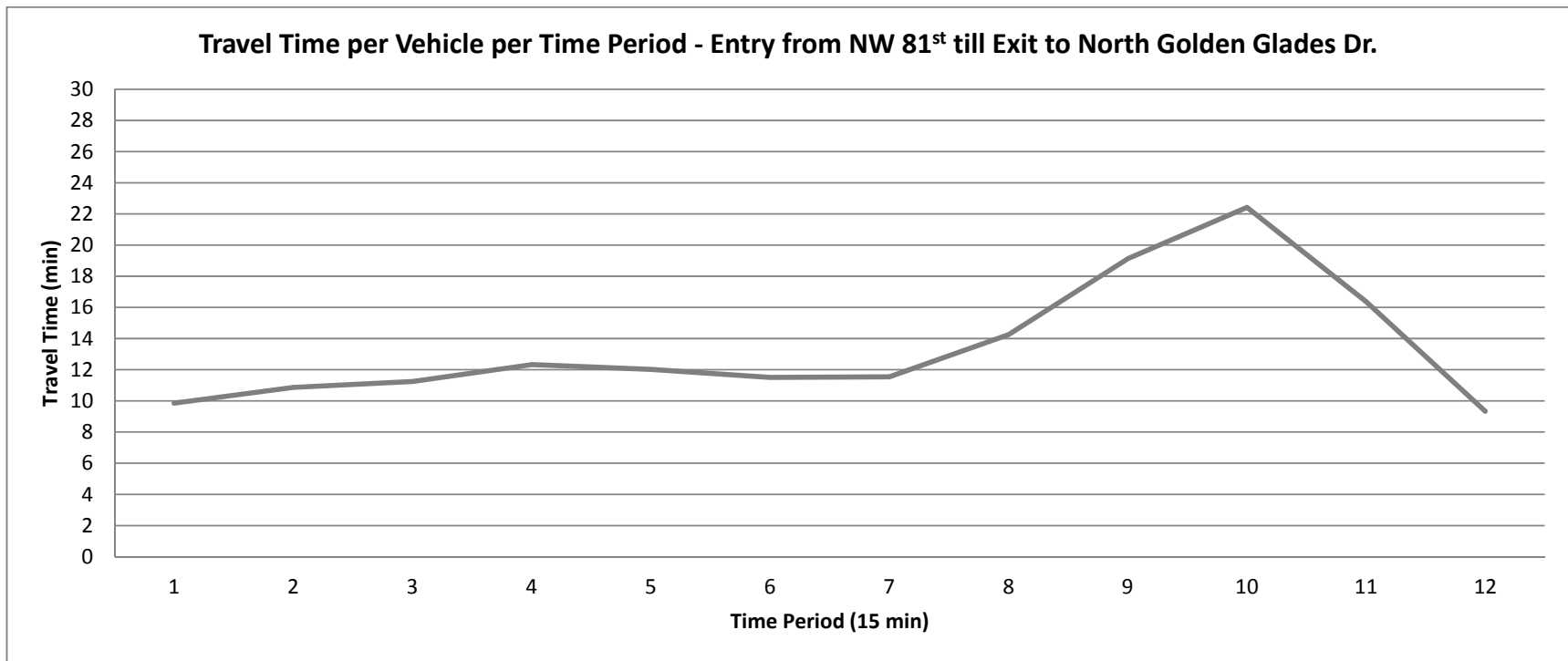


FIGURE 2.56 Scenario #1: Average travel time per vehicle from NW 81st St. to North Golden Glades

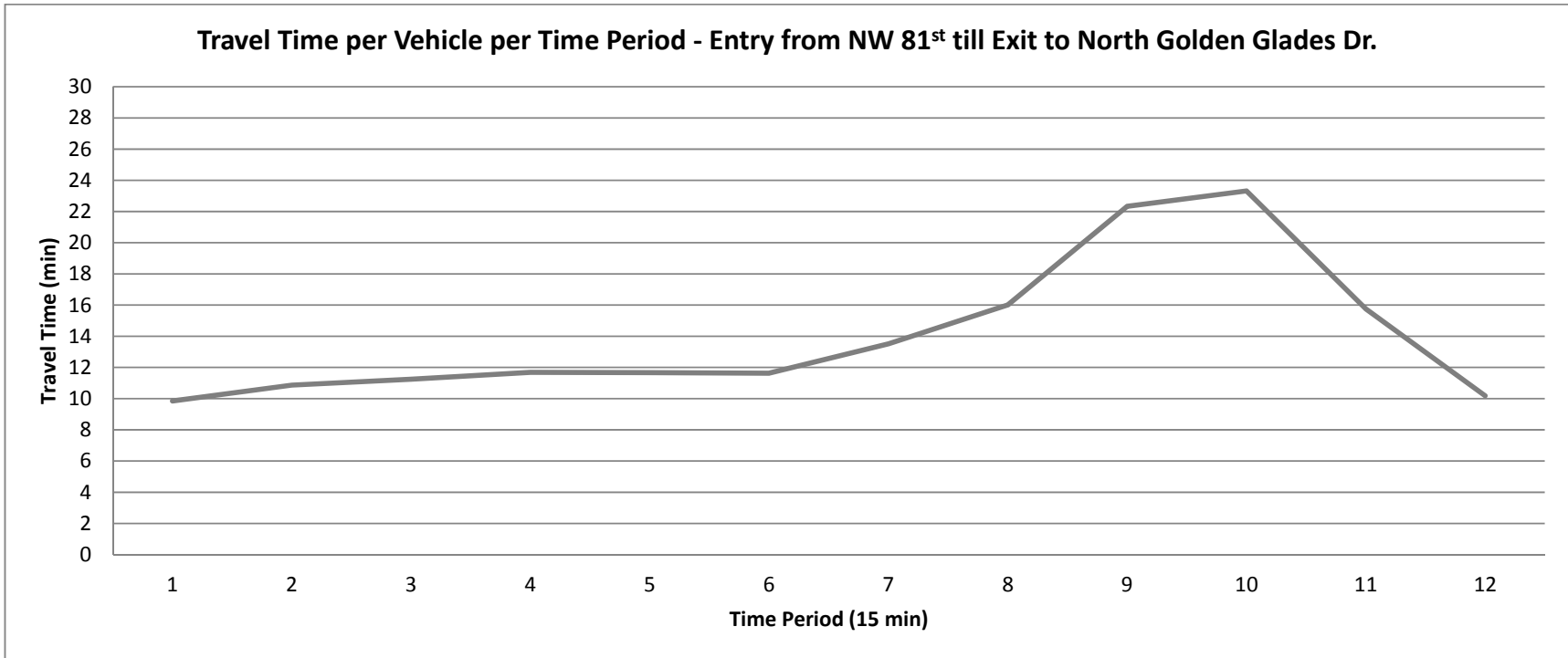


FIGURE 2.57 Scenario #2: Average travel time per vehicle from NW 81st St. to North Golden Glades

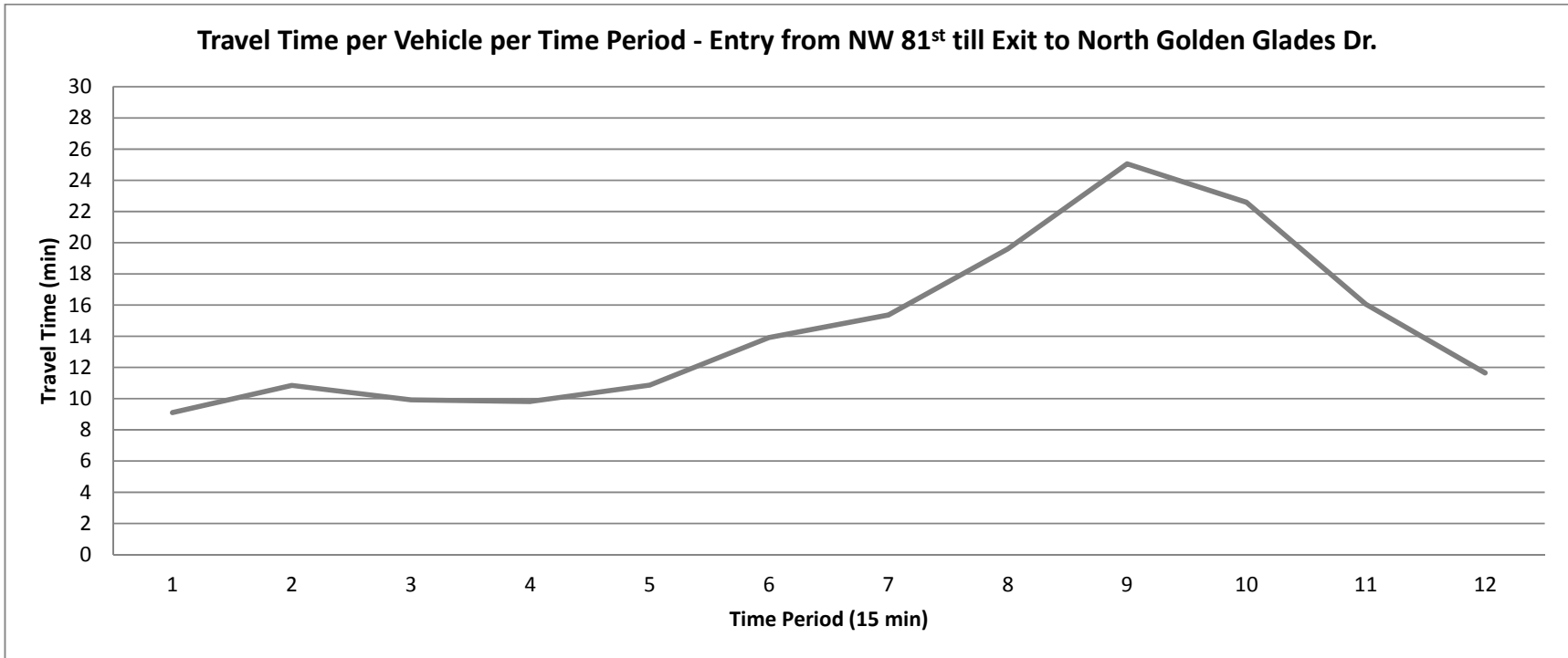


FIGURE 2.58 Scenario #3: Average travel time per vehicle from NW 81st St. to North Golden Glades

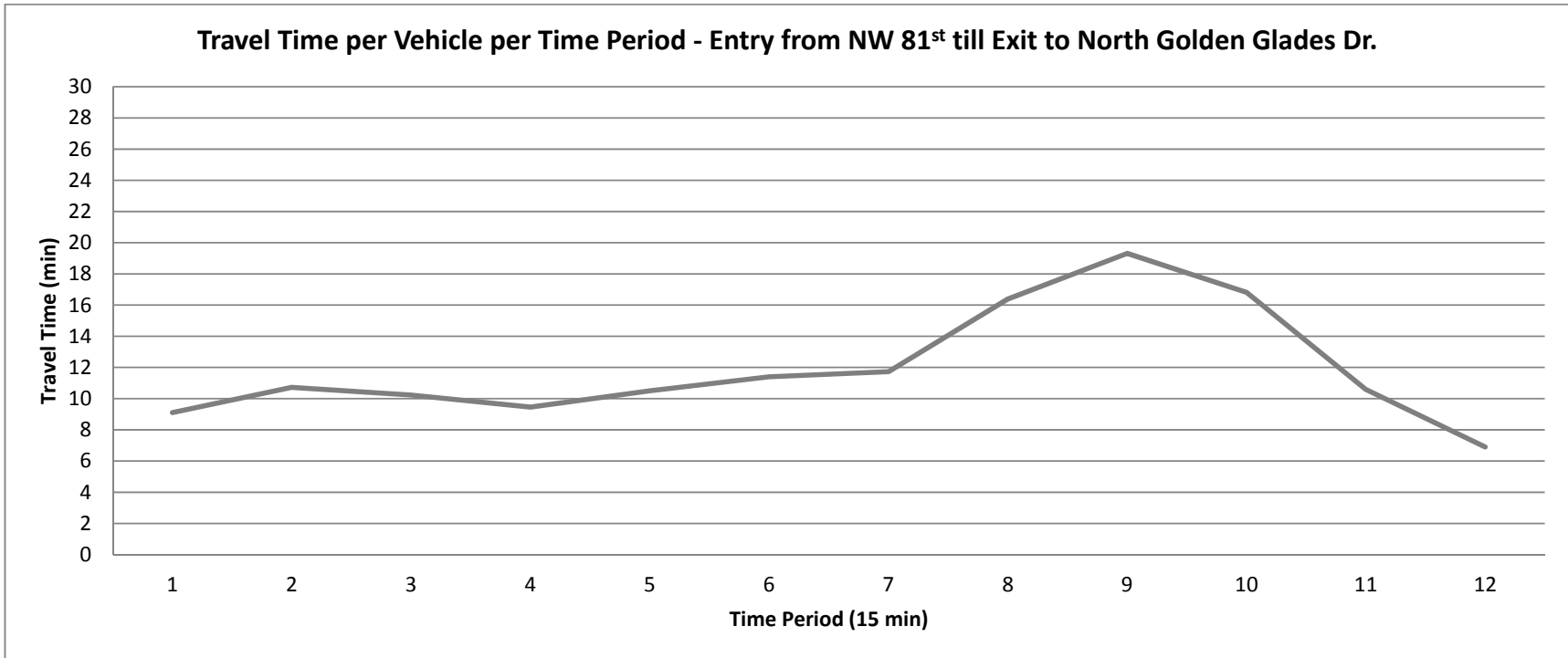


FIGURE 2.59 Scenario #4: Average travel time per vehicle from NW 81st St. to North Golden Glades

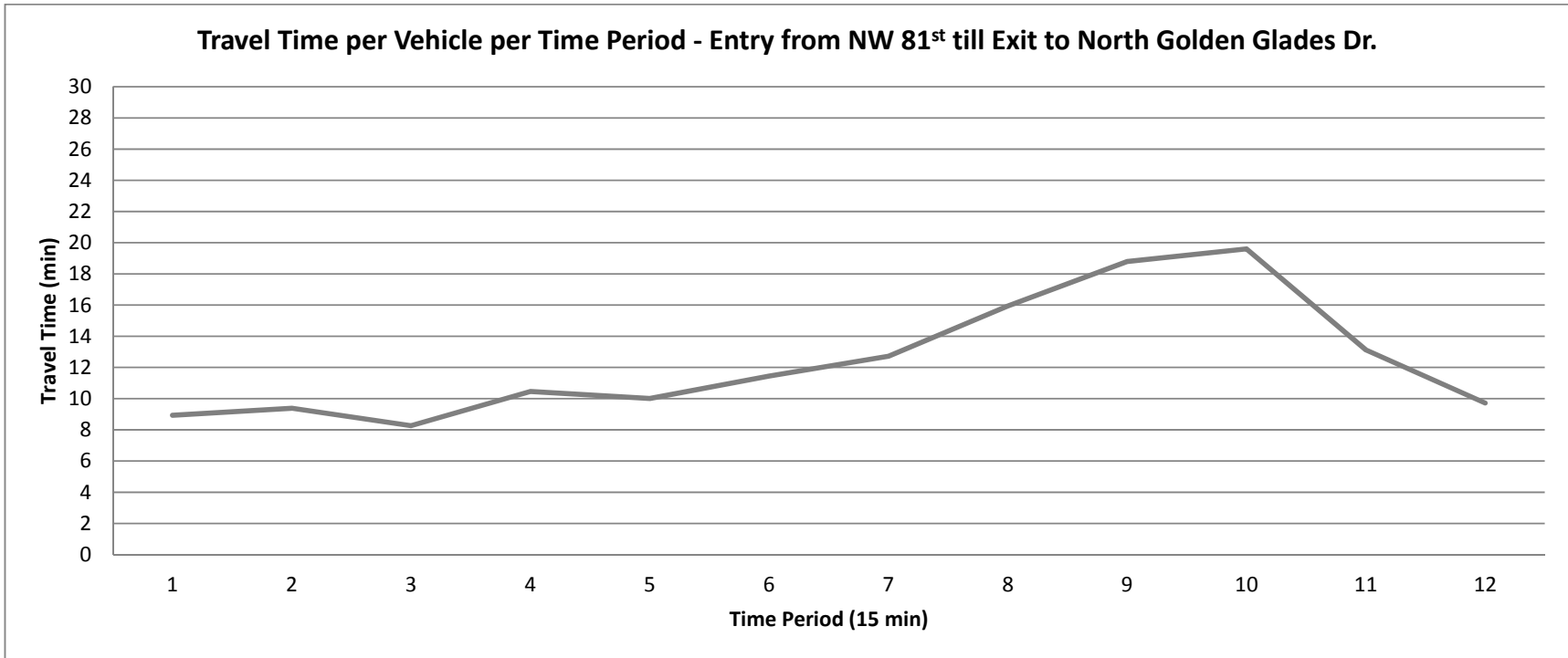


FIGURE 2.60 Scenario #5: Average travel time per vehicle from NW 81st St. to North Golden Glades

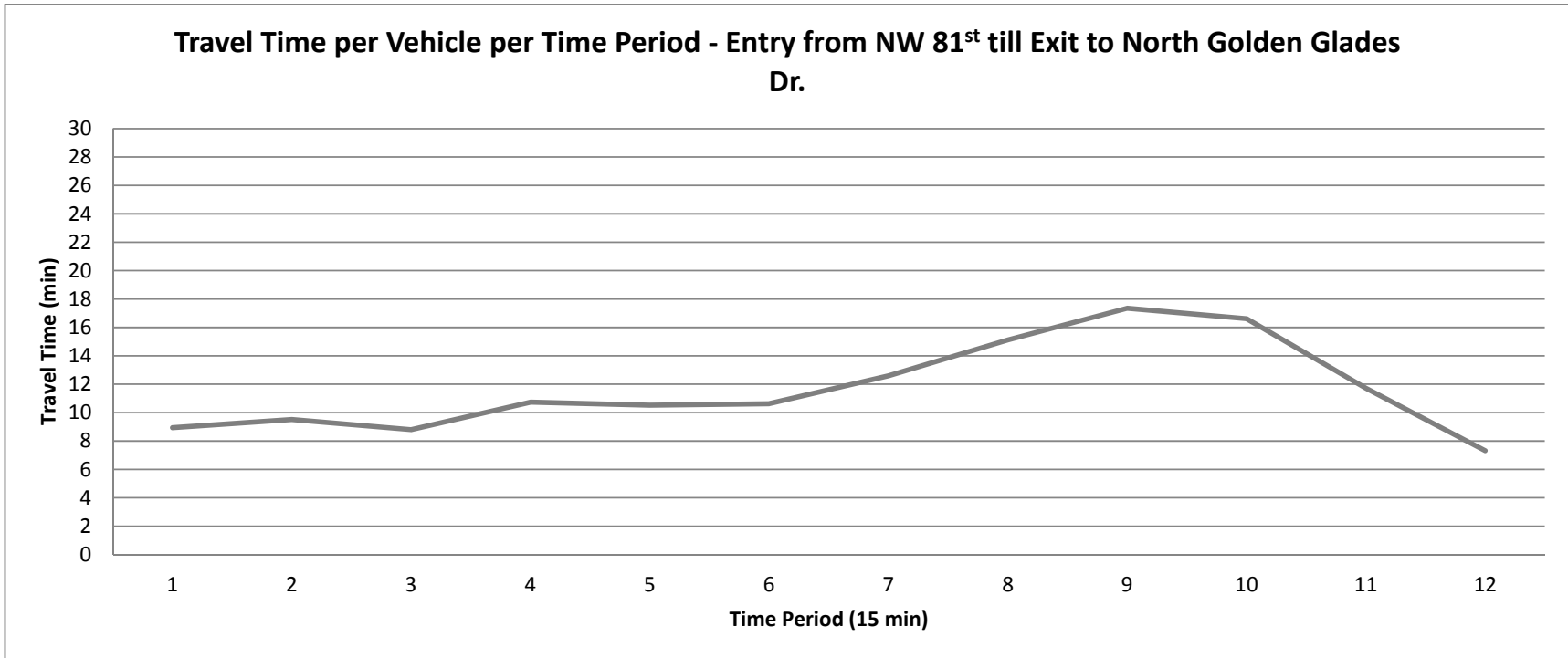


FIGURE 2.61 Scenario #6: Average travel time per vehicle from NW 81st St. to North Golden Glades

Next, we investigate the total delay at each of the on-ramps under each management scheme. Figures 2.62 to 2.64 provide the total delay of all vehicles on the ramp entering from 95th St. during the 9th time period for scenarios 2, 4 and 6 respectively. As shown, the delay is significantly lower when the dynamic metering and tolling scheme is implemented. The same pattern exists at the other three on-ramps that are located within this route.

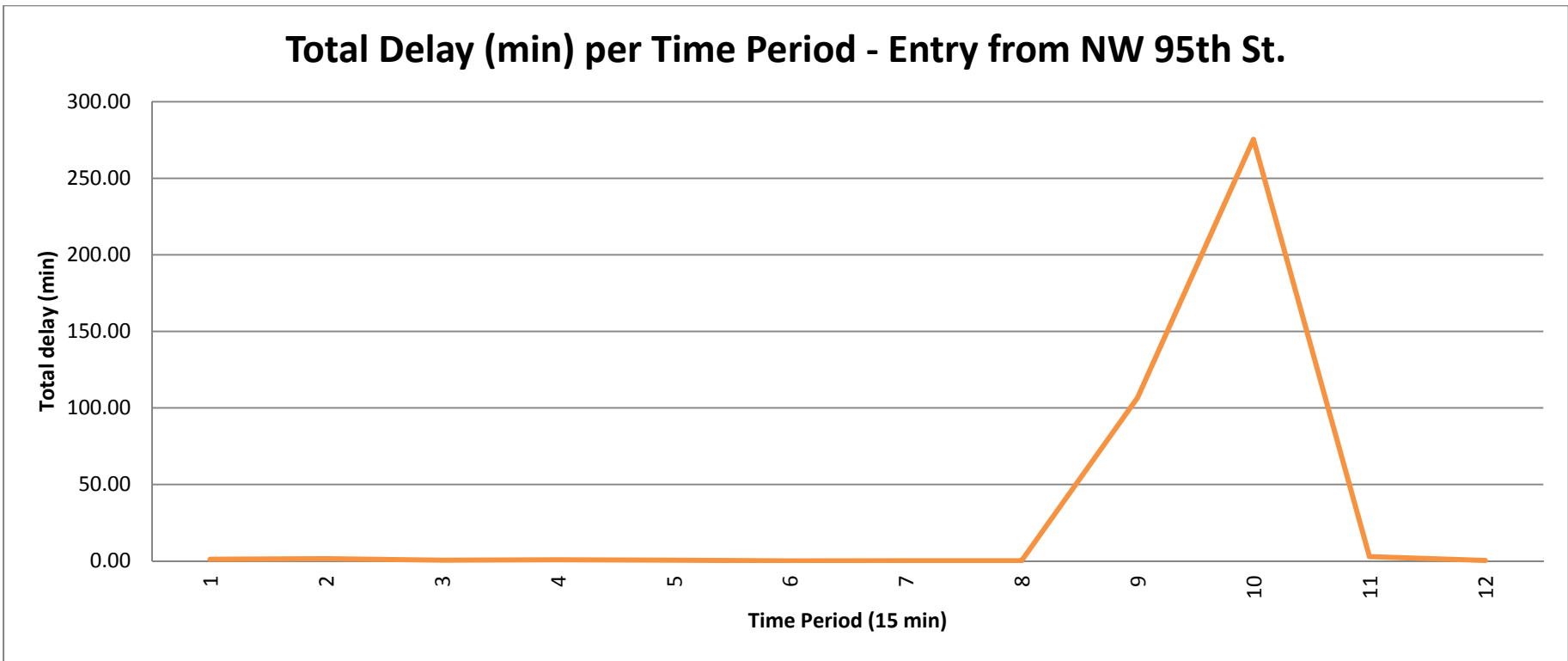


FIGURE 2.62 Scenario #2: Total delay at the first on-ramp downstream of NW 95th Street

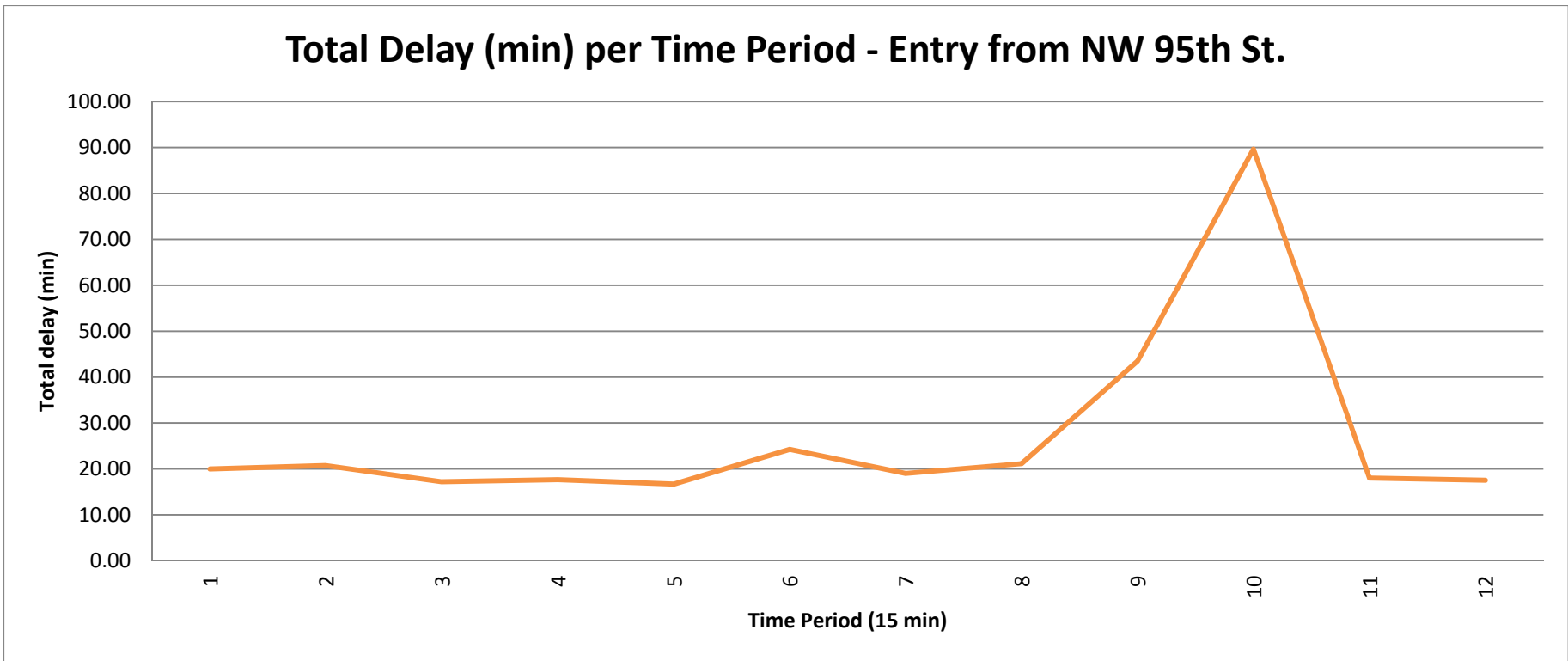


FIGURE 2.63 Scenario #4: Total delay at the first on-ramp downstream of NW 95th Street

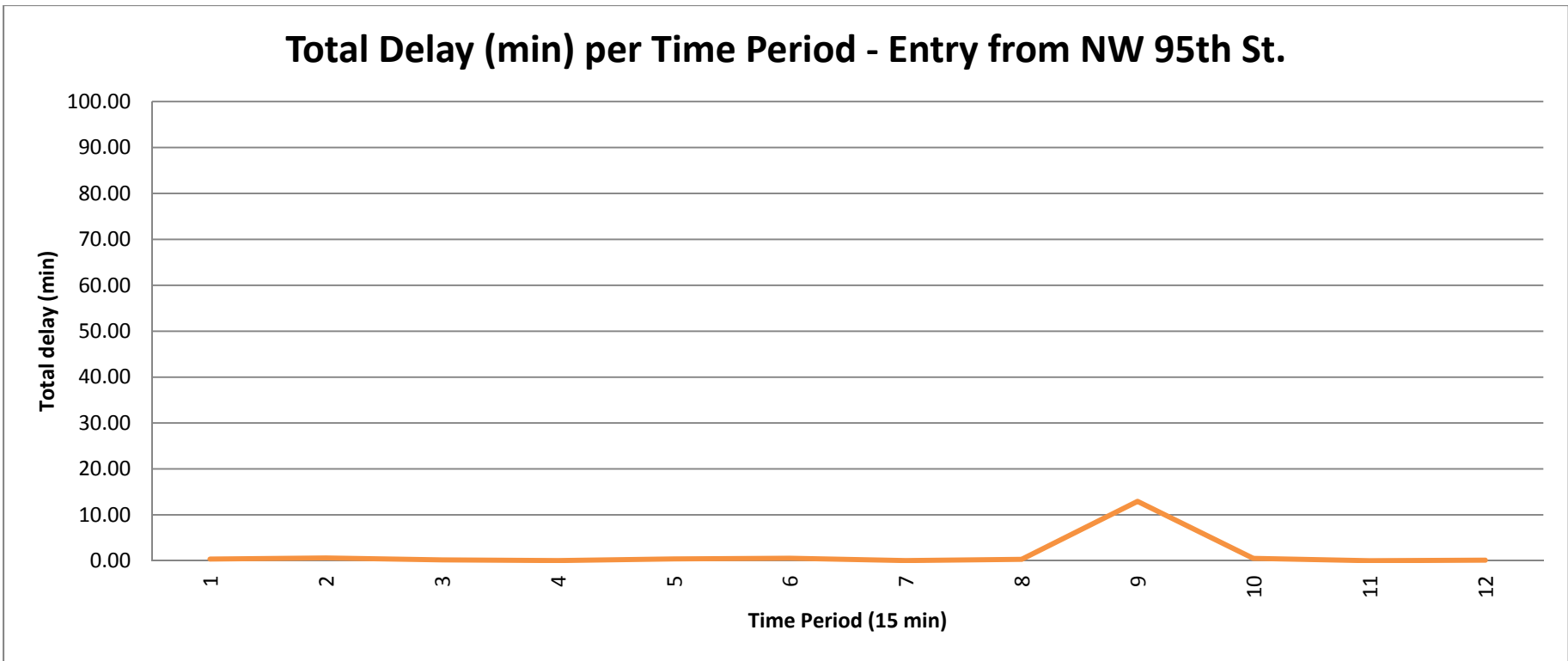


FIGURE 2.64 Scenario #6: Total delay at the first on-ramp downstream of NW 95th Street

3 VARIABLE SPEED LIMITS ON I-95 EXPRESS

This chapter is organized as follows. Section 3.1 describes the formulation of the experiments, including the study site characteristics, the development of the RTE and the scenarios tested. Section 3.2 presents the simulation results for individual signs and a coordinated VSL system.

3.1 Formulation of the Experiments

This section provides first a description of the study site and potential VSL implementation locations and briefly discusses the calibrated CORSIM file to be used in the experiments. The second subsection discusses the VSL algorithms selected for use in the simulation, along with the threshold and sign location scenarios to be tested for each algorithm. The last subsection discusses the RTE implementation.

3.1.1 Study site

The study site is a 13-mile section of I-95 in Miami, Florida, from I-395 to Miami Gardens Dr. in the northbound direction. This section of I-95 has two High Occupancy Tolling (HOT) lanes, as well as ramp metering. The VSL control is limited to the general purpose lanes and does not have a direct effect on the HOT lane operations. The roadway is already equipped with inductive loop detectors that can obtain speed, volume, and occupancy. These same sensors will be simulated, and it will be assumed that these will be used to relay information that triggers VSL control.

The researchers examined the speed profile along this facility to identify the bottleneck locations so that the VSL can be installed to mitigate these. The speed profile over the entire I-95 section analyzed is displayed in Figure 3.1. These speeds were averaged over a 15-minute period during the onset of congestion. As shown, there were two noticeable bottlenecks; one is located immediately before the exit to the turnpike, and the other is at the entry to NW 103rd street. This report evaluates the operations of the corridor if VSL is implemented at each of these locations separately one at a time, as well as simultaneously.

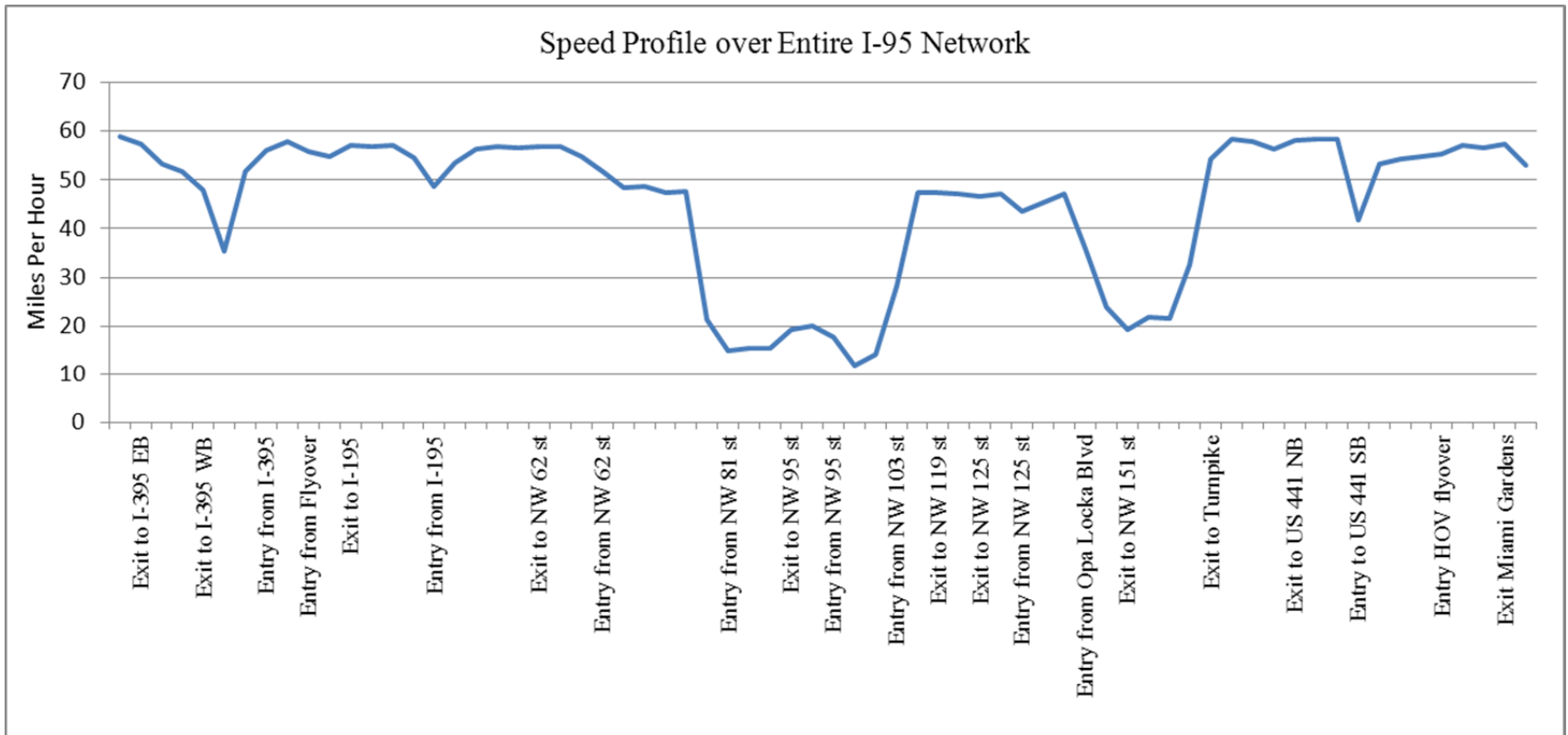


FIGURE 3.1 Speed profile of the I-95 section at the onset of congestion (4:15 p.m. to 4:30 p.m.).

The CORSIM network used for this study was developed in Task 5 of this project and replicates traffic operations on the stretch of I-95 (Chapter 2 of the Project Final Report). The field data used in this task for calibration of the network were obtained from the STEWARD database. The data were obtained on October 7, 2009, from 3:30 p.m. to 6:30 p.m. These three hours were selected to include the p.m. peak period and the associated congestion formation and dissipation. The network was calibrated to match field-recorded volumes and speeds for each 15-min period of the simulation, and it replicated both the ramp metering and HOT lane operations. The ramp metering used a constant metering rate that is not demand sensitive, and thus it was not expected to interact with the VSL algorithms in these simulations. The HOT lanes were modeled as a separate parallel facility with interchanges at various access points.

3.1.2 VSL Algorithms

The study selected algorithms that use different measures for triggering a speed limit change, to evaluate the impacts of different types of algorithms. Based on the literature review (Appendix B), three algorithms were selected for simulation: occupancy-based, volume-based, and combined flow/occupancy/speed algorithm. These represent the major types of algorithms that have been tested and implemented to-date. The occupancy-based algorithm was selected because it is currently implemented on I-4 in Orlando, Florida. The volume-based algorithm was selected because it is implemented on the M25 in England (Robinson, 2000) with very good overall results. The third algorithm selected is based on a combination of flow, occupancy, and average travel speed, and it is based on a study of a freeway in Toronto, Canada (Allaby et al., 2007). This algorithm was selected because it seemed a promising alternative to the other two; however, this one has not been implemented in the field.

Each algorithm functions similarly within the freeway system. An inductive loop detector is located at the bottleneck, and relays 1-minute averages of speed, occupancy, and/or volume to a VSL sign upstream of this location. When a particular threshold value is reached the speed limit is reduced at the associated VSL sign. Similarly, when a parameter drops below one of the reverse thresholds the speed limit is allowed to increase back to a higher speed. To prevent a rapid fluctuation of speed limits, each algorithm has one set of thresholds for lowering the speed limit and another set of thresholds for raising them. The speed limit is only allowed to drop by

one increment at a time. For instance, if the current speed limit is 55 mph, and a threshold is reached that notifies the sign to drop to 45 mph, the speed limit is only reduced to 50 mph. This prevents drastic changes in the speed limit that might create driver confusion.

Each algorithm can operate under a broad range of threshold values. The following paragraphs describe each algorithm along with the threshold values and scenarios tested for that algorithm.

3.1.2.1 Algorithm Based on Occupancy

The algorithm based on occupancy has two sets of threshold values; one for the decreasing of speed limits and one for the increasing of speed limits. The VSL sign is linked to a downstream detector, and the average occupancy is calculated for all lanes. The traffic is classified as either free-flow, light congestion, or heavy congestion. If the occupancy crosses a threshold the speed limit is decreased by an increment of five miles per hour. Similarly the speed limit may increase back to its previous value but not more than 5 mph at a time. This algorithm is based on the current operating algorithm of the I-4 system (PBS&J, 2009). The I-4 implementation evaluates the speed limit every 120 seconds, while this study evaluates the speed limit every 60 seconds. The first threshold scenario uses the same values as the I-4 system. The next two threshold scenarios are generated based on findings from NCHRP Report 3-87 (Elefteriadou et al. 2011). That report studied occupancy values as a function of the probability of breakdown at merge junctions. The three threshold scenarios are shown in Table 3.1, Table 3.2, and Table 3.3.

TABLE 3.1 Occupancy thresholds for displayed speed limits (scenario 1)

Traffic Category	Occupancy for decreasing speed limit (%)	Occupancy for increasing speed limit (%)	Speed limit (mph)
Free flow	< 16	< 12	55
Light congestion	16 - 28	12 - 25	50
Heavy congestion	> 28	>25	45

TABLE 3.2 Occupancy thresholds for displayed speed limits (scenario 2)

Traffic category	Occupancy for decreasing speed limit (%)	Occupancy for increasing speed limit (%)	Speed limit (mph)
Free flow	< 10	< 8	55
Light congestion	10 - 30	8 - 27	50
Heavy congestion	> 30	>2	45

TABLE 3.3 Occupancy thresholds for displayed speed limits (scenario 3)

Traffic category	Occupancy for decreasing speed limit (%)	Occupancy for increasing speed limit (%)	Speed limit (mph)
Free flow	< 20%	< 17%	55
Light congestion	20 - 35%	17 - 32%	50
Heavy congestion	> 35%	>32%	45

3.1.2.2 Algorithm Based on Flow

The algorithm based on volumes also uses two threshold values; one for the decreasing of speed limits and one for the increasing of speed limits. The VSL sign is linked to a downstream detector location, and average volume is computed in vehicles per hour per lane. When a volume drops below a specified threshold, the speed limit is decreased accordingly. To return to the original speed the volume must cross a different threshold. The first set of threshold values were obtained from a study conducted on the M25 in England (Robinson, 2000), and are shown in Table 3.4. The second set of thresholds are obtained from speed flow diagrams in the 2000 Highway Capacity Manual (HCM, 2000), and are shown in Table 3.5. The thresholds are obtained by locating the volume of traffic where speeds drop for a given speed, using the associated volume as the threshold point.

TABLE 3.4 Volume thresholds for displayed speed limits (scenario 1)

Flow for decreasing speed limit (vphpl)	Flow for increasing speed limit (vphpl)	Speed limit (mph)
< 1650	-	55
> 1650	< 1450	50
> 2050	<1850	45

TABLE 3.5 Volume thresholds for displayed speed limits (scenario 2)

Flow for decreasing speed limit (vphpl)	Flow for increasing speed limit (vphpl)	Speed limit (mph)
< 1450	-	55
> 1450	< 1250	50
> 2000	<1800	45

3.1.2.3 Algorithm Based on a Logic Tree including Flow, Occupancy, and Average Speed

In this algorithm, speed limits are determined based on a logic tree that includes flow, occupancy, and average travel speed. The decision making logic is shown in Figure 3.2. The algorithm first takes into account flow data from a downstream loop detector. If the volume is less than or equal to 1650 vphpl, the next step is to consider occupancy. If occupancy is less than or equal to 10%, the maximum speed limit is posted. If the occupancy is greater than 10%, average speed determines which speed is displayed. Going back to the first step, if the volume is greater than 1650 vphpl, the logic skips straight to the average speed calculation. The speed to be displayed is then sent to the appropriate VSL sign. This algorithm is based on research conducted on a candidate VSL system in Toronto, Canada (Allaby, 2007).

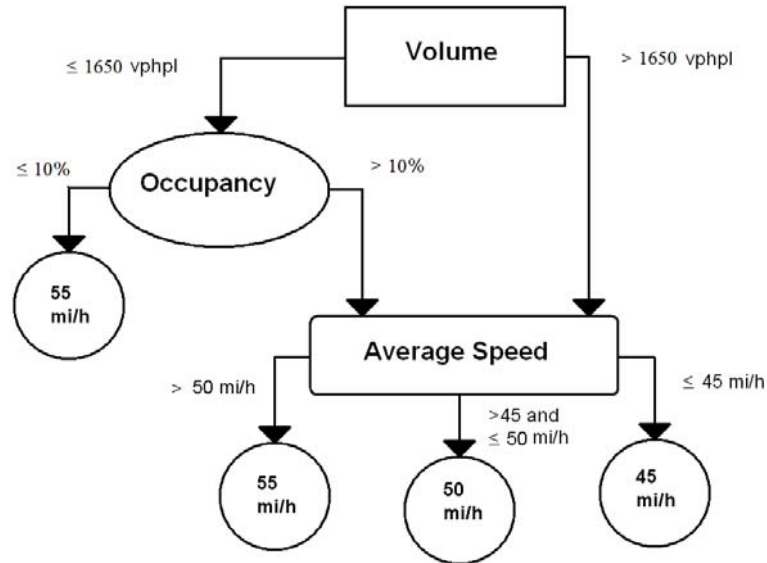


FIGURE 3.2 Decision tree logic for combined flow/occupancy/speed algorithm

3.1.3 Sign location variations

In addition to the three VSL algorithms and various threshold values, four different sign location scenarios were tested for each bottleneck. Each scenario used the same detectors but varies the location of VSL signs, which is where drivers are advised of the change in the speed limit. In each case the same detector location was used for control, and was located at the source of congestion. The first scenario used one VSL sign spaced approximately one-half mile from the bottleneck. The second scenario used one sign spaced approximately one mile from the bottleneck. The third scenario used two signs: the first sign was placed approximately one-half mile from the bottleneck and the second one-half mile upstream from the first sign. The fourth scenario used two signs: the first sign was placed approximately one mile from the bottleneck and the second sign one mile upstream of the first sign. In the two-sign scenario, the downstream sign was linked to the detector and the speed limit was updated based the relayed data. The upstream sign always displayed a speed limit 5 mph higher than the downstream sign, except during normal operation. For example, if the downstream sign displays 55 mph, the upstream sign also displays 55 mph. If the downstream sign displays 50 mph, the upstream sign still displays 55 mph. If the downstream sign displays 45 mph, the upstream sign displays 50 mph. The purpose of this operation is to create a smooth transition between speed limits. The four sign location scenarios for each bottleneck are shown visually in Figures 3.3 through 3.10.

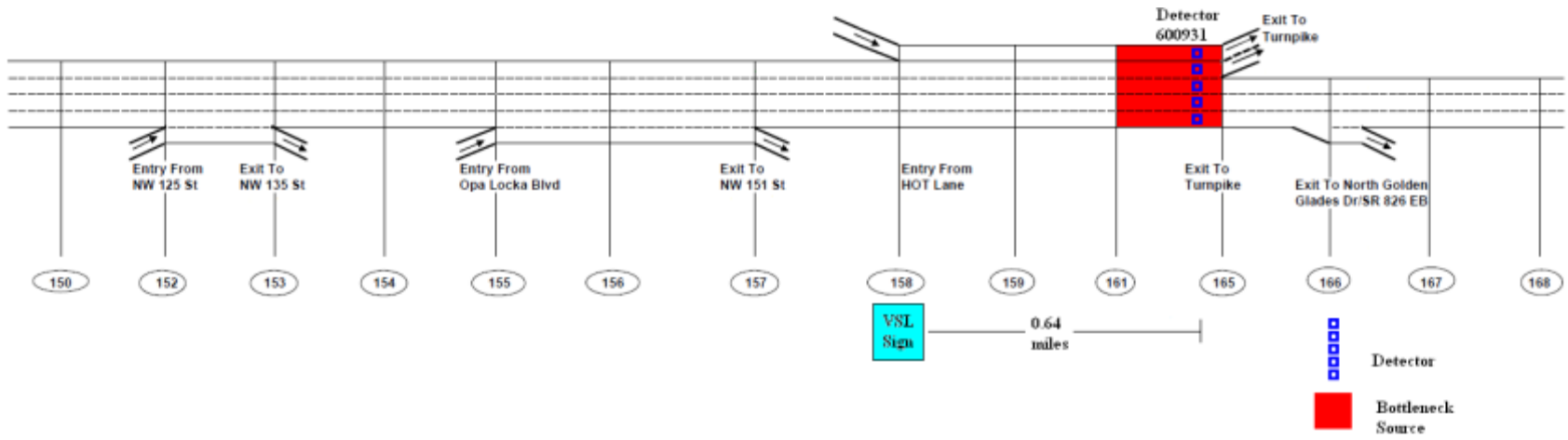


FIGURE 3.3 Use of one sign located approximately one-half mile upstream of Bottleneck 1

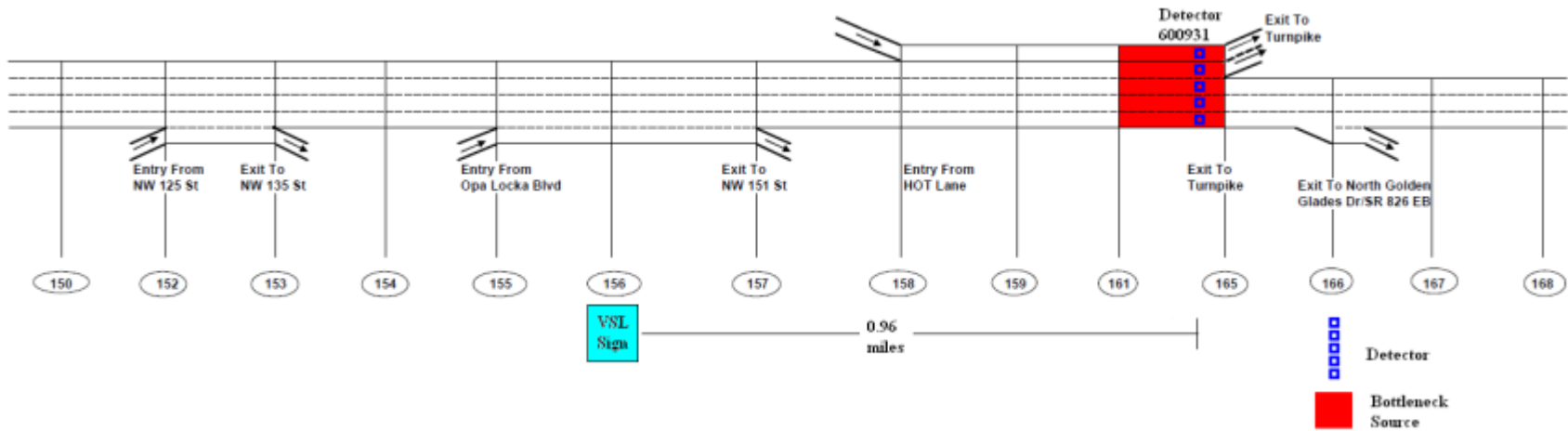


FIGURE 3.4 Use of one sign located approximately one mile upstream of Bottleneck 1

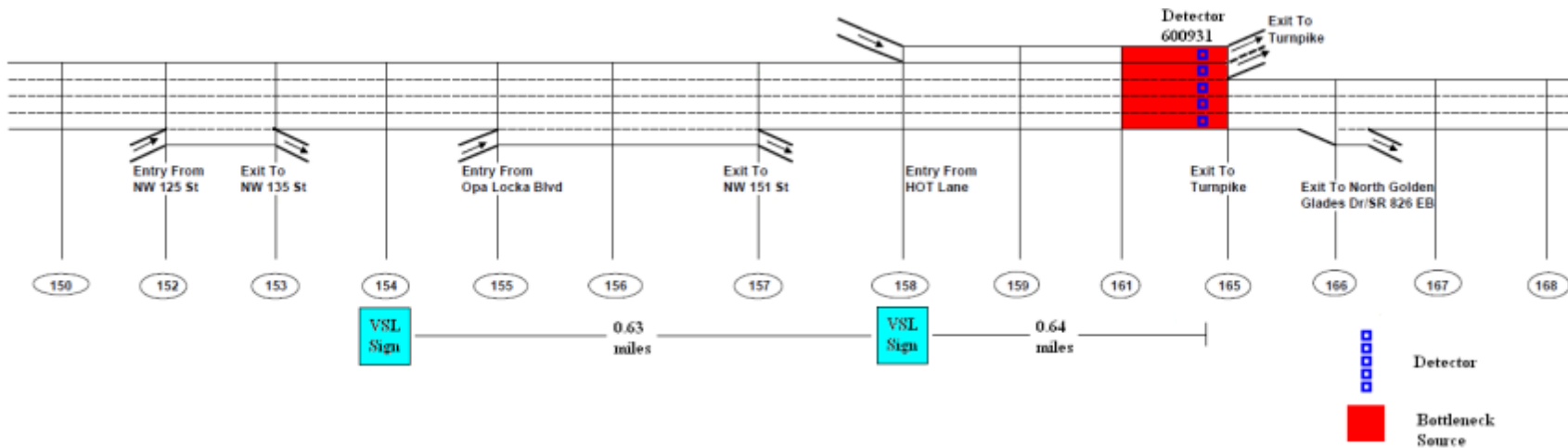


FIGURE 3.5 Use of two signs spaced approximately one-half mile apart upstream of Bottleneck 1

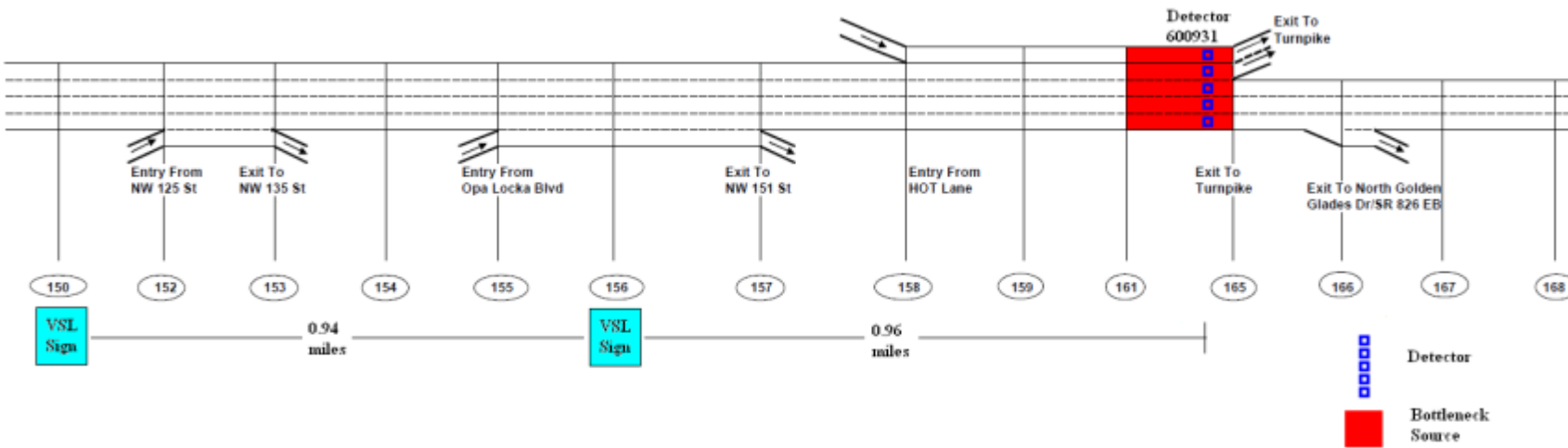


FIGURE 3.6 Use of two signs spaced approximately one mile apart upstream of Bottleneck 1

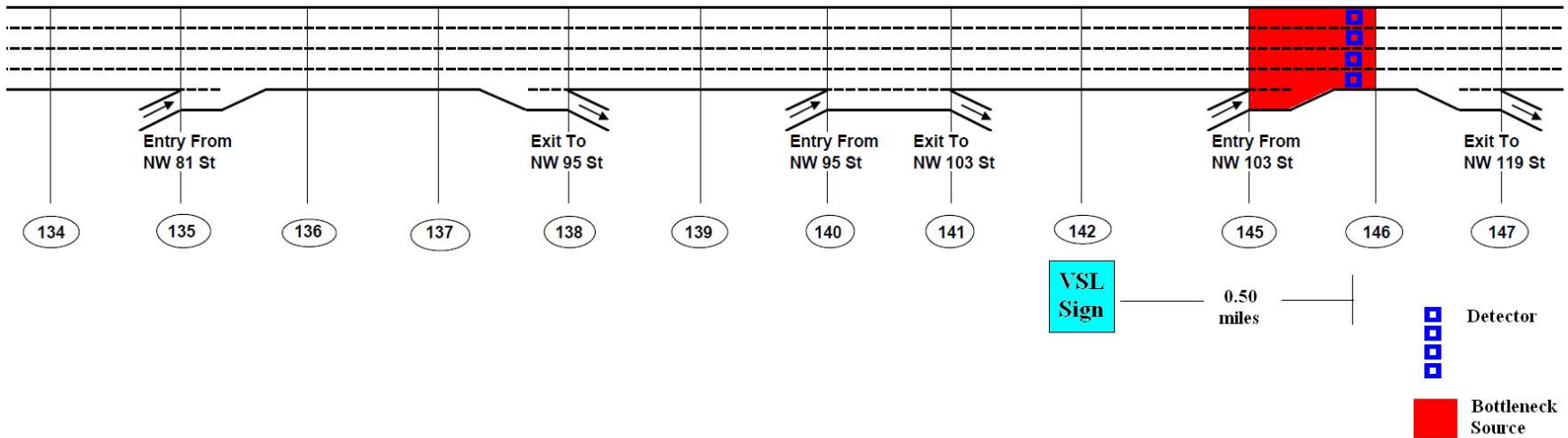


FIGURE 3.7 Use of one sign located approximately one half mile upstream of Bottleneck 2

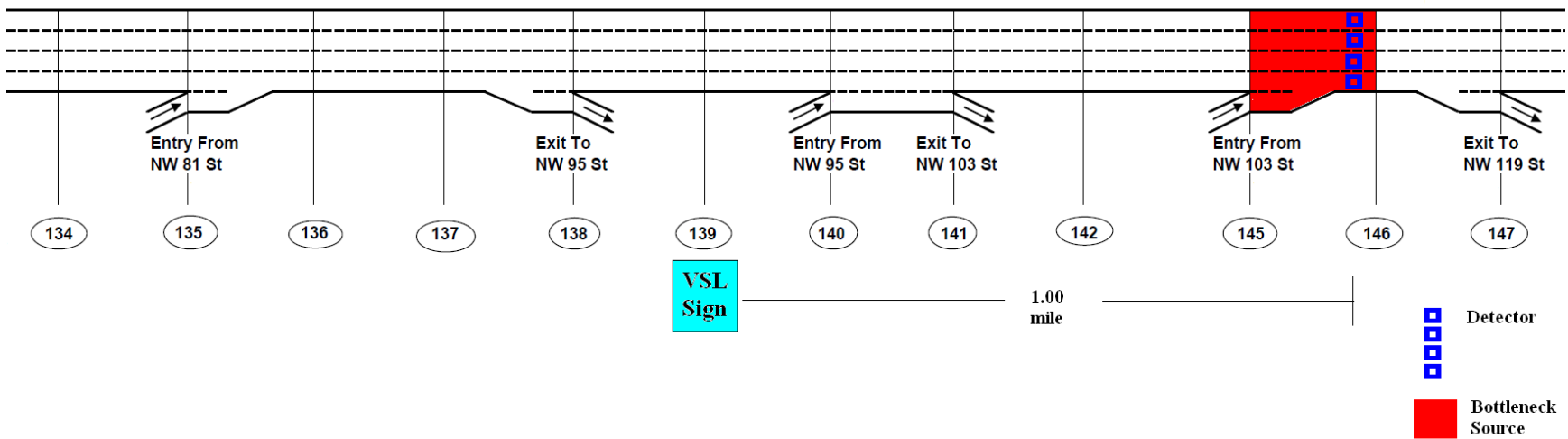


FIGURE 3.8 Use of one sign located approximately one mile upstream from Bottleneck 2

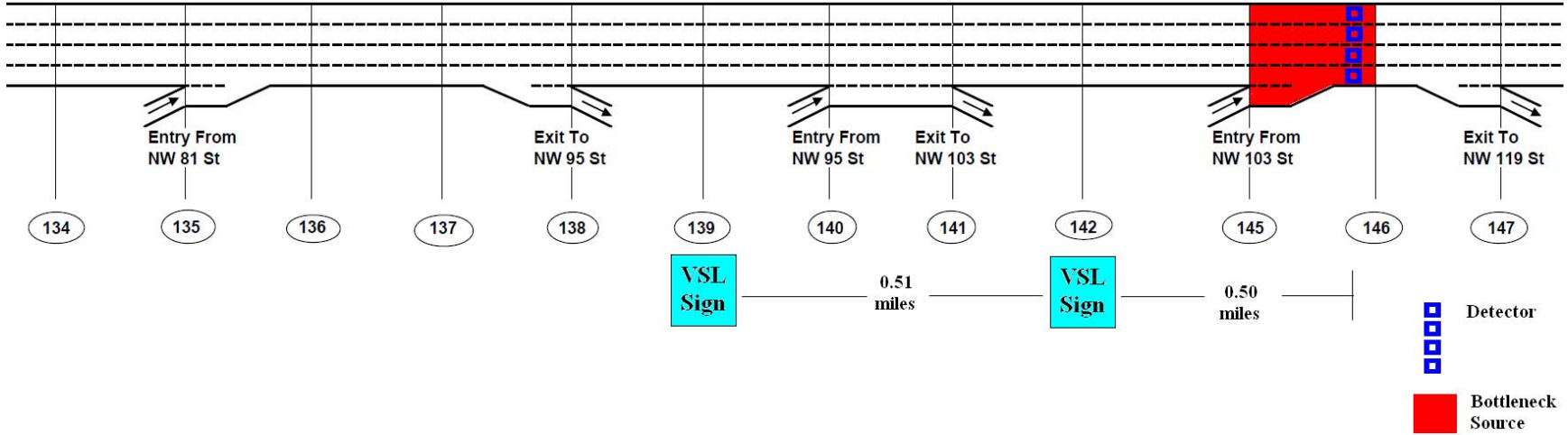


FIGURE 3.9 Use of two signs spaced approximately one half mile apart upstream of Bottleneck 2

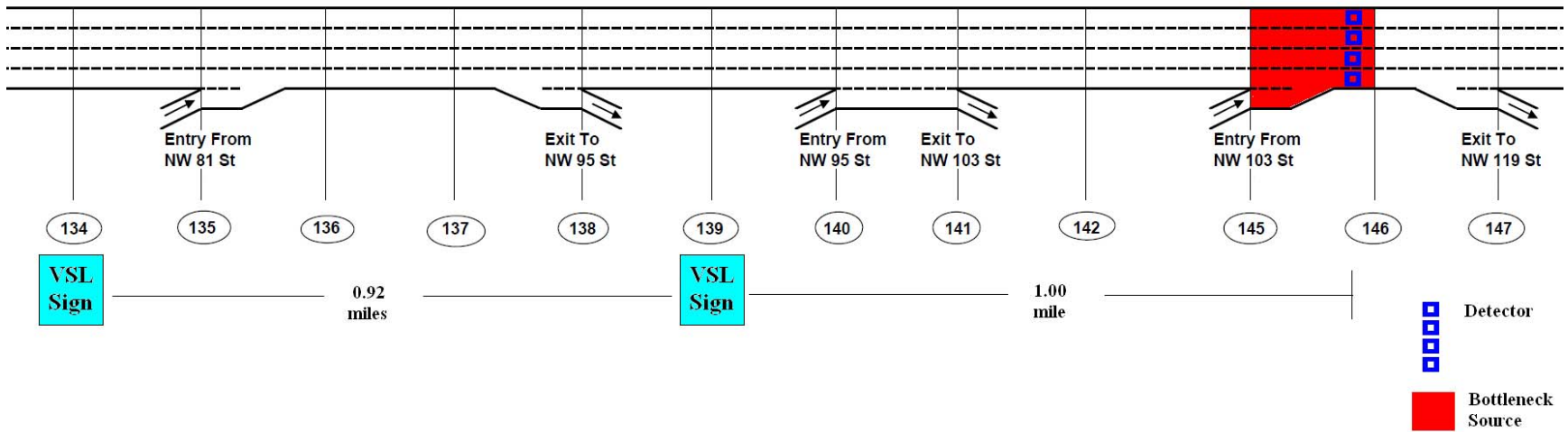


FIGURE 3.10 Use of two signs spaced approximately one mile apart upstream of Bottleneck 2

3.1.4 The CORSIM RTE Interface

Implementing the algorithms on the CORSIM network required a dynamic link library (DLL) that interfaces with the CORSIM simulation in real-time. CORSIM allows this DLL to be imported through an RTE interface. The interface allows the DLL to import and export variables internal to CORSIM. Three different DLLs were built, one for each type of algorithm. The general structure of the program worked similarly for each case, but the rules and thresholds for the speed change logic differ between each program. A flowchart with the general logic of the program is shown in Figure 3.11.

Upon initialization of the simulation, the DLL program identifies where VSL signs have been specified, and what detectors are used to control the VSL operation. The links affected by the VSL sign are also identified. This allows the speeds on the downstream links to be updated when a speed limit change occurs. During the initialization period the point processing interval is also defined. This determines how data are aggregated from the inductive loop detectors. For this set of scenarios the point processing interval has been set to 60 seconds.

After initialization is complete, the DLL is accessed at the call point PREFRESIMVEHICLE. This occurs every time-step (one second) during the simulation before vehicle movement takes place. First the program checks to determine whether the simulation is still in the initialization period (which is at the beginning of the simulation as the simulated network fills up with vehicles.) If so, the program exits the function and this is reassessed at the next time step. If the simulation is not in the initialization period the current speed limit is assessed based on average values relayed from the specified detectors. If it is determined that a speed change is to occur, the free-flow speed is updated on the link containing the VSL sign. At the same time a message is displayed on the computer as the simulation runs to indicate a speed change has occurred in the network. An example of a speed change message during the CORSIM simulation with the occupancy algorithm is displayed in Figure 3.12.

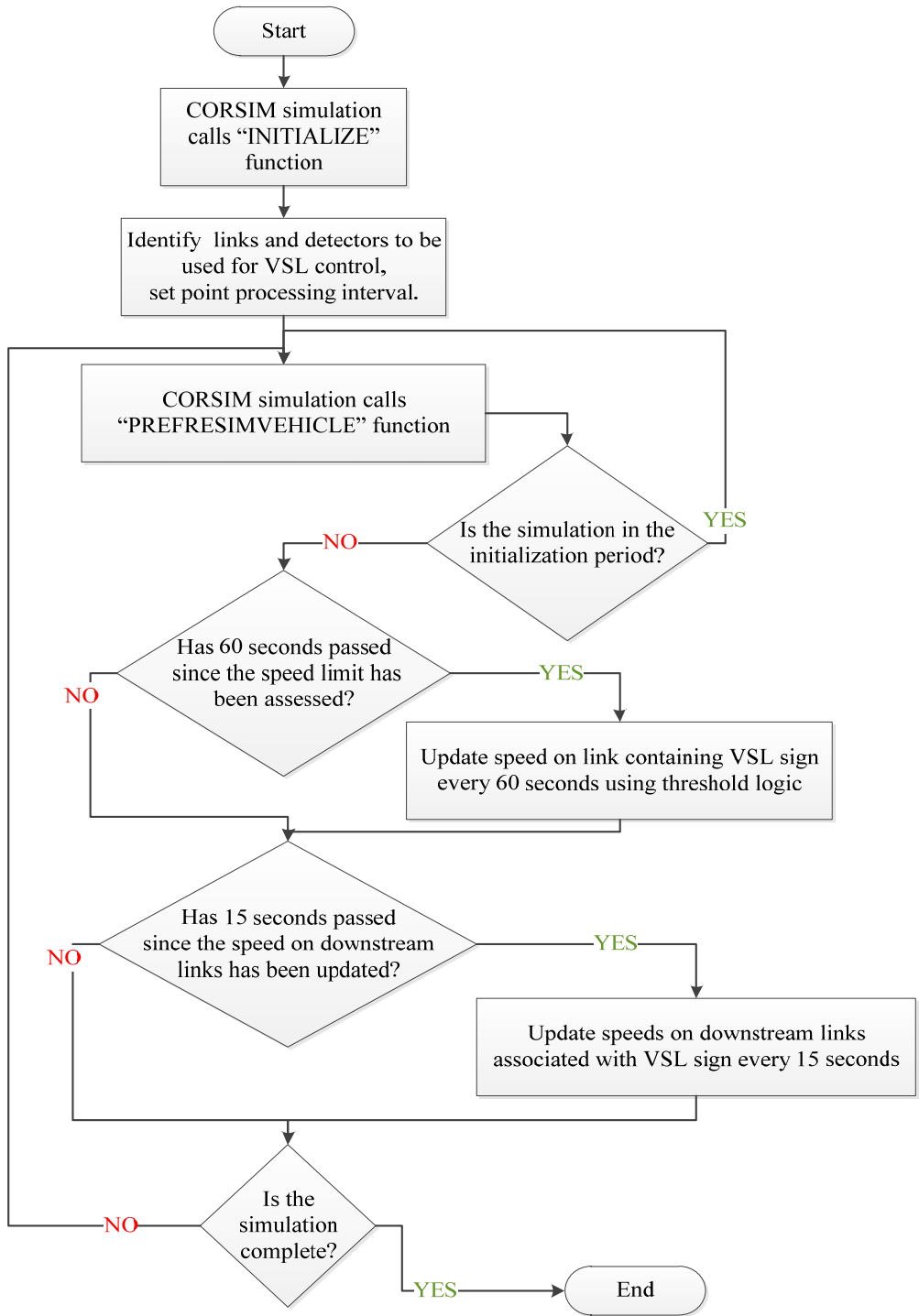


FIGURE 3.11 Flowchart of RTE logic

```

NETWORK HAS REACHED EQUILIBRIUM.
COMPLETED 60 SECONDS OF SIMULATION..... (CORSIM) ( 2.83 CPU Seconds)
Speed Limit has been reduced to 50 MPH, with Average Occupancy:29.257435

COMPLETED 120 SECONDS OF SIMULATION..... (CORSIM) ( 3.28 CPU Seconds)
COMPLETED 180 SECONDS OF SIMULATION..... (CORSIM) ( 3.14 CPU Seconds)
COMPLETED 240 SECONDS OF SIMULATION..... (CORSIM) ( 3.27 CPU Seconds)
COMPLETED 300 SECONDS OF SIMULATION..... (CORSIM) ( 3.40 CPU Seconds)
COMPLETED 360 SECONDS OF SIMULATION..... (CORSIM) ( 3.33 CPU Seconds)
COMPLETED 420 SECONDS OF SIMULATION..... (CORSIM) ( 3.21 CPU Seconds)
COMPLETED 480 SECONDS OF SIMULATION..... (CORSIM) ( 3.28 CPU Seconds)
COMPLETED 540 SECONDS OF SIMULATION..... (CORSIM) ( 3.86 CPU Seconds)
COMPLETED 600 SECONDS OF SIMULATION..... (CORSIM) ( 3.47 CPU Seconds)
COMPLETED 660 SECONDS OF SIMULATION..... (CORSIM) ( 3.69 CPU Seconds)
COMPLETED 720 SECONDS OF SIMULATION..... (CORSIM) ( 3.76 CPU Seconds)
COMPLETED 780 SECONDS OF SIMULATION..... (CORSIM) ( 4.09 CPU Seconds)
COMPLETED 840 SECONDS OF SIMULATION..... (CORSIM) ( 4.28 CPU Seconds)
COMPLETED 900 SECONDS OF SIMULATION..... (CORSIM) ( 6.30 CPU Seconds)
TOTAL CPU TIME FOR THIS RUN = 134.97 SECONDS
**** THERE WERE 1 WARNING MESSAGES.

```

FIGURE 3.12 Screen shot of computer run indicating a change in the speed limit

After the free flow speed has been updated on the link containing the VSL sign, the free flow speed is updated gradually on the downstream links. The free flow speeds at the downstream links are updated every 15 seconds, and the time of the speed change depends on the free flow speed and distance between the VSL sign and the downstream link. This creates a rolling speed change so that all the downstream links are not updated simultaneously. This method mimics a real world scenario where the first vehicle observing a speed change represents a rolling speed change through the downstream links. Figure 3.13 shows how the speed change would propagate downstream for a sample speed limit change. In the diagram the speed limit drops from 55 to 50 mph starting at the VSL sign. The downstream link speeds are then updated every 15 seconds based on the length of the link and the free flow speed.

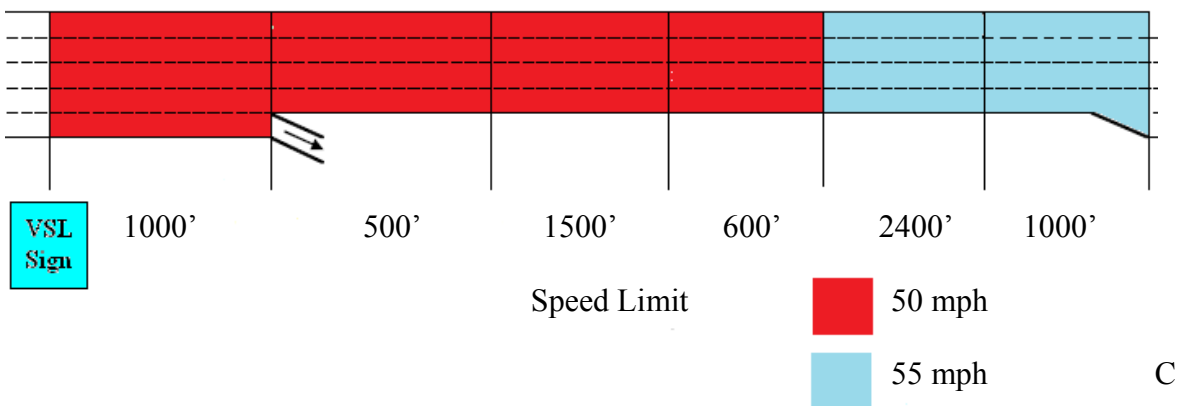
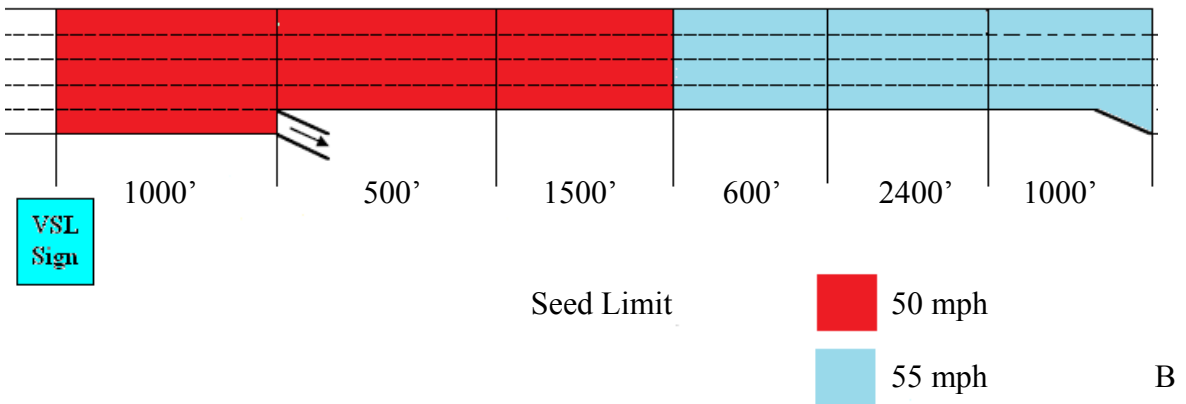
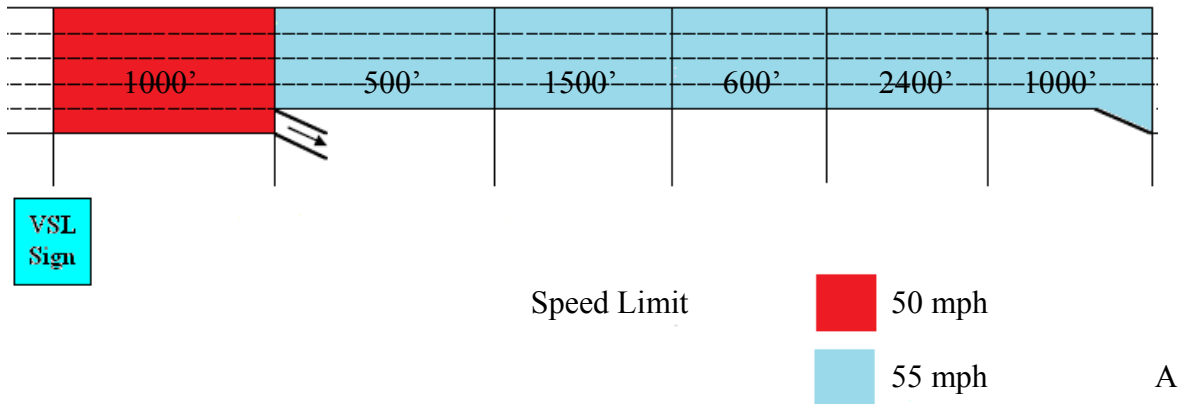


FIGURE 3.13 Speed limit propagation downstream from VSL sign location. Simulation time from change of speed limit: A) 0 seconds; B) 15 seconds; C) 30 seconds; D) 45 seconds; E) 60 seconds; F) 75 seconds

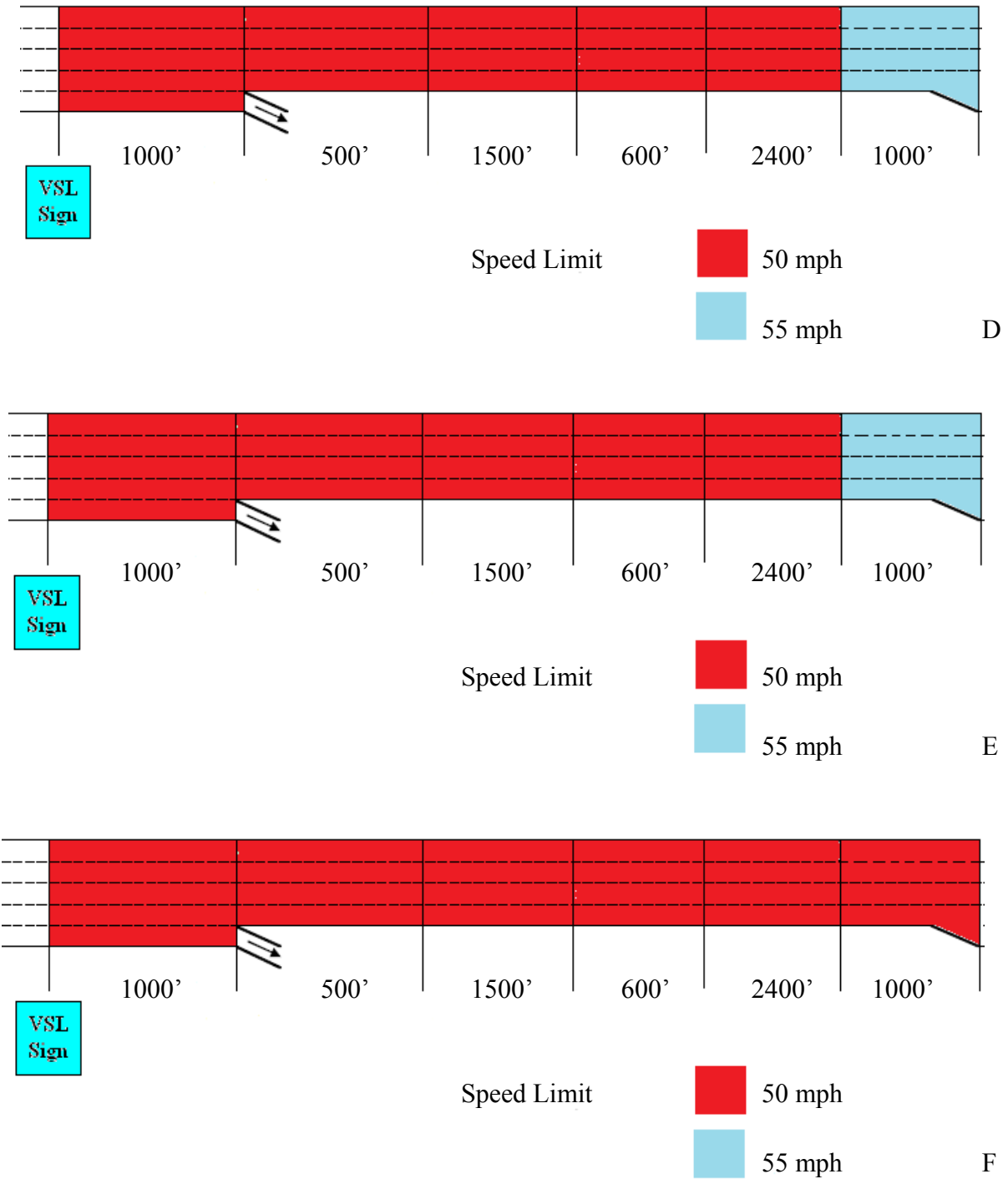


FIGURE 3.13 (Continued) Speed limit propagation downstream from VSL sign location. Simulation time from change of speed limit: A) 0 seconds; B) 15 seconds; C) 30 seconds; D) 45 seconds; E) 60 seconds; F) 75 seconds

3.2 Implementation and Analysis of Algorithms in CORSIM

This section presents the implementation of the algorithms and results obtained from the simulations. The first subsection describes all the scenarios that are implemented and how the simulations are carried out. The second subsection examines the results of the no-control scenario, and identifies the bottleneck sources. The third subsection presents the simulation results for VSL control along the first (downstream) bottleneck, while the fourth subsection presents the simulation results for the second (upstream) bottleneck. The fifth section describes the results of the simulation for VSL implemented along both bottlenecks. The last section provides a summary of the conclusions from all the simulations.

3.2.1 Implementation of RTE Scenarios in CORSIM

A different run time extension (RTE) was created for each algorithm and a total of 24 scenarios were tested at each of the bottlenecks. The scenarios are summarized in Table 3.6. Initially ten runs were conducted for the no-control scenario to obtain the final number of runs needed. The number of runs required for each scenario was based on the average speed of vehicles in the network in miles per hour. The standard deviation of the initial ten runs was 0.2865. The acceptable error was set to be 0.2 mph, and a confidence interval of 95% was used. The acceptable number of runs computed was approximately eight. Since originally ten runs were used and this value exceeded the minimum of eight, tens runs are used for all scenarios.

Output processing was performed to provide averages over the ten runs. The simulation generates a comma-separated value file that aggregates evaluation parameters by time period. On the network level the parameters include average travel speed, vehicle miles traveled, total travel time, and throughput. On the link level speed profile plots were created, displaying the average speeds over a 3-mile section of roadway upstream from the bottleneck location. Each scenario consists of twelve time periods, fifteen-minutes each. This is a total of 3 hours of simulation

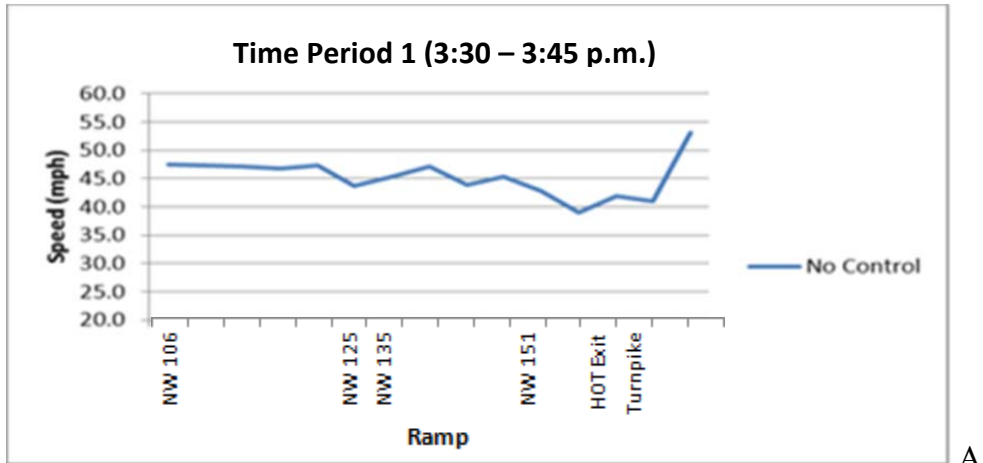
time for each scenario. Each simulation requires 3000 seconds of initialization period to properly load the network with vehicles at the beginning of the simulation.

TABLE 3.6. Description of scenarios tested

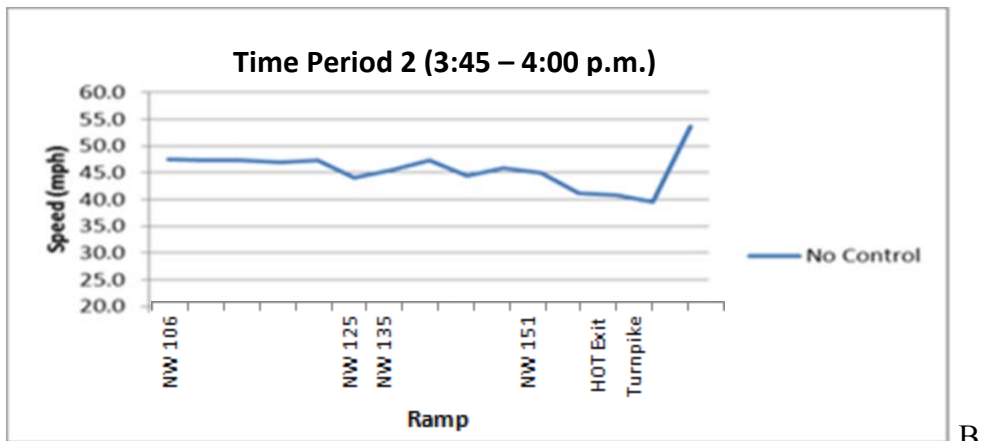
Algorithm	Threshold scenario	Sign location
No VSL control	-	-
Occupancy based	1	One sign - half mile spacing
Occupancy based	2	One sign - half mile spacing
Occupancy based	3	One sign - half mile spacing
Occupancy based	1	One sign - one mile spacing
Occupancy based	2	One sign - one mile spacing
Occupancy based	3	One sign - one mile spacing
Occupancy based	1	Two signs - half mile spacing
Occupancy based	2	Two signs - half mile spacing
Occupancy based	3	Two signs - half mile spacing
Occupancy based	1	Two signs - one-mile spacing
Occupancy based	2	Two signs - one-mile spacing
Occupancy based	3	Two signs - one-mile spacing
Volume based	1	One sign - half mile spacing
Volume based	2	One sign - half mile spacing
Volume based	1	One sign - one mile spacing
Volume based	2	One sign - one mile spacing
Volume based	1	Two signs - half mile spacing
Volume based	2	Two signs - half mile spacing
Volume based	1	Two signs - one-mile spacing
Volume based	2	Two signs - one-mile spacing
Multiple parameter	-	One sign - half mile spacing
Multiple parameter	-	One sign - one mile spacing
Multiple parameter	-	Two signs - half mile spacing
Multiple parameter	-	Two signs - one-mile spacing

3.2.2 Analysis of the No VSL Control Scenario

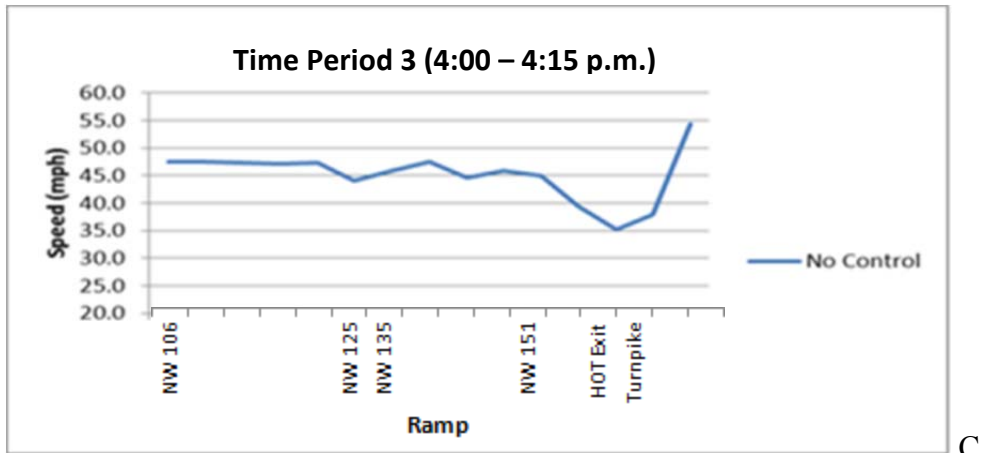
The speed profile of the no-control scenario for a portion of the downstream section of the corridor is displayed in Figure 3.14.



A

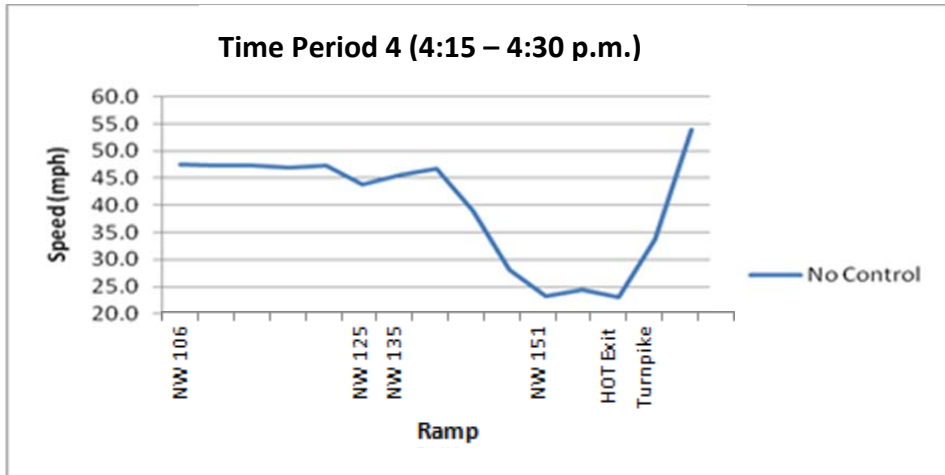


B

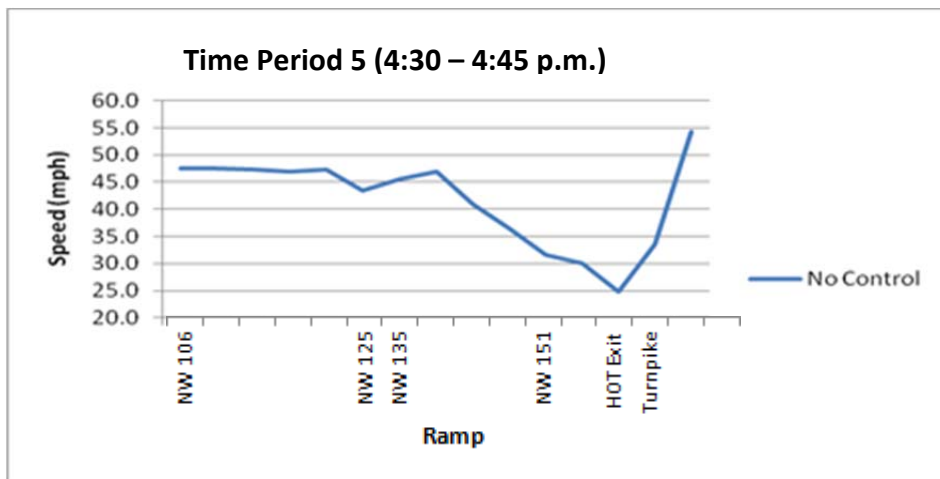


C

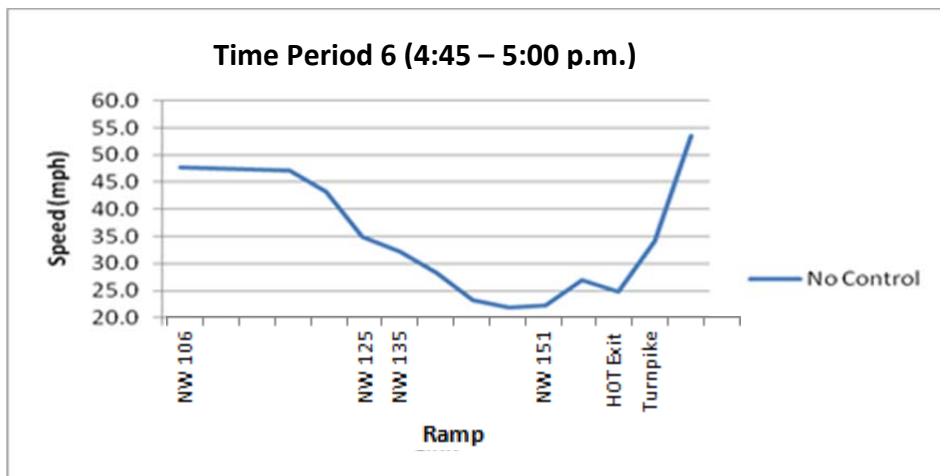
FIGURE 3.14 Speed profile for no-control scenario over time the 12 periods at Bottleneck 1 A) Time period 1; B) Time Period 2; C) Time period 3; D) Time period 4; E) Time period 5; F) Time Period 6; G) Time Period 7; H) Time Period 8; I) Time Period 9; J) Time Period 10; K) Time Period 11; L) Time Period 12.



D

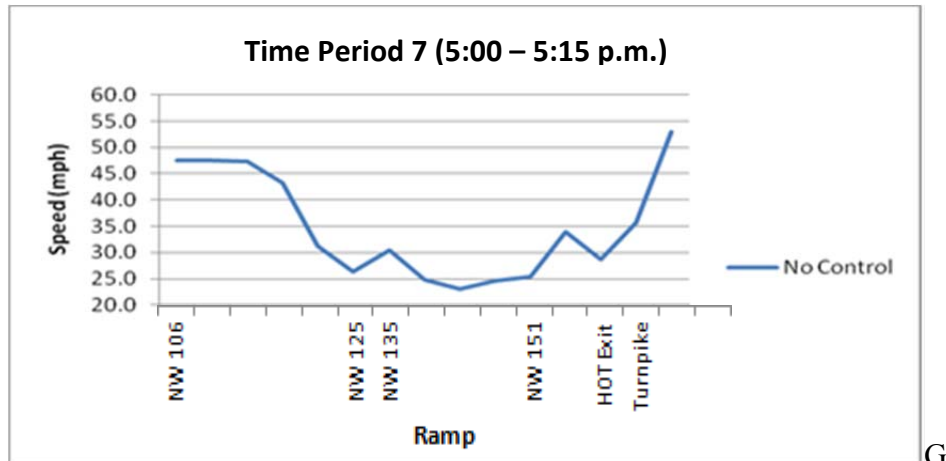


E

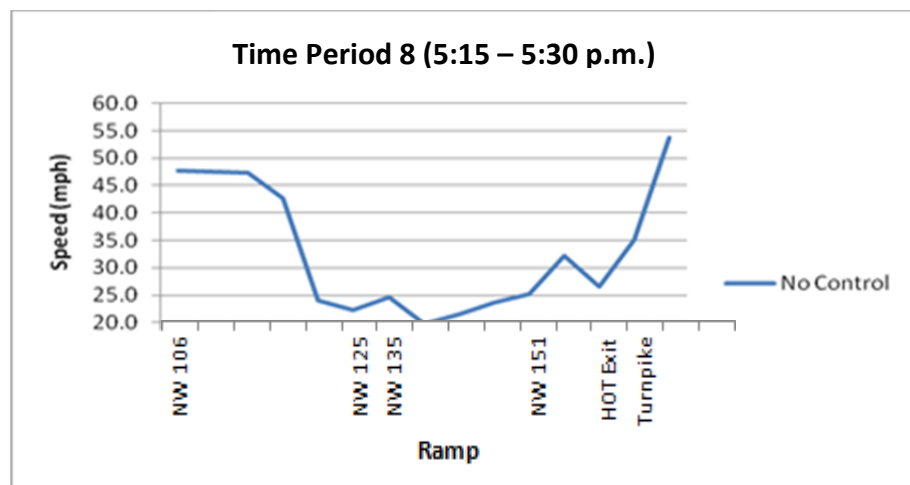


F

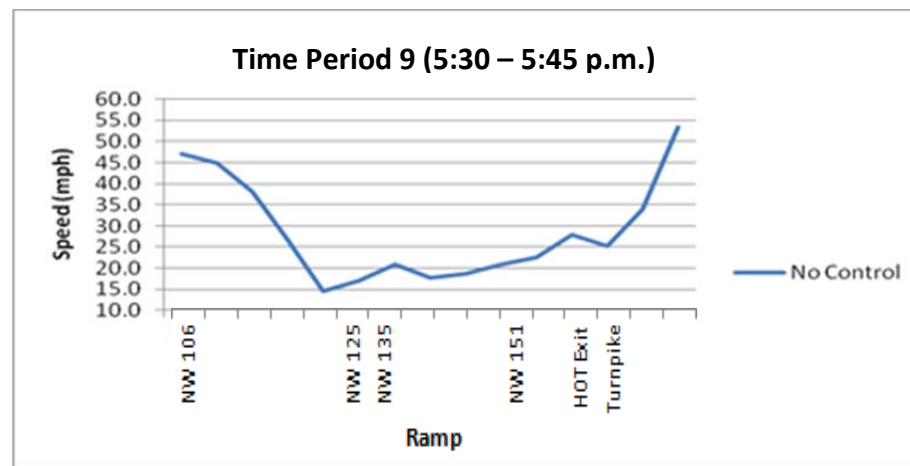
FIGURE 3.14 (Continued) Speed profile for no-control scenario over time the 12 periods at Bottleneck 1 A) Time period 1; B) Time Period 2; C) Time period 3; D) Time period 4; E) Time period 5; F) Time Period 6; G) Time Period 7; H) Time Period 8; I) Time Period 9; J) Time Period 10; K) Time Period 11; L) Time Period 12.



G

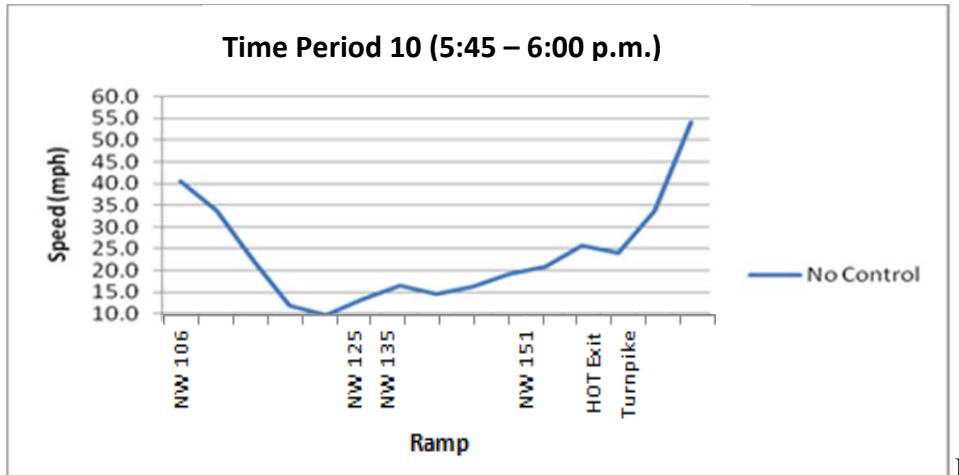


H

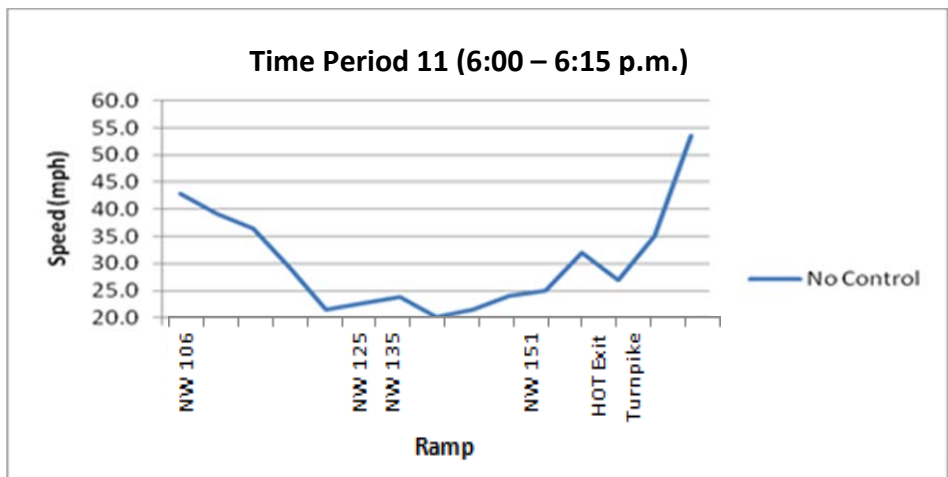


I

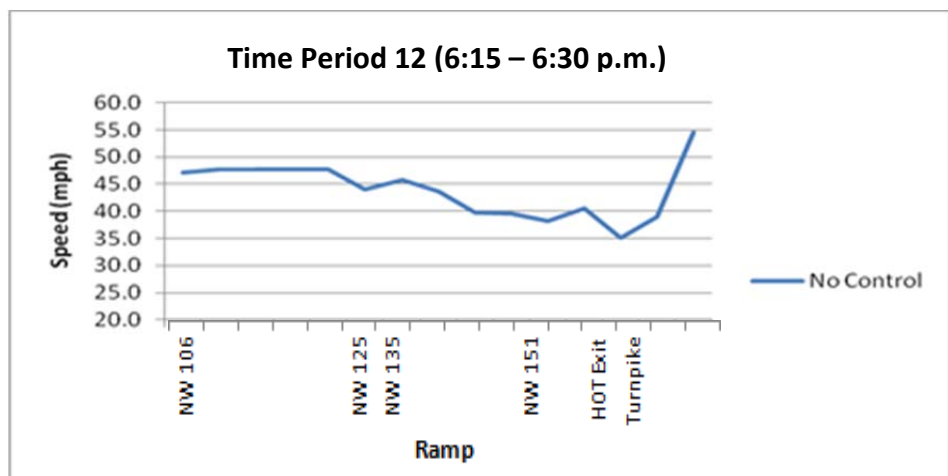
FIGURE 3.14 (Continued). Speed profile for no-control scenario over time the 12 periods at Bottleneck 1 A) Time period 1; B) Time Period 2; C) Time period 3; D) Time period 4; E) Time period 5; F) Time Period 6; G) Time Period 7; H) Time Period 8; I) Time Period 9; J) Time Period 10; K) Time Period 11; L) Time Period 12.



J



K



L

FIGURE 3.14 (Continued). Speed profile for no-control scenario over time the 12 periods at Bottleneck 1 A) Time period 1; B) Time Period 2; C) Time period 3; D) Time period 4; E) Time period 5; F) Time Period 6; G) Time Period 7; H) Time Period 8; I) Time Period 9; J) Time Period 10; K) Time Period 11; L) Time Period 12.

From the results, it is clear that a bottleneck forms on link 159-161, beginning sometime between time periods 3 and 4. This location is approximately 1000 ft upstream from the exit to the turnpike. This off-ramp is located on the left side of the freeway, and the high volume diverge creates traffic breakdown. During time period 3 the speed at this location drops to 35 mph, and at time period 4 below 25 mph. The congestion moves upstream and affects links as far as link 147-148, which is over 2 miles upstream of the bottleneck. Congestion does not dissipate until time period 12, which is approximately two hours after the breakdown. This represents a typical evening peak period with recurring congestion on the I-95 network, and an ideal scenario to test the selected VSL algorithms. In this report, this location is referred to as Bottleneck 1.

Figure 3.15 shows the speed profile of the no-control scenario over another section. From the figure it can be concluded that a bottleneck forms on the entry from NW 103rd St. This bottleneck extends upstream approximately 2 miles. Again, congestion does not dissipate until time period 12. This will be referred to as Bottleneck 2.

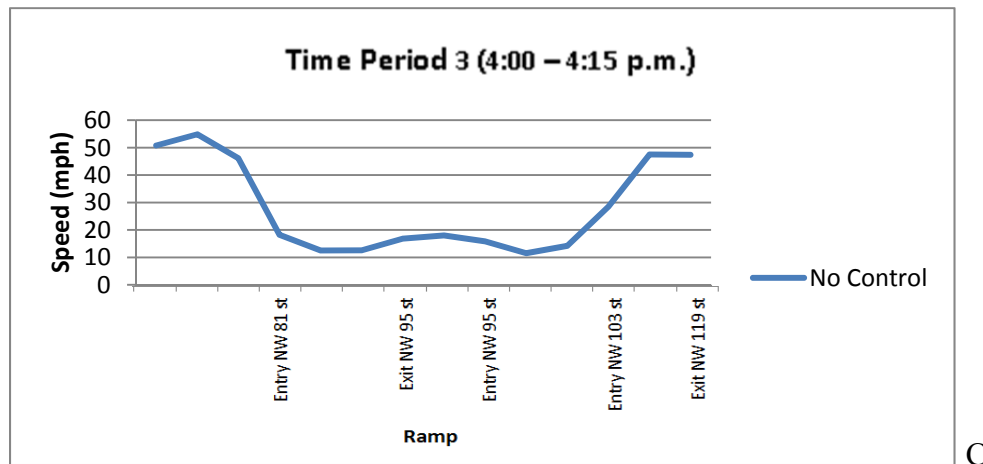
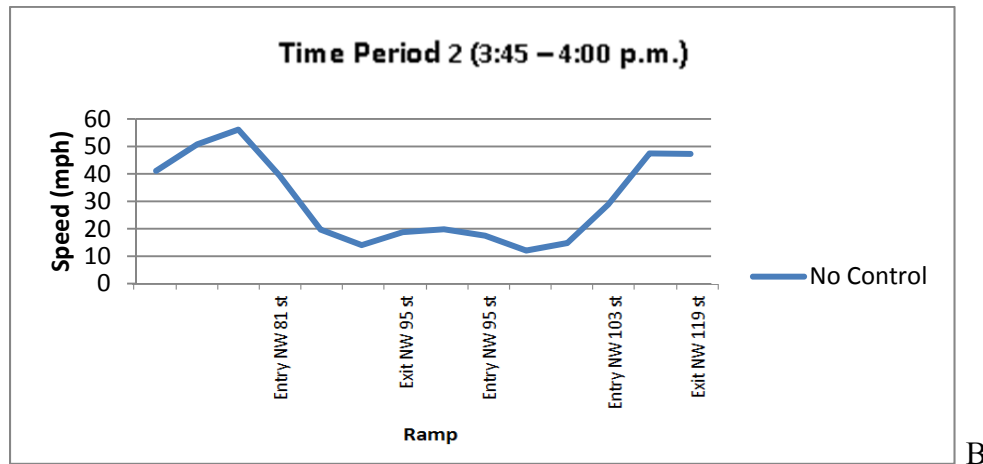
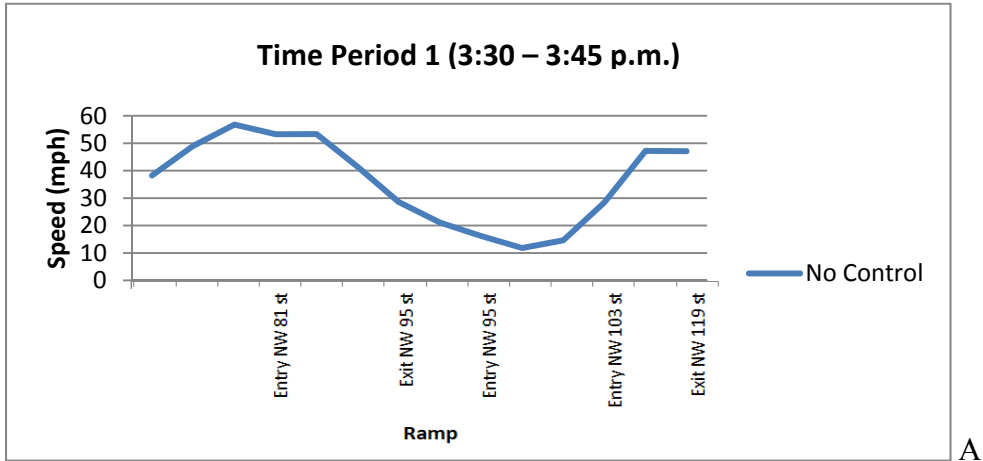
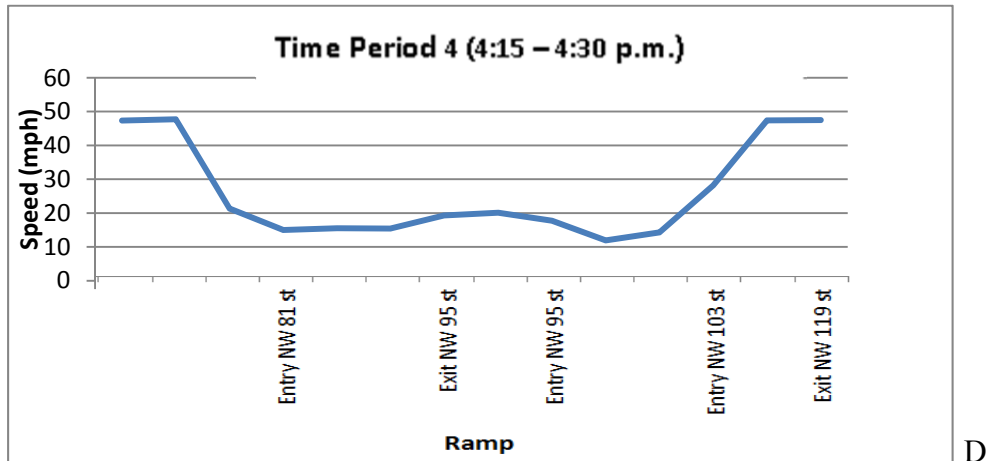
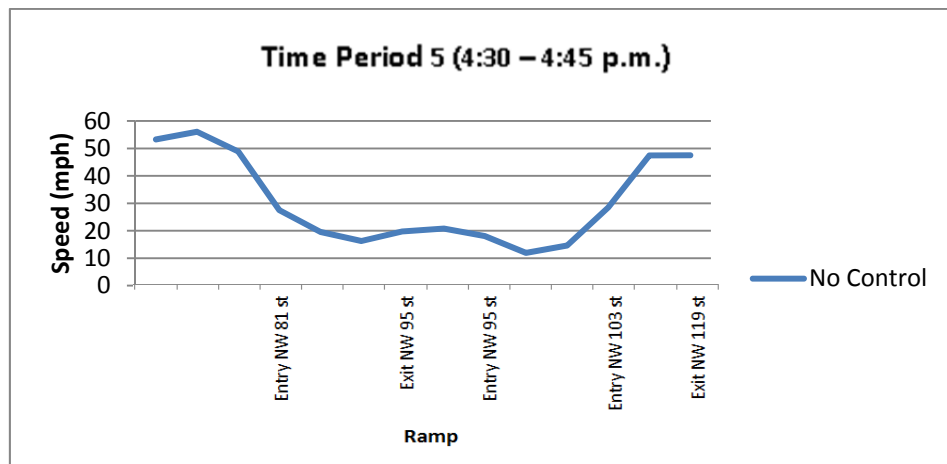


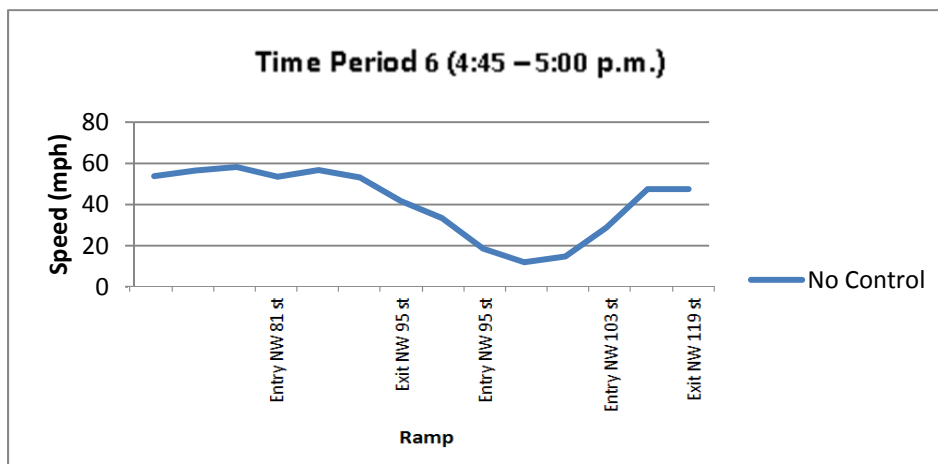
FIGURE 3.15. Speed profile for no-control scenario over time the 12 periods at Bottleneck 2 A) Time period 1; B) Time Period 2; C) Time period 3; D) Time period 4; E) Time period 5; F) Time Period 6; G) Time Period 7; H) Time Period 8; I) Time Period 9; J) Time Period 10; K) Time Period 11; L) Time Period 12.



D



E



F

FIGURE 3.15 (Continued). Speed profile for no-control scenario over time the 12 periods at Bottleneck 2 A) Time period 1; B) Time Period 2; C) Time period 3; D) Time period 4; E) Time period 5; F) Time Period 6; G) Time Period 7; H) Time Period 8; I) Time Period 9; J) Time Period 10; K) Time Period 11; L) Time Period 12.

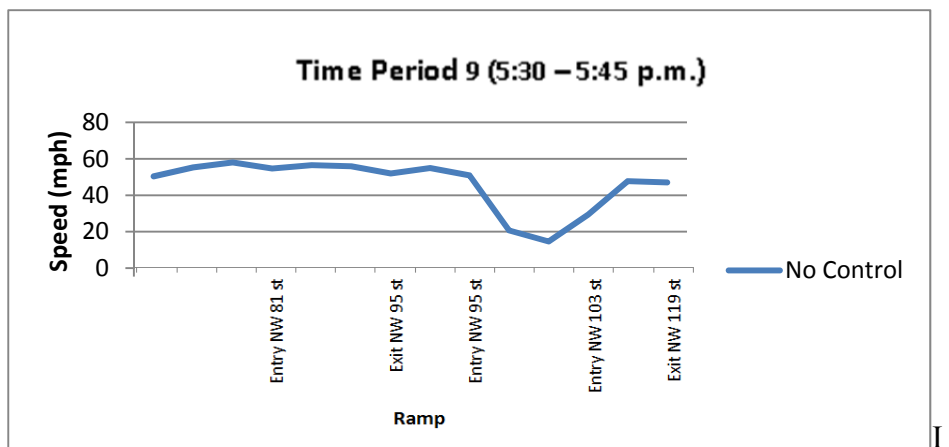
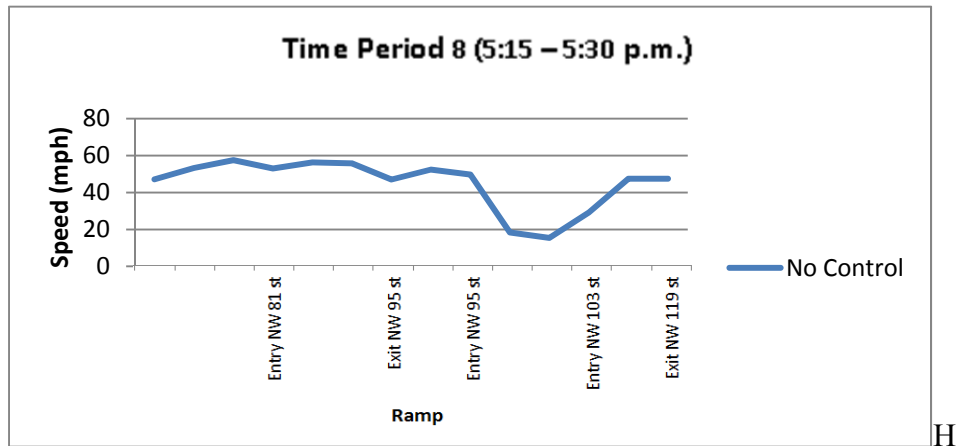
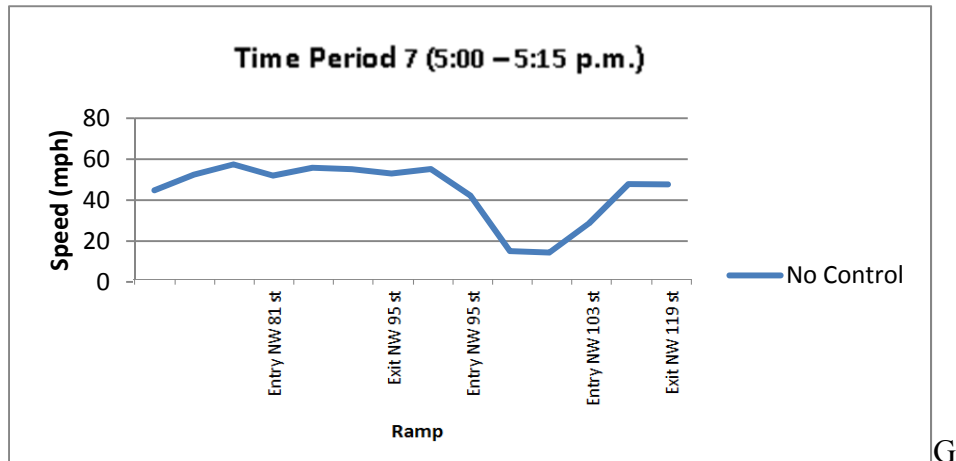


FIGURE 3.15 (Continued). Speed profile for no-control scenario over time the 12 periods at Bottleneck 2 A) Time period 1; B) Time Period 2; C) Time period 3; D) Time period 4; E) Time period 5; F) Time Period 6; G) Time Period 7; H) Time Period 8; I) Time Period 9; J) Time Period 10; K) Time Period 11; L) Time Period 12.

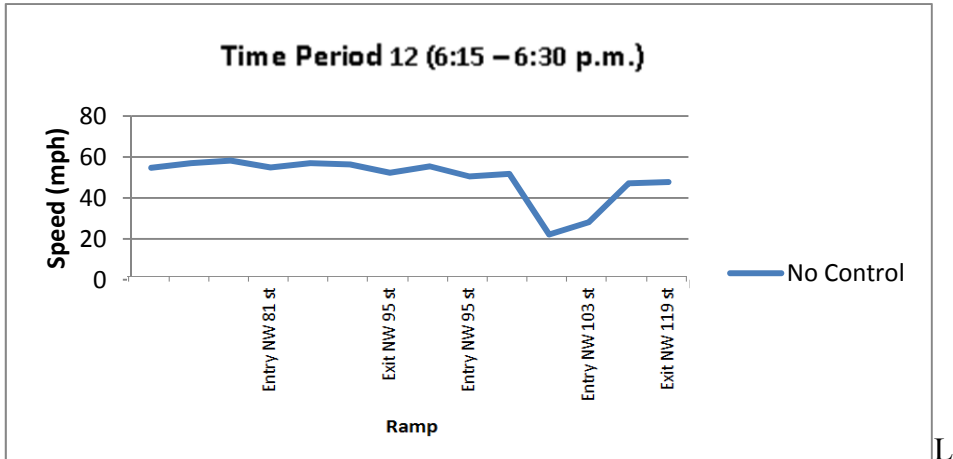
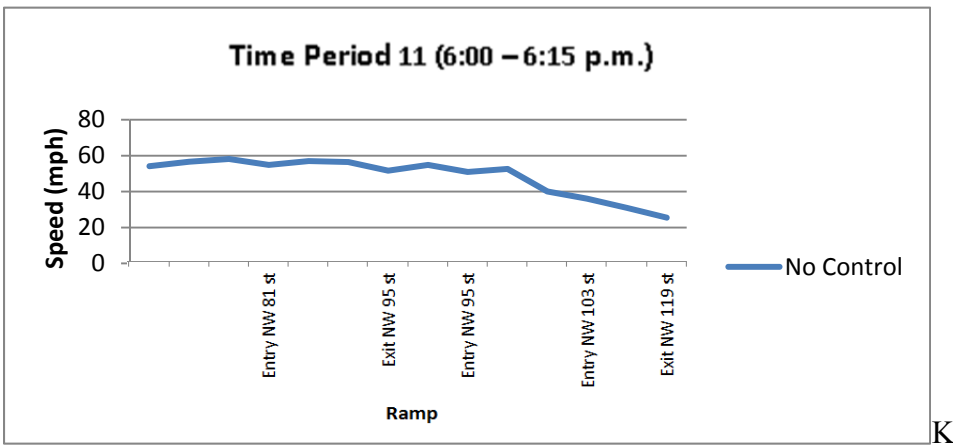
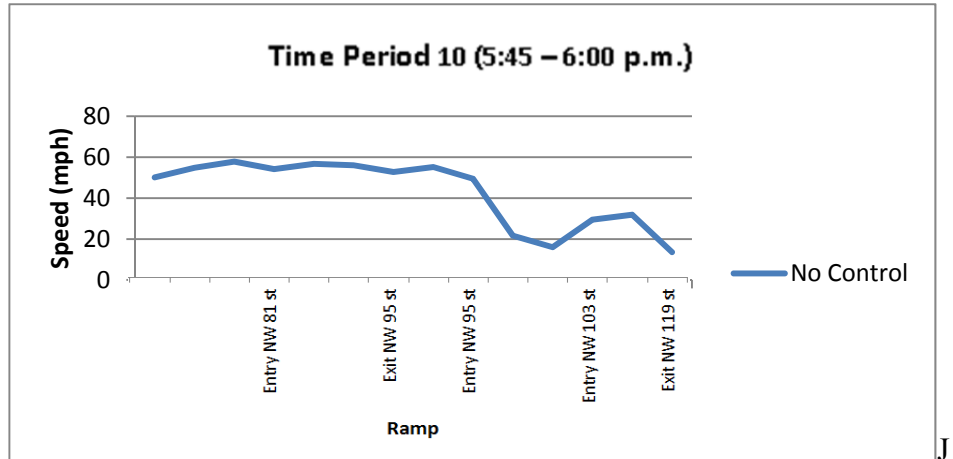


FIGURE 3.15 (Continued). Speed profile for no-control scenario over time the 12 periods at Bottleneck 2 A) Time period 1; B) Time Period 2; C) Time period 3; D) Time period 4; E) Time period 5; F) Time Period 6; G) Time Period 7; H) Time Period 8; I) Time Period 9; J) Time Period 10; K) Time Period 11; L) Time Period 12.

3.2.3 Implementation of VSL along Bottleneck 1

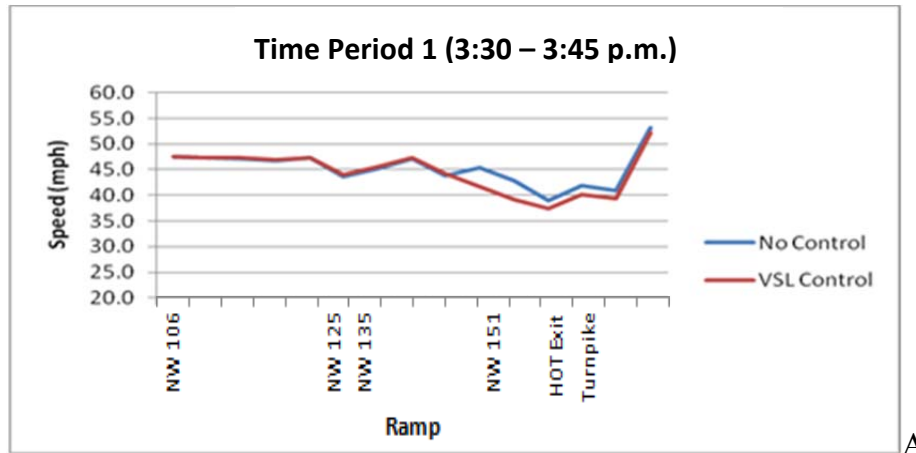
This subsection examines the operational effects of implementing VSL along Bottleneck 1. A total of 24 scenarios were developed and tested. Evaluation parameters include average travel speed, total travel time, and throughput over the entire network. At the link level, speed profile plots and throughput plots are created over a 3-mile section of the roadway upstream from the bottleneck. Each scenario consists of twelve time periods, fifteen-minutes each. This is a total of 3 hours of simulation time for each scenario. A summary of the results of every scenario are shown in Table 3.7.

As shown, the volume-based scenario using one sign spaced one mile from the bottleneck, and using threshold scenario 1 had the greatest improvement over the no-control scenario. This scenario had the greatest improvement in network average travel speed with a 3.64 % (1.44 mph) increase. It also had the greatest decrease in total travel time by 3.41% (260 hours).

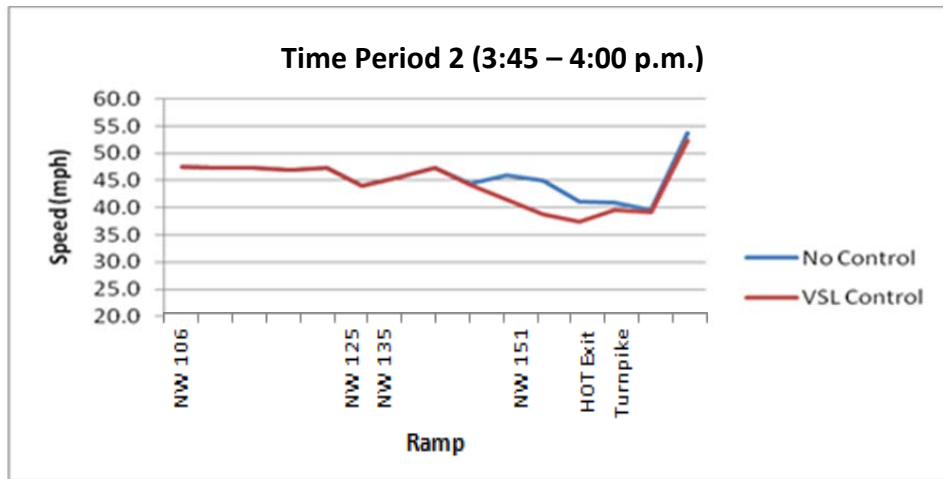
The speed profile for this scenario compared to the no-control scenario is shown in Figure 3.16. During free flow conditions and at the beginning of congestion the VSL control showed slightly reduced speeds when compared to the no-control scenario. At the onset of congestion the VSL control scenario mirrors the no-control scenario almost identically. As time progresses the VSL-control scenario showed improved speeds starting at the bottleneck and moving upstream. The VSL-control scenario showed consistent average speed improvements by as much as 13 mph. During the recovery phase the VSL-control scenario again showed speed improvement over the no-control scenario. All but one scenario tested showed similar improvements in average speeds over the entire length and duration of congestion.

TABLE 3.7. Network performance measures for Bottleneck 1

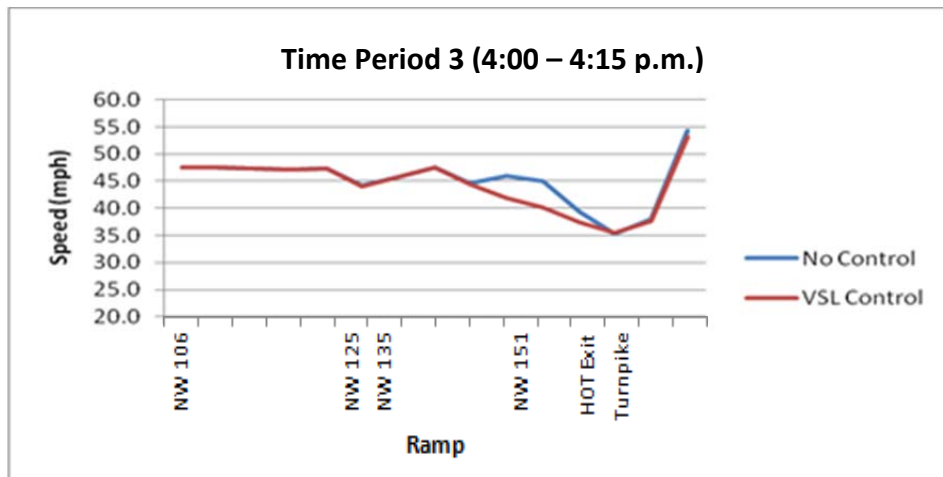
Algorithm	# of signs	Spacing (miles)	Threshold scenario	Average speed	% Change from no-control	Total travel time (hours)	% Change from no-control
No control	NA	NA	NA	39.57	0.00	7624.55	0.00
Occupancy	1	1/2	1	40.13	1.41	7514.82	-1.44
Occupancy	1	1/2	2	40.39	2.05	7475.28	-1.96
Occupancy	1	1/2	3	40.60	2.60	7425.28	-2.61
Occupancy	1	1	1	40.15	1.46	7512.60	-1.47
Occupancy	1	1	2	40.82	3.14	7380.71	-3.20
Occupancy	1	1	3	40.11	1.35	7523.84	-1.32
Occupancy	2	1/2	1	40.37	2.02	7471.69	-2.00
Occupancy	2	1/2	2	40.91	3.38	7369.21	-3.35
Occupancy	2	1/2	3	40.33	1.90	7471.87	-2.00
Occupancy	2	1	1	40.82	3.14	7380.71	-3.20
Occupancy	2	1	2	39.89	0.79	7570.62	-0.71
Occupancy	2	1	3	40.03	1.15	7535.28	-1.17
Volume	1	1/2	1	40.52	2.40	7445.97	-2.34
Volume	1	1/2	2	40.36	1.97	7467.51	-2.06
Volume	1	1	1	41.01	3.64	7364.17	-3.41
Volume	1	1	2	40.18	1.52	7498.70	-1.65
Volume	2	1/2	1	40.63	2.67	7433.17	-2.51
Volume	2	1/2	2	40.39	2.06	7462.65	-2.12
Volume	2	1	1	40.86	3.25	7388.90	-3.09
Volume	2	1	2	39.64	0.18	7619.88	-0.06
Multiple	1	1/2	1	40.00	1.08	7538.87	-1.12
Multiple	1	1	1	38.73	-2.14	7791.58	2.19
Multiple	2	1/2	1	40.48	2.29	7448.92	-2.30
Multiple	2	1	1	39.94	0.92	7543.46	-1.06



A

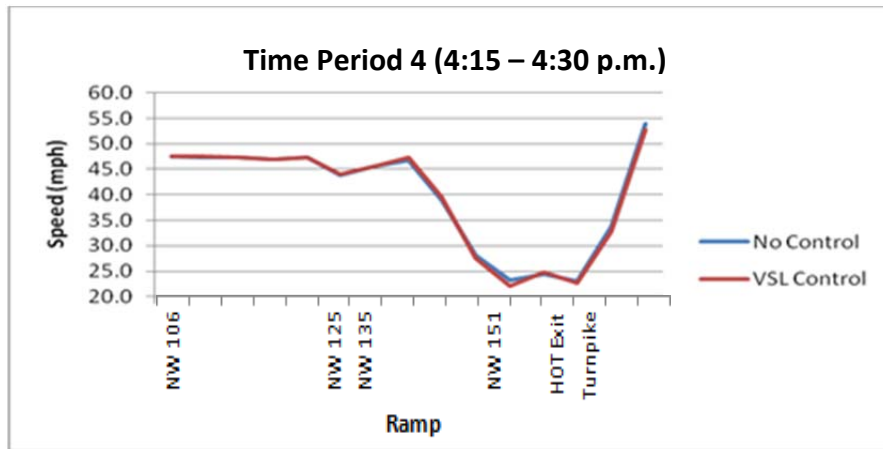


B

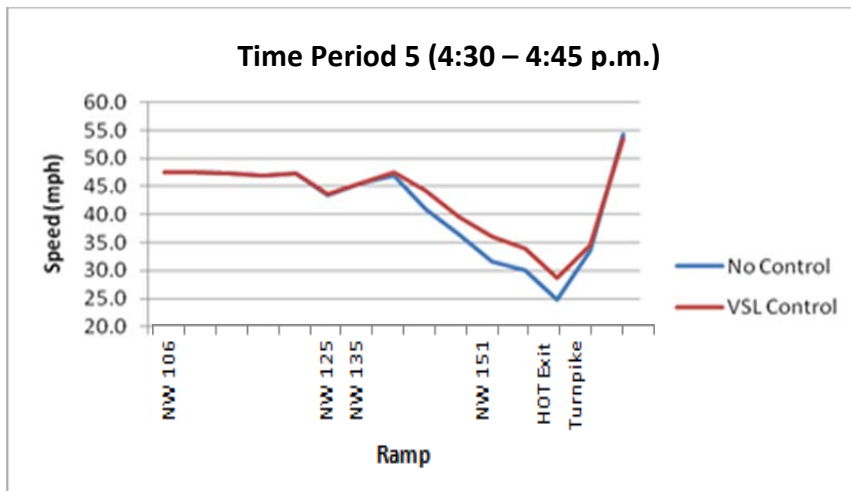


C

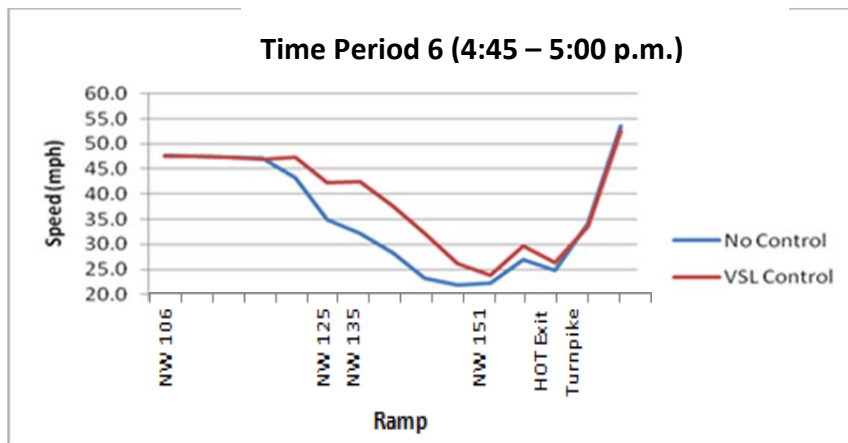
FIGURE 3.16. Speed profile for the volume-based algorithm using one sign spaced 1 mile from the bottleneck (threshold scenario 1) compared to the no-control scenario A) Time period 1; B) Time Period 2; C) Time period 3; D) Time period 4; E) Time period 5; F) Time Period 6; G) Time Period 7; H) Time Period 8; I) Time Period 9; J) Time Period 10; K) Time Period 11; L) Time Period 12.



D



E



F

FIGURE 3.16 (Continued). Speed profile for the volume-based algorithm using one sign spaced 1 mile from the bottleneck (threshold scenario 1) compared to the no-control scenario A) Time period 1; B) Time Period 2; C) Time period 3; D) Time period 4; E) Time period 5; F) Time Period 6; G) Time Period 7; H) Time Period 8; I) Time Period 9; J) Time Period 10; K) Time Period 11; L) Time Period 12.

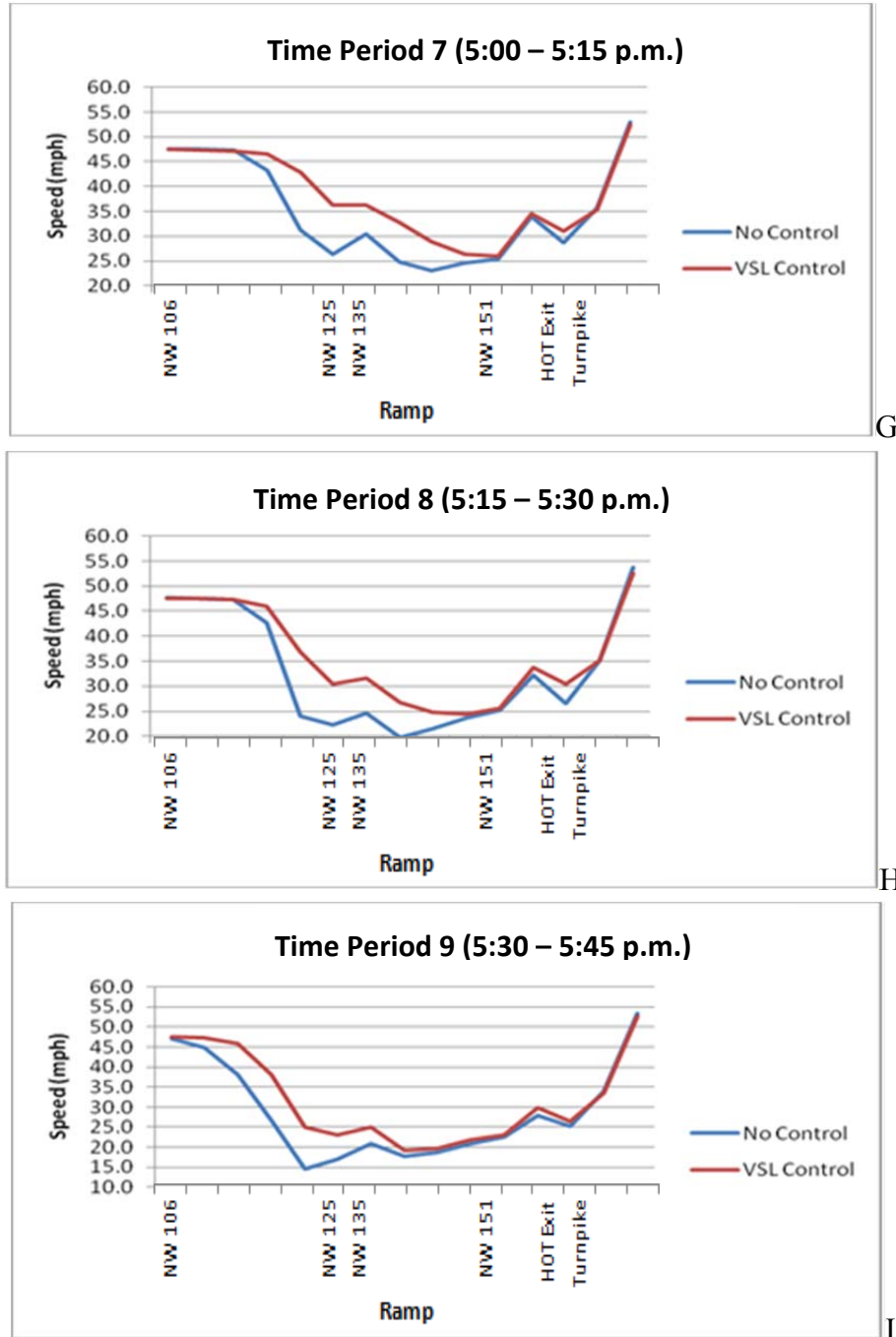


FIGURE 3.16 (Continued). Speed profile for the volume-based algorithm using one sign spaced 1 mile from the bottleneck (threshold scenario 1) compared to the no-control scenario A) Time period 1; B) Time Period 2; C) Time period 3; D) Time period 4; E) Time period 5; F) Time Period 6; G) Time Period 7; H) Time Period 8; I) Time Period 9; J) Time Period 10; K) Time Period 11; L) Time Period 12.

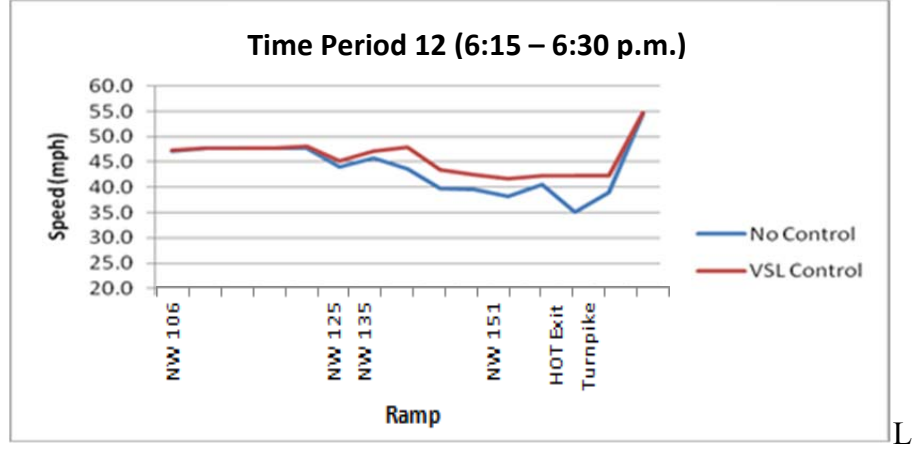
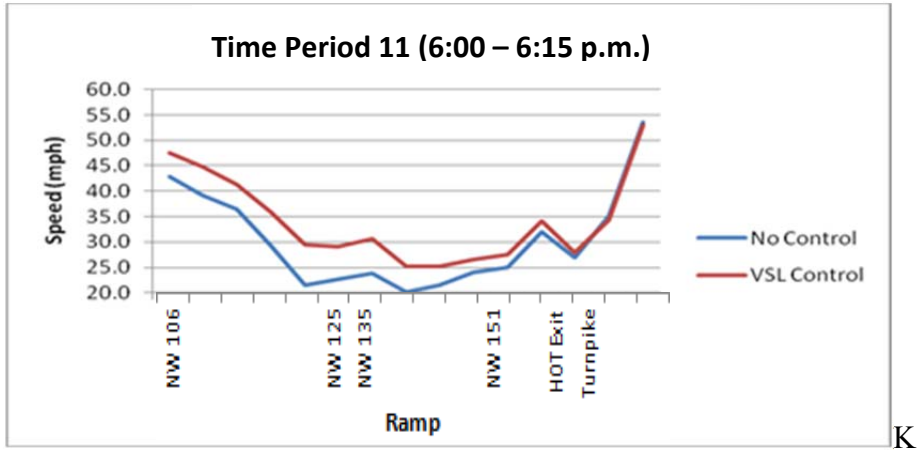
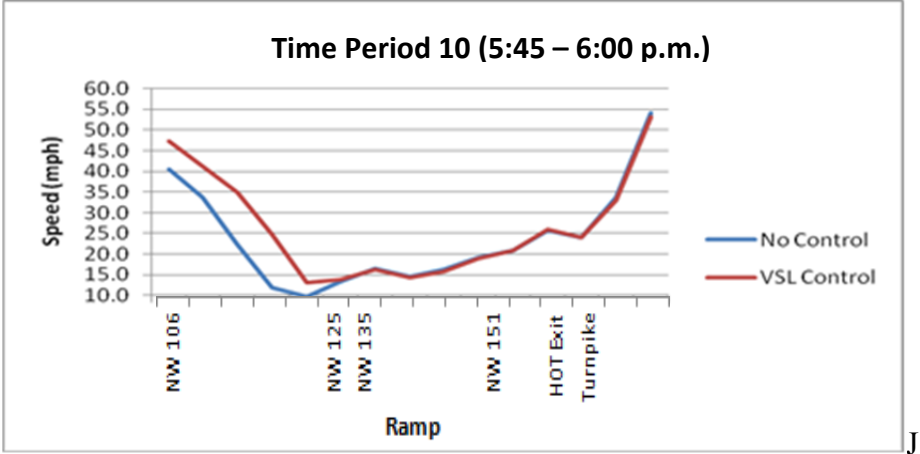


FIGURE 3.16 (Continued). Speed profile for the volume-based algorithm using one sign spaced 1 mile from the bottleneck (threshold scenario 1) compared to the no-control scenario A) Time period 1; B) Time Period 2; C) Time period 3; D) Time period 4; E) Time period 5; F) Time Period 6; G) Time Period 7; H) Time Period 8; I) Time Period 9; J) Time Period 10; K) Time Period 11; L) Time Period 12.

To evaluate the throughput of the section, scaled cumulative curves were constructed to provide the throughput at key locations around the bottleneck. The scaled cumulative departures are used because they can show much more clearly the differences between the control and no-control case. The scaled cumulative departures are obtained by subtracting the time multiplied by a base flow rate from the cumulative departures. This relationship is as follows:

$$\text{scaled cum. departures} = \text{cum. departures} - \text{base flow rate} * \text{time period} \quad (2)$$

The throughput for this scenario at the bottleneck and locations upstream is shown in Figure 3.17. A clear improvement in throughput over the duration of congestion (88 vehicles over a 15 minute period) can be observed when comparing to the no-control case. This improved throughput accounts for the increased average travel speed, and reduced travel time. This finding was observed in nearly all the scenarios tested.

Overall, the results show that implementation of VSL increased average speeds and decreased travel times during the simulation. All but one scenario tested showed improvement in both of these categories, and these improvements were clearly seen when evaluating the study section on a link-by-link basis. However, the magnitude of the improvement when viewed as an average over the analysis period was very small (a maximum of 3.6% improvement in average travel). In general, the throughput over the section affected by the bottleneck showed improvement over the no-control scenario. This improved throughput explains the improvement in average travel speed and reduced travel time. In these simulations the volume-based algorithm showed the best overall improvement. The multiple-parameter algorithm showed the least improvement overall, and one of its scenarios showed worsening of conditions compared to the no-control scenario. One of the possible explanations for why the volume-based algorithm performed better than the occupancy-based one is that occupancy remains relatively flat over a wide set of volumes; thus the volume-based algorithm is quicker to trigger a speed limit drop upstream.

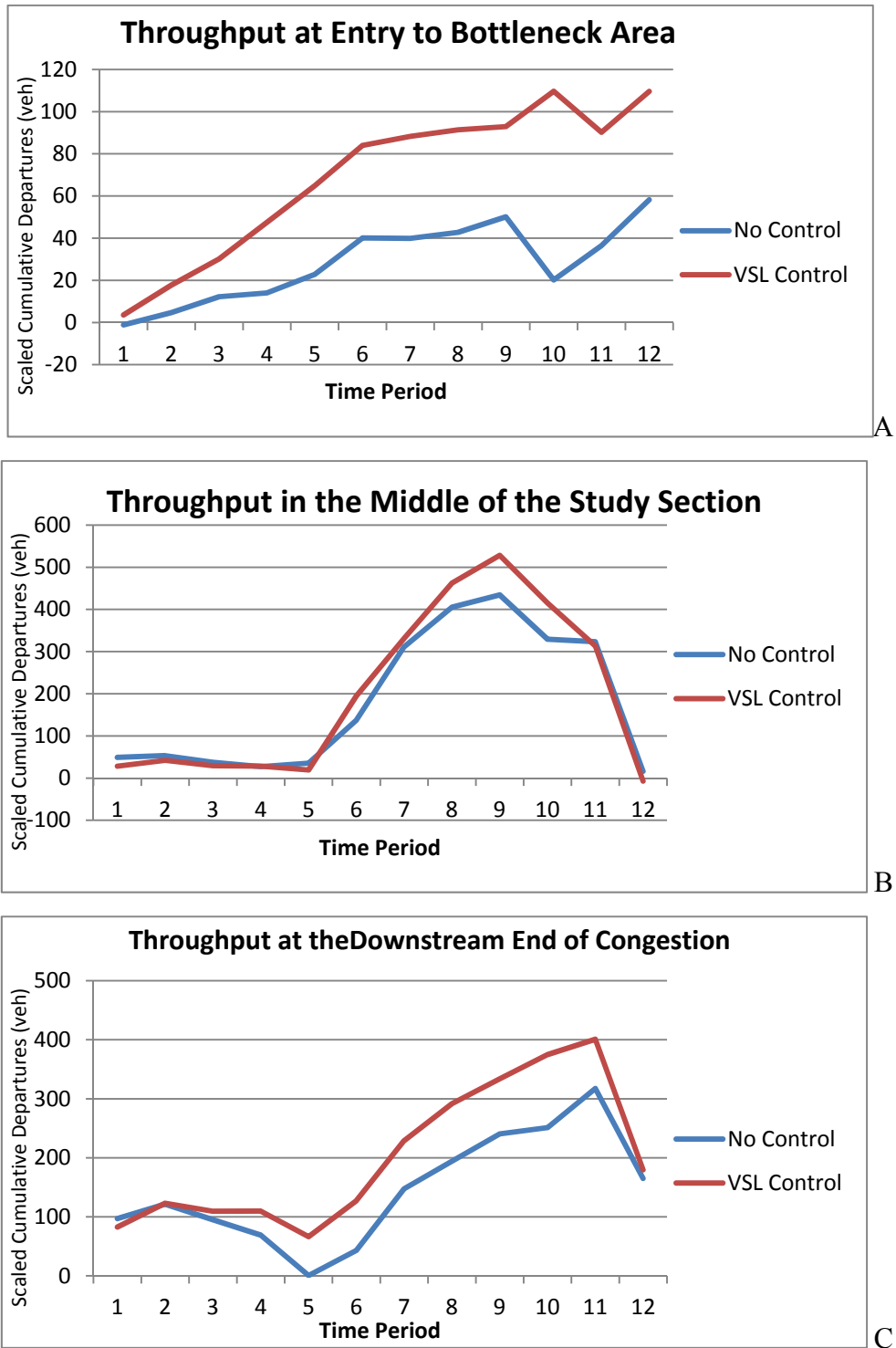


FIGURE 3.17. Throughput for the volume-based algorithm using one sign spaced 1 mile from the bottleneck (threshold scenario 1) compared to the no-control scenario A) At entry to the bottleneck area (NW 125th ST). B) At the middle of the study section (NW 151st ST). C) At the downstream end of congestion (Turnpike).

With respect to the multiple-parameter algorithm, it appears that it results in breakdown earlier than in the no-control case. Perhaps this is related to the particular thresholds used, and would not occur for higher thresholds. Note that this analysis has not sought to thoroughly evaluate and compare these algorithms. To completely assess each algorithm and document their relative merits and preferred applications, a full optimization of thresholds and sign positioning would have to be performed.

Comparing scenarios with one sign to those with two signs, it appeared that using only one sign creates a sharp transition between speeds and results in lower speeds before the onset of congestion. Using two signs resulted in a smoother transition between speeds and as a result these configurations have less reduction in speeds before the onset of congestion. However, the best sign spacing is not the same for every algorithm. Each algorithm performs best with a different sign spacing.

3.2.4 Implementation of VSL along Bottleneck 2

This subsection examines the operational effects of implementing VSL along Bottleneck 2. Similarly to the analysis of Bottleneck 1, a total of 24 scenarios were tested, and evaluation parameters include average travel speed, total travel time, and throughput over the entire network. Speed profile plots and throughput plots were created over a 3-mile section upstream from the bottleneck. Each scenario consists of twelve time periods, fifteen-minutes each. This is a total of 3 hours of simulation time for each scenario. A summary of the results for every scenario is provided in Table 3.8.

As shown, the occupancy-based scenario using two signs spaced one half mile apart, and using threshold scenario 1 had the greatest improvement over the no-control scenario. This scenario displayed the greatest improvement in network average travel speed with a 3.38 % (1.34 mph) increase. It also resulted in the greatest decrease in total travel time by 3.40% (259 hours). The speed profile for this scenario compared to the no-control scenario is shown in Figure 3.18.

TABLE 3.8. Network performance measures for Bottleneck 2

Algorithm	# of signs	Spacing (miles)	Threshold scenario	Average speed	% Change from no-control	Total travel time (hours)	% Change from no-control
No control	NA	NA	NA	39.57	0.00	7624.55	0.00
Occupancy	1	1/2	1	39.96	0.98	7543.39	-1.06
Occupancy	1	1/2	2	39.83	0.65	7583.00	-0.55
Occupancy	1	1/2	3	38.65	-2.34	7553.96	-0.93
Occupancy	1	1	1	40.18	1.53	7518.28	-1.39
Occupancy	1	1	2	39.99	1.04	7550.39	-0.97
Occupancy	1	1	3	38.96	-1.54	7746.66	1.60
Occupancy	2	1/2	1	40.91	3.38	7365.52	-3.40
Occupancy	2	1/2	2	40.72	2.90	7401.65	-2.92
Occupancy	2	1/2	3	40.11	1.36	7522.64	-1.34
Occupancy	2	1	1	40.58	2.55	7431.82	-2.53
Occupancy	2	1	2	39.99	1.04	7550.39	-0.97
Occupancy	2	1	3	38.98	-1.51	7745.94	1.59
Volume	1	1/2	1	39.93	0.91	7557.06	-0.89
Volume	1	1/2	2	40.00	1.09	7546.39	-1.03
Volume	1	1	1	39.73	0.40	7596.20	-0.37
Volume	1	1	2	40.55	2.47	7432.40	-2.52
Volume	2	1/2	1	40.50	2.34	7453.42	-2.24
Volume	2	1/2	2	40.61	2.61	7425.06	-2.62
Volume	2	1	1	39.57	-0.01	7616.30	-0.11
Volume	2	1	2	40.55	2.47	7432.40	-2.52
Multiple	1	1/2	1	40.08	1.28	7516.71	-1.41
Multiple	1	1	1	40.20	1.59	7492.70	-1.73
Multiple	2	1/2	1	40.16	1.49	7513.31	-1.46
Multiple	2	1	1	40.65	2.71	7415.88	-2.74

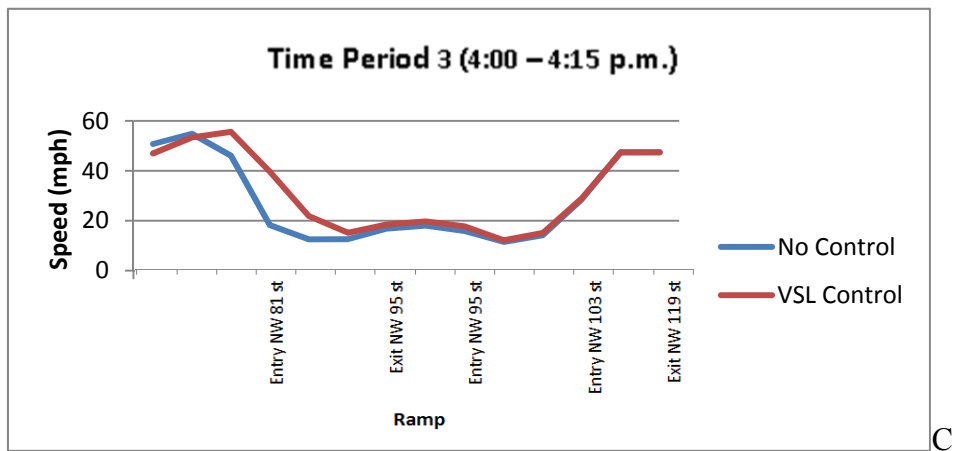
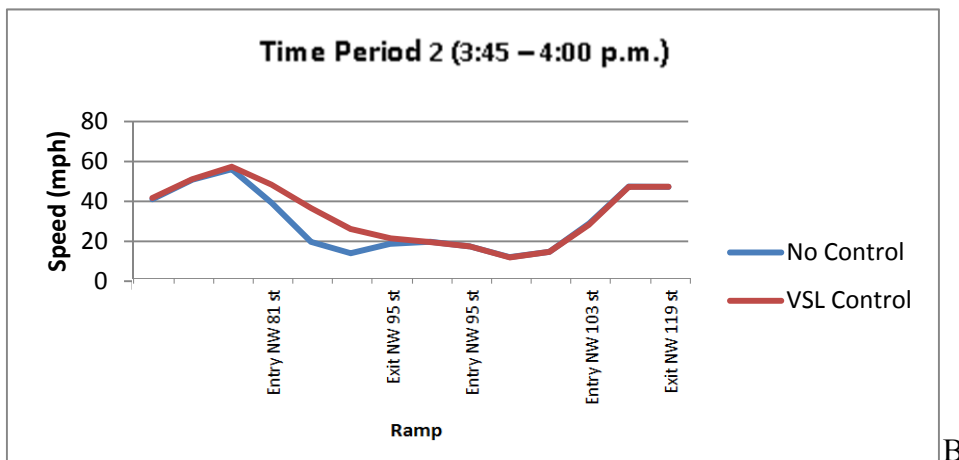
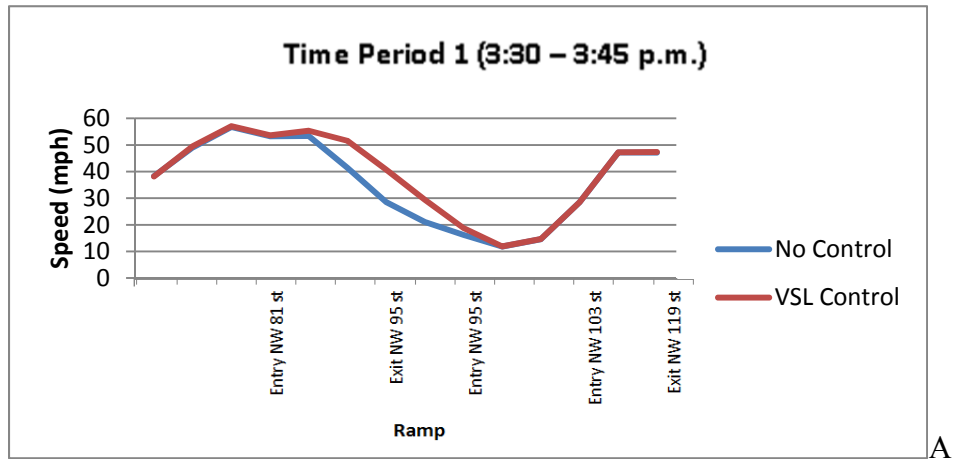
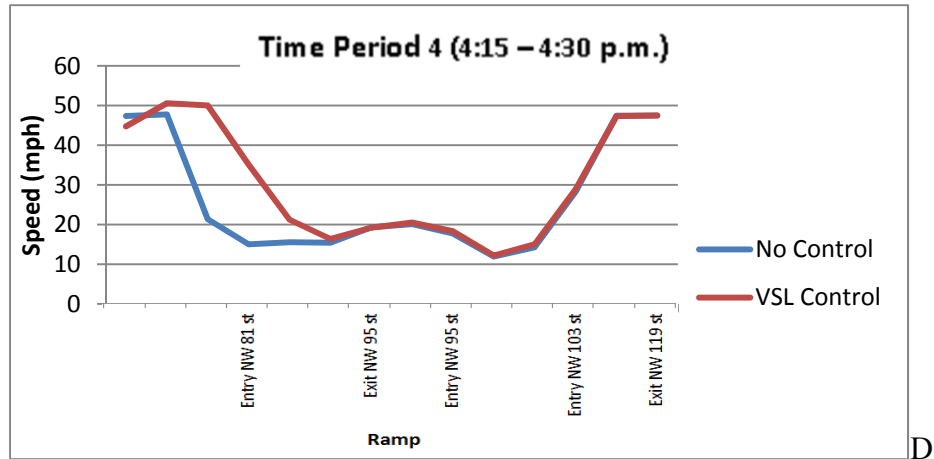
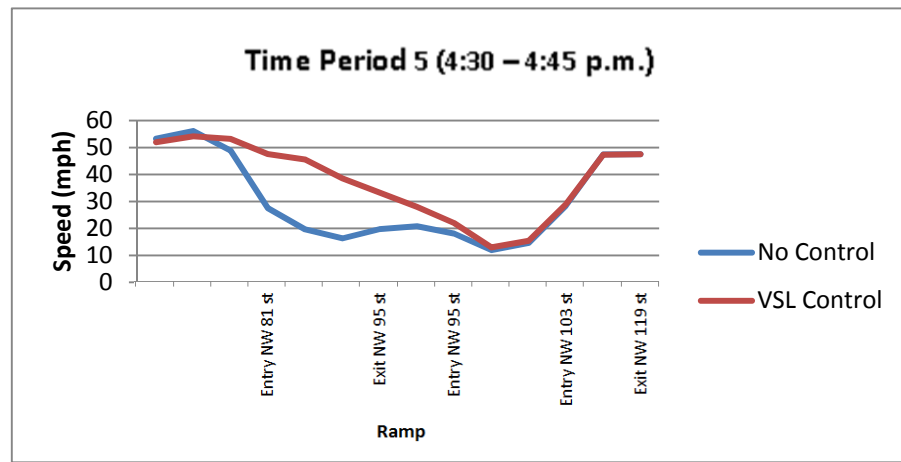


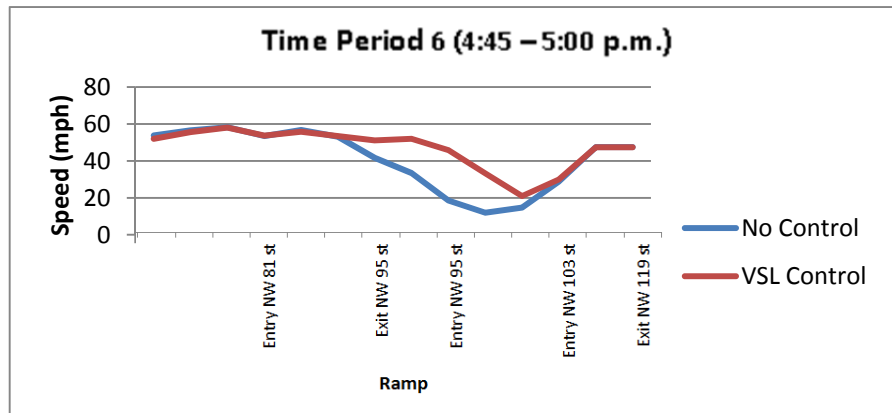
FIGURE 3.18. Speed profile for the occupancy-based algorithm using two signs spaced 1/2 mile apart (threshold scenario 1) compared to the no-control scenario A) Time period 1; B) Time Period 2; C) Time period 3; D) Time period 4; E) Time period 5; F) Time Period 6; G) Time Period 7; H) Time Period 8; I) Time Period 9; J) Time Period 10; K) Time Period 11; L) Time Period 12.



D



E



F

FIGURE 3.18 (Continued). Speed profile for the occupancy-based algorithm using two signs spaced 1/2 mile apart (threshold scenario 1) compared to the no-control scenario A) Time period 1; B) Time Period 2; C) Time period 3; D) Time period 4; E) Time period 5; F) Time Period 6; G) Time Period 7; H) Time Period 8; I) Time Period 9; J) Time Period 10; K) Time Period 11; L) Time Period 12.

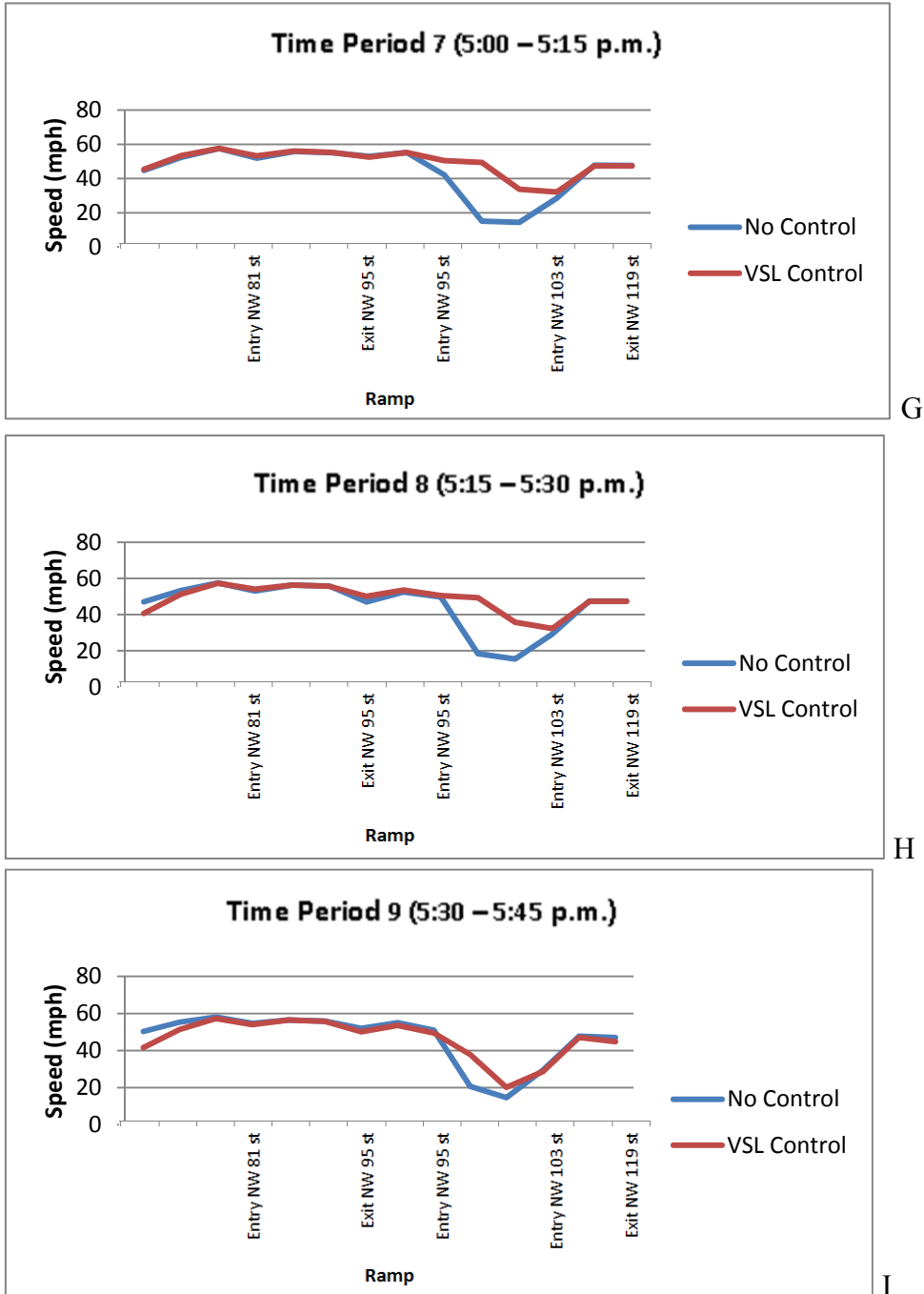


FIGURE 3.18 (Continued). Speed profile for the occupancy-based algorithm using two signs spaced 1/2 mile apart (threshold scenario 1) compared to the no-control scenario A) Time period 1; B) Time Period 2; C) Time period 3; D) Time period 4; E) Time period 5; F) Time Period 6; G) Time Period 7; H) Time Period 8; I) Time Period 9; J) Time Period 10; K) Time Period 11; L) Time Period 12.

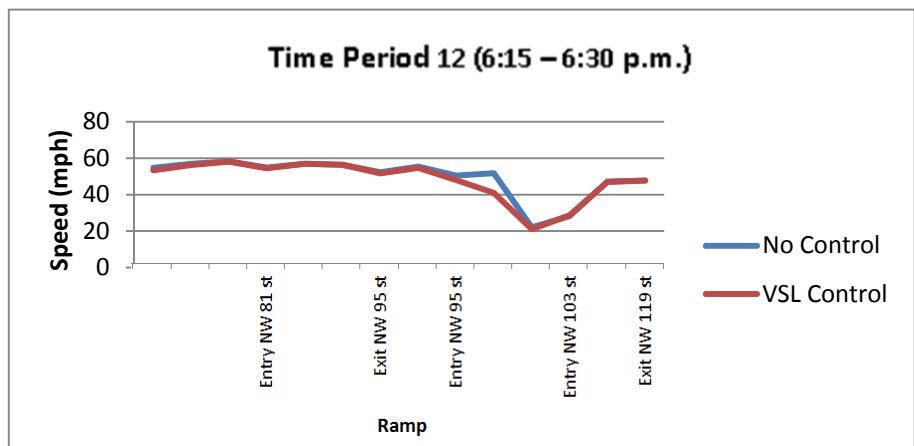
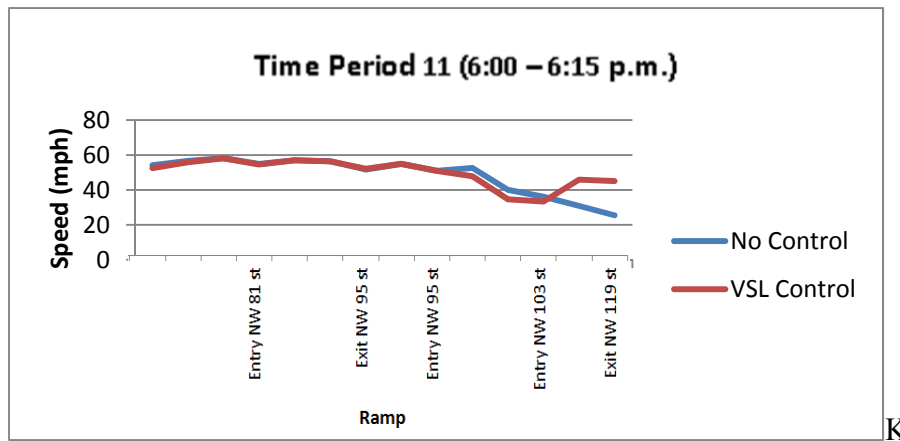
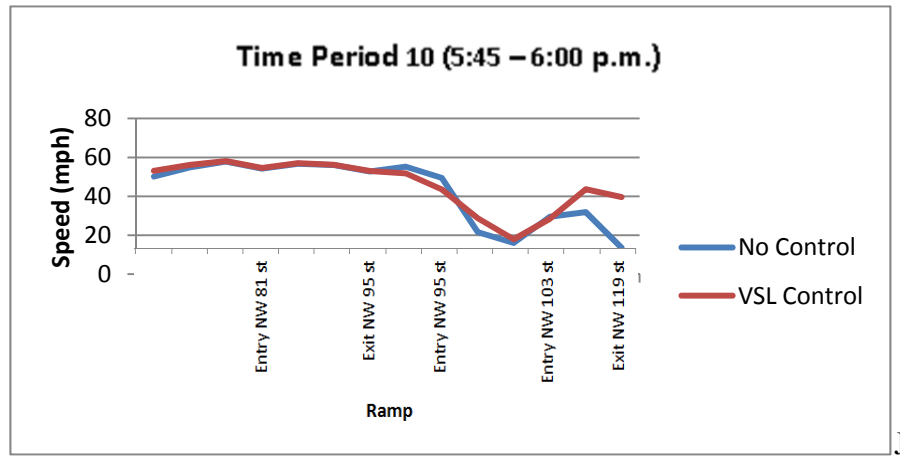


FIGURE 3.18 (Continued). Speed profile for the occupancy-based algorithm using two signs spaced 1/2 mile apart (threshold scenario 1) compared to the no-control scenario A) Time period 1; B) Time Period 2; C) Time period 3; D) Time period 4; E) Time period 5; F) Time Period 6; G) Time Period 7; H) Time Period 8; I) Time Period 9; J) Time Period 10; K) Time Period 11; L) Time Period 12.

Starting with free flow conditions and during the beginning of congestion, the VSL control showed slightly increased speeds when compared to the no-control scenario. At the onset of congestion the VSL control scenario showed significantly improved speeds. As time progresses the VSL-control scenario showed improved speeds starting at the bottleneck and moving upstream. The VSL-control scenario showed consistent average speed improvements by as much as 30 mph. During the recovery phase the VSL-control scenario shows similar speeds to the no-control scenario. Most scenarios tested showed improvements in average speed, and reduced travel time.

The throughput for this scenario at the bottleneck and locations upstream is shown in Figure 3.19. A clear improvement in the early time periods (71 vehicles over a 15 minute period) can be observed when comparing to the no-control case. This improved throughput accounts for the increased average travel speed, and reduced travel time. This finding was observed in nearly all the scenarios tested. In the later time periods the throughput is the same or even lower than the no control scenario.

In general, the throughput over the section affected by the bottleneck showed improvement over the no-control scenario. This improved throughput explains the improvement in average travel speed and reduced travel time. In these simulations the occupancy-based algorithm showed the best overall improvement. The multiple-parameter algorithm showed some improvement, while the occupancy threshold scenario 3 performed very poorly, and occupancy threshold scenario 1 performed consistently well. For all scenarios tested using two signs spaced $\frac{1}{2}$ mile apart gave the best results.

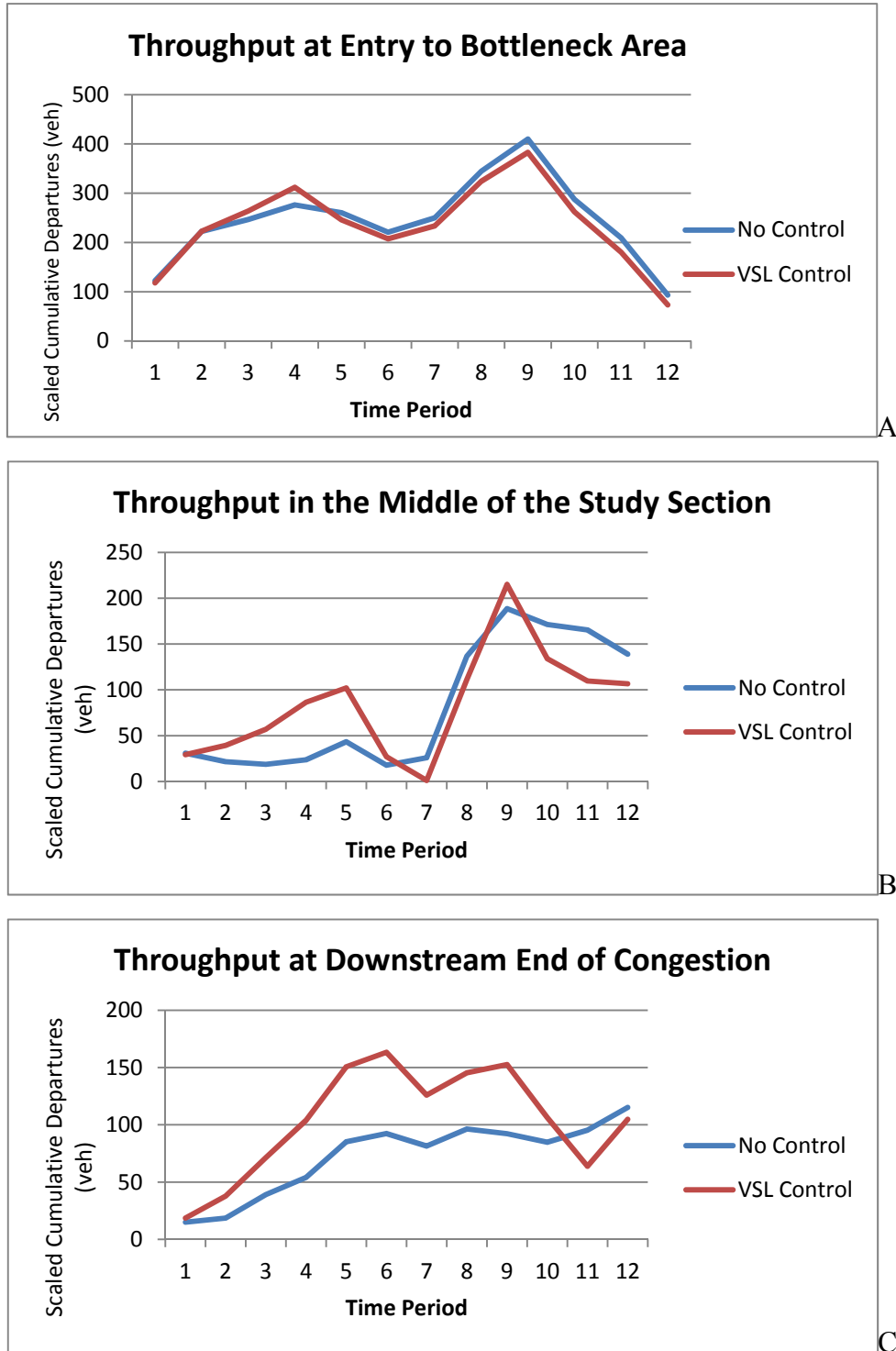


FIGURE 3.19 Throughput for the occupancy-based algorithm using two signs spaced 1/2 mile apart (threshold scenario 1) compared to the no-control scenario A) At entry to the bottleneck area (Exit to NW 95th ST); B) At the middle of the study section (Entry to NW 95th ST); C) At the downstream end of congestion (Entry to NW 103rd ST).

3.2.5 Simultaneous VSL control at the two bottlenecks

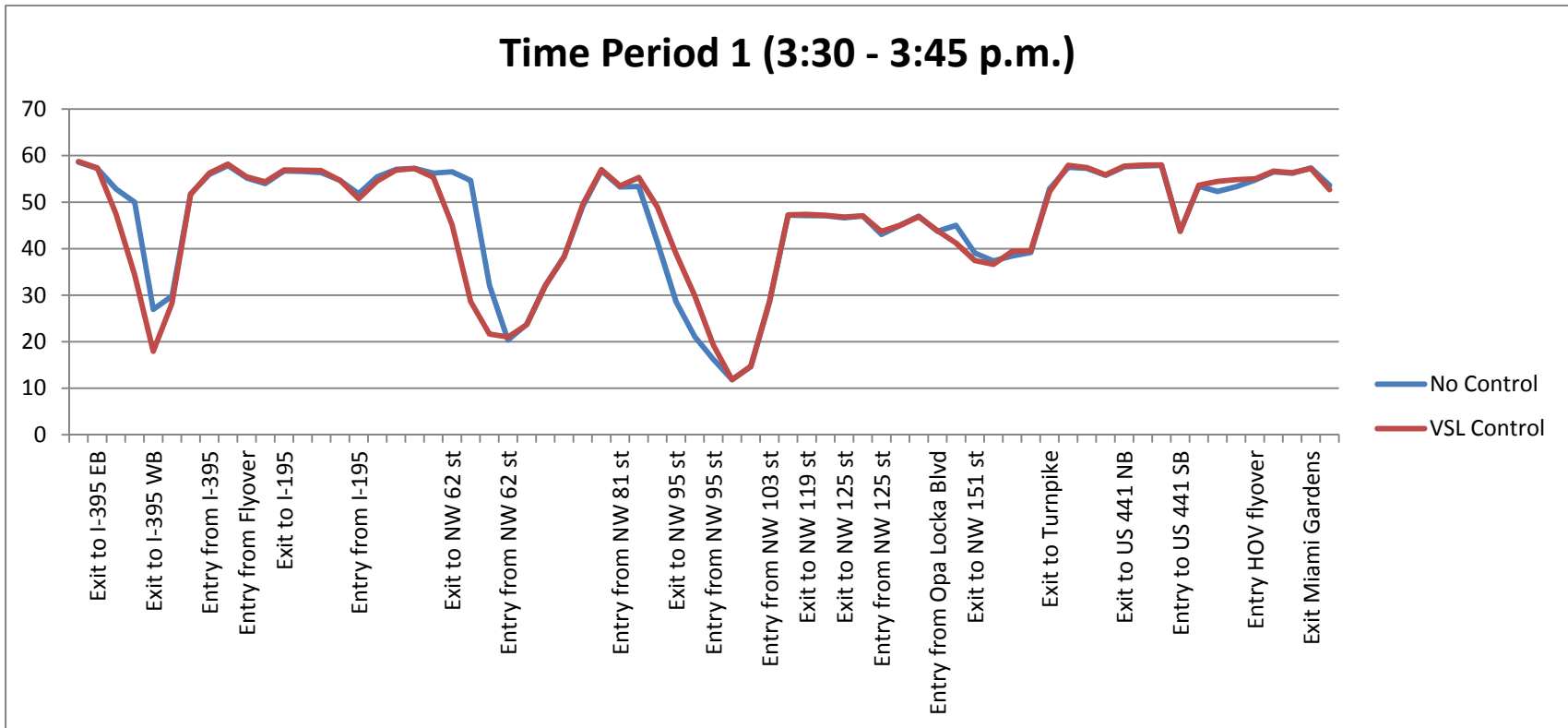
This subsection examines the operational effects of implementing VSL at both bottlenecks simultaneously. The best performing algorithm scenario from the upstream bottleneck was paired with five of the best performing scenarios from the downstream bottleneck. This approach was taken to account for the fact that the downstream section would be affected by the upstream VSL and the resulting changes in throughput. Thus the best performing algorithm may not be the same as when Bottleneck 1 is analyzed in isolation.

As indicated in Section 3.4, the best performing scenario was the use of two signs spaced one half mile apart, using the occupancy scenario 1. This scenario was paired with five of the best performing scenarios from Section 3.3. Each simulation was run ten times and the average was taken from all ten runs. The average speed over the entire network, and the total travel time were obtained and are shown in Table 3.9. As shown, the combination producing the best results is using two signs spaced one half mile apart, using the occupancy Scenario 1 at the upstream bottleneck. This was paired with the use of two signs spaced 1 mile apart, using the volume threshold scenario 1. This combination results in the greatest improvement in network average travel speed with a 2.31 % (0.92 mph) increase. This scenario also resulted in the greatest decrease in total travel time by 2.24% (259 hours). The speed profile for this scenario compared to the no-control scenario is shown in Figure 3.20.

It was anticipated that the combination of the two VSL sections would improve conditions even more, but the improvements of the combined scenario are not as high as either scenario working by itself. It is possible that the traffic conditions have changed due to the upstream VSL operation, and a different VSL strategy would need to be implemented downstream. To completely assess each algorithm and document their relative merits and preferred applications, a full optimization of thresholds and sign positioning would have to be performed.

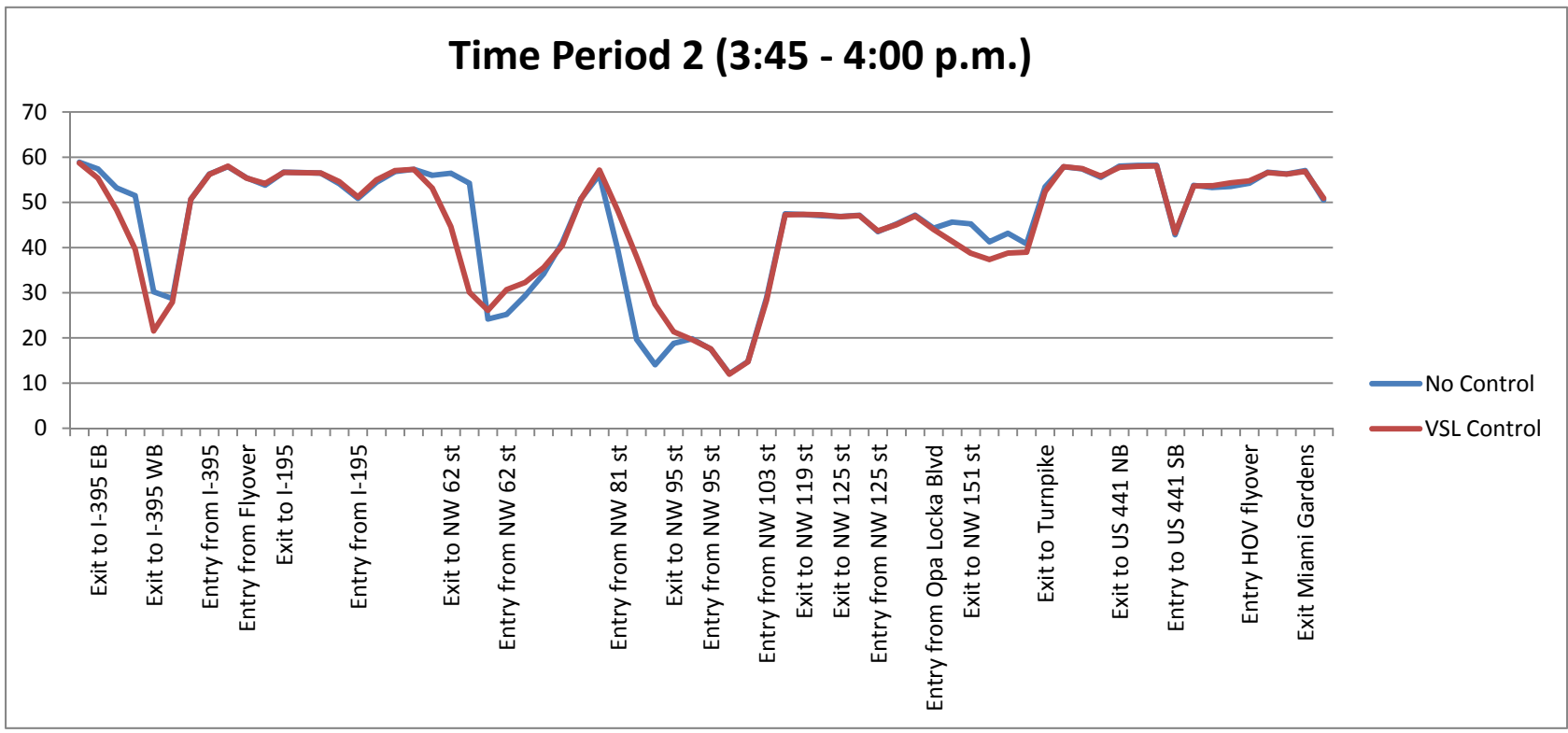
TABLE 3.9 Network performance measures for corridor analysis

Algorithm	# of signs	Spacing (miles)	Threshold scenario	Average speed	% Change from no-control	Total travel time (hours)	% Change from no-control
No control	NA	NA	NA	39.57	0.00	7624.55	0.00
Occupancy	2	1/2	1	40.08	1.29	7528.56	-1.26
Occupancy	2	1/2	2				
Occupancy	2	1/2	1	39.83	0.64	7589.62	-0.46
Occupancy	1	1	2				
Occupancy	2	1/2	1	40.22	1.62	7513.61	-1.46
Occupancy	2	1/2	1				
Occupancy	2	1/2	1	39.64	0.97	7564.87	-0.78
Volume	1	1	1				
Occupancy	2	1/2	1	40.49	0.92	7453.47	-2.24
Volume	2	1	1				



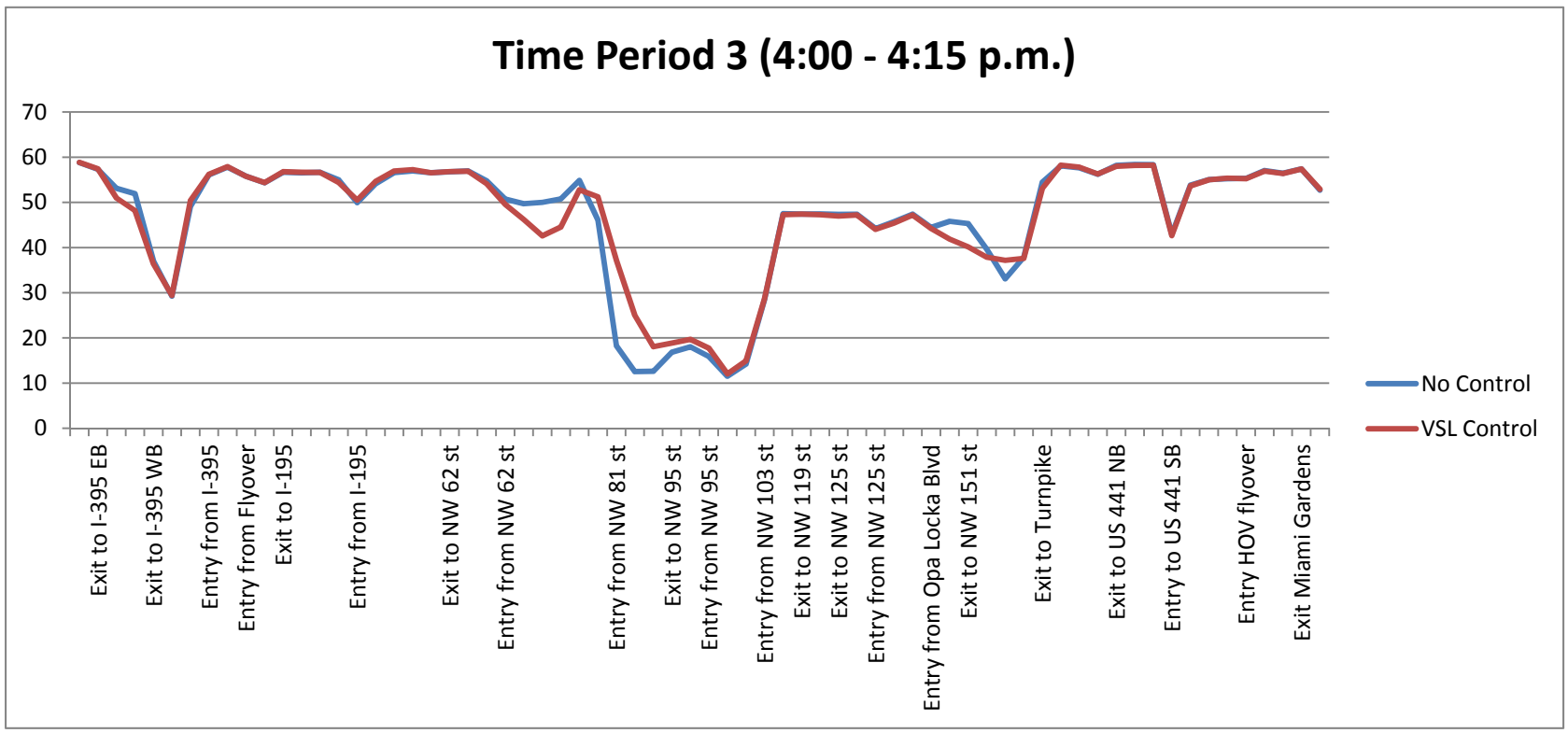
A

FIGURE 3.20 Speed profile for the combination VSL control compared to the no-control scenario A) Time period 1; B) Time Period 2; C) Time period 3; D) Time period 4; E) Time period 5; F) Time Period 6; G) Time Period 7; H) Time Period 8; I) Time Period 9; J) Time Period 10; K) Time Period 11; L) Time Period 12.



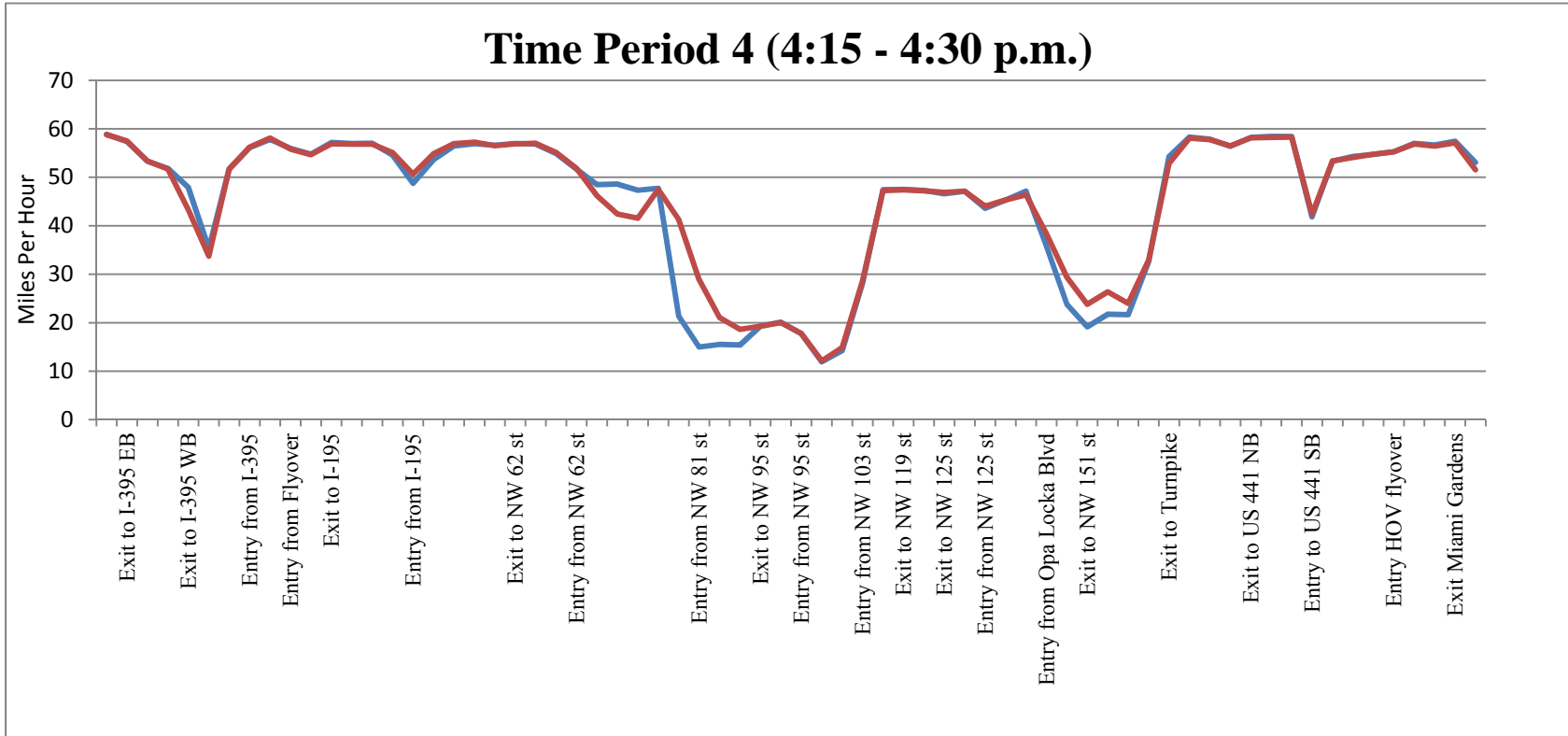
B

FIGURE 3.20 (Continued) Speed profile for the combination VSL control compared to the no-control scenario A) Time period 1; B) Time Period 2; C) Time period 3; D) Time period 4; E) Time period 5; F) Time Period 6; G) Time Period 7; H) Time Period 8; I) Time Period 9; J) Time Period 10; K) Time Period 11; L) Time Period 12.



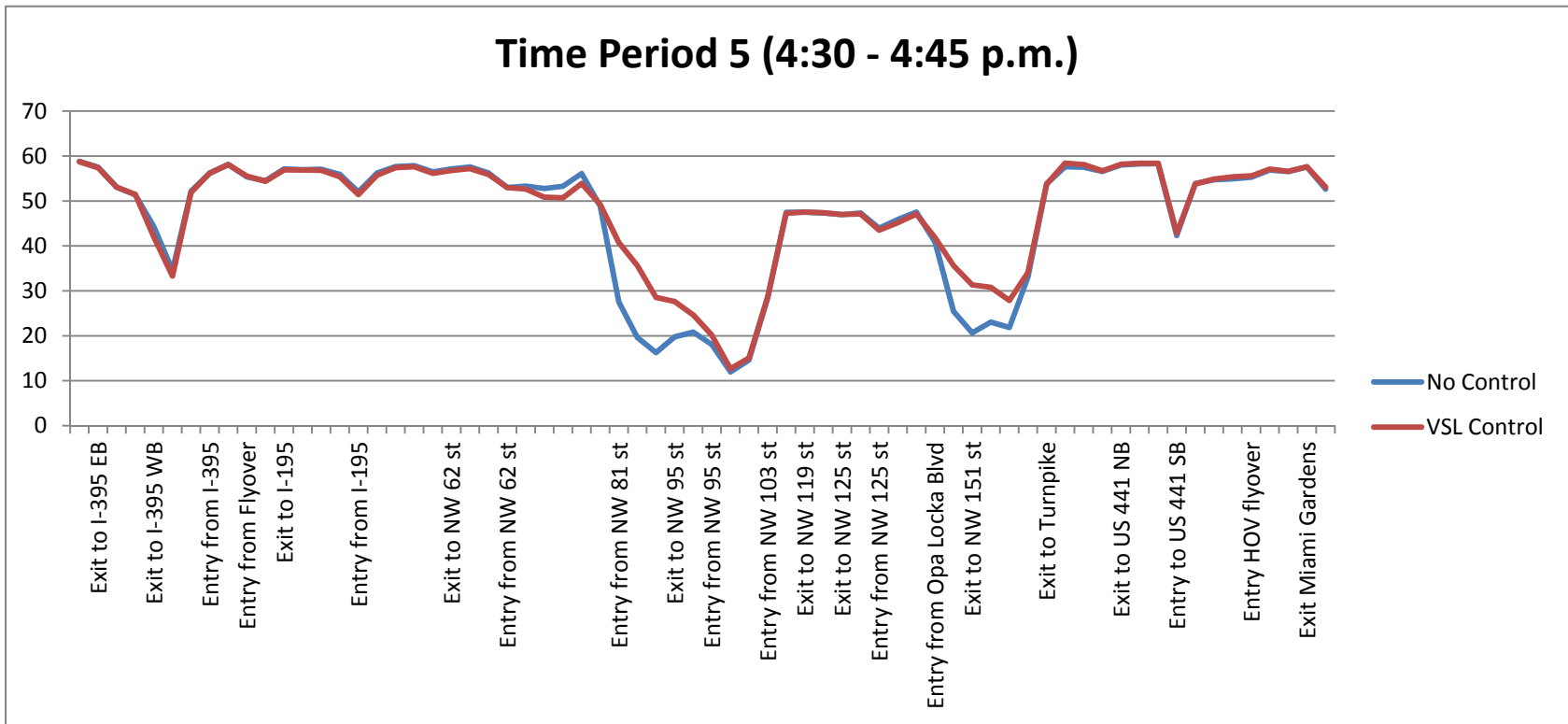
C

FIGURE 3.20 (Continued) Speed profile for the combination VSL control compared to the no-control scenario A) Time period 1; B) Time Period 2; C) Time period 3; D) Time period 4; E) Time period 5; F) Time Period 6; G) Time Period 7; H) Time Period 8; I) Time Period 9; J) Time Period 10; K) Time Period 11; L) Time Period 12.



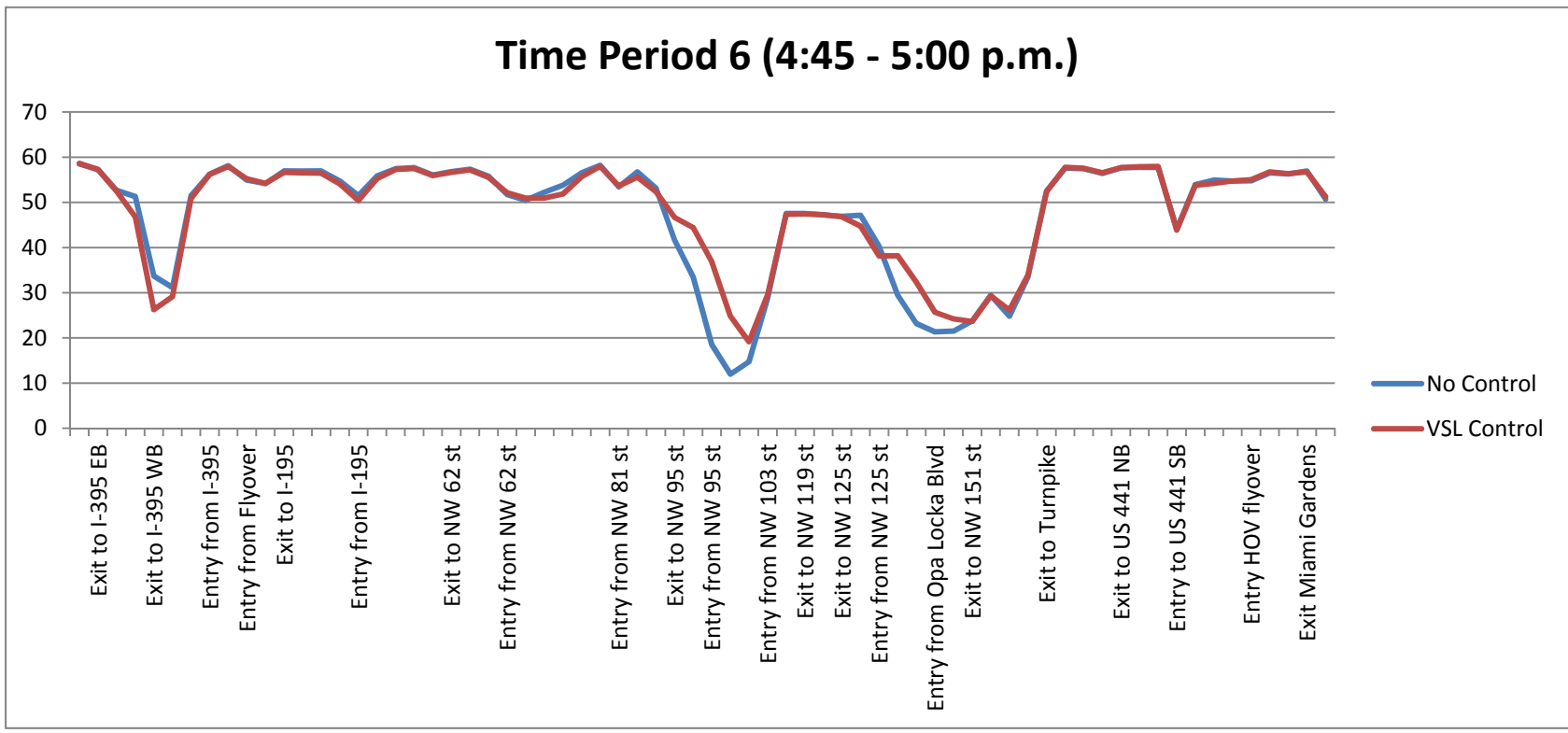
D

FIGURE 3.20 (Continued) Speed profile for the combination VSL control compared to the no-control scenario A) Time period 1; B) Time Period 2; C) Time period 3; D) Time period 4; E) Time period 5; F) Time Period 6; G) Time Period 7; H) Time Period 8; I) Time Period 9; J) Time Period 10; K) Time Period 11; L) Time Period 12.



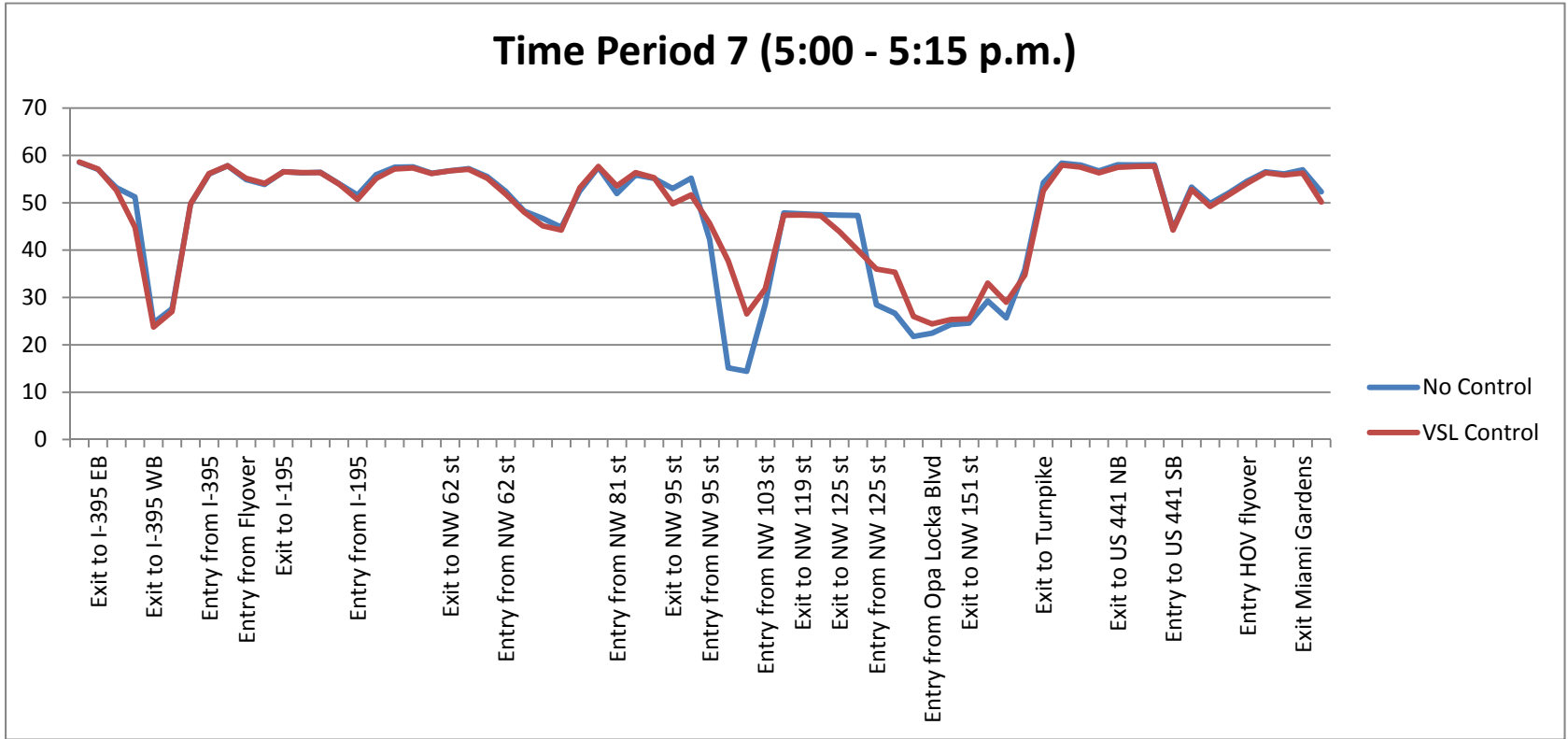
E

FIGURE 3.20 (Continued) Speed profile for the combination VSL control compared to the no-control scenario A) Time period 1; B) Time Period 2; C) Time period 3; D) Time period 4; E) Time period 5; F) Time Period 6; G) Time Period 7; H) Time Period 8; I) Time Period 9; J) Time Period 10; K) Time Period 11; L) Time Period 12.



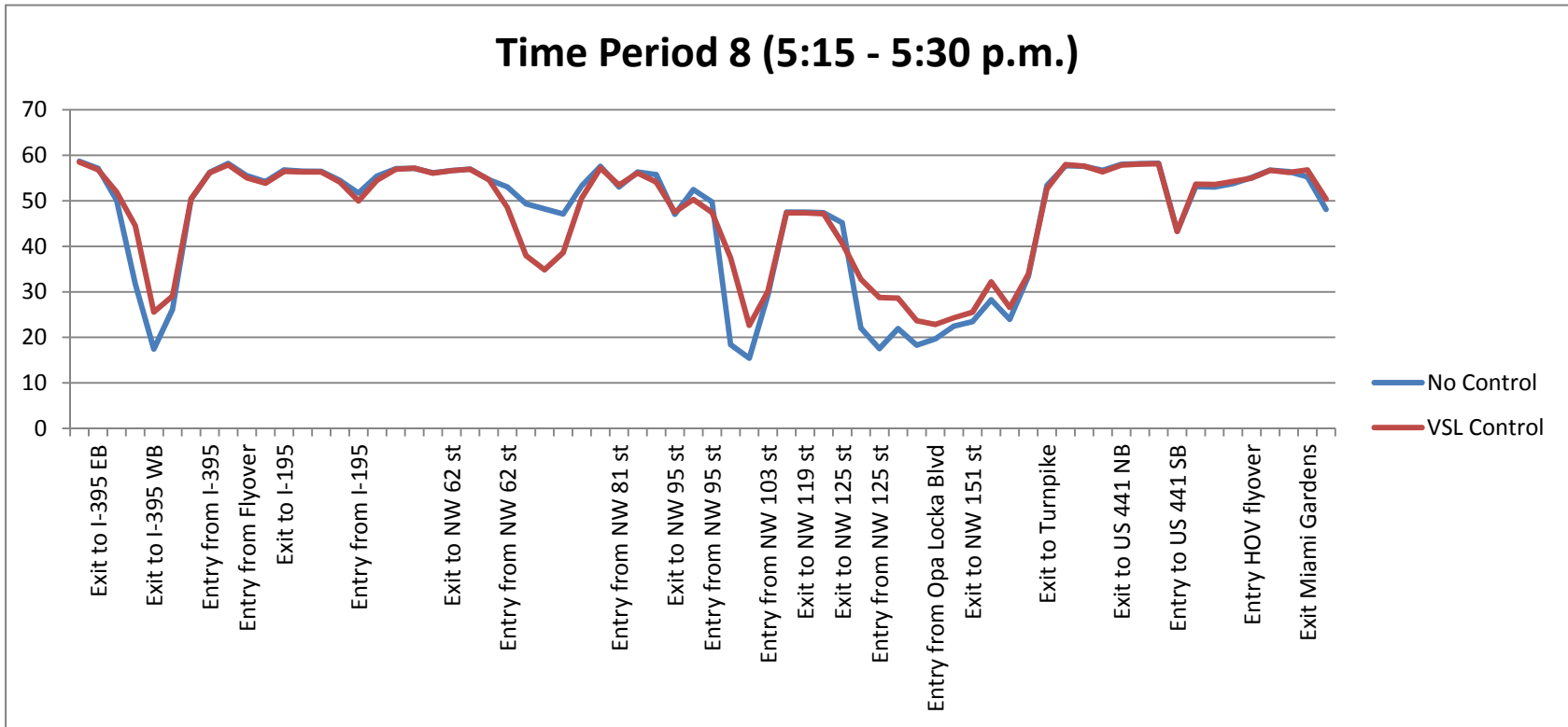
F

FIGURE 3.20 (Continued) Speed profile for the combination VSL control compared to the no-control scenario A) Time period 1; B) Time Period 2; C) Time period 3; D) Time period 4; E) Time period 5; F) Time Period 6; G) Time Period 7; H) Time Period 8; I) Time Period 9; J) Time Period 10; K) Time Period 11; L) Time Period 12.



G

FIGURE 3.20 (Continued) Speed profile for the combination VSL control compared to the no-control scenario A) Time period 1; B) Time Period 2; C) Time period 3; D) Time period 4; E) Time period 5; F) Time Period 6; G) Time Period 7; H) Time Period 8; I) Time Period 9; J) Time Period 10; K) Time Period 11; L) Time Period 12.



H

FIGURE 3.20 (Continued) Speed profile for the combination VSL control compared to the no-control scenario A) Time period 1; B) Time Period 2; C) Time period 3; D) Time period 4; E) Time period 5; F) Time Period 6; G) Time Period 7; H) Time Period 8; I) Time Period 9; J) Time Period 10; K) Time Period 11; L) Time Period 12.

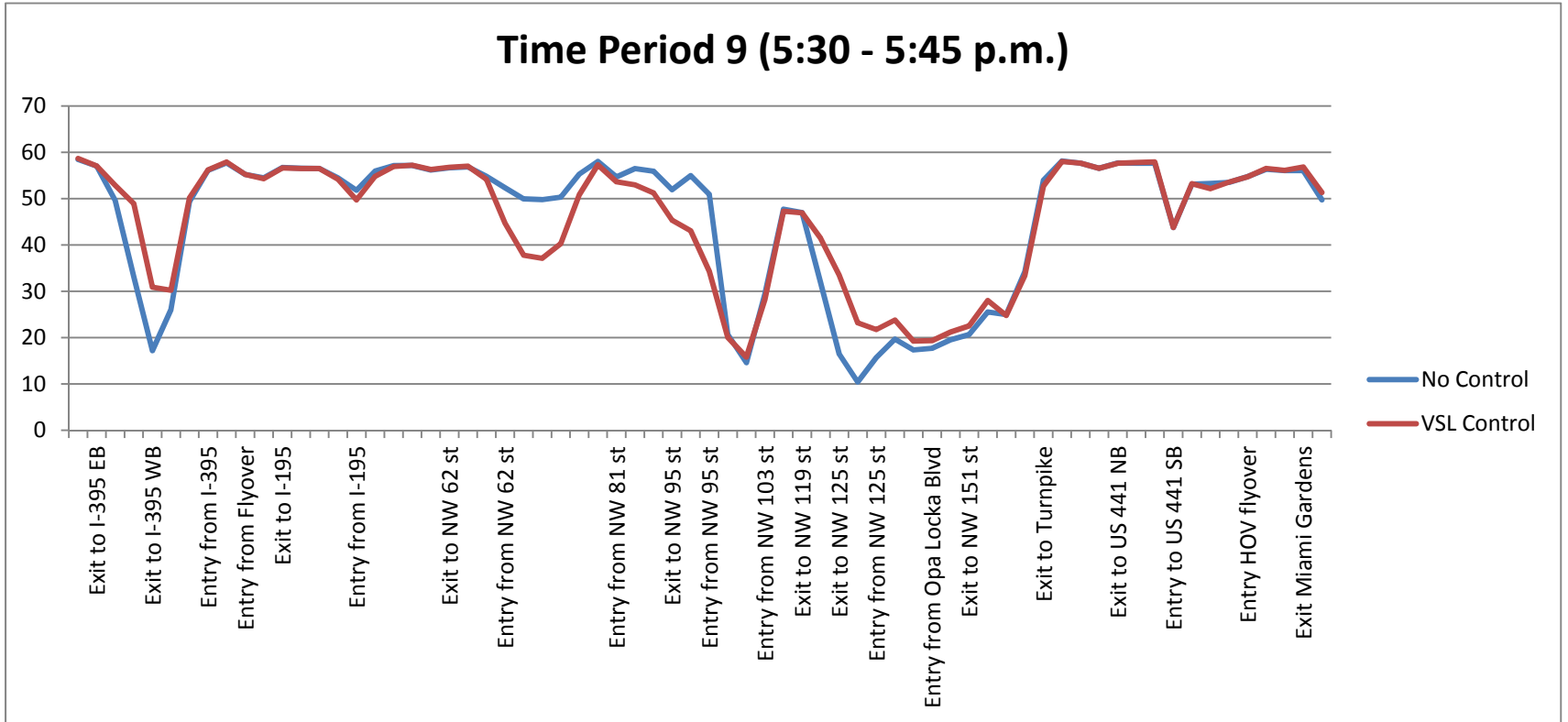


FIGURE 3.20 (Continued) Speed profile for the combination VSL control compared to the no-control scenario A) Time period 1; B) Time Period 2; C) Time period 3; D) Time period 4; E) Time period 5; F) Time Period 6; G) Time Period 7; H) Time Period 8; I) Time Period 9; J) Time Period 10; K) Time Period 11; L) Time Period 12.

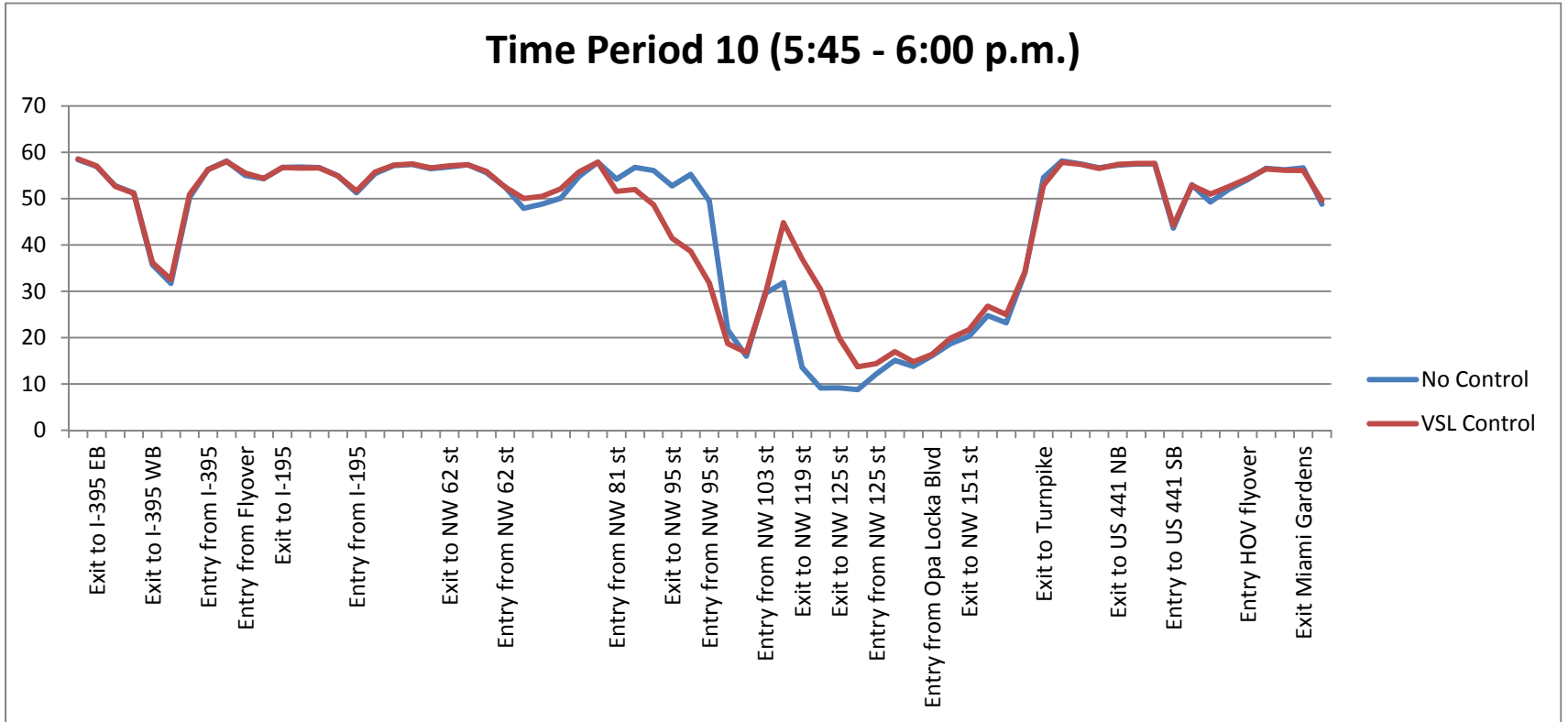
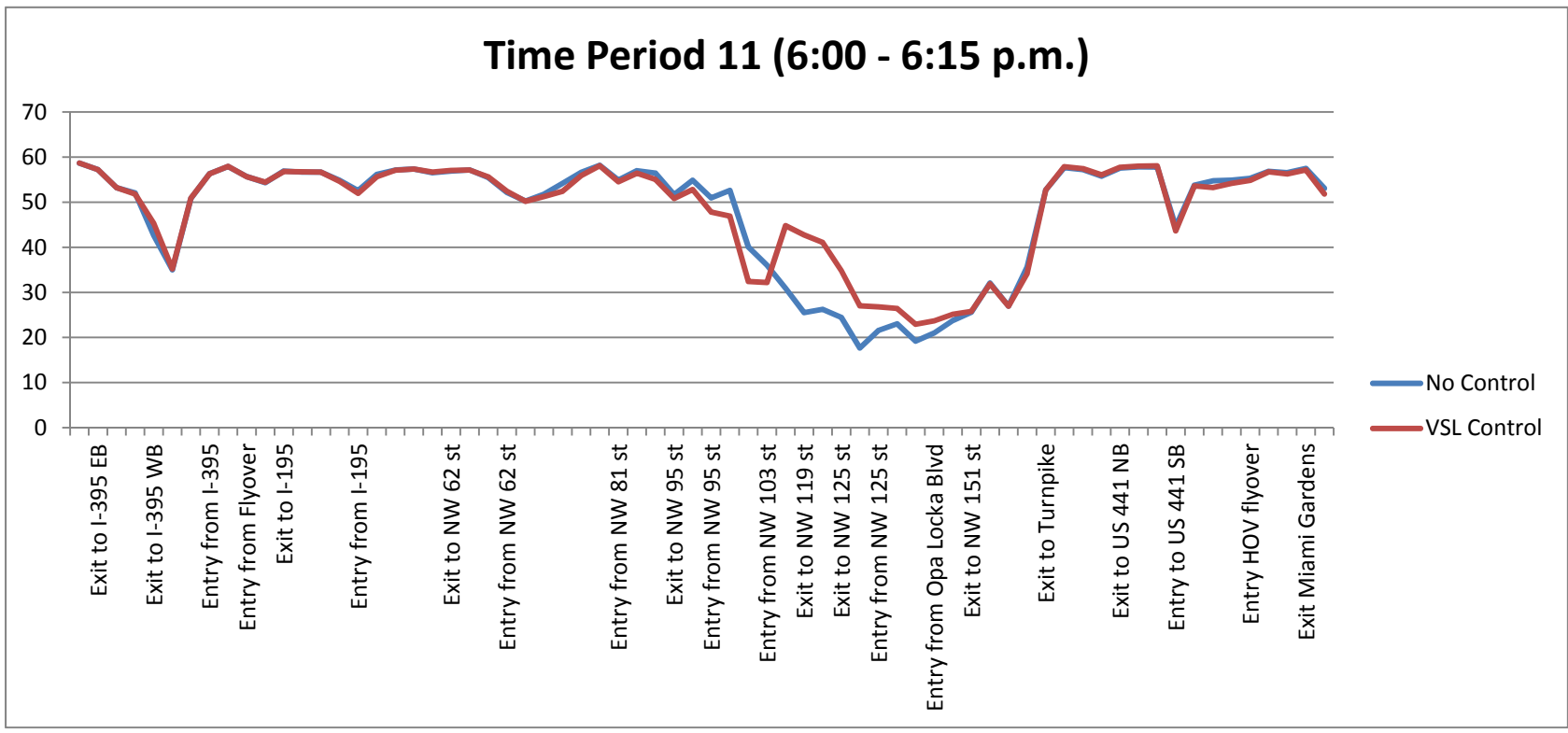
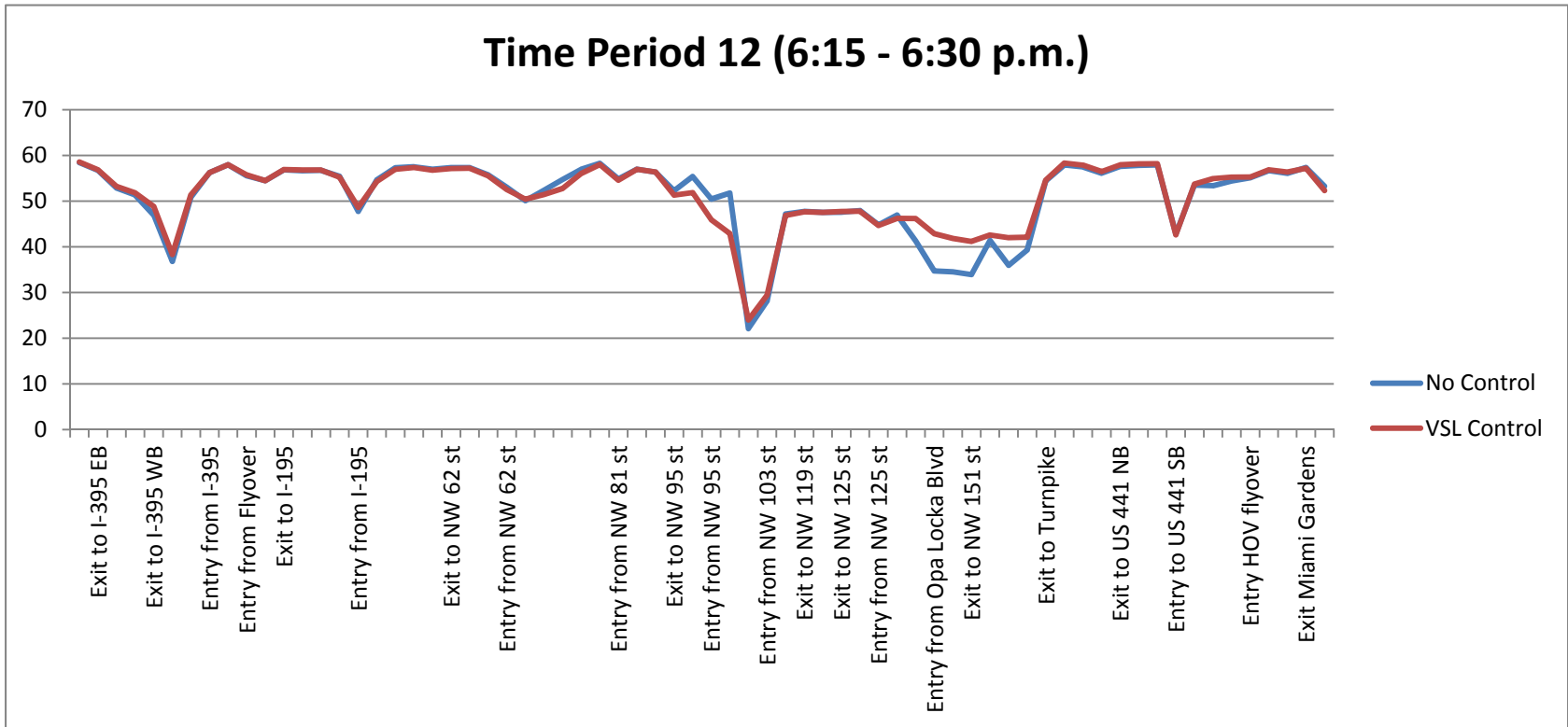


FIGURE 3.20 (Continued) Speed profile for the combination VSL control compared to the no-control scenario A) Time period 1; B) Time Period 2; C) Time period 3; D) Time period 4; E) Time period 5; F) Time Period 6; G) Time Period 7; H) Time Period 8; I) Time Period 9; J) Time Period 10; K) Time Period 11; L) Time Period 12.



K

FIGURE 3.20 (Continued) Speed profile for the combination VSL control compared to the no-control scenario A) Time period 1; B) Time Period 2; C) Time period 3; D) Time period 4; E) Time period 5; F) Time Period 6; G) Time Period 7; H) Time Period 8; I) Time Period 9; J) Time Period 10; K) Time Period 11; L) Time Period 12.



L

FIGURE 3.20 (Continued) Speed profile for the combination VSL control compared to the no-control scenario A) Time period 1; B) Time Period 2; C) Time period 3; D) Time period 4; E) Time period 5; F) Time Period 6; G) Time Period 7; H) Time Period 8; I) Time Period 9; J) Time Period 10; K) Time Period 11; L) Time Period 12.

4 CONCLUSIONS AND RECCOMENDATIONS

This section provides conclusions and recommendations regarding each of the tasks addressed in this report. Section 4.1 relates to the coordination between pricing and ramp metering. Section 4.2 provides conclusions and recommendations related to the evaluation of VSLs along the I-95 corridor.

4.1 Coordination Between Pricing and Ramp Signaling

The primary purpose of this task was to explore the interactions between ramp metering and pricing, and to propose a method of coordinating them in order to improve traffic operations along the freeway network. The research team first developed a theoretical framework regarding the interaction of congestion pricing and ramp metering according to their respective locations on the network. This analysis suggested that an increase in the toll rates would cause a decrease in the metering rates at the ramp meters that are installed along the HOT lanes.

This hypothesis was examined using simulation. The I-95 in Miami was simulated in CORSIM. A dynamic pricing algorithm (i.e., I-95 HOT Tolling Algorithm) and a dynamic ramp metering algorithm (i.e., Fuzzy Logic Ramp Metering Algorithm) were programmed and interfaced with CORSIM to conduct the experiments. The simulation results were in agreement with the hypothesis made in the early stages of this task. An increase in the toll rate is rendering the HOT lanes less preferable with respect to travel cost, shifting traffic to the GP lanes. This causes the metering rate to become more restrictive.

Based on the analysis conducted, the optimal operation of the system would rely on maximizing the utilization of the HOT lanes. Therefore, it is suggested that one of the objectives of the pricing algorithm should be the maximization of the utilization of the HOT lanes. The toll rate should always remain at a level that prevents the occurrence of breakdowns on the HOT lanes.

The more traffic HOT lanes manage to service without the risk of congestion, the easier it becomes for ramp metering to regulate the mainline and on-ramp traffic.

Concurrently with the investigation of the interactions between ramp metering and pricing, the researchers evaluated the operation of different tolling algorithms and different combinations of ramp metering and pricing algorithms. This evaluation revealed that the integrated control (i.e., ramp metering plus tolling) regulates traffic much more efficiently compared to the tolling only case. However, when both algorithms are implemented it is recommended that they operate in a dynamic way in order to mitigate congestion successfully both on the ramps and the mainline freeway.

4.2 Variable Speed Limits on I-95 Express

This task evaluated whether VSL could/should be considered for incorporation into managed lanes along the I-95 HOT lanes facility. The researchers used the CORSIM simulation model developed under Task 5 to replicate VSL operations along the facility. Various types of VSL algorithms were implemented at specific locations along the simulated I-95 freeway section to evaluate the effectiveness of these algorithms. The following were concluded:

- Most of the algorithms tested improved average travel speed and total travel time, though different thresholds were tested to obtain a “best case” scenario.
- The throughput was found to increase for most of the VSL scenarios tested by a maximum of 30 to 90 vehicles over a given 15-minute time period.
- The effect of the VSL may not be immediately seen if one examines conditions only at the bottleneck. The area upstream of the bottleneck shows much greater traffic improvements than the bottleneck itself.
- Improper selection of thresholds or sign positioning can cause traffic conditions to deteriorate compared to the no VSL control case.

- The best performing algorithm and scenario was different between the two bottleneck locations, suggesting that there is no best implementation that applies to every bottleneck.
- There was no consistent trend in traffic performance as a function of the number and location of speed limit signs. The best sign positioning was found to be highly dependent on the type of algorithm and specific thresholds selected.
- Implementing VSL at both bottlenecks simultaneously did not improve operations beyond those observed when implementing VSL at one bottleneck only. However, additional testing of combinations of algorithms at the two bottlenecks might reveal that another combination can further improve performance.
- The results and conclusions of this study assume speed limit compliance from motorists. In order for the I-95 corridor to operate at similar levels, the same level of compliance must be achieved. Thus there is a need for enforcement of the speed limits when they are implemented in the field.

In conclusion, VSL has the potential to improve traffic operations along the I-95 corridor, if applied appropriately. Several issues must be addressed before implementation of such a system. It is recommended that a study be completed to assess the performance of the VSL system working in unison with the dynamic tolling, and the fuzzy logic ramp signaling currently employed on I-95 in Miami, FL. Few studies have been conducted on the interaction between these three control strategies. Such a study could provide a clearer picture of how the VSL would function as a piece of a larger control strategy. It is expected that coordination/ optimization with these other control strategies would further increase the benefits observed from the VSL system. Another issue that needs to be addressed is the compliance of motorists to reduced speed limits. Another study currently underway for the Florida Department of Transportation by the University of Florida Transportation Research Center, is examining those issues for the I-4 corridor (FDOT Contract BDK77-TWO977-11.)

This study did not attempt to thoroughly evaluate and compare the three selected VSL algorithms, nor to obtain optimal thresholds for each type of algorithm. An optimization-type study could be performed to obtain optimal thresholds, sign locations, and detector locations. To

fully consider the implementation of this system on I-95 in Miami, a feasibility study must be completed, weighing the potential benefits and the cost of deployment, maintenance, and operations.

REFERENCES

- Allaby P., Hellenga B., and Bullock M., 2007. Variable Speed Limits: Safety and Operational Impacts of a Candidate Control Strategy for Freeway Applications. *IEEE Transactions on Intelligent Transportation System* 8 (4), pp. 671-680.
- Elefteriadou, L., Brilon, W., Jacobson, L., 2011. Proactive Ramp Management Under the Threat of Freeway Flow Breakdown. NCHRP Report 3-87.
- FHWA, 2008. Technologies That Complement Congestion Pricing: A Primer.
- Florida Department of Transportation (FDOT), 2011. Managed Lane Operations – Adjusted Time of Day Pricing vs. Near-Real Time Dynamic Pricing. Tallahassee, FL.
- Highway Capacity Manual (HCM), 2000. Transportation Research Board. Washington, DC, ISBN: 0-309-06681-6.
- Meldrum, D. & Taylor, C., 2000. Algorithm Design, User Interface, and Optimization Procedure for a Fuzzy Logic Ramp Metering Algorithm: A Training Manual for Freeway Operations Engineers. Technical Report to Washington State Department of Transportation, Seattle.
- PBS&J., 2009. I-4 Variable Speed Limit Effectiveness Study. Prepared for the Florida Department of Transportation, District 5.
- Robinson, M. D., 2000. Examples of Variable Speed Application. In: Proceedings of the 79th Annual Meeting of the Transportation Research Board, Washington, D.C.
- Shen, W., & Zhang, H. M., 2009. Pareto-Improving Ramp Metering Strategies for Reducing Congestion in the Morning Commute. Transportation Research Board, 88th Annual Meeting.
- Sisiopiku V., 2001. Variable Speed Control: Technologies and Practices. In: Proceedings of the 80th Annual Meeting of the Transportation Research Board, Washington, D.C.
- Swenson, C. R., & Poole, Jr. R. W., 2009. Reducing Congestion in Lee County, Florida. Reason Foundation.

APPENDIX A – CALIBRATION DATA

This appendix provides details regarding the inputs and calibration of the CORSIM file. Table A-1 includes information regarding the entering traffic in the simulated network along with the exiting percentages at each off-ramp during every time interval. Table A-2 shows the values of the car following sensitivity factor and free flow speed (mph) for each network link.

TABLE A-1 Entering and exiting percentages in the simulated network

		Mainline Volume Data											
Description	Type	Time Period											
		1	2	3	4	5	6	7	8	9	10	11	12
		15:30	15:45	16:00	16:15	16:30	16:45	17:00	17:15	17:30	17:45	18:00	18:15
Begin I-95 NB		1330	1354	1297	1298	1350	1474	1477	1534	1464	1435	1431	1491
Exit to I-395 EB	exit	140	154	155	163	153	159	182	230	211	193	195	249
I-95 NB		1190	1200	1142	1135	1197	1315	1295	1304	1253	1242	1236	1242
Exit to I-395/SR 836 WB	exit	256	255	270	239	265	248	237	161	180	153	238	236
I-95 NB		935	945	872	895	932	1067	1059	1144	1073	1089	998	1006
Entry from NW 8th St./NW 3rd Ave.	entry	222	227	279	189	187	215	224	152	161	140	158	115
I-95 NB		1157	1172	1151	1084	1118	1282	1282	1296	1234	1228	1156	1121
Exit to Flyover	exit	324	258	161	249	268	295	256	350	259	284	207	202
I-95 NB		833	914	989	835	850	987	1026	946	975	944	949	919
Entry from I-395 EB/WB	entry	628	601	602	629	641	630	629	621	582	582	611	622
I-95 NB		1461	1515	1591	1464	1491	1617	1655	1567	1557	1526	1560	1541
Entry from Flyover	entry	324	258	161	249	268	295	256	350	259	284	207	202
I-95 NB		1785	1773	1752	1714	1760	1912	1912	1917	1816	1810	1768	1743
Exit to I-195 EB/WB	exit	431	438	436	429	432	458	466	481	455	438	432	441
I-95 NB		1353	1334	1316	1285	1328	1454	1446	1436	1361	1372	1336	1302
Entry from I-195 EB/WB	entry	681	678	675	720	660	638	623	681	575	465	473	559
I-95 NB		2035	2012	1991	2005	1988	2092	2069	2117	1936	1838	1809	1861
Exit to HOT Lanes	exit	203	201	259	301	298	272	269	254	271	257	235	279
I-95 NB		1831	1811	1732	1704	1690	1820	1800	1863	1665	1580	1574	1582
Exit to NW 62nd St.	exit	220	127	69	278	186	218	357	149	271	237	79	79
I-95 NB		1612	1684	1663	1426	1504	1602	1443	1714	1394	1343	1495	1503
Entry from NW 62nd St.	entry	213	194	207	186	201	199	204	213	198	196	194	175
I-95 NB		1825	1878	1870	1612	1705	1801	1647	1927	1592	1539	1689	1678
Entry from NW 69th St.	entry	185	104	152	180	87	144	200	197	188	145	197	175
I-95 NB		2010	1982	2022	1792	1792	1945	1847	2124	1780	1684	1886	1853
Exit to NW 79th St.	exit	100	258	182	125	108	156	111	191	160	236	189	214
I-95 NB		1909	1725	1840	1667	1684	1789	1736	1933	1620	1448	1698	1639
Entry from NW 81st St.	entry	214	196	201	194	207	204	189	202	149	182	176	183
I-95 NB		2123	1921	2041	1861	1891	1993	1925	2135	1769	1630	1874	1822
Exit to NW 95th St.	exit	190	153	135	242	178	219	193	107	106	130	56	73
I-95 NB		1933	1767	1906	1619	1713	1774	1733	2028	1663	1500	1817	1749
Entry from NW 95th St.	entry	133	119	116	122	118	129	121	112	81	96	89	114
I-95 NB		2066	1886	2022	1741	1831	1903	1854	2140	1744	1596	1906	1863
Exit to NW 103rd St.	exit	145	113	121	122	146	114	167	214	87	160	95	296
I-95 NB		1922	1773	1900	1619	1685	1789	1687	1926	1656	1436	1811	1567
Entry from NW 103rd St.	entry	185	212	161	186	168	235	240	239	236	219	254	174
I-95 NB		2107	1985	2061	1805	1853	2024	1927	2165	1892	1655	2065	1741
Exit to NW 119th St.	exit	42	40	41	36	222	40	39	43	38	149	207	209
I-95 NB		2065	1945	2020	1769	1631	1983	1888	2122	1855	1506	1859	1532
Exit to NW 125th St.	exit	41	39	40	53	33	40	38	42	37	151	223	184
I-95 NB		2023	1906	1980	1716	1598	1944	1851	2079	1818	1356	1636	1348
Entry from NW 125th St.	entry	185	188	190	251	270	273	268	247	255	190	192	156
I-95 NB		2208	2094	2170	1967	1868	2217	2119	2326	2073	1546	1828	1504
Exit to NW 135th St.	exit	199	251	174	315	56	66	64	70	104	201	219	78
I-95 NB		2010	1843	1996	1652	1812	2150	2055	2256	1969	1345	1572	1426
Entry from Opa Locka Blvd	entry	238	239	239	238	238	238	238	238	238	214	195	182
I-95 NB		2247	2081	2235	1890	2050	2388	2292	2494	2206	1559	1767	1608
Exit to NW 151st St.	exit	51	50	46	189	38	167	33	28	22	35	41	50
I-95 NB		2196	2032	2189	1701	2011	2220	2260	2466	2184	1524	1726	1558
Entry from HOT Lane	entry	301	225	345	247	255	255	221	202	346	237	218	238
I-95 NB		2497	2257	2534	1948	2266	2475	2481	2668	2530	1761	1944	1796
Exit to Turnpike	exit	874	880	1039	820	929	916	992	1067	1012	822	830	782
I-95 NB		1623	1377	1495	1128	1337	1560	1488	1601	1518	939	1114	1014
Exit to North Golden Glades Dr./SR 826 EB	exit	243	159	254	124	174	125	194	208	76	94	111	101
I-95 NB		1380	1218	1241	1004	1163	1435	1295	1393	1442	845	1003	912
Exit to US 441 NB	exit	519	386	199	130	116	215	614	695	72	34	150	23
I-95 NB		861	832	1042	873	1047	1220	681	698	1370	811	852	889
Entry from US 441 NB	entry	220	210	228	219	229	239	247	273	234	251	221	215
I-95 NB		1081	1042	1270	1092	1276	1459	928	971	1604	1062	1073	1104
Entry from NW 2nd Ave./167th St.	entry	327	353	324	380	315	285	394	355	357	368	317	303
I-95 NB		1408	1395	1594	1472	1591	1744	1322	1326	1961	1430	1390	1407
Entry from HOV Flyover	entry	212	200	213	215	195	234	271	250	235	241	246	218
I-95 NB		1620	1595	1807	1687	1786	1978	1593	1576	2196	1671	1637	1625
Exit to Miami Gardens Dr.	exit	162	160	181	169	179	198	159	158	220	167	164	163
I-95 NB		1458	1436	1627	1519	1607	1780	1434	1418	1976	1504	1473	1463
Entry from Miami Gardens Dr.	entry	165	203	174	206	188	219	194	242	215	225	187	197
End I-95 NB		1623	1639	1801	1725	1795	1999	1628	1660	2191	1729	1660	1660
NB HOT Lanes													
Entry from GP Lanes		309	284	349	384	360	341	338	363	344	341	290	369
Entry from I-195 EB HOV		292	232	317	184	167	251	246	147	223	138	261	118
Begin NB HOT lanes		601	516	666	568	527	592	584	510	567	479	551	487
Exit to I-95 NB GP Lanes	exit	361	270	400	288	288	288	249	255	397	287	243	292
I-95 NB HOV Flyover (Golden Glades)		240	246	266	280	239	304	335	255	170	191	308	195
Exit to Park and Ride	exit	53	54	59	62	53	67	74	56	37	42	68	43
I-95 NB HOV Entrance Ramp		188	192	208	219	187	237	262	199	133	149	240	152

TABLE A-2 Car-following sensitivity parameter by link

Link #	Free-Flow Speed (mph)	Car-following Sensitivity Multiplier	Link #	Free-Flow Speed (mph)	Car-following Sensitivity Multiplier
[105, 106]	60	1.00	[139, 140]	60	1.65
[106, 107]	60	1.00	[140, 141]	55	1.50
[107, 108]	55	1.00	[141, 142]	55	1.00
[108, 109]	55	1.00	[142, 145]	50	1.50
[109, 111]	55	1.00	[145, 146]	50	1.80
[111, 112]	55	2.00	[146, 147]	50	1.00
[112, 113]	55	2.00	[147, 148]	50	1.00
[113, 114]	60	1.00	[148, 149]	50	1.00
[114, 115]	60	1.00	[149, 150]	50	1.00
[115, 116]	60	1.00	[150, 152]	50	1.00
[116, 117]	60	1.00	[152, 153]	50	1.50
[117, 118]	60	1.00	[153, 154]	50	1.65
[118, 119]	60	1.00	[154, 155]	50	1.50
[119, 120]	60	1.00	[155, 156]	50	1.50
[120, 121]	60	1.00	[156, 157]	50	1.50
[121, 122]	60	1.00	[157, 159]	50	1.80
[122, 123]	60	1.00	[158, 159]	50	1.80
[123, 124]	60	1.00	[159, 161]	55	1.80
[124, 125]	60	1.00	[161, 165]	55	1.80
[125, 126]	60	1.00	[165, 166]	60	1.00
[126, 127]	60	1.00	[166, 167]	60	1.00
[127, 128]	60	1.00	[167, 168]	60	1.00
[128, 129]	60	1.60	[168, 170]	60	1.00
[129, 130]	60	1.60	[170, 171]	60	1.00
[130, 131]	60	1.70	[171, 172]	60	1.00
[131, 132]	60	1.90	[172, 174]	60	1.00
[132, 133]	60	2.00	[174, 177]	60	1.20
[133, 134]	60	1.50	[177, 178]	60	1.20
[134, 135]	60	1.00	[178, 179]	60	1.00
[135, 136]	60	1.00	[179, 180]	60	1.00
[136, 137]	60	1.00	[180, 181]	60	1.20
[137, 138]	60	1.00	[181, 182]	60	1.00
[138, 139]	60	1.65	[182, 185]	60	1.00

APPENDIX B - LITERATURE REVIEW ON VARIABLE SPEED LIMITS (VSL)

Static speed limits are designed to provide motorists with a safe speed at which to drive. While these safe speeds are effective during ideal conditions, they fail to provide recommended safe speeds during adverse weather or congested driving conditions (Sisiopiku 2001). Thus, variable speed limits (VSLs) are implemented to commend safe driving speeds during less than ideal conditions. These systems can result in improved safety and possible performance improvements. This appendix summarizes first the literature review findings regarding implementation of VSLs, followed by research related to driver behavior around VSLs. The third part discusses evaluations of VSLs using simulation. The fourth part provides an overview of VSL algorithms, while the fifth part summarizes the types of VSL signs used.

Implementation of VSLs

The first part of this section provides an overview of VSL systems implemented in the US, while the second part summarizes the findings regarding implementations in Europe. Information regarding many of the evaluations was obtained from Robinson (2000). That report does not list the source documents of each evaluation, and thus it is difficult to obtain additional information regarding these evaluations.

Implementation of VSL in the USA

In the United States variable speed limits have been implemented in a number of locations. These systems typically set a safety speed limit according to the weather, traffic, or road conditions (CTC and Associates LLC, 2003, Abdel-Aty et al., 2006A). Another use of variable speed limits are at school zones and at construction or work zone (Hines, 2002). The main objective of most freeway implementations in the US has been to improve safety, and very few have focused on congestion. Congestion-related benefits have been shown mostly using simulation. However, safety benefits have been documented for several of the systems.

The first variable speed limit system in the US was implemented along the M-10 (Lodge Freeway) in Detroit, Michigan, between the Edsel Ford Freeway (I-94) and the Davison Freeway

in 1960. The system was designed to alert motorists to slow down when approaching congestion and accelerate when leaving a congested area. The system was 3.2 miles long and had 21 VSL sign locations. The speed limits were chosen by the operator based on CCTV and plots of freeway speed. The VSL signs were manually switched at the control center with an increment of 5 mph from 20 to 60 mph. The evaluation results showed that the VSL system did not significantly increase or decrease the vehicle speeds (Robinson, 2000). The system was disbanded sometime after 1967.

In New Jersey, a VSL system was implemented along the New Jersey Turnpike in the 1960s. This system was designed to reduce speed limits during congested conditions, and is currently part of a larger ITS system, that warns drivers of lane closures and crashes to improve safety and avoid large delays. The system is over 148 miles in length and utilizes approximately 120 signs. Since the implementation of the system there have been updates to controllers and detectors, but the system is still running without problems. The posted speed limits are based on average travel speeds and are displayed automatically. The posted speed limit can be reduced from the normal posted speed limit (65 mi/h, 55 mi/h, or 50 mi/h) in increments of 5 mi/h to a minimum speed of 30 mi/h under six conditions: vehicle collisions, traffic congestion, construction, icy road conditions, snowfall, and fog. No formal evaluation of the system has been performed, but the Turnpike Authority observes the system 24 hours a day and deemed its performance to be satisfactory. They did note that the system needed enforcement by State Police (CTC and Associates LLC, 2003, Steel et al., 2005).

In New Mexico, a VSL system was implemented along I-40 in Albuquerque in March of 1989. The system was set up as a test-bed for VSL equipment and was later disbanded in 1997 due to road widening. The six kilometer-long system used three roadside detector stations, and a variable message sign to vary the posted speed limit. The posted speed limit was generated using a look-up table based on the smoothed (90 percent old data plus 10 percent current data) average speed plus a constant based on the environmental conditions. The speed and environmental data such as light level and precipitation were collected by detectors. Evaluation results showed that there was a slight reduction in accidents after the system was implemented. It has been suggested that the implementation of the National Maximum Speed Limit (55 mph) hindered the effect of

the system, as posted speeds were generated based on older data, and field conditions didn't match the expected conditions. (Robinson, 2002, CTC and Associates LLC, 2003, Steel et al., 2005).

In Tennessee, a variable speed limit system was implemented along a 19-mile section of I-75 in 1993 to respond to the reduction in visibility causing crashes during adverse weather conditions (especially fog). The system has 10 VSL signs, 8 fog detectors, 44 radar speed detectors, highway advisory radio, and 6 swinging gates. The posted message and speed limit are determined by a central computer in the Highway Patrol office, based on the transmitted data collected using environmental sensor and vehicle detectors. The system has the capability to close down the entire stretch of roadway during severe fog conditions, and divert traffic onto US Highway 11. This requires coordination with highway patrol officers closing swinging gates. The effect of the VSL on actual travel speeds has not been formally evaluated, but the enforcement agency observed a slight (5 to 10 percent) reduction in speed, and there have been no crashes due to fog after the system was implemented. (Robinson, 2002, Road Weather Management, 2003, Steel et al., 2005).

In Colorado, a variable speed limit system was implemented along the Eisenhower Tunnel on I-70 west of Denver in 1995. This system is designed to improve truck safety by displaying vehicle-specific safe operating speeds for long downgrades. The system consists of a weigh-in motion sensor, variable message sign, inductive loop detectors, and computer hardware and software. A safe speed is computed by an algorithm within the computer system based on the truck weight, speed, and axle configuration. The recommended safe speed is then displayed on a variable message sign. Moreover, each truck receives a vehicle-specific recommended safe speed message. The speed limit was advisory and evaluation results showed that truck-related accidents declined on the steep downhill grade sections after the implementation of the VSL system, even though the truck volume increased (Robinson, 2000).

The Washington Department of Transportation implemented a VSL system on I-90 across the Snoqualmie Pass in 1997. The system was implemented to improve safety and inform motorists of road conditions and weather information and is still active. Speed limits are recommended by the central computer based on information collected from a variety of sources, including wide

aperture radar that tracks speeds, roadside cabinets that collect and control roadside data, and packetized data radio on three mountaintop relay sites that use microwaves to communicate to the control center. The computer automatically computes the speed from relayed data and recommends a VSL value, which an operator implements. It was found that VSLs may lose their effectiveness without enforcement by the State Patrol, and that they reduced the mean speed and increased the speed standard deviation (CTC and Associates LLC, 2003, TravelAid et al., 2001, Steel et al., 2005).

In 1998, Northern Arizona University and the Arizona Department of Transportation developed a VSL system based on a fuzzy control algorithm along the I-40 corridor in rural Arizona. This was an experimental system designed to display appropriate speeds for different weather conditions. It was unclear from the study whether the system was actually ever implemented, or just simulated. The system used a Road Weather Information System to gather atmospheric and road surface conditions. The system then displayed a corresponding speed limit according to the fuzzy control algorithm. Placer (2001) summarized upgrades made to this Road Weather Information System. No performance measures or quantitative impacts of the VSL system were given.

In 2000 a VSL system was implemented along I-80 in Nevada. The system was remotely controlled without human intervention. It consisted of four VSL signs (two eastbound and two westbound), visibility detectors, speed loops, RWIS weather stations, and “reduced speed ahead when flashing” signs upstream of the VSL signs. Speed limits were updated every 15 minutes and computed using a logic tree based on the 85th percentile speed, visibility, and pavement conditions. The results found that the sensors were unreliable and could not accurately relay visibility conditions (Robinson, 2000, Robinson, 2002). This limited the effectiveness of the VSL system. No information was found on the current operational status of the system.

In Florida, VMS were placed along a 9-mile portion of I-4 in Orlando. The system was installed from a period of September 2008 to January 2009. The system is designed to improve safety along I-4 through more steady flow during congested periods, and to provide advance warning of slowing traffic ahead. Detectors are used to measure speed, volume, and occupancy for each lane at 30-second intervals. The SunGuide software monitors the occupancy level and classifies

traffic conditions as either free-flow, light congestion, or heavy congestion. On the basis of these classifications, the software recommends speed limits of 30 mph for heavy congestion, 40 mph for light congestion, and the normal speed limit (i.e., 50 or 55 mph) for free flow. The software also ensures that the posted speed limit does not change by more than 10 mph between two adjacent sets of VSL signs (Haas et al., 2009). A study prepared for the FDOT evaluated the performance of the current VSL operation (PBS&J, 2009). The study concluded that the VSL system was not effective at reducing vehicle speeds because vehicles were not complying to the reduced speed limits. Since vehicles were not affected by the signs no traffic improvements or safety benefits were shown.

A study was conducted in southeast Wyoming (Young, 2010) to assess the effectiveness of VSL signs in a rural setting on a 100 mile stretch of I-80 through Elk Mountain. The system is designed to reduce speed limits during adverse weather conditions. When a reduced speed limit is in effect a yellow flashing light on top of the sign is activated and a reduced speed message is displayed. The study showed that vehicle speeds were reduced by 0.47 – 0.75 mph for every 1 mph reduction in posted speed (Young, 2010).

In Seattle, Washington variable speed limits have been installed recently on a stretch of I-5 from Boeing access road to I-90. The project began in 2009 with the installation of fifteen new overhead sign bridges. The system was activated in August 2010. The overhead signs feature individual displays for each lane and warn of approaching lane closures and traffic congestion. The project is designed to reduce the number of collisions and collision-related congestion. The displayed speed limit ranges from 40 mi/h to 60 mi/hr, and is based on speed and volume data. The speed limit is enforced by the Washington State Patrol. There has yet to be a formal assessment of the effectiveness of the system (WSDOT, 2010).

Implementation of VSL in Europe

According to Hines (2002), numerous VSL systems have been implemented in European countries. Based on European case studies, he reported that VSLs can stabilize traffic flow in congestion and thus decrease the probability of crashes.

A VSL system was implemented along an 18-km (11-mi) section of Autobahn 9 near Munich, Germany, in the 1970s. The system was originally implemented to improve safety, but the effects of the VSL system on other key parameters were also evaluated. The system displays speeds based on three control strategies: incident detection, harmonization, and weather conditions. Boice et al. (2006) investigated the effects of the system on key parameters around bottleneck formation, based on one-day data along the site. It was found that once a bottleneck had formed there was an 11% reduction in flow in the northbound direction and a 6% reduction in flow in the southbound direction. Capacity values were provided by lane and they were compared to the Highway Capacity Manual (HCM, 2000), and the German Handbuch für die Bemessung von Strassenverkehrsanlagen (HBS, 2002). The capacity values for the median lane were consistent with both the HCM and the HBS values. The capacity value for the middle lane was consistent with the HBS but slightly lower than the HCM. The shoulder lane capacity was consistently lower than both manuals. It was concluded that there was no improvement in the capacity values over recognized standards.

In the Netherlands, a VSL system was installed along the A16 motorway near Breda in 1991. This system was designed to improve driving safety during fog conditions. The system has signs every 0.4-0.5 miles over 7.4 miles, 20 visibility sensors, and automatic incident detection. The speed limit was reduced to 80 km/h (50 mi/h) from 100 km/h (62 mi/h) if visibility dropped below 140 meters, and was reduced to 60 km/h (37 mi/h) from 100 km/h (62 mi/h) if visibility dropped below 70 meters. When an incident was detected, a speed limit of 50 km/h (31 mi/h) was posted on the first sign upstream and 70 km/h (43 mi/h) on the second sign upstream (Robinson, 2000). The results of an evaluation (Zarean et. al, 1999) showed that drivers reduced their mean speeds by about 8-10 km/h (5-6 mi/h) during fog conditions. No information could be found on the current status of the system, but it was operational in 2000.

Another VSL system was installed in the Netherlands along a 20 km (12 mi) rural section of the A2 motorway between Amsterdam and Utrecht in 1992 (Robinson, 2002). The system is designed to reduce the risk of shockwaves, crashes, and congestion. Variable message signs are spaced approximately every one kilometer and loop detectors spaced every half kilometer. The posted speed limits are determined by a system control algorithm based on 1-minute averages of speed and volume across all lanes. If an incident is detected, a speed of 50 km/h (31 mi/h) is displayed. The evaluation results showed that the severity of shockwaves and speed in all lanes were reduced (Van de Hoogen and Smulders, 1994). The vehicle speed and speed deviation decreased leading to fewer short headways as well as reduced severity of shockwaves. The study showed no positive effect on capacity or flow, but cited the safety benefits of traffic homogenization.

Speed limits were adjusted in England in response to the level of congestion on the M25 motorway in 1995. The objective of the system was to smooth traffic flow by reducing stop-start driving. The 22.6 km long system has VSL stations spaced at 1 km intervals, loop detectors at 500-meter intervals, and CCTV. Using loop detectors measuring traffic density and speed, speed limits are lowered in increments as congestion increases. The speed limits are lowered from 70 mph to 60 mph when volume exceeds 1,650 veh/h/ln, and lowered to 50 mph when volume exceeds 2,050 veh/h/ln. Results showed that traffic accidents decreased by 10-15% and there was a very high compliance with the VSL system (Robinson, 2000). The VSL system is still functioning today.

Rämä (1999) investigated the effects of weather-controlled speed limits and signs on driver behavior on the Finnish E18 site in Finland. The study looked at two scenarios compared to a control case: one in the summer where the maximum speed limit is 120 km/h (75 mi/h), and one in the winter where the maximum speed limit is 100 km/hr (62mi/h). The control cases were the normal operating procedures in the summer and winter months. In the winter, during adverse road conditions the speed was lowered from 100 km/h (62 mi/h) to 80 km/hr (50 mi/h). A 3.4 km/h (2.1 mi/h) decrease in speeds was observed. It was noted that during adverse conditions that are harder to observe by drivers (such as “black ice”), the VSL was very effective at reducing speeds compared to the control case. It was concluded that the system is very beneficial

for improving safety when drivers have a difficult time perceiving adverse conditions. In the summer, results showed that the 85th percentile speed was decreased more than the mean speed, essentially reducing high end speeds. Both winter and summer scenarios showed that VSLs decreased the mean speed and standard deviation of speeds and demonstrated traffic homogenization. This was an experimental site and no information could be found as to the current status of the system.

Variable speed limits have been implemented in Sweden at 20 locations. Lind (2006) looked at the impacts of weather controlled VSLs on the E6 motorway in Halland, and the traffic controlled VSLs on the E6 in Mölndal, south of Gothenburg. The E6 in Mölndal is a low-speed urban motorway with normal speed limit of 70 km/h (43 mi/h). The VSLs in Mölndal were implemented as advisory speed limits in 2004 and changed to enforceable speed limits in 2006. This was part of a study to determine how VSLs were perceived by motorists in both enforceable and advisory conditions. The speed limit for free flow conditions was raised to 90 km/h (56 mi/h). In dense traffic the speed is reduced in a stepwise manner. At 950 veh/h/ln the speed is reduced to 70 km/h (43 mi/h) and can be reduced to 50 or 30 km/h (31 and 17 mi/h) depending on the density. Two thirds of interviewed drivers indicated that they supported the VSL system and said that it made them more attentive as to changes in traffic conditions. The same proportion reported a less hectic driving scenario and reduction of queue lengths. When the advisory speed limit was displayed crashes were reduced by 20% and when the enforceable speed limit was displayed crashes were reduced by 40%. The results showed an increase in average speed for all driving conditions and as much as a 40 km/h (25 mi/h) increase in potential queue formation scenarios. The study concluded there was an improvement in driving behavior for congested conditions, and a homogenization of traffic.

Papageorgiou et al. (2008) studied the impact of VSLs on traffic flow behavior (flow-occupancy diagrams) through simulation of a motorway in Europe. The displayed speed was based on a threshold control algorithm, with possible speed limits of 60 mi/h, 50 mi/h, and 40 mi/h. The study showed that the 50 mi/h setting showed the most changes in traffic flow that could be used for improving traffic efficiency. The 40 mi/h setting was useful at high occupancies for displaying safe speeds, but not for improving traffic efficiency. The average occupancy was

found to be higher when the VSL is implemented. The study concluded that the effect on capacity was not clear.

In summary, VSLs have been implemented in numerous areas throughout the United States, and are widespread throughout Europe. Table B-1 provides an overview of the VSL systems in the US, while Table B-2 provides an overview of these systems elsewhere. Most of the VSL systems in the US have been implemented to address adverse weather conditions. Several of the European systems however have been implemented to smooth flow and reduce congestion-related crashes. Several studies showed that mean speeds will decrease when a VSL is implemented, indicating that the VSLs do affect the speed at which motorists drive. Several studies showed the speed standard deviation to decrease as well, and that decrease has been associated with safety benefits. There has been little evidence to suggest that implementing VSLs has the potential to increase capacity. The systems using weather and road conditions to display VSLs have been shown to reduce crashes and homogenize traffic conditions. It is important for VSL control algorithms to display a safe speed for drivers to travel, especially when dealing with adverse weather and road conditions.

Among active systems, the minimum speed limits provided in the US are typically between 40 mi/h and 50 mi/h, while those in Europe typically vary between 60 km/h (37 mi/h) and 80 km/hr (50 mi/hr). It is also common in European systems to display a speed of 50 km/h (31 mi/h) during a detected accident scenario.

Table B-1. Summary of VSL Systems in the US

Name	Location / Time	VSL Algorithm	Observed Impacts	Status/Goal of System
Michigan, USA	M-10 in Detroit / 1960	Manually modified by operator based on CCTV and plots of freeway speed, from 20 to 60 mph	No significant effect on vehicle speeds	Inactive; improve safety by making drivers aware of downstream congestion
New Jersey, USA	New Jersey Turnpike / 1960s	Based on average travel speeds: normal speed to 48 km/h, 8 km/h increments	Authority concluded the signs are effective	Active; improve safety and reduce delays during congestion
New Mexico, USA	I-40 in Albuquerque/ 1989	Generated using a look-up table based on average speed plus a constant as a function of environmental conditions	A slight reduction in accidents, hindered by National Maximum Speed Limit (55 MPH)	Inactive; improve safety and smooth flow by displaying proper speeds
Tennessee, USA	19-mile section of I-75 / 1993	Determined by a central computer based on data collected using environmental sensors and vehicle detectors	5 to 10 percent reduction in speed, no crashes due to fog after implementation	Active; safety during adverse fog conditions
Colorado, USA	Eisenhower Tunnel on I-70 / 1995	Automatically computed based on the truck weight, speed, and axle configuration	Truck-related accidents declined on steep downhill sections	Active; improve truck safety on long downgrades
Washington, USA	I-90 across the Snoqualmie Pass / 1997	Automatically computed using speed, roadside data. Display confirmed by operator	Reduced the mean speed, increased the deviation	Active; improve safety by informing users of hazardous conditions
Arizona, USA	Rural section of I-40 in Flagstaff / 1998	Determined by a fuzzy logic controller based on atmospheric data and road surface conditions	Fuzzy logic worked well with the imprecision inherent in the input data	Inactive; improve safety during adverse weather conditions
Nevada, USA	I-80 / 2000	Using a logic tree, based on the 85th percentile speed, visibility, and pavement conditions, remotely controlled	Reliability of the visibility sensor limited the operation	Active; no specific consideration for congestion
Florida, USA	I-4 in Orlando / Sept/Oct 2008 and Jan 2009	Speed limits of 30 mph for heavy congestion, 40 mph for light congestion, normal limit for free flow	Analysis showed drivers were not complying with speed limits and system was ineffective	Active; improve safety and create a more steady flow
Wyoming, USA	Rural part of I-80 on Elk Mountain / 2010	Reduces speed during adverse weather	Speeds reduced by 0.47-0.75mi/h for every 1 mi/h reduction in VSL	Active; improve safety during adverse weather
Seattle, USA	I-5 from Boeing access road to I-90 / 2010	Algorithm unknown, bases changes on average speed and volume	No formal evaluation yet	Active; reduce accidents and congestion

Table B-2. Summary of VSL Systems Outside the US

Name	Location / Time	VSL Algorithm	Observed Impacts	Status/Reason for System
Germany	18-km section of Autobahn 9 near Munich / 1970s	Based on the fundamental relationships of speed, flow, and density between detector stations	Traffic during congested periods at speeds between 30 and 40 km/h	Active; stabilize traffic flow even under heavy flow conditions
Netherlands	A16 motorway near Breda /1991	Normal 100 km/h, reduced to 80 km/h if visibility <140 m, reduced to 60 km/h if visibility < 70 m	Mean speeds reduced by about 8-10 km/h during fog conditions	Unknown; improve safety during fog
Netherlands	A2 between Amsterdam and Utrecht / 1992	Based on 1-minute averages of speed and volume across all lanes, 50 km/h if incident occurs	Severity of shockwaves and speed in all lanes were reduced	Active; reduce risk of shockwaves, crashes, congestion
England	M25 / 1995	Flow > 1650: 70 mph to 60 mph Flow > 2050: lowered to 50 mph (unit: veh/h/ln)	Accidents decreased by 10-15%, very high compliance	Active; smooth traffic flow, speed limits are enforced
Finland	E18 / 1998	Lowered from 100 to 80 km/h in winter, from 120 to 100 km/h in summer	Decreased both the mean speed and the standard deviation of speed	Active; influence driver behavior and improve safety; speed limits are mandatory
Sweden	E6 motorway in Mölndal / 2006	Based on density: Free flow = 90 km/h 950 veh/h/ln = 70 km/h Can be reduced as low as 50 to 30 km/h	Advisory = 20% crash reduction Enforceable = 40% crash reduction Average speed increase Homogenization of traffic Reduction in queue length	Active; improve safety during adverse weather conditions
Europe	Motorway in Europe (2008)	Based on a threshold control algorithm	Efficiency optimized at 50 mph. Capacity effects not clear.	Specific location not provided; improve traffic flow efficiency

Driver Behavior Around VSLs

One of the important issues in implementing VSLs which is crucial to their success is whether drivers will obey the speed limit signs. This section summarizes the literature regarding driver behavior around VSLs and driver acceptance of such systems.

In the Netherlands Van den Hoogen and Smulders (1994) studied the VSL system on sections of the A2 motorway between Amsterdam and Utrecht (this is the same section as discussed earlier in the literature review). A user survey showed driver acceptance of the system was good, and the consensus from drivers was that it resulted in less stressful driving.

Tignor et al. (1999) suggest that the key to gaining compliance of variable speed limits is automated enforcement. Automated speed limit enforcement is not common in the United States, but has shown great benefits in Europe. The study by Tignor et al. (1999) in England showed improvements of compliance to VSLs due to automated enforcement. These improvements to compliance also improved facility performance measures with a 5-10% increase in the roadway capacity, and a 25-30% decrease in the number of rear-end collisions. After the initial installation of auto-enforcement cameras, they discovered that they did not have to keep cameras in every enforcement station. The flash produced by the cameras was enough to deter users from exceeding the speed limit as long as there were active cameras at a few locations. They could rotate the locations of actual cameras so drivers would never know which cameras were actually taking pictures.

Rämä (2001) studied the effect of weather controlled speed limits on driver behavior in Finland. The study took place in two scenarios; one in the winter and one in the summer. During the winter the study experimented with increasing the speed limit from 80 km/h to 100 km/h during good road conditions, and displaying a slippery road message during adverse road conditions at the normal speed limit (80 km/h). It was shown that during poor weather conditions in the winter, providing a warning message as well as the normal speed limit (80 km/h) reduced mean speed by 2.5 km/hr. If the normal speed limit was displayed during poor conditions without a warning message, the mean speed was higher. During good road conditions and operating at the normal speed limit, the average speed was lower when compared to that measured when a static

speed sign was present. When during good road conditions the speed limit was increased to 100 km/h, the average speed increased by 3.9 km/h. This shows that drivers recognize the displayed speed as the maximum they should travel, and also as the safest recommended speed. In the summer the normal speed limit is 100 km/h and the speed could be reduced to 80 km/h during adverse road conditions. During the summer, when the speed limit was reduced to 80 km/h the average travel speed decreased by 3 km/h. When the normal speed was displayed during good road conditions the average travel speed increased by approximately 1 km/h. In both summer and winter scenarios if the 100 km/h speed limit was shown during poor conditions the average speed increased and the headways decreased causing short headways and unsafe conditions. The percentage of drivers recalling the displayed VSL speed in both scenarios was good compared to fixed signs, and there was an overall positive response to the system. The author suggested that there would be more of an acceptance of VSLs if the driver was aware of why the speed limits were being reduced. He surmised that if the driver knew the theory behind the VSL system they might be more accepting of it.

Ulfarsson et al. (2005) looked at the effect of variable speed limit signs on mean speeds and speed deviations. They concluded that VSLs significantly reduce mean speed and that speed deviation was decreased for the uphill direction, but increased for the downhill direction. They recommended that VSLs should only be used under adverse weather or traffic conditions. They show that during favorable conditions VSL signs increased the average speed and speed deviation, leading to unsafe conditions. The study also analyzed an area downstream of the VSL section and suggested that while reducing speeds is effective within the variable speed limit zone, drivers may compensate by driving faster once out of a reduced zone which can lead to short headways and dangerous conditions downstream.

Brewer et al. (2006) investigated the effectiveness of several speed control devices on compliance of speed control in work zones. The study investigated the effectiveness of three separate devices: a speed display trailer, changeable message sign with radar, and orange border speed limit signs. The results showed that drivers will reduce their travel speed when their actual speed is displayed by radar detection signs. Radar devices show great potential for increasing speed compliance. Adding an orange border to a speed sign increases the visibility of the sign

but does not greatly increase the compliance. Based on data from the study, the authors concluded that drivers will travel at the speed at which they feel the most comfortable, unless they are aware of potential enforcement.

Lee and Abdel-Aty (2008) investigated the effects of warning messages and variable speed limits on driver behavior using a driving simulator. He found that under congested conditions and during gradual transitions of speed limits drivers followed speed limits well. If the speed was reduced abruptly there was greater speed variation and shorter headways. The use of a gradual reduction of speed limits reduced the variation in speeds and resulted in safer conditions. The author recommended placing VSLs upstream of the congestion and to gradually reduce the speed limit for a smooth transition. He concluded that VSLs are effective at reducing mean speeds and variation of speeds in congested areas. He also noted that the use of a simulator may not depict real world driving situations as the driver is aware that someone is monitoring their speed.

A study by PBS&J (2009) assessed the effectiveness of the current VSL system implemented on a 9-mile stretch of I-4 in Orlando, FL. The study analyzed driver speed through correlation testing. It was determined that driver's speeds were reduced by the VSL signs but that occupancy had increased as well. It was also shown that most of the traffic exceeded the speed limit by more when the VSL was reduced compared to the baseline speed limit. Through hypothesis testing it was also shown that flashing beacons had no significant effect on speed compliance rates, meaning they were ineffective at increasing compliance rates. Overall the study concluded that a true assessment of the system is not possible because the drivers were not traveling at speeds displayed by the signs. The speeds were correlated to the occupancy values; however the average speeds and occupancies were not correlated to the posted VSL speed.

Trout et al. (2010) studied the effectiveness of different work zone speed limit displays on driver behavior through use of a laboratory survey. The study compared four types of signs: static work zone, electronic speed limit, portable changeable message signs, and "Your Speed" signs. The study recommended the use of electronic speed limit signs using white LEDs in order for the sign to be perceived as enforceable. However, 97% of people found both the white and orange LED signs to be enforceable.

In summary, research has shown that drivers tend to travel at their desired speed whenever there is no enforcement. Automated enforcement, highway patrol enforcement, and signs that display drivers' speeds have all been shown to be effective enforcement strategies. In Europe most systems have had a positive response from drivers, and previous studies have concluded that drivers are more accepting of these systems if they know why they are implemented. The effectiveness of a VSL system is dependent on the driver's acceptance of the system. Gaining increased compliance of variable speed limits can be accomplished through some method of enforcement, or by making drivers aware to the specific strategies of VSL implementation. Research also suggests that gradual speed limit reduction is more effective than sudden speed reduction.

Evaluation of VSLs Using Simulation

Simulation is a very valuable tool for assessing the impact of changes in the transportation system and selecting optimal alternatives without actually implementing and testing them in the field. Several studies have been conducted to evaluate various VSL algorithms prior to their implementation. This section provides an overview of such studies and summarizes their findings.

Hegyi et al. (2003) present a predictive model for coordination of variable speed limits to suppress shockwaves at highway bottlenecks. The objective of this control mechanism is to minimize the time a vehicle spends in the given network. The METANET model is used to simulate the network, but was modified to incorporate the effect of speed limits into the calculation logic. METANET is a second order macroscopic traffic flow model. The controller predicts the evolution of the network based on the current state of the network and a control input. The algorithm bases speed increments on calculations of traffic flow, density, and mean speed. The data are relayed to the controller every interval, and the speed increments are updated based on the calculations. The specific time interval used for this study was not specified. Safety constraints are implemented into the model to prevent large speed limit fluctuations (e.g., 10 km/h). The model was applied to a benchmark freeway segment consisting of two nodes connecting one link. The study compared the use of continuous valued speed limits and discrete valued speed limits to a base scenario with no control. The results showed that in all control

cases the coordination of speed limits eliminated the shockwave, and restored the volume exiting the section to capacity sooner.

Hegyi et al. (2005) continued work on model predictive control through coordination of VSLs and ramp metering. The study compared the results of simulated ramp metering, and ramp metering with variable speed limits on a simple network. The results showed that when used in conjunction the total time spent in the system was lower and resulted in higher outflow. The decision of which method to use depends on the demand of the on-ramp and the freeway. It is suggested that VSLs should be used if speed limits can limit the flow sufficiently, however if the flow becomes too large, ramp metering should be implemented. The authors suggest that integrated use of both technologies will produce more favorable results than the use of each technology by itself.

Lin et al. (2004) presented two online algorithms for VSL controls at highway work zones. The first VSL algorithm was aimed to reduce approaching traffic speed so as to increase the average headway for vehicles to merge onto adjacent lanes. It consisted of two modules: one to compute the initial speed of each VSL sign, and the second responsible for updating the displayed speed on each VSL sign. The algorithm computes the appropriate speeds starting on the link directly upstream of the work-zone. The algorithm computes the target density and appropriate speed for that segment and works upstream to calculate appropriate speed limits. The second VSL algorithm was aimed to maximize the total throughput from the work zone under some predefined safety constraints. The model looks at projected queue lengths and changes the upstream speed control signs based on the optimization of a throughput function. The simulation results by CORSIM indicated that VSL algorithms can increase work-zone throughputs and reduce total vehicle delays. Moreover, when VSL was implemented, speed variances were lower than other non-controlled scenarios, although the average speed didn't change significantly.

Lee et al. (2004) used a real-time crash prediction model integrated with the microscopic simulator PARAMICS to assess the safety effects of variable speed limits on a 2.5 km stretch of a sample freeway segment. The algorithm for changing speeds was relatively simple. Three detector locations relay information to the controller which averages their values into one crash potential value. A crash threshold is predefined, and when the crash potential exceeds this

threshold the speed limit for all three detector locations was set based on a set of criteria. When crash potential exceeded the threshold, the speed limits were reduced from the design speed limit (90 km/h) based on the average speeds: reduced to 50 km/h if average speed \leq 60 km/h , reduced to 60 km/h if average speed $>$ 60 and \leq 70 km/h , reduced to 70 km/h if average speed $>$ 70 and \leq 80 km/h, and reduced to 80 km/h if average speed $>$ 80 km/h. The results found that reduction in speed limits can reduce average total crash potential, and the greatest reduction in crash potential occurred at the location of high traffic turbulence such as a bottleneck. However, the reduction in speed limit also increased the travel time. Thus, there was a trade-off between safety benefits and system travel time increase. The results were not based on real traffic data and many assumptions in the simulation were not calibrated to field conditions. The authors speculated that this may account for the increase in travel time.

Lee et al. (2006) continued work using the simulator PARAMICS in combination with the real-time crash prediction model described earlier, to analyze the effect of variable speed limits on safety. Simulation results showed that the system obtained the greatest safety benefit when speed changes were gradually introduced (5 mi/h every 10 minutes). It was also found that it is best to base the displayed speed on the average speed of detectors immediately upstream and immediately downstream of the VSL location. However, the study has several limitations. First, it assumed that drivers would comply with the speed limit. Second, it ignored the potential of ‘driver compensation’ (driving faster downstream after reducing speed).

Mitra and Pant (2005) evaluated the impact of a VSL system on a freeway work zone using the model VISSIM. The authors considered three scenarios: base scenario (no work zone), reduced speed on the work zone link, and reduced speed with reduced lane width. The displayed speed was only changed through the work-zone and only one value indicating lowered speed was displayed. Through analysis of the data, a process was carried out for developing an equation to calculate expected delays for a reduced speed through a work zone. The authors concluded that this equation could help determine the proper speed through a work-zone without the use of repeated simulation.

Abdel-Aty et al. (2006B) evaluated the safety effects of variable speed limits on I-4 in Orlando, Florida using PAPAMICS. This was part of a series of papers which reported research related to

the I-4 system. The algorithm not only investigated lowering speeds upstream of congestion, but also raising speeds limits after a congested area. The VSL signs were changed based on data from a detector directly associated with the sign. The study evaluated two speed regimes: low speed, and medium to high speed. The results found that there was a safety benefit in medium-to-high-speed regions but not in low-speed situations (congested situations). It was also shown that the greatest improvement in safety was achieved by abruptly changing speeds (15 mi/h) rather than gradually changing them. A travel time study was also conducted and showed a significant reduction in travel time through the segment. It was further recommended that decreasing speed limits before congestion and increasing them after congestion has positive impacts on safety and travel time.

In a subsequent study, Abdel-Aty et al. (2008) studied the effects of VSL on reducing crash risk on I-4 at different volume loading scenarios using PARAMICS. There were a total of 24 treatments in the experiment based on the extent of speed change, speed change distance, and speed change duration (5 to 10 minutes). The study investigated the benefits of reducing the speed (5 -10 mi/h) entering a congested area and increasing the speed (5 mi/h) past the congested area. Crash risks were computed from a crash prediction model that was based on traffic parameters. The study found that VSLs could reduce the rear-end and lane-change crash risk at low volume conditions, especially when lowering the upstream speed limit by 5 mph and raising the downstream speed limit by 5 mph. Again, VSLs were not found to be effective in reducing crash risk during congested conditions.

Abdel Aty and Dhindsa (2007) also conducted a micro-simulation study using PARAMICS in order to determine the impact that VSLs and ramp metering would have on the safety of a 9-mile stretch of I-4 in Orlando. The study also investigated the impact of VSLs and ramp metering on operational parameters like speed and travel time. The speed limits were changed based on thresholds of 5 minute averages of travel speed, and the ALINEA feed-back algorithm was used for the ramp metering. It was concluded that implementation of VSL can increase average speeds and decrease speed variation in the network as well as improve the risk index. It was also shown that the best implementation strategy is one where the speeds are incremented by 5 mi/h over a half mile. It was also shown that for safety improvements, a scenario where only downstream

speeds are increased, outperformed a scenario where upstream speeds are decreased and downstream speeds increased. A third conclusion drawn by the authors was that VSL and ramp metering are more effective when integrated together. When used in conjunction they showed shorter travel times and higher speeds than ramp metering or VSL alone.

Jiang and Wu (2006) used a cellular automaton model and showed that using multiple speed limits (where the speed limits decrease gradually from upstream to downstream) can help remove traffic jams. For a single small jam the concept is that by altering the speeds appropriately one can decrease the inflow toward a jammed area and increase the outflow. This will eventually result in the jam being dissipated. Their model was not based on field data.

Allaby et al. (2007) evaluated the impact of a candidate VSL system on an 8-km section of the eastbound Queen Elizabeth Way, an urban freeway in Toronto, Canada. The study was conducted using the microscopic simulator PARAMICS combined with a categorical crash model developed by Lee (2003). The VSL algorithm used was based on a logic tree that uses threshold values for flow, occupancy, and average travel speed. The base speed used was 100 km/h (62 mi/h) and it could be reduced to 80 km/h (50 mi/h) and 60 km/h (37 mi/h). The signs were arranged so there was never an abrupt change of speed limits (10 km/h difference) between signs. Each VSL sign was linked to an adjacent loop detector, and each sign operates individually. The results of the simulation showed that implementation of VSL signs could significantly improve safety, however the authors concluded that the use of VSL signs increased the travel time for all traffic scenarios considered.

Piao and McDonald (2008) assessed the safety benefits of in-vehicle variable speed limits on motorways using the microscopic simulation model AIMSUN. Traffic on UK motorway M6 with speed limit of 70 mi/h was simulated under different scenarios. Variable speed limits were applied when the speed difference between a queuing section and the upstream section was larger than 20 km/h (12.4 mi/h), and were provided to drivers through in-vehicle information. The simulation assumed that all vehicles were equipped with the in-vehicle devices. The adjusted speed limits could be 60 km/h (37 mi/h), 70 km/h (43 mi/h), 80 km/h (50 mi/h), 90 km/h (56 mi/h), or 100 km/h (62 mi/h). The simulation results showed that VSL reduced speed differences creating homogenization, reduced very small time headways, small time-to-collision (TTC)

events, and lane change frequency. This in effect reduced crash potential. The authors also indicated that there were potential safety risks in using the in-vehicle VSL compared with roadside VSL: large speed variations in speed could occur because some vehicles didn't have the in-vehicle device.

Papageorgiou et al. (2008) used a quantitative model to investigate the impact of VSL implementation on traffic flow. VSLs were incorporated into the general second-order traffic flow model METANET as a control component. The study evaluated the system based on a no-control case, coordinated ramp metering, VSL, and integrated scenario. The freeway was set up as a constrained discrete-time optimal control problem and solved using a feasible direction algorithm. It was shown that VSLs can substantially improve the traffic flow efficiency of a stretch of roadway especially when combined with coordinated ramp metering. The study concluded that when the optimal solution is applied to real motorway traffic, the solution will inevitably become non-optimum due to uncertainties in the real traffic stream. It is suggested that future research address using the optimal solution to develop a suitable feedback control strategy and update the solution in real time.

Carlson et al. (2010) expanded on the work of Papageorgiou (2008) by using a similar method, to explore the parallels between ramp metering and applying VSL upstream of a potential bottleneck or high volume merging situation. The METANET second order macroscopic model was altered to allow the VSLs to be incorporated. The study showed that when applied upstream, the VSL can act similarly to ramp metering where the flow is held back on the mainstream rather than on the ramp. The traffic arriving at the bottleneck is temporarily reduced and the system delays propagation of the congestion. Four scenarios were evaluated: no-control, VSL control, ramp metering, and integrated control. The VSL case decreased total time spent in the system (TTS) by 15.3%, and when VSLs and ramp metering are used in conjunction the TTS was reduced by as much as 19.5%. The study concluded that traffic flow and capacity can be improved through VSL use by reducing the capacity drop at bottlenecks. However, if the VSL is applied at under-critical conditions without the potential for bottleneck mitigation, mean speed is lowered and flow efficiency is decreased.

Popov et al. (2008) proposed a speed limit control approach to eliminate shockwaves based on a

distributed controller design. The METANET environment was used for the simulation. In this design, each variable speed limit sign has its own controller, but they all use the same structure and parameters. The proposed method requires using the appropriate amount of upstream and downstream data. Different scenarios were presented where each controller uses data from as many as 5 downstream controllers and one upstream controller. The maximum speed limit was 120 km/h (75 mi/h), and could be lowered in increments of 10 km/hr to a minimum of 50 km/h (31 mi/h). The authors showed that a simple, linear, static controller using immediate neighbor information successfully resolves a shockwave. The control scenario when compared to a scenario without controllers reduced total time spent in the network by 20%.

Ghods et al. (2009) used METANET to investigate the use of ramp metering and VSL in order to reduce peak hour congestion. An adaptive genetic-fuzzy control was used and was compared to the traditional ALINEA controller. Local density, local speeds, and queue length of the on-ramp were used as input data to develop the fuzzy controller. The fuzzy controller processes this input data and provides a corresponding metering rate and two variable speed limits. The idea behind fuzzy logic is to have a controller that resembles human decision making. It can process imprecise input data to arrive at a definitive conclusion. Rather than having precise threshold values that determine the output values of the controller, approximate multi-valued boundaries are used. This allows for input data to have partial membership to a category as opposed to the traditional “crisp” membership or non-membership options only. The study showed that the genetic fuzzy ramp metering and VSL control improved TTS by 15.3%.

In summary, much research has been conducted on the potential benefits of VSLs through the use of simulation. Table B-3 provides an overview of the studies discussed. One set of studies has used VSLs as a control mechanism similar to that employed in ramp metering. These studies concluded that VSLs can be used to suppress shockwaves at bottlenecks by implementing the VSL upstream of a bottleneck. Those studies reported that VSLs were effective in reducing TTS in the network, and their effect was more beneficial when combined with ramp metering. Another set of studies investigated the use of VSLs in microsimulators (VISSIM, PARAMICS, AIMSUN) and evaluated the safety benefits of such systems. These studies generally conclude

that VSLs can improve safety, as they tend to reduce speed variability.

Table B-3. Summary of VSL Evaluations Using Simulation

Author	Software	VSL Algorithm	Impacts	Other Comments
Hegyi et al. (2003)	METANET	Modified the METANET model to incorporate variable speed limits using continuous-valued speed limits based on the fundamental diagram.	Damped shockwaves and decreased the total travel time	Used a safety constraint to prevent large speed limit drops (e.g., 10 km/h)
Lin et al. (2004)	CORSIM	Two online algorithms: 1. minimize the queue in advance of the work zone by dynamically reducing the speed limit. 2. maximize the throughput over the entire work-zone area	Increased work-zone throughputs and reduced total vehicle delays, lowered speed variance	Evaluated the algorithms on three types of work zones. Used speed variances as safety indicator
Lee et al. (2004)	PARAMICS	50 km/h if ave.speed \leq 60 km/h, 60 km/h if $60 < \text{ave.speed} \leq 70$ km/h, 70 km/h if $70 < \text{ave.speed} \leq 80$ km/h, 80 km/h if ave. speed > 80 km/h	Reduced average total crash potential, especially at the bottleneck. Increased the travel time	Results were not based on real traffic data, many assumptions not calibrated
Mitra and Pant (2005)	VISSIM	Three scenarios: base, reduce speed on one link, reduce speed with lane width variation on link	Significant changes in speed, density, and lost time when reduced speed is implemented with lane width variation	Limited to a static network modeling due to scope and data
Hegyi et al. (2005)	METANET	Use of ramp metering with variable speed limits to provide optimum control.	TTS was lower and a higher outflow was achieved.	Did not perfect method for switching from ramp metering to VSL but gave general guidelines
Abdel-Aty et al. (2006B)	PARAMICS	Lower speed limits upstream and higher speed limits downstream of a hazard location	Safety benefit in medium-to-high-speed regions, travel time reduced, no benefit in congested situations	
Lee et al. (2006)	PARAMICS	Speed limit change for a pre-specified duration if the estimated crash potential (predicted from loop detector data) exceeded a specific threshold	Most safe when speed limit equal to the average speeds at the upstream and downstream detectors	Assumed that drivers would comply with the speed limit. Ignored the potential of 'driver compensation'
Jiang and Wu. (2006)	Cellular Automation Model	Used multiple speed limits at a traffic jam: Used decreased speed limits at the jam and increased the speed limit gradually upstream.	Traffic jams were shown to dissipate faster than the control case when the new varied speed limits were in place.	The speed limit reduction resulted in lower flow into the jammed area

Table B-3. Summary of VSL Evaluations Using Simulation (continued)

Author	Software	VSL Algorithm	Impacts	Other Comments
Allaby et al. (2007)	PARAMICS	Uses a logic tree based on flow, occupancy, and average travel speeds.	Improved safety but increased travel time for all traffic scenarios	Used several different combinations of threshold values to get optimum solution
Abdel Aty and Dhindsa (2007)	PARAMICS	Used 5 minute averages of speed to determine switching. Used 5 mph and 10 mph increments.	Improved speeds and decreased speed variation. Improved the risk index.	Used 24 scenarios to identify best implementation of upstream and downstream increments
Piao and McDonald (2008)	AIMSUN	In-vehicle system, could be 60km/h, 70km/h, 80km/h, 90km/h, and 100km/h	Reduced speed differences, small time headways, small time-to-collision (TTC) events	Needed in-vehicle device. Need to study how to achieve balance of safety and efficiency
Abdel-Aty et al. (2008)	PARAMICS	24 treatments based on the speed change extent (-10 to 5 mph), speed change distance, speed change duration (5 to 10 minutes) et al.	Reduced rear-end and lane-change crash risk at low volume conditions. No safety benefit in congested situations	crash risk were computed from crash prediction model that based on traffic parameters
Papageorgiou et al. (2008)	METANET	Modified METANET environment to incorporate variable speed limits and ramp metering.	VSL improved traffic flow efficiency, especially when used in conjunction with ramp metering	Considered no-control, VSL, ramp metering, and integrated cases.
Popov et al. (2008)	METANET	Used upstream and downstream data, and based threshold values on the fundamental diagram of flow and density.	Shockwave was resolved and total time spent was reduced by 20% when compared to the no control scenario.	
Ghods et al. (2009)	METANET	Used local density, local speeds, and queue length of the on-ramp to develop the fuzzy controller	ALINEA ramp metering controller: 4.8% Fuzzy-genetic ramp metering controller: 5.0% Fuzzy-genetic ramp metering and VSL: 15.3% (percentages signify improvements in TTS)	The genetic-fuzzy control proved to be superior to the ALINEA control.
Carlson et al. (2010)	METANET	Modified METANET to incorporate VSL data through use of a b-value	Reduced TTS by 15.3% in VSL case and 19.5% in integrated case	Four scenarios: no-control, VSL, ramp metering, and integrated

VSL Algorithms

This section provides more detailed information regarding the various VSL algorithms that have been developed. Different algorithms have been developed based on the purpose of the VSL. The first part of this section discusses VSL algorithms developed to mitigate congestion and improve safety, while the second part focuses on algorithms developed to address weather and other issues.

Congestion and Safety-Related Algorithms

The following three algorithms aim to mitigate shockwaves and are based on a combination of parameters:

- **Along A2 between Amsterdam and Utrechtin / 1992 Netherlands (implemented)**
 - Based on 1-minute averages of speed and volume across all lanes
 - 50 km/h if incident occurs
 - Severity of shockwaves and speed in all lanes were reduced
 - Detailed information regarding location of signs and detectors was not provided
- **Hegy 2003 (METANET simulation, not implemented)**
 - Bases speed increments through real time calculations of traffic flow, density, and mean speed
 - Uses rolling horizon values to continuously update the optimal solution
 - Showed that during a developing shockwave the model predictive control created a scenario with less congestion and higher outflow
- **Popov et al. 2008 (METANET simulation, not implemented)**
 - Used individual controller for each VSL sign using data from as many as 5 downstream controllers and one upstream controller
 - Reduced speeds in 10 km/h increments from 120 km/h to as low as 50 km/h

- Showed that a simple, linear, static controller using immediate neighbor information successfully eliminates a shockwave

The following two algorithms are based on flow:

- **M25 / 1995 England (implemented)**

- When flow > 1650 veh/h/ln: 70 mph to 60 mph.
- When flow > 2050 veh/h/ln: lowered to 50 mph
- Accidents decreased by 10-15%, very high compliance
- Detailed information on location of signs and detectors not provided

- **On the E6 motorway in Mölndal / 2006 Sweden (implemented)**

- Free flow = 90km/h
- 950veh/h/ln = 70km/h
- Speed can be reduced as low as 50 to 30 km/h
- When speeds were advisory there was a 20% crash reduction observed. For enforceable speed limits the crash reduction improved to 40%. Other impacts included average speed increase, homogenization of traffic, and reduction in queue length.

The following algorithm is based on occupancy:

- **I-4 Orlando, Florida (implemented)**

The software, SunGuide, uses in-ground inductive loops to measure traffic speed, volume, and occupancy for each lane in both directions of I-4. The speed displayed on the VSL sign depends upon the traffic occupancy level observed by these inductive loops. Each sign is linked to two or three downstream detectors and the occupancy value is averaged between them. There are three categories of traffic for this system: free, light, and heavy. The SunGuide software recommends an increase or decrease in speed based on the current occupancy level. An operator at the District 5 Regional Traffic Management Center either accepts or declines the recommendation. Table B-4 provides the thresholds used by the I-4

system to set variable speed limits.

Table B-4. Orlando I-4 Control Thresholds

	Occupancy for Decreasing Speed Limit	Occupancy for Increasing Speed Limit	Speed Limit
Free Flow	< 16%	< 12%	50 mph
Light Congestion	16 - 28%	12 - 25%	40 mph
Heavy Congestion	> 28%	>25%	30 mph

For the software to recommend a change between categories, the occupancy level must be sustained and observed for at least 120 consecutive seconds.

The following algorithm is based on average travel speeds:

- **Lee et al. 2004 (PARAMICS simulation, not implemented)**
 - Each VSL has an associated loop detector located adjacent to it
 - Three signs are grouped together and data for these signs was averaged into one value
 - If a crash potential threshold is reached the displayed speed is dropped at all signs using a set of criteria (all signs display the same speed)
 - 50 km/h if ave.speed \leq 60 km/h,
 - 60 km/h if $60 <$ ave.speed \leq 70 km/h,
 - 70 km/h if $70 <$ ave.speed \leq 80 km/h,

- 80 km/h if ave. speed > 80 km/h
- Reduced average total crash potential, especially at the bottleneck, but increased the overall travel time

This algorithm is based on a combination of flow, occupancy, and average speed, using a logic tree.

- **Allaby et al. 2007 (PARAMICS simulation, not implemented)**

- Figure B-1 summarizes the logic used in this algorithm.
- Each VSL sign is linked to an adjacent detector that operates individually
- For low volumes (less than 1,600 vphpl) occupancy is used as part of the criterion for reducing speeds. For higher volumes (more than 1,600 vphpl) occupancy is not considered.
- Ultimately average speed determines the displayed speed. This algorithm does not address gradual speed limit reduction as drivers are approaching the bottleneck.
- The simulation results showed that VSL signs could improve safety but that the travel time for all traffic scenarios considered were increased.

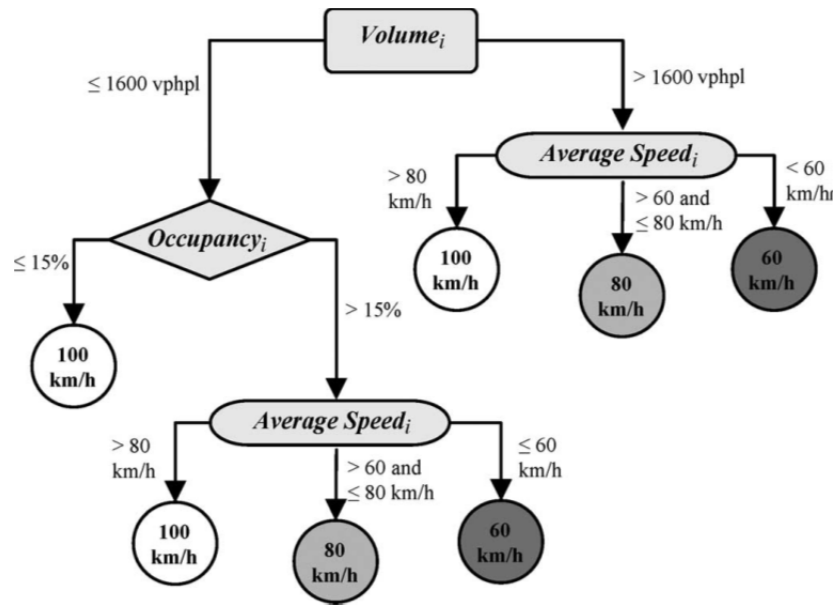


Figure B-1. Decision path for determining the new posted speed of the trigger VSLs.

(Source: Allaby P., Hellinga B., and Bullock M. **Variable Speed Limits: Safety and Operational Impacts of a Candidate Control Strategy for Freeway Applications**. IEEE Transactions on Intelligent Transportation System, 2007. Vol.8, No.4, pp.671-680)

Weather-Related and Other Algorithms

The following four algorithms were developed to address weather-related issues (visibility, wind speed, precipitation severity, etc.):

- **Along A16 motorway near Breda /1991 Netherland (implemented)**
 - 100 km/h (normal)
 - 80 km/h if visibility <140 meters
 - 60 km/h if visibility < 70 meters

- Mean speeds reduced by about 8-10 km/h during fog conditions
- **25 km, between Hammina and Kotka / 1997 Finland (implemented)**
 - 120 km/h for good road conditions
 - 100 km/h for moderate road conditions
 - 80 km/h for poor road conditions
- **On the Finnish E18 site / 1998 Finland (implemented)**
 - Lowered from 100 to 80 km/h in winter
 - Lowered from 120 to 100 km/h in summer
 - Decreased both the mean speed and the standard deviation of speed
- **Along a 19-mile section of I-75 / 1993 Tennessee, USA (implemented)**
 - Lowered to 55 mi/h with fog warning sign
 - Lowered to 35 mi/h with fog warning sign
 - Close Interstate during extreme fog
 - 5 to 10 percent reduction in speed
 - no crashes due to fog after implementation

In summary, there are a number of existing algorithms based on different performance measures. For algorithms involving congestion mitigation or shockwave dampening, VSL signs are almost always associated with downstream detectors to decrease flow entering a congested area. Algorithms based on weather or road condition parameters usually deal with VSLs associated with adjacent detectors. In both cases it is most common to gradually lower the speed limit in increments of 5 or 10 mi/h. Most algorithms also use a safety measure that prevents adjacent signs from having more than a 10 mi/h difference between them. In addition, nearly all systems will use a mechanism to prevent hysteresis, or rapid fluctuation between displayed speeds. Some

systems use minimum time durations, and others use reverse thresholds to avoid this event.

Types of VSL Sign Displays

There are several different types of variable speed limit signs utilized. The signs can be categorized into two groups: overhead signs and roadside signs. Either of these technologies can be accompanied by changeable message signs or flashing beacons displaying a “Reduced Speed When Flashing” message. This section provides a few examples of these two technologies.

In Seattle, Washington large overhead sign bridges (Figure 2) display the variable speed limits. This is part of a system that can also display changeable messages and symbols. During normal conditions the speed limit is displayed on either side of the road, and overhead displays are blank. During reduced speed zones the speed is displayed above each lane and the roadside signs display “Reduced Speed Zone” messages (as shown in Figure B-2). The sign also has the ability to display lane closures and warn drivers of approaching congestion or incidents (WSDOT

2010).

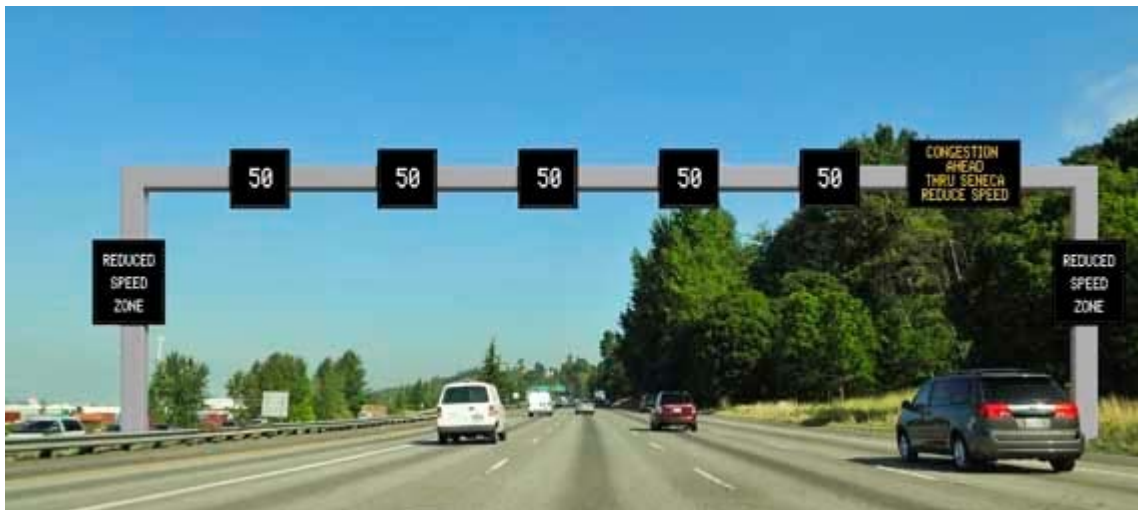


Figure B-2. VSL sign on I-5 in Seattle Washington (WSDOT 2010)

Similarly, the M25 in the United Kingdom also has an overhead variable speed limit display (Figure B-3). Each lane has a display of the reduced speed limit outlined by a red border to signify that it is enforceable. Automatic speed enforcement is also installed to capture vehicles violating the speed limit through photo-radar enforcement. This practice is prevalent throughout

Europe and the technology for “fake” photo enforcement exists as well. In those cases a flash goes off when a vehicle is exceeding the speed limit, but no picture is taken. This makes the driver believe they have been issued a ticket (Robinson 2000).



Figure B-3. VSL Sign on M25 Motorway in the UK (Robinson 2000)

The variable speed limits used on I-4 in Orlando, Florida are displayed on LED illuminated roadside signs (Figure B-4). These signs employ a flashing beacon, and are designed to look similar to the surrounding static speed limit signs (Haas, 2009).



Figure B-4. Variable Speed Limit Sign on I-4 in Orlando, FL

Luoma and Rämä studied the effects of VSLs on speed behavior and memory of signs using two different sign technologies in southern Finland. They interviewed drivers after passing variable speed limit signs, and asked them if they could recall seeing the sign, and if so what the speed limit was. The two technologies were fiber-optic and electromechanical VSL signs. The study showed that fiber-optic signs had a significantly greater effect on speed reduction than the electromechanical signs. The fiber-optic signs also had a 91% recall where the electromechanical signs only had a recall of 71.6%. It should be noted that the average recall of fixed speed limit signs is 76 – 80%.

There has not been much direct comparison between types of signs, but the general consensus is that overhead signs are more visible than roadside signs. However the cost of building these overhead signs is significantly higher than that of roadside signs.

Appendix B References

Abdel-Aty M., Dilmore, J., and Hsia, L. Applying Variable Speed Limits and the Potential for Crash Migration. Transportation research record No.1953, Transportation Research Board of the National Academies, Washington, DC, 2006A. pp. 21-30.

Abdel-Aty, M., Dilmore, J., Dhindsa, A. Evaluation of Variable Speed Limits for Real-Time Freeway Safety Improvement. *Accident Analysis and Prevention*, 38, 2006B pp. 335-345.

Abdel-Aty, M., and Dhindsa, A. Coordinated Use of Variable Speed Limits and Ramp Metering for Improving Traffic Safety on Congested Freeways. Preprint No. TRB 07-0008, 86th Annual Meeting of the Transportation Research Board, Transportation Research Board, Washington, D.C., 2007.

Abdel-Aty M., Cunningham R. J., Gayah V. V., and Hsia L. Dynamic Variable Speed Limit Strategies for Real-Time Crash Risk Reduction on Freeways. Transportation research record No. 2078, Transportation Research Board of the National Academies, Washington, DC, 2008. pp. 108-116.

Allaby P., Hellinga B., and Bullock M. Variable Speed Limits: Safety and Operational Impacts of a Candidate Control Strategy for Freeway Applications. *IEEE Transactions on Intelligent Transportation System*, 2007. Vol.8, No.4, pp.671-680

Boice, S., Bertini, R. L., Ahn, S., and Bogenberger, K. Dynamics of Variable Speed Limit System Surrounding Bottleneck on German Autobahn. Transportation research record 1978, Transportation Research Board of the National Academies, Washington, DC, 2006. pp. 149-159.

Brewer, M., Pesti, G., and Schneider, W. Effectiveness of Selected Devices on Improving Work Zone Speed Limit Compliance. College Station, Tex.: Texas Transportation Institute, Texas A&M University 2005.

Buddemeyer, J., Young, R.K., Dorsey-Spitz, B. Rural Variable Speed Limit System for Southeast Wyoming. Transportation Research Board Annual Meeting, Washington DC, 2010 Paper #10-2444.

Borough, Peter. In England, an variable speed limit system on the M25 freeway increases average travel times, but promotes proper following distances between vehicles and creates smoother traffic flow. Published By: The Urban Transportation Monitor. March 14, 1997.

<http://www.benefitcost.its.dot.gov/ITS/benecost.nsf/ID/8FD5EA59EFFF390F852569610051E25B>; accessed 22 March, 2010.

Carlson, R.C., Papamichail, I., Papageorgiou, M., Messmer, A. Variable Speed Limits as a Mainline Metering Device for Freeways. Transportation Research Board Annual Meeting, Washington DC, 2010 Paper #10-1529.

CTC and Associates LLC. Variable Speed Limit Signs for Winter Weather. Transportation Synthesis Report, Bureau of Highway Operations, Division of Transportation Infrastructure Development, Wisconsin Department of Transportation, 2003. (CTC and Associates LLC, <http://www.ctcandassociates.com/index.html>).

The Department of Transport and Regional Services (DoTARs), submission no. 5.

Elefteriadou, L., Brilon, W., Jacobson, L., 2011. Proactive Ramp Management Under the Threat of Freeway Flow Breakdown. NCHRP Report 3-87.

<http://www.infrastructure.gov.au/>, accessed July 25th, 2010.

Ghods, A.H., Rahimi-Kian, A., Tabibi, M. Adaptive Freeway Ramp Metering and Variable Speed Limit Control: A Genetic-Fuzzy Approach, IEEE ITS Magazine, Vol. 1, No. 2, Spring 2009. pp. 27-36.

Haas R., Carter M., Perry E., Trombly J., Bedsole E., Margiotta R. iFlorida Model Deployment Final Evaluation Report. Report No. FHWA-HOP-08-050. 2009.

Hegy A., De Schutter B., and Hellendoorn J. MPC-based Optimal Coordination of Variable Speed Limits to Suppress Shock Waves in Freeway Traffic. Proceedings of the 2003 American Control Conference, Denver, Colorado, June 2003, pp. 4083–4088.

Hegy A., De Schutter B., and Hellendoorn J. Model predictive control for optimal coordination of ramp metering and variable speed limits. Transportation Research Part C, 13 (3):185–209, June 2005.

Hines, M. Judicial Enforcement of Variable Speed Limits. NCHRP Legal Research Digest Number 47, Transportation Research Board, Washington D.C., March 2002.

Jiang R., Wu Q. Suppressing Jams by Multiple Speed Limits: a Simulation Study Based on Cellular Automaton Model. Transportation Research Board, Washington DC, 2006.

Kwon, E., Brannan, D., Shouman, K., Isackson, C., and Arseneau, B. Development and Field Evaluation of Variable Advisory Speed Limit System for Work Zones. Transportation research record No. 2015, Transportation Research Board of the National Academies, Washington, DC, 2007. pp. 12-18. and 55-64.

Lee, C., Hellinga, B., Saccomanno, F. Assessing Safety Benefits of Variable Speed Limits. Transportation research record 1897, Transportation Research Board of the National Academies, Washington, DC, 2004. pp. 183-190.

Lee, C., Hellinga, B., Saccomanno, F. Evaluation of Variable Speed Limits to Improve Traffic Safety. Transportation Research, Part C (14) 200, 213-228. 2006.

Lee, C. and Abdel-Aty, M. Testing Effects of Warning Messages and Variable Speed Limits on Driver Behavior Using Driving Simulator. Journal of the Transportation Research Board, Vol. 2069, 2008.

Lin, P., Kang, K., and Chang, G. Exploring the Effectiveness of Variable Speed Limit Controls on Highway Work-Zone Operations. Intelligent Transportation Systems, Vol. 8, 2004, pp.1-14.

Lind, G. Weather and Traffic Controlled Variable Speed Limits in Sweden. Report, Movea trafikonsult AB, Stockholm, Sweden, 2006.

Luoma, J., and Rämä, P. Effects of Variable Speed Limit Signs on Speed Behavior and Recall of Signs. Traffic Engineering + Control pp. 234-237. 1998.

Mitra A. and Pant P. D. A Framework to Evaluate the Impact of Variable Speed Limit Systems on Work Zone Traffic Operation Using VISSIM. Institute of Transportation Engineers, 2005 District 6 Annual Meeting. 2005.

Papageorgiou, M., E. Kosmatopoulos, M. Protopappas, and I. Papamichail. "Effects of Variable Speed Limits on Motorway Traffic". Internal Report 2006-25. Dynamic Systems and Simulation Laboratory, Technical University of Crete, Chania, Greece, 2006.

Papageorgiou, M., Kosmatopoulos, E., and Papamichail, I., 2008. Effects of Variable Speed Limits on Motorway Traffic Flow. Transportation Research Record 2047, pp. 37-48.

Papamichail, I., Kampitaki, K., Papageorgiou, M., Messmer, A., 2008. Integrated Ramp Metering and Variable Speed Limit Control of Motorway Traffic Flow. Proceedings of the 17th IFAC World Congress, Seoul, Korea, pp. 14084–14089.

PBS&J., 2009. I-4 Variable Speed Limit Effectiveness Study. Prepared for the Florida Department of Transportation, District 5.

Popov, A., Babuska, R., Hegyi, A. and Werner, H., Distributed Controller Design for Dynamic Speed Limit Control Against Shock Waves on Freeways. 17th IFAC World Congress, Seoul, Korea, 2008, pp 14060-14065.

Piao J. and McDonald M. Safety Impacts of Variable Speed Limits – A Simulation Study. Proceedings of the 11th International IEEE, Conference on Intelligent Transportation Systems, 2008.

Placer J., Fuzzy Variable Speed Limit Device Modification and Testing—Phase II, Arizona Department of Transportation, July 2001.

Rämä, P., Effects of Weather-Controlled Variable Speed Limits and Warning Signs on Driver Behavior. Transportation research record 1689, ISSN 0361-1981. Annual Meeting of the Transportation Research Board, National Research Council, Washington, DC, 1999.

Rämä, P., Raitio, J., Anttila, V. and Schirokoff, A. Effects of Weather Controlled Speed Limits on Driver Behaviour on a Two-Lane Road. VTT Communities and Infrastructure, Finland. 2001.

Robinson M. D. Safety Applications of ITS in Rural Areas. U.S. Department of Transportation, Washington D.C., Sept 2002.

Robinson, M. D. Examples of Variable Speed Application. Prepared for the Speed management workshop at Transportation Research Board, 79th annual meeting, 2000.
<http://safety.fhwa.dot.gov/speedmgt/vslimits/docs/vslexamples.ppt>, Accessed March 26, 2010.

Road Weather Management, Best Practices for Road Weather Management, Office of Transportation Operations, FHWA, U.S. Department of Transportation, 2003.

Sisiopiku V., Variable Speed Control: Technologies and Practices, Transportation Research Board 80th Annual Meeting 2001.

Special Report 254: Managing Speed: Review of Current Practice for Setting and Enforcing Speed Limits. TRB, National Research Council, Washington, D.C., 1998.

Steel, P., R.V. McGregor, A.A. Guebert and T.M. McGuire. Application of Variable Speed Limits along the Trans Canada Highway in Banff National Park. Annual Conference of the Transportation Associate of Canada. 2005.

TravelAid, Gudmundur F. Ulfarsson et al., Washington State Transportation Center, University of Washington, Washington, Dec 2001.

Tignor S.C, Brown L.L., Butner J. L., Cunard R., Davis S.C., Hawkins H.G., Fischer E.L., Kehrl M.R, Rusch P.F., Wainwright W. S., Innovative Traffic Control-Technology and Practice in Europe, International Technology Exchange Program Report to the U.S. Department of Transportation, August 1999.

Trout, N., Finley, M., Ullman, G. Motorist Understanding of Alternative Work Zone Speed Limit Displays. Transportation Research Board, Washington, DC 89th Annual Meeting, 2010.

Ulfarsson, G.F., Shankar, V.N., and Vu, P. The effect of variable message and speed limit signs on mean speeds and speed deviations. *Int. J. Vehicle Information and Communication Systems*, Vol. 1, Nos. 1/2, 2005 pp. 69 – 87.

Van den Hoogen, E., and Smulders, S. Control by variable speed signs: results of the Dutch experiment. Seventh International Conference on 'Road Traffic Monitoring and Control' (CP391). London, UK, 26-28 April 1994. pp.145–149.

Washington State Department of Transportation.
<http://www.wsdot.wa.gov/Projects/I5/ActiveTrafficManagement/>; accessed September 13, 2010.

WESH Orlando. Speed Limit Changes Coming to I-4.
<http://www.wesh.com/news/4154842/detail.html>; accessed 13 September, 2010.

Young, R., Rural Variable Speed Limit for Southeast Wyoming. Transportation Research Board, Washington, DC 89th Annual Meeting, 2010.

Zarean, M., Pisano, P., Dirnberger, K., and Robinson, M. Variable Speed Limit Systems: The-State-Of-The-Practice. Proceedings of the 1999 Rural Advanced Technology & Transportation Systems Conference, Flagstaff, AZ.

Zarean, Robinson, and Warren. Applications of Variable Speed Limit Systems to Enhance Safety. Office of Safety R&D, FHWA, U.S. Department of Transportation, 2000.